7.7 CORROBORATION OF RESULTS WITH AUXILIARY ANALYSES

The auxiliary analyses, described in this section and listed in Table 7.1-1, play an important part in building confidence that the TSPA-LA Model results are reasonable for the model's intended purpose. To gain confidence in the TSPA-LA Model, auxiliary analyses include analyses of single realizations (Section 7.7.1), comparisons of the TSPA-LA Model results with a simplified TSPA analysis produced using a FORTRAN code (Section 7.7.2), and with the TSPA results independently produced by EPRI using its Integrated Multiple Assumptions and Release code (IMARC) (Section 7.7.3). In addition, performance margin analyses (PMA) were performed using the same modeling cases and dose computation methodology as was used for the compliance modeling cases of the TSPA-LA Model (Section 7.7.4). While the results of all four groups of these auxiliary analyses add confidence in making the determination as to whether the model results are reasonable and ensure achievement of the required validation status for the model's intended purpose, the PMA results were of special significance in this regard. As required by the technical work plan, the PMA utilized revisions to selected component models in the TSPA-LA compliance model, including conceptual or uncertainty alternatives, to assess the performance margin in the compliance model, and to evaluate the degree to which the compliance model results are conservative.

The analysis of single realizations examines coupling of the model components and processes that constitute the foundation for the nature of the TSPA-LA annual dose history plots and validate reasonableness of the calculated dose by the TSPA-LA Model. Single realizations are analyzed for the Waste Package and Drip Shield EF Modeling Cases, the Igneous Intrusion Modeling Case, and the Seismic GM Modeling Case. The Simplified TSPA Analysis results are compared with results of the TSPA-LA Model of repository performance to demonstrate that the more complex TSPA-LA Model yields results that would be expected. The Simplified TSPA Analysis conducted simulations of the Nominal Scenario Modeling Case, Waste Package EF Modeling Case, Seismic GM Modeling Case and Igneous Intrusion Modeling Case. For the EPRI comparison, the TSPA-LA Nominal Scenario Modeling Case and Waste Package EF Modeling Case results were compared with the EPRI PA results for the equivalent modeling cases. The differences between the two model results are found reflective of the modeling approach and input differences between them. The PMA analysis (Section 7.7.4) confirmed that the implicit and explicit conservatisms in the TSPA-LA model components are indeed conservative and do not introduce undue risk dilution in the TSPA-LA results. The analysis also revealed the presence of performance margins, which is especially large for the Seismic GM Modeling case. The PMA analysis was performed on the same set of modeling cases as the TSPA-LA Model.

INTENTIONALLY LEFT BLANK

7.7.1 Analysis of Single Realizations

Analysis of single realizations provides a unique insight into the coupling of various submodel processes within the TSPA-LA Model. A comprehensive explanation detailing how the transport of key radionuclides is affected by coupling various components of the EBS, UZ, and SZ domains following the WP failure under varying physical-chemical-thermal-mechanical conditions provides confidence that the various submodel processes are working as expected and in-turn helps in providing confidence in the TSPA-LA Model.

Four different modeling cases are chosen to cover the range of WP failure mechanisms considered in TSPA-LA and to highlight the various processes affecting and controlling the radionuclide releases under various thermal and chemical conditions. The four modeling cases are: (1) Waste Package EF Modeling Case (Section 7.7.1.1), (2) Drip Shield EF Modeling Case (Section 7.7.1.2), (3) Igneous Intrusion Modeling Case (Section 7.7.1.3), and (4) Seismic GM Modeling Case (Section 7.7.1.4).

The methodology for calculating the expected annual dose (expectation of annual dose over aleatory uncertainty) for the various modeling cases is described in Section 6.1.2, which discusses differentiating epistemic uncertainty from aleatory uncertainty in the TSPA-LA Model. Although the treatment of aleatory uncertainty varies by the modeling case, the general methodology for selecting a realization for detailed analysis is similar in all four modeling cases. First, an epistemic uncertainty vector is chosen from the set of epistemic uncertainty realizations. The criteria for selecting an epistemic uncertainty vector is such that the general behavior of the expected annual dose (from that vector) is similar to the mean annual dose (expectation over both aleatory and epistemic uncertainty) and the magnitude of the expected annual dose is somewhat higher than the mean annual dose over time periods of interest. This choice is intended to select epistemic realizations that highlight processes of interest in each modeling case. Since the expected annual dose for an epistemic vector is calculated by taking the expectation over aleatory uncertainty, each expected annual dose is further broken down to select the realization(s) representing individual aleatory uncertainty vectors. The aleatory vectors are chosen by comparing each realization's dose contribution to the dose from other aleatory vectors in the set and selecting aleatory realizations which best describe the behavior of the expected annual dose. For the Igneous Intrusion and Seismic GM Modeling Cases, one GoldSim realization representing a unique combination of epistemic and aleatory uncertainty is chosen for detailed analysis while in the Waste Package EF and Drip Shield EF Modeling Cases, two GoldSim realizations representing two aleatory uncertainty vectors (representing CSNF and CDSP WP locations) for a given epistemic uncertainty vector are selected, to best describe the expected annual dose for the chosen epistemic uncertainty vector. More details regarding the selection of a single realization for analysis are presented in each subsection. All single realization analyses discussed here are carried out by running the single realization using GoldSim software (GoldSim V9.60.100, STN: 10344-9.60-01 [DIRS 181903]). However, the expected annual dose results presented are based on calculations performed using EXDOC_LA software (EXDOC_LA V2.0 STN: 11193-2.0-00 [DIRS 182102]) with proper weighting of scenario specific probabilities and expectation over aleatory and epistemic uncertainties.

7.7.1.1 Waste Package Early Failure Modeling Case

This section presents analyses of two realizations selected from the 6,000-realization base case run performed for calculating the expected annual dose from the Waste Package EF Modeling Case (GoldSim filename: LA_v5.000_EW_006000_012.gsm; output DTN: MO0709TSPAREGS.000 [DIRS 182976]). The distribution of expected annual dose along with the mean and various quantiles is shown on Figure 7.7.1-1a on a linear time scale and on Figure 7.7.1-1b with a log time scale to show the variation in dose at early time more clearly. The 300 displayed expected annual dose histories correspond to the 300 epistemic uncertainty vectors. Each expected annual dose history is calculated as a weighted average of twenty aleatory uncertainty vectors (Eq. 6.1.2-13). The twenty aleatory uncertainties are derived by considering the five spatial percolation subregions, two environments (dripping and non-dripping environments) for each percolation subregion, and two WP types for each environment (Section 6.1.2.4). One early failed WP is modeled in each of the aleatory vectors. From the Figure 7.7.1-1, the epistemic vector 281 is chosen for detailed analysis as it has an expected annual dose curve similar to the mean. The twenty aleatory uncertainty vectors which correspond to epistemic vector 281 are GoldSim realizations 5601 through 5620 (Figure 7.7.1-2).

The mean annual dose from this modeling case has several peaks (Figure 7.7.1-1b). The first broad peak is between 1,000 and 2,000 years due to contribution from CDSP WPs predominantly, when the relative humidity in the CDSP packages in the various percolation subregions goes above 95 percent and diffusive transport starts (Section 5.1.4). The second set of peaks that occur between 10,000 and 30,000 years are due to contribution from CSNF WPs when the relative humidity of the CSNF packages in the various percolation bins go above 95 percent. The last broad peak occurs after the DSs fail (between around 250,000 and 300,000 years) and water flux through the WPs starts.

The radionuclides contributing to the mean annual dose are shown on Figure 7.7.1-3. ^{99}Tc and ^{129}I are the top contributors at the peak of the mean annual dose, which occurs around 12,500 years. Beyond about 30,000 years, ^{239}Pu and ^{242}Pu become major contributors, with additional contribution from ^{237}Np and ^{226}Ra. In the sections that follow, transport characteristics of ^{99}Tc will be discussed as an example of high-solubility, non-sorbing radionuclides, while ^{239}Pu and ^{242}Pu will be discussed as examples of low-solubility, high-sorbing radionuclides.

In order to investigate the peaks in the mean annual dose curve, it was necessary to inspect two GoldSim realizations (representing two aleatory uncertainty vectors for the same epistemic uncertainty vector), one with an early CSNF WP failure and one with an early CDSP WP failure, because they each affect the expected annual dose at different time periods. Realization 5,608 is chosen to represent the early failure of CSNF WP while realization 5618 is chosen to represent the early failure of CDSP WP. These realizations were chosen because they have early failure of CSNF and CDSP packages within percolation subregion 3, which represents 40 percent of the repository area, and the dripping environment where releases are typically greater than from the non-dripping environment. The annual dose from the two realizations, are highlighted on Figure 7.7.1-2 along with other 18 realizations representing aleatory uncertainty vectors. These two realizations are examined more closely in the sections that follow.

Early Failure CSNF Package—Realization 5608

Figure 7.7.1-4 shows the annual dose from the major radionuclides for realization 5608 (GoldSim filename: LA_v5.000_EW_006000_020.gsm; output DTN: MO0708TSPAVALI.000 [DIRS 182985]). ^{99}Tc and ^{129}I dominate the first sharp peak at 11,500 years. There is a broad peak due to ^{239}Pu between 20,000 and 100,000 years and a broad peak due to ^{242}Pu and ^{237}Np after the DS fails at 292,000 years. At no time do the irreversibly attached colloids significantly contribute to the dose.

The peak dose is due to the almost pulse-like release of ^{99}Tc and ^{129}I from CSNF packages that transport unretarded through EBS, UZ, and SZ. In the Waste Package EF Modeling case, the CSNF matrix is modeled to instantaneously degrade when the WP is breached and while the temperature is above 100°C. However, release of the radionuclides cannot occur until there is a continuous water film within the WP to support diffusion that is modeled to occur once the relative humidity rises above the threshold of 95 percent in the absence of flow. In realization 5608 this occurs at 11,500 years, causing the diffusive release to start. All of the highly soluble radionuclides such as technetium and iodine from the CSNF inventory dissolve into the available water volume establishing a large concentration gradient between the waste form domain and the invert that drives diffusion and rapidly depletes the mass. Figure 7.7.1-5 shows the technetium release rate from the WF, EBS, UZ, and SZ for realization 5608. The initial pulse-like release rate from the waste form is lowered and broadened only slightly by the transport through the WP corrosion products domain and the invert domain, and on this plot, the curves are virtually on top of each other. There is small but observable lowering and broadening of the release rate peak in the UZ and SZ due to hydrodynamic dispersion caused by fracture-matrix interaction in the volcanic units and transport through alluvium. The small but sharp increase in the SZ release rate around 164,000 years is due to a step-change in the SZ breakthrough curve from Source Region 2 that results from coarse time discretization.

Plutonium, in contrast, is a low-solubility and high-sorbing element so its behavior is quite different from technetium. Unlike technetium, which had a large pulse-like release, the plutonium release from the waste form rises to a lower value and stays constant for a long time (Figure 7.7.1-6a). This is because the plutonium concentration is solubility limited unlike unbounded technetium concentration. As a result, degraded plutonium mass precipitates within the waste form domain. Figure 7.7.1-7a shows the plutonium solubility and concentrations within the CSNF waste form domain. The isotopes share the element solubility in proportion to their mass in the waste form cell, so ^{239}Pu dominates the plutonium inventory at early times and ^{242}Pu dominates at late times as ^{239}Pu decays away. The plutonium remains precipitated in the waste form domain throughout the simulation period in realization 5608. The drop in solubility observed around 292,000 years is due to the change in in-package chemistry calculations (Figure 7.7.1-7b) that occur following the failure of DS and as flow through the WP starts resulting in the switch from vapor-influx chemistry calculations to flow-through chemistry calculations. Note that at no point during the transport calculations do the pH and ionic strength go outside the range of instability for CSNF colloids (Figure 6.3.7-11b).

Besides precipitation within the waste form domain, sorption onto WP corrosion products is very important to controlling plutonium release from the WP. The effect of sorption on the plutonium concentration within the WP corrosion products can be seen in Figure 7.7.1-6b, where after an

initial spike, the concentration is maintained below the solubility limit within that domain. The initial spike results from the initial calculation of low corrosion products K_ds, when the competitive sorption regression uses a minimum value for the radionuclide concentrations. Once the radionuclide concentrations rise above the minimum, the K_ds adjust to higher values. The low initial K_d allows a pulse of radionuclides, most notably ^{239}Pu and ^{243}Am, to be released through the WP corrosion products and sorbed onto the invert before significant K_ds are calculated in the corrosion products. This is a model limitation due to the explicit-in-time solution method for the competitive sorption calculations. However, the current implementation is adequate because it causes only a minor over-prediction of the ^{239}Pu release to the invert in a single time step and is conservative. Because of decay of ^{243}Am to ^{239}Pu, the dissolved concentration of ^{239}Pu in the WP corrosion products is calculated to exceed that in the waste form domain. In the subsequent time steps, the higher K_ds cause the WP corrosion products domain ^{239}Pu concentration to drop below that of the waste form domain and then below that of the invert. As a result, there is backward diffusion from the invert into the WP corrosion products (represented by a negative release rate in Figure 7.7.1-6a). Flow through the invert eventually drops the concentration in the invert below that in the WP corrosion products and positive release from the WP to the invert is reinstated. The diffusion gradient between the invert and the UZ remains positive, however, resulting in continuous downgradient releases (Figure 7.7.1-6a). The release rates decrease in the UZ and further in the SZ, due to dispersion, sorption, and radioactive decay during transport. The small concentration of ^{239}Pu irreversibly attached to CSNF colloids in the waste form domain (referred as Ic on Figure 7.7.1-6b) shows that colloidal transport is not important in CSNF WPs.

The release rates of ^{242}Pu (Figure 7.7.1-8a) correlates well with its concentrations (Figure 7.7.1-8b). The share of ^{242}Pu relative to the elemental solubility increases with time as mentioned earlier, so its concentration and release rate also increases. Release from the WP corrosion product domain is significantly reduced due to sorption onto the WP corrosion products. Unlike ^{239}Pu where the concentration in the WP corrosion products domain exceeded that in the waste form domain in the initial timestep (at 11,500 years), ^{242}Pu is not the daughter of a significant short-lived parent, and the concentration in the WP corrosion products domain remains below that of the waste form domain. At 292,000 years the DS breaches, so water flux through the WP starts increasing the release rate from the WP. Delay and lowering of the release rates can be seen from the EBS (at invert), UZ, and SZ.

Early Failure CDSP Package—Realization 5618

Figure 7.7.1-9 shows the annual dose from the major radionuclides for realization 5618 (GoldSim filename: LA_v5.000_EW_006000_021.gsm; output DTN: MO0708TSPAVALI.000 [DIRS 182985]). ^{14}C, ^{99}Tc, and ^{129}I dominate the first peak which starts at about 1,000 years when relative humidity of the CDSP package rises above 95 percent. Although the CDSP WP is failed at the start of the simulation, only the DSNF is assumed to degrade instantaneously; the HLW glass degrades more slowly based on its degradation rate. This process can be seen from the plot of the cumulative release of selected isotopes from the waste form domain (Figure 7.7.1-10). The DSNF release is seen at the end of the first timestep (250 year timestep), with a gradual rise in the cumulative release, as the HLW glass degrades. The line for ^{14}C is flat because there is no ^{14}C inventory in the HLW glass. The slow degradation of HLW leads to a gradual release of ^{99}Tc from the HLW waste form domain (Figure 7.7.1-11) compared to that

from the CSNF waste form (Figure 7.7.1-5). The lower inventory of ^{99}Tc within the DSNF compared to that within CSNF (on a per package basis) results in a lower initial release rate. Once again there is small but observable lowering and delay of the release rate peak in the UZ and SZ.

Figure 7.7.1-12a shows the release rates of ^{239}Pu from the different domains. Figure 7.7.1-12b shows the concentration of ^{239}Pu in each domain of the EBS transport model: the HLW glass, DSNF, WP corrosion products, and invert. Each domain has its own chemistry and plutonium solubility. The plutonium starts out precipitated in both the HLW glass domain and the DSNF domain, but is depleted first in the DSNF domain by about 4,000 years. After that time its concentration in DSNF domain is controlled by transport from the upstream HLW cell. Kinetic sorption and desorption processes that are modeled in the WP corrosion products domain control the concentration of plutonium and maintain it at the solubility limit. As diffusive release continues to the invert, the plutonium mass is depleted from the corrosion products domain. By 75,000 years, the dissolved concentrations cannot be maintained at the solubility limits leading to its gradual decline. This reduction in corrosion product domain concentrations increases the concentration gradient between the HLW and WP corrosion products domains and increases the release rate from the waste form domain (Figure 7.7.1-12a). After 176,000 years, the plutonium within the HLW glass waste form domain is depleted, so the total release from the waste form domain drops to zero. In addition to the dissolved concentrations, Figure 7.7.1-12b also shows the concentrations of ^{239}Pu irreversibly attached to glass waste form colloids. The ionic strength (Figure 7.7.1-13) remains above the threshold for glass waste form colloid stability (Figure 6.3.7-11a) until 50,000 years. After that time, the ^{239}Pu concentration irreversibly associated with the glass waste form colloids remain orders of magnitude below the dissolved concentration, so significant colloidal release of ^{239}Pu is not observed in realization 5,618.

The release rate curves of ^{242}Pu from CDSP packages (Figure 7.7.1-14a) are similar to the curves for ^{239}Pu (Figure 7.7.1-12a), except that ^{242}Pu does not decay away as quickly (half life is 375,000 years), leading to significant late time releases. Once again, the ^{242}Pu becomes depleted in the DSNF domain at 4,000 years, but the concentration in the WP corrosion products domain is held steady due to sorption-desorption processes. The concentration of ^{242}Pu in the HLW waste form domain is low at early times as the elemental solubility is dominated by the ^{239}Pu concentration. As ^{239}Pu concentration declines due to radioactive decay the concentration of ^{242}Pu increases to match the elemental solubility (Figure 7.7.1-14b), and reaches a maximum around 176,000 years when ^{239}Pu concentration drops. As a result, the diffusion gradient which was from the WP corrosion products domain to the upstream waste form domains reverses leading to increasing downgradient (positive) release and depletion of the mass in the waste form domain. Once the mass is depleted the concentration in the waste form domain decreases and the backward diffusion from the WP corrosion products domain resumes. Release of ^{242}Pu irreversibly attached to glass waste form colloids (referred as Ic) is low but increases after the DS fails due to advective release from the WP. This is the only significant release of colloidal radionuclides for this modeling case, with the release rate of irreversibly attached plutonium nearly equal to that of dissolved plutonium.

7.7.1.2 Drip Shield Early Failure Modeling Case

This section presents analysis of two realizations selected from the 3,000-realization base case run performed for calculating the expected annual dose from the Drip Shield EF Modeling Case (GoldSim filename: LA_v5.000_ED_003000_008.gsm; output DTN: MO0709TSPAREGS.000 [DIRS 182976]). The 3,000 realizations in GoldSim represent 300 epistemic uncertainty vectors where each epistemic vector is used for 10 aleatory uncertainty vectors.

In the stylized Drip Shield EF Modeling Case, a single CSNF or CDSP WP is modeled in a dripping environment under a DS that is assumed to be completely failed (breached) at the start of the simulation. Furthermore, the WP is assumed to fail completely from localized corrosion at the onset of drift seepage when the in-drift temperatures are still hot. This stylized analysis is used to calculate the dose from WP failure by localized corrosion conditional on the early failure of the DS.

The expected annual dose from all 300 epistemic vectors, along with the statistics on the distribution of expected annual dose, is shown on Figure 7.7.1-15. Figure 7.7.1-16 shows the major radionuclides that contribute to the mean annual dose. There is an early peak due to ^{99}Tc, later, ^{239}Pu, and ^{242}Pu are the top contributors. Based on Figure 7.7.1-15, epistemic vector 228 is chosen for further analysis because it has a shape similar to the mean annual dose curve but has higher dose near the early peak.

The expected annual dose from this epistemic vector is calculated as a weighted average of annual dose for ten aleatory vectors (Eq. 6.1.2-14). The ten annual dose histories for epistemic vector 228 are GoldSim realizations 2,271 to 2,280 (Figure 7.7.1-17). The ten aleatory vectors represent dripping environments in five percolation subregions for both CSNF and CDSP WP types. As outlined in Equation 6.1.2-14, the dose from each realization is then multiplied by the probability of early DS failure, the waste type fraction, the seepage fraction, and the percolation bin fraction, which is equal to the number of WPs in the percolation subregion divided by the total number of WPs in the repository. These weighted doses are then summed to get the expected annual dose for epistemic vector 228 on Figure 7.7.1-15. Two GoldSim realizations (2,273 and 2,278) are highlighted on Figure 7.7.1-17 to show the relative difference in unweighted dose behavior between a CSNF WP type (realization 2,273) and CDSP WP type (realization 2,278) located in the same percolation subregion (percolation subregion 3). Both realizations are considered for further analysis (GoldSim filenames: LA_v5.000_ED_003000_016.gsm and LA_v5.000_ED_003000_017.gsm; output DTN: MO0708TSPAVALI.000 [DIRS 182985]). The major dose contributors for realization 2,278 are shown on Figure 7.7.1-18a, and they are similar to the major dose contributors for the mean annual dose (Figure 7.7.1-16): the early part of the dose curve is controlled by ^{99}Tc, the middle part is controlled by ^{239}Pu, and the late time part is controlled by ^{242}Pu after the decay of ^{239}Pu. The major dose contributors for realization 2,273 are similar to the ones shown for realization 2,278. ^{79}Se is also important early on as there is no solubility controlling phase and it is retarded moderately during transport. It shows spiky behavior due to the particle tracking algorithm used in the UZ Transport Model to track mass.

In the first 5,000 years, annual dose is controlled by the unretarded species that have no solubility constraints, such as ^{99}Tc, ^{79}Se, and ^{14}C. After 5,000 years and until 250,000 years,

^{239}Pu is the dominant radionuclide. As shown on Figure 7.7.1-18b, the dose from ^{239}Pu is a combination of dissolved plutonium and plutonium irreversibly sorbed on colloids. The dose from ^{239}Pu mass irreversibly associated with slow traveling fraction of colloids (defined by symbol Ic) is comparable to the dose from dissolved ^{239}Pu. At late times (past 300,000 years), ^{242}Pu is the dominant contributor to dose, just like in the Waste Package EF Modeling Case previously discussed. Here again, the dose from ^{242}Pu is a combination of dissolved and irreversibly sorbed colloidal plutonium (Figure 7.7.1-18b). Note that the colloidal plutonium was not important in the Waste Package EF Modeling Case (7.7.1.1) until the DS failure because of only diffusive releases from the WP. In this Drip Shield EF Modeling Case, the releases from the WP are mainly advective and colloids become important.

This type of transport behavior is expected because ^{99}Tc, ^{79}Se, and ^{14}C are transported as solutes with little or no retardation in the engineered barrier and natural system. Despite their similar transport properties and travel times to the biosphere, these radionuclides exhibit variations in terms of dose due to differences in the initial inventory, decay rates, and BDCFs for each of the radionuclides. Unlike the above radionuclides, the transport characteristic of ^{239}Pu is affected by retardation in the EBS, UZ, and SZ. This retardation is due to reversible sorption on the WP corrosion products and invert material (crushed tuff) in the EBS and on the lithologic units in the UZ and SZ. Almost all of the ^{239}Pu that is associated irreversibly with colloids (embedded in HLW glass waste form colloids) is transported faster than the dissolved ^{239}Pu due to a lesser degree of fracture-matrix interaction in the UZ and SZ, so it is observed earlier than dissolved ^{239}Pu.

The first ^{99}Tc release out of the EBS occurs at approximately 500 years for the CDSP WP even though the WP failures occur at the start of the simulation (Figure 7.7.1-19). Temperature effects cause this delay as no transport (diffusive or advective) is modeled to occur while the temperatures are above the boiling point of water (100°C). Figure 7.7.1-19 shows that the temperature within a CDSP WP does not fall below 100°C until approximately 500 years and, for CSNF WPs, the temperature does not fall below 100°C until approximately 700 years.

Releases from Engineered Barrier System—A number of processes in both the WP and invert influence the release of radionuclides from the EBS. Figure 7.7.1-19 shows the mass flux of ^{99}Tc out of the EBS into the UZ from both CSNF and CDSP WPs (from realizations 2,273 and 2,278, respectively).

The ^{99}Tc release curve for the CDSP WP starts at 500 years and initially decreases as the drift wall condensation changes from Stage 2 to Stage 3, as discussed next. The change in climate state is marked by an instantaneous increase in seepage rates through the EBS (Figure 7.7.1-20). The climate changes are at 600 years, 2,000 years, and 10,000 years. The small spike in release rates at around 2,000 years is in response to the switch from monsoonal to glacial-transition climate state. Another spike occurs around 10,000 years in response to the change to the long-term average climate state with its higher infiltration and higher seepage rate.

Figure 7.7.1-20 shows the flow rate into the WP as a function of time for the CDSP and CSNF WPs. The initial high CDSP seepage rate is from Stage 2 drift wall condensation (Section 6.3.3.2). The flow into the WP becomes equal to the seepage rate after 500 years when Stage 2 ends. The CSNF package shows low initial seepage because there is no CSNF Stage 2

drift wall condensation. The figure shows the flow into the WP increases at each climate change because the percolation rate increases.

Figure 7.7.1-21 shows the fraction of the waste form degraded for CDSP and CSNF. The CSNF waste form is completely degraded when the WP fails at the start of simulation because the temperature exceeds 100°C. The CDSP waste form, however, degrades slowly with the degradation rate declining gradually as WP temperature decreases; the entire waste form is completely degraded by about 10,000 years.

Unsaturated Zone–After their releases from the EBS, the radionuclides enter the UZ and are partitioned among the UZ fractures and matrix. For the major contributors to dose (^{99}Tc, ^{129}I, ^{237}Np, ^{239}IcPu (irreversible mass associated with colloids ^{239}Pu, and ^{242}Pu), most of the radionuclide mass released from EBS is partitioned into the UZ fractures where there is very little delay in transport. The release is mainly into the fractures because most of the release is by advection because the DS is failed and the WP is in the seeping percolation subregion in this modeling case. Figure 7.7.1-22 shows the fraction of each radionuclide partitioned into the fractures for percolation subregion 3 (CDSP WP) releases. (The results for CSNF WP releases are similar.) Figure 7.7.1-22 shows that, at a minimum, 80 percent of the mass flux enters the UZ fractures, but generally more than 95 percent of the mass flux is partitioned into the UZ fractures. The spikes down to zero (near the end of the simulation) are due to numerical approximations in the partitioning algorithm when essentially all of the ^{239}IcPu and ^{239}Pu have decayed and the actual release is approximately zero. Because of the fast transport times in the UZ fractures there is very little delay of radionuclides within the UZ, as shown on Figure 7.7.1-23.

Saturated Zone—Transport of radionuclides through the SZ has the potential for significant retardation due to sorption in the SZ volcanics and alluvium for some radionuclides. Because there is no sorption of ^{99}Tc in the SZ, its transport is relatively fast (Figure 7.7.1-23). This realization does not show much retardation for plutonium in the SZ. The combined UZ and SZ, delays and reduces the cumulative release of ^{242}Pu, with the majority of the reduction in the UZ.

7.7.1.3 Igneous Intrusion Modeling Case

This section presents analyses of a single realization selected from the 3,000-realization base-case run performed for calculating the expected annual dose from the Igneous Intrusion Modeling Case for one-million year simulation duration (GoldSim filename: LA_v5.000_IG_003000_017.gsm; output DTN: MO0709TSPAREGS.000 [DIRS 182976]). The 3,000 realizations are the combination of 300 epistemic vectors that are sampled over all the epistemic uncertainties and 10 aleatory samples that specify the time of an igneous intrusion event. In other words, each realization of this modeling case has one igneous intrusion event occurring at a specified time with one given epistemic vector. The duration of simulation for this modeling case is 1,000,000 years. The reader is referred to Sections 6.1.2 and 6.1.3 for how aleatory uncertainties and epistemic uncertainties are treated and how expected annual dose is calculated for the Igneous Intrusion Modeling Case. Section 6.5.1 provides the details of the conceptual model, model abstraction, and TSPA-LA implementations for the Igneous Intrusion Modeling Case.

It should be noted that all WPs and DSs are assumed to completely fail from the igneous intrusion event and the barrier capability of WP and DS to water flow is conservatively ignored. In addition, before the intrusion time, the nominal corrosion processes are included in this modeling case such that the WPs could be breached by either SCC or general corrosion and could release the radionuclides.

The mean annual dose and contributing radionuclides for the base case are shown on Figure 7.7.1-24. This figure shows that the mean annual dose increases rapidly for the first 100,000 years to about 1 mrem, then decreases slowly until around 200,000 years to a low value of 0.76 mrem, and then increases gradually for the remaining time to a maximum of 1.3 mrem. ^{239}Pu is the dominant radionuclide early on (for the first 200,000 years) with decreasing contribution as it undergoes radioactive decay. While the contribution from ^{239}Pu decreases, the contributions from ^{226}Ra, ^{242}Pu, and ^{237}Np increases. Around 200,000 years, ^{226}Ra overtakes ^{239}Pu as the dominant radionuclide. After 250,000 years, ^{226}Ra, ^{242}Pu, and ^{237}Np are the major radionuclides.

The expected annual dose from all 300 epistemic vectors is shown on Figure 7.7.1-25. The expected annual dose of epistemic vector 286 is very similar to the mean annual dose and thus this epistemic vector was chosen for this analysis. Figure 7.7.1-26 presents the annual dose for the ten aleatory vectors paired with epistemic vector 286 (GoldSim realizations 2851 through 2860). Among these, realization 2,855, which has an igneous event occurring at 10,000 years, was chosen for the single realization analysis as its dose contribution starts early. The model for realization 2,855 was run twice to first save information for all the percolation subregions and then to specifically save EBS cell-pathway details related to percolation subregion 3 under dripping environment (GoldSim filenames: LA_v5.000_IG_003000_032.gsm and LA_v5.000_IG_003000_033.gsm; output DTN: MO0708TSPAVALI.000 [DIRS 182985]).

This analysis of realization 2,855 focuses on 5 major contributors to dose. They are ^{239}Pu; ^{226}Ra; ^{242}Pu; and ^{237}Np mentioned above; plus ^{234}U. ^{234}U is included in this analysis because ^{226}Ra is a decay product of ^{234}U and is largely controlled by the transport behavior of ^{234}U. Note that the annual dose from realization 2,855 slowly decreases, which is somewhat different from the late-time trend of the expected annual dose shown for epistemic vector 286, which also has contribution from other aleatory vectors with late igneous event times.

Figure 7.7.1-27 shows the time history of annual dose and the contributions to annual dose from the selected radionuclides for realization 2855. A spike in dose (1,000 mrem) is noticeable immediately after the igneous intrusion event. This spike is caused by mobile radionuclides such as ^{99}Tc, ^{129}I, and ^{14}C. Dose contributions from those mobile elements decrease very quickly. In about 6,000 years their doses decrease by more than two orders of magnitude from their peak and for this reason, these radionuclides are not analyzed in detail hereafter. While the contributions from these mobile radionuclides decrease, dose from ^{239}Pu, ^{237}Np, and ^{242}Pu increases and a plateau (400 to 700 mrem) forms between 36,000 and 126,000 years. The annual dose starts decreasing gradually after that.

Note in the Igneous Intrusion Modeling Case, there are differences in the EBS environment that affect the waste form degradation and radionuclide mobilization (discussed in Section 6.5.1.1.2) from that in the Nominal Scenario Class (discussed in Section 6.3.4).

Igneous Event—For realization 2,855, the igneous intrusion event occurs at 10,000 years. The event fails all CSNF and CDSP WPs (total number = 11,629) as well as the DSs. None of the WPs and DSs have failed by the nominal corrosion processes prior to this igneous event. The WPs and waste forms experience a high temperature (the peak temperature is 1,150°C) because of the heat of the magma. The high temperature converts the uranium in CSNF WPs to U_3O_8 that has a very high specific surface area (BSC 2004 [DIRS 169987], Section 6.2.2.2). The increased surface area of the U_3O_8 results in an essentially instantaneous degradation of CSNF. The high temperature also results in a very fast degradation of HLW glass. After 500 years (the following GoldSim specified timestep after the intrusive event), the WP temperature drops to 52°C.

EBS Releases—The high degradation rates of CSNF and HLW lead to quick release of the waste inventories into solution. Because of solubility constraints, some of the radionuclides precipitate within the waste form domain of the EBS transport model. As shown on Figure 7.7.1-28, following the igneous event, the dissolved concentrations of neptunium, plutonium, and uranium from CSNF waste form domain reach and maintain at their solubilities for variable time durations. The solution is saturated with neptunium for about 40,000 years after the intrusion event, while it is saturated with plutonium for about 200,000 years. The solution is always saturated with uranium due to its large inventory. However, Ra concentration is below its solubility in the CSNF waste form domain. The dissolved concentration of Ra increases first followed by gradual decrease, due to the decay chain ingrowth from ^{234}U and the decay of itself. The dissolved concentrations of neptunium and plutonium decrease rapidly once their precipitated mass is depleted. As a result, their releases at later time are not solubility controlled.

The gradual declines in uranium, neptunium, and plutonium solubilities between 10,000 and 170,000 years are caused by the slow shift of pH towards neutral and the decrease of P_{CO2} with time for that period of time, as shown on Figure 7.7.1-29. The sudden increase in neptunium solubility at 172,000 years (Figure 7.7.1-28) is because at this time the neptunium solubility controlling phase switches from NpO_2 to Np_2O_5 due to complete degradation of steel inside the waste form domain, which acts as a reductant (Section 6.3.7.5). The releases of plutonium, uranium, neptunium, and radium from CDSP waste form domain have similar characteristics.

As discussed in Section 6.5.1.1.1, in the Igneous Intrusion Modeling Case, every WP and DS is rendered incapable of protecting its contents after the igneous intrusion event. As a result, high seepage fluxes, which are set equal to the local percolation flux after igneous intrusion (Section 6.5.1) and range from 0.18 to 3.54 m^3/yr, flow through each WP. This in turn causes rapid release of radionuclides from the WPs once the temperature drops below the boiling point of water (Figure 7.7.1-30). Among the selected radionuclides, the highest peak release rate is observed for ^{237}Np (approximately 553 g/yr), and its release rate decreases gradually as its inventory is consumed. The releases of ^{242}Pu, ^{234}U, and ^{226}Ra have a similar trend, but the release of ^{239}Pu decreases rapidly because of its relatively short half-life (2.41×10^4 years). Figure 7.7.1-30 also shows that a large percentage (>90 percent) of ^{239}Pu is transported in the form of dissolved species with the rest in the form of colloidal species. In addition, the dissolved component of total ^{239}Pu increases with time. For ^{242}Pu, the dissolved species is more than 99 percent of its total. For this reason, only the dissolved component of plutonium will be analyzed hereafter.

Figure 7.7.1-31 shows the advective and diffusive release rates of major radionuclides from CSNF WPs. It shows that advection is the major transport mechanism for radionuclides released from WPs for the Igneous Intrusion Modeling Case. Diffusion contributes less than one percent of the total release from WPs except for ^{242}Pu at late time. Comparing Figure 7.7.1-31 with Figure 7.7.1-30 reveals that CSNF WPs are the dominant source for those major radionuclides.

Figure 7.7.1-32 presents the dissolved concentrations of neptunium, uranium, plutonium, and radium and their solubilities in the CSNF corrosion products domain for percolation subregion 3 under dripping environment. It shows that in the corrosion products domain, neptunium and plutonium concentrations maintain at their solubilities for a longer time than in the waste form domain (see Figure 7.7.1-28). However, unlike in the waste form domain, uranium concentration does not reach its solubility. Similar to the waste form domain, radium concentration does not reach its solubility. Moreover, the dissolved concentrations of neptunium and plutonium decrease at slower rates than in the waste form domain, because in the corrosion products domain, the corrosion products gradually release neptunium and plutonium that were once sorbed onto them. The solubility controlled releases of ^{237}Np and ^{239}Pu are responsible for the dose curve plateau between 36,000 and 126,000 years presented on Figure 7.7.1-27.

The changes in radium solubility at 57,500 and 340,000 years are due to pH changes that cause switches between the two values of the radium solubility (Section 6.3.7.5.2). The changes in uranium solubility at those times are also due to pH changes that cause switches between Na-boltwoodite controlled uranium solubility and schoepite controlled uranium solubility (Section 6.3.7.5.2 and Tables 6.3.7-56 and 6.3.7-57).

Natural System—The cumulative releases for ^{237}Np, ^{242}Pu, ^{234}U, and ^{226}Ra from the EBS, UZ, and SZ are presented on Figures 7.7.1-33 (a) through (d).

Figure 7.7.1-33(a) shows that there is a small delay for ^{237}Np in the UZ and SZ (500 years or one timestep for the UZ and another 500 years for the SZ). This small delay is due to predominance of fast transport along fracture pathway with limited diffusion into the matrix. At the end of the simulation (one-million years), 99 percent of neptunium that was released from the EBS has migrated through the UZ and 96 percent of that has migrated through the SZ. In other words, the UZ and SZ provide insignificant retardation for ^{237}Np in the Igneous Intrusion Modeling Case. This is attributed to the relatively small K_d values of neptunium. Similarly, ^{234}U is not retarded significantly by the UZ and SZ, as shown on Figure 7.7.1-33(b). The figure shows that the cumulative release of ^{234}U from the SZ after 330,000 years is higher than that from the EBS. This is not a numerical error but is caused by the inventory boosting performed at the UZ-SZ interface for transport through the SZ (Section 6.3.10.3).

The cumulative release curves for ^{242}Pu, presented on Figure 7.7.1-33(c), show that the UZ delays plutonium release for a few thousand years, while the SZ delays plutonium release for more than 10,000 years. At the end of the simulation, about 24 percent of ^{242}Pu that was released from the EBS was held in the UZ, and 29 percent of ^{242}Pu that was released from the UZ was held in the SZ. The UZ and SZ provide significant retardation for ^{242}Pu. This is attributed to sorption of plutonium in the SZ alluvium and the volcanic matrix as a result of fracture-matrix interaction.

The cumulative release history for ^{226}Ra is presented on Figure 7.7.1-33(d). It shows that a large amount of ^{226}Ra that was released from the EBS did not enter the biosphere. Without considering decay and decay chain ingrowth, at 1,000,000 years, only 25 percent of ^{226}Ra that was released from the EBS migrates through the UZ and less than 0.1 percent of ^{226}Ra that was released from the UZ migrates through the SZ. The significant reduction of ^{226}Ra mass at the UZ and SZ is caused by the high K_d values in the UZ and SZ (Tables 6.3.9-2 and 6.3.10-2). It not only retards the transport of ^{226}Ra through the UZ and SZ, but also causes a large percentage of ^{226}Ra to decay during the prolonged transport processes through the UZ and SZ due to the short half-life of ^{226}Ra (1,600 years; see Figure 6.3.7-4).

As pointed out previously, Figure 7.7.1-27 shows that the annual dose curve has a plateau that appears between 36,000 and 126,000 years. This plateau corresponds to the SZ groundwater concentration plateau of ^{237}Np and ^{239}Pu at the RMEI location for the same time period as shown on Figure 7.7.1-34. The concentration plateaus correspond to the solubility controlled releases of neptunium and plutonium from the corrosion products domain shown on Figure 7.7.1-32. Note that the SZ groundwater concentrations shown on Figure 7.7.1-34 are obtained by dividing the annual releases of radionuclides from the SZ by the 3,000 acre-ft/yr annual water usage, as required by federal regulations. Although the SZ groundwater concentration of ^{237}Np is higher than that of ^{239}Pu, the latter has a higher concentration-dose conversion factor, as shown in Table 7.7.1-1. As a result, ^{239}Pu dose is higher than ^{237}Np dose.

Table 7.7.1-1 gives the specific activities for major radionuclides and the sampled BDCF values for realization 2,855. The last column of the table lists the Concentration-Dose Conversion Factors for the individual radionuclides, which are obtained by multiplying specific activities by the sampled BDCF values. This table shows that ^{226}Ra has the highest concentration-dose conversion factor (2.90×10^{13} (mrem/yr)/(g/L)), while ^{237}Np has the lowest concentration-dose conversion factor (8.81×10^{8} (mrem/yr)/(g/L)). The annual doses for the major radionuclides, presented on Figure 7.7.1-27, are the products of the SZ groundwater concentrations (Figure 7.7.1-34) and the concentration-dose converting factor for realization 2,855.

Figure 7.7.1-34 shows that for the first 500,000 years, the ^{234}U concentration increases with time and then decreases, so does the ^{226}Ra concentrations. This suggests that ^{226}Ra concentration is largely controlled by ^{234}U concentration, since the former is a decay product of the latter.

This single realization analysis examined important aspects that control the release of radionuclides from WPs to the environment in the Igneous Intrusion Modeling Case. It demonstrated that submodels are connected properly and the model as a whole functions as constructed and designed, to the extent of single realization level. The objective of this confidence building activity has been achieved.

7.7.1.4 Seismic Ground Motion Modeling Case

This section presents an analysis of a single realization from the 9,000-realization base case run performed for calculating the expected dose from the Seismic GM Modeling Case (GoldSim filename: LA_v5.000_SM_009000_000.gsm; output DTN: MO0709TSPAREGS.000 [DIRS 182976]) for the million-year simulation duration. The expected annual dose is presented on Figure 7.7.1-35, where each of the 300 realizations represent expected annual dose for one

epistemic uncertainty vector. The expected annual dose for each epistemic uncertainty vector is generated by taking an expectation over a sample of 30 aleatory uncertainty vectors (for more details on the computational methodology, refer to Sections 6.1.2.4.4 and 7.3.2.6.2). A single epistemic vector is selected for further analysis in such a manner that the expected annual dose is broadly representative of the modeling case and similar in behavior to the mean annual dose curve (Figure 7.7.1-35).

The epistemic uncertainty vector 155 is selected. The thirty corresponding aleatory sampling sequences are GoldSim realizations 4,621 through 4,650 (Figure 7.7.1-36). Of these, GoldSim realization 4,641 is selected for further analysis (solid red curve). Note that realization 4,641 represents epistemic uncertainty vector 155 and aleatory uncertainty vector (sampling sequence) 21. The GoldSim file for realization 4,641 was run twice to first save information for all the percolation subregions and then to specifically save EBS cell-pathway details related to percolation subregion 3 for the dripping environment (GoldSim filenames: LA_v5.000_SM_009000_016.gsm and LA_v5.000_SM_009000_017.gsm; output DTN: MO0708TSPAVALI.000 [DIRS 182985]).

The annual dose from realization 4,641 is presented on Figure 7.7.1-37 along with the dose contribution from major radionuclides. In general, the annual dose profile shows four peaks, of which two of them occur before 100,000 years and the remaining two around 200,000 years. Before 300,000 years, the dominant radionuclides are ^{99}Tc, ^{129}I, ^{79}Se, ^{239}Pu, but afterwards the dose is predominantly from ^{242}Pu with minor contribution from ^{135}Cs and ^{237}Np. The dose increases gradually past 300,000 years and there is no dose prior to 24,500 years.

Seismic events are modeled as a Poisson process that are generated randomly with the specified rate of 4.287×10^{-4} yr^{-1} (equal to the difference between maximum annual exceedance frequency of 4.287×10^{-4} yr^{-1} and the minimum annual exceedance frequency of 1×10^{-8} yr^{-1}) (Section 6.6.1.3.2). Over the course of any simulation several seismic events can occur with an average value of 428 events (computed by multiplying the specified rate of the Poisson process, 4.287×10^{-4} yr^{-1}, by the simulation time-period of one-million years). For realization 4,641, as shown on Figure 7.7.1-38, a total of 460 seismic events occur over the simulated duration. The horizontal component of the PGV corresponding to each seismic event is also shown, which is calculated from the mean bounded seismic hazard curve (Figure 6.6-6) by uniformly sampling the annual exceedance frequency between the minimum and maximum values for each event and reading the corresponding PGV value.

The probability of damage from an event is calculated separately for the CDSP and CSNF packages due to the inclusion of TAD canister in the CSNF packages, which increases its structural strength. Though the response surface for the probability of damage is different among CDSP and CSNF packages they are both functions of the PGV and the residual stress threshold of Alloy 22. The PGV value varies by each seismic event (as shown on Figure 7.7.1-38) while the residual stress threshold of Alloy 22 is treated as an epistemic uncertainty with a sampled value of 91.92 percent of the yield strength which is held constant over the realization. The residual stress threshold can vary uniformly from 90 percent to 105 percent of the yield strength and thus the value of 91.92 percent indicates a sample from the lower end of the distribution. A lower residual stress threshold value typically results in a greater probability of damage to the WP during a given seismic event; however, the actual

damage depends on a number of other conditions, such as whether the WP has intact internals or degraded internals, whether the DS framework and plate are intact or not, or whether the WP is covered by rubble or not. These conditions are determined separately.

Based on the DS plate and framework fragility analysis (Section 6.6.1.3.5), which is a function of DS plate and framework thickness at the event time, the fraction of the drift filled by rubble (in lithophysal zones) at the event time, and the PGV of the event, it is calculated that the DS framework does not fail until after 90,485 years and the DS plate does not fail until 268,000 years (Figure 7.7.1-39). It should be noted that at the time of DS plate failure the fraction of drift filled by rubble is still less than half. The failure time of the DS from rubble fill due to seismic events is computed to be much earlier than the DS failure time from general corrosion processes, which is computed to occur around 307,000 years.

The first damage time from a seismic event for the WP (Section 6.6.1.3.8) is determined separately for CDSP and CSNF WP, and it is calculated as the earliest of (a) the first damage time to the WP surrounded by rubble (using degraded internals damage abstraction) after the DS (either framework or plate) is failed or (b) the first damage time to the intact WP moving freely beneath the intact DS (the probability of damage is a function of PGV and residual stress threshold, assuming a 23-mm thickness of the WP outer barrier).

For CDSP WP, the first damage is caused by the seismic event at about 24,100 years, which is much earlier than the DS failure time (DS framework fails at 90,485 years). The PGV of the seismic event is about 0.7 m/s and at the sampled residual stress threshold of 91.92 percent, based on results presented on Figure 6.6-11a, the probability of damage is computed to be about 0.22. This value is compared to a random number generated by sampling a uniform distribution between 0 and 1 for each seismic event, such that if the probability of damage exceeds the random number then the WP damage would occur. At the event time of about 24,100 years, the random number value is 0.15 and thus the CDSP WP damage occurs. All CDSP WPs fail at this time as there is no spatial variability from seismic damage. The number of CDSP WPs failing in each percolation subregion for both dripping and non-dripping environments is shown on Figure 7.7.1-40.

For CSNF WP, the first damage that could result from a seismic event is calculated to be around 850,000 years. This evaluation is based on the damage abstraction of WP surrounded by rubble (using the degraded internals damage abstraction) after the DS is failed. This is to be expected since the probability of the WP getting damaged directly from a seismic event is extremely small (Figure 6.6-10a). However, the breach times from stress corrosion cracking by nominal processes, as calculated by WAPDEG, are much earlier than the seismic damage time. The WAPDEG calculated breach times differ for each percolation subregion due to spatial variability in the corrosion processes and thermal profiles of the WP. The first breach on CSNF WPs in percolation subregion 1 occurs at around 192,000 years, at around 168,000 years in percolation subregion 2, and around 204,000 years in percolation subregions 3, 4, and 5. Once any WP in a given percolation subregion is breached by the nominal corrosion processes, then to evaluate the damage from the subsequent seismic events, the degraded internals abstraction is conservatively applied to all WPs in that percolation subregion. Since the DS plate has not failed yet (failure time is 268,000 years), the seismic damage abstraction for fully degraded internals under intact DS is used (Figures 6.6-10b and 10c). The total number of CSNF packages that fail in each

percolation subregion for both dripping and non-dripping environment is shown on Figure 7.7.1-41. Since the first CSNF WP breach in the percolation subregion 2 occurs the earliest, one of the seismic events that occurs within the next timestep leads to failure of all WPs in that percolation subregion. All other percolation subregions following their first breaches undergo gradual failures of CSNF WPs from nominal processes until around 224,000 years, when a seismic event occurs that causes failure of all the CSNF WPs in the given percolation subregion. Note that the WP outer barrier thickness is greater than 23 mm in all percolation subregions when the seismic damage occurs. This highlights that even when the outer barrier thickness is near its maximum value, there is high probability of WP failure from seismic event when fully degraded WP internals abstraction under intact DS is used.

Although all CDSP WPs fail around 24,100 years, the damaged area on a WP increases gradually from subsequent seismic events. At each seismic event the probability of damage is computed and if it exceeds the random number then the corresponding damage area is added to the previous damaged area. The probability of damage from seismic event is based on using the damage abstractions for CDSP WPs with degraded internals under intact DS as shown on Figures 6.6-11b and 11c. When the outer barrier thickness is between 23 mm and 17 mm, the probability of damage is linearly interpolated between these two end member damage abstractions based on the thickness. Similarly, the damaged areas are computed from sampling gamma distributions for 23 mm and 17 mm outer barrier thickness as a function of the PGV and residual stress threshold and linearly interpolated. The mean damaged area of a CDSP WP with degraded internals under intact DS is shown on Figure 6.6-13. The failure-area time history for percolation subregion 3 for dripping environment is shown on Figure 7.7.1-42. Before 600,000 years the predominant damage area is from stress corrosion cracks due to seismic events, while the breach area from general corrosion patches becomes dominant afterwards. The initial damage area increases sharply around 49,000 years followed by a few more increases from events that cause damage, but after the DS plate failure (around 268,000 years) the WP is assumed to be surrounded by rubble and the probability of damage becomes even smaller leading to no failure from subsequent seismic events until the seismic event that occurs about 850,000 years.

Since the general corrosion patches on the WP do not appear until much later (500,000 years or more), all of the release from the WP is diffusive through stress corrosion cracks (at least until 500,000 years). The comparison of diffusive mass flux of ^{99}Tc out of the WP, which is the major dose contributor in the first 280,000 years (Figure 7.7.1-37), for various percolation subregions for CDSP WPs, is shown on Figure 7.7.1-43a. The releases start when the WP is first damaged, then decrease with time as steady state conditions get established, but then increase again around 49,500 years due to increase in the damage area (Figure 7.7.1-42). Most of the ^{99}Tc mass in the inventory is released out of the WP in the following few timesteps as there is no solubility controlling mineral phase for ^{99}Tc. The small diffusive areas associated with the WP outer barrier exert a strong control on the diffusive release of ^{99}Tc out of the EBS. In contrast, the diffusive mass flux of ^{242}Pu out of the WP, which is the major dose contributor past 280,000 years (Figure 7.7.1-43b), follows the WP outer barrier area curve indicating that the diffusive release is proportional to the opening area. The release is maintained for the simulated time because of various factors, such as: (a) ^{242}Pu has a comparatively long half life (~ 375,000 years), (b) the dissolved concentration inside the waste form domain is controlled by the solubility controlling mineral phase and thus not all of the degraded mass is available for

release, (c) the sorption of ^{242}Pu in the corrosion products domain retards the transport and further reduces the concentration gradient for diffusive flux, and (d) the small diffusive areas associated with the WP outer barrier reduces the mass flux. Of these factors, the most important is the sorption onto the corrosion products. For example, in the percolation subregion 3 for dripping environment, 1,055 CDSP WPs fail around 24,100 years. The total initial ^{242}Pu mass in the inventory, combined for HLW and DSNF mass, is about 38.66 g/pkg (from Table 6.3.7-5 with adjustment based on the uncertainty in the inventory). Using the decay rate of 1.85×10^{-6} yr^{-1}, the maximum mass at breach time would be about 36.97 g/pkg and about 35.31 g/pkg at 49,000 years (the time when the breach area increases). Based on the results of the calculation, the sorbed mass on corrosion products at 49,000 years is about 35.3 g/pkg, which accounts for almost all of the available mass. The mass gets slowly released by desorption from corrosion products into the solution, thus controlling the dissolved concentration (Figure 7.7.1-44) and the diffusive flux. Note that a mechanistic competitive sorption model that considers kinetic sorption-desorption processes is implemented for plutonium in the corrosion products domain. As a result, the concentration variations in the corrosion products domain are moderated even though the upstream concentrations (in waste form domain) could vary over a larger range based on degradation rates and solubility.

The diffusive flux of ^{99}Tc and ^{242}Pu from all five percolation subregions for CSNF WPs is shown on Figures 7.7.1-45a and b. The release from percolation subregion 2 is earlier than others as expected since the WP failure in percolation subregions 2 occurs earlier as shown on Figure 7.7.1-41. Figure 7.7.1-46 shows the WP outer barrier opening area with time for CSNF WPs that belong to the percolation subregion 3 for dripping environment. As discussed for CDSP packages, the ^{99}Tc diffusive release starts at the time of first breach and increases as the WP area increases. The inventory is quickly depleted and the concentrations fall rapidly. In contrast, the ^{242}Pu release is gradual and follows the breach area curve. The breached area increases after about 800,000 years after the patch area becomes significant. Although all CSNF WPs in a given percolation subregion undergo failure from seismic event at the same time, the release of ^{242}Pu is gradual due to sorption on the corrosion products. Figure 7.7.1-47 shows the example for percolation subregion 3 for dripping environment, where most of the ^{242}Pu mass released is sorbed on the corrosion products and then is gradually released by desorption thereby controlling the dissolved concentration and diffusive release out of the WP.

The pH and ionic strength time history in the corrosion products domain is shown on Figure 7.7.1-48. The first sharp decline in ionic strength occurs around 380,000 years because that is the time when rubble fills the drift (a consequence of multiple seismic events). At that time, the differential temperature and relative humidity time histories for a high thermal conductivity rubble is imposed leading to a small increase in relative humidity from 0.9956 to 0.9984. Since this increase in relative humidity corresponds to an equivalent increase in activity of water, it causes an appreciable decrease in ionic strength, indicating its high degree of sensitivity to relative humidity under vapor influx conditions (see Section 6.3.7.2.2 for details on ionic strength abstraction). The second decline in ionic strength that occurs around 724,000 years is caused by water flowing through the WP after general corrosion patches have formed and exceeding a threshold of 0.1 L/yr, thereby leading to a change in the in-package chemistry abstraction from calculations based on vapor influx to calculations based on liquid influx. Despite the changes in ionic strength over the course of the simulation, pH in the corrosion

products domain remains nearly constant as a result of buffering by surface complexation reactions.

Most of the ^{242}Pu mass released from the WP is in the dissolved state and very little is associated with colloids. This is because (a) the groundwater colloids in the WP are not present until 600,000 years as there is no flow through the WP, (b) the iron oxyhydroxide colloids and CSNF waste form colloids are unstable under the given pH and ionic strength conditions throughout the simulated duration (see Figure 6.3.7-11 for colloid stability relationships), and (c) the uranium colloids, which become stable around 384,000 years when the ionic strength drops from about 0.3 mol/kg to about 0.1 mol/kg, have limited carrying capacity as both the colloid concentration (about 3.7 mg/L) and the K_d for plutonium (about 247 ml/g) is small.

The total EBS release (summed over all percolation subregions) of ^{99}Tc and ^{242}Pu from CSNF and CDSP WPs is shown on Figure 7.7.1-49. As expected, the mass release from CSNF WPs is higher than that for CDSP WPs due to greater number of WPs and larger inventory on a per package basis (Tables 6.3.7-1 and 6.3.7-5). The majority of the mass passed to the UZ from EBS at the repository horizon goes into the fracture nodes of the UZ as compared to the matrix nodes, as shown on Figure 7.7.1-50 for ^{242}Pu. This is because the majority of the WPs in a given percolation subregion are in the dripping environment where drift seepage that flows out through the invert carries the mass advectively through the fractures even though most of the mass is diffusing out of the WP. For percolation subregion 1, the fraction of mass going into the fracture is relatively small (around 0.4) and increases (to around 0.9) at 396,000 years. This behavior is due to the change in seepage flux, which remains relatively small (about 0.005 m^3/yr) until around 396,000 years and then increases to a value of about 0.08 m3/yr. This is because at this time, the nonlithophysal locations are considered to be collapsed from drift degradation based on the drift seepage model abstraction, resulting in the seepage flux for such locations to change from the non-collapsed drift seepage to the percolation flux (Section 6.3.3.1.2). The effect of this change is greatest for percolation subregion 1 because, compared to other percolation subregions, it has (a) the smallest ambient seepage rates prior to the drift collapse and (b) he highest fraction of nonlithophysal locations (about 32 percent).

The cumulative mass release from EBS, UZ, and SZ are compared on Figure 7.7.1-51 for ^{99}Tc and ^{242}Pu. The transport characteristics are quite different for ^{99}Tc and ^{242}Pu in the UZ and SZ domains as ^{99}Tc is transported as unretarded species while ^{242}Pu undergoes significant retardation due to sorption on the tuff matrix and alluvium. Almost all of the mass that is released from the EBS for ^{99}Tc is also released out of the SZ model boundary within a relatively short period compared to the simulation time. In contrast, the amount of ^{242}Pu mass released from the UZ and SZ model boundaries at the end of simulation (one-million years) is appreciably smaller than that released out of the EBS (about 67 percent in UZ and 34 percent in SZ), indicating significant retardation. Since most of the mass is passed to the fracture nodes of the UZ, the mass mostly diffuses from the fracture continuum into the matrix continuum due to fracture-matrix interaction in the UZ with some also advecting due to lateral flow. Even though the free water diffusion coefficient in the UZ (as in EBS) varies by species (Table 6.3.9.3), the difference is relatively small between ^{99}Tc and ^{242}Pu and can be ignored for all practical purposes. Thus, both are likely to equally diffuse (assuming equal concentrations) into the matrix continuum from the fracture continuum. Because of the sorption of ^{242}Pu in the UZ matrix, the concentration gradient from the fracture to matrix is higher for ^{242}Pu compared to

^{99}Tc leading to its greater diffusive flux into the matrix and lesser cumulative release at the UZ-SZ boundary. In the SZ domain, the mass release from each of the four UZ regions is passed to the corresponding SZ region. In each SZ region, a location is randomly selected as the starting point for transport, which is manifested through sampling one of the 200 pre-generated SZ breakthrough curves for a given species (Section 6.3.10.2). Separate sets of breakthrough curves are available for ^{99}Tc and ^{242}Pu due to their different transport characteristics through the volcanic units and alluvium. The breakthrough curves are pre-generated as an impulse response function to a unit pulse and are convolved with the incoming UZ mass flux using the convolution integral approach to produce the SZ mass flux at the location of the RMEI. In this realization, the SZ breakthrough curve 122 is selected and the breakthrough times for all four zones for ^{99}Tc and ^{242}Pu are compared on Figure 7.7.1-52. The breakthrough of ^{99}Tc from all four SZ regions is much earlier than that for ^{242}Pu, with almost half of the mass input recovered after a few hundred years of travel in the SZ for ^{99}Tc compared to almost 100,000 years of travel time required for ^{242}Pu. However, there is a long tail in the breakthrough curve for ^{99}Tc for the remaining half of the input mass that results from longitudinal and transverse dispersion in the volcanic units and alluvium are due to fracture-matrix diffusive interaction in the dual porosity volcanic domain of the SZ transport model. The ^{242}Pu breakthrough is further impacted by sorption in the volcanic matrix and by sorption to the alluvium. For SZ breakthrough curve 122, the initially sampled plutonium K_d for volcanic matrix units is around 120 ml/g and that for the alluvium is 107 ml/g, which are modified to calculate effective K_d values but nevertheless introduce significant retardation. Most of the transport of plutonium occurs in the dissolved phase with a small fraction (less than 0.001) being transported via reversible sorption on the groundwater colloids. This is because the groundwater colloid concentration sampled is about 0.11 mg/L and the K_d for plutonium on the colloid is sampled to be about 6,560 ml/g, which when multiplied together, provided the mass associated with colloids compared to mass in dissolved state per unit water volume.

The SZ release rates for ^{99}Tc and ^{242}Pu are shown on Figure 7.7.1-53 for realization 4,641. They more or less follow the release rates out of the EBS (Figure 7.7.1-49). The SZ releases are converted into annual dose by taking the annual releases out of the SZ for each radionuclide, dissolving them in the 3,000 acre-ft of water (annual usage at RMEI as defined by the regulation) to compute the mass concentrations, converting the mass concentration into concentration of radioactivity (in curies per liter of water), and then multiplying with the corresponding BDCFs computed for the modern-interglacial climate (present-day climate). The end result of this is Figure 7.7.1-37.

7.7.1.5 Summary

The single realization analyses, of the four modeling cases, provide a useful insight into the interaction of several submodels under varying thermal-mechanical-chemical-physical conditions in the repository. They help in understanding the coupling of the EBS, UZ, and SZ transport models for calculating the annual dose to RMEI in a given realization. Within each transport model domain, the interaction of various submodels (and their abstractions) under a given set of physicochemical conditions is described in detail, which provides confidence that the submodels are coupled as intended and their behavior can be explained in a logical manner leading to the dose calculations. Besides explaining the interaction of submodels, the transport behavior of major dose contributing radionuclides is also described and highlighted in the

various modeling cases. For example, the Waste Package EF and Drip Shield EF Modeling Cases highlight the controls on transport at early times when the repository is hot and show the effect of climate changes while the DS are still intact. In contrast, the Igneous Intrusion and Seismic GM Modeling Cases show the effects of various processes occurring late in time and when the DSs are breached. In all cases the early release following the WP breach is dominated by non-sorbing and non-solubility limited radionuclides such as ^{99}Tc and ^{129}I, while the late time release is dominated by longer-lasting solubility-limited radionuclides that undergo sorption such as ^{242}Pu, ^{237}Np, and ^{239}Pu.

INTENTIONALLY LEFT BLANK

Table 7.7.1-1. Calculation of Dose Per Unit Concentration of Selected Radionuclides for the Igneous Intrusion Modeling Case (for Realization 2855)

Radionuclide	Specific Activity (Ci/g)[a]	BDCF (mrem/yr)/(pCi/L)[b]	Concentration-Dose Converting Factor[c] (mrem/yr)/(g/L)
^{237}Np	7.05E-04	1.25E+00	8.81E+08
^{239}Pu	6.21E-02	3.57E+00	2.22E+11
^{242}Pu	3.94E-03	3.39E+00	1.34E+10
^{234}U	6.21E-03	4.03E-01	2.50E+09
^{226}Ra	9.89E-01	2.93E+01	2.90E+13

[a] Taken from the species element of GoldSim file: LA_v5.000_IG_003000_032.gsm (output DTN: MO0708TSPAVALI.000) [DIRS 182985]).
[b] Taken from BDCF_Nominal element of GoldSim file: LA_v5.000_IG_003000_032.gsm (output DTN: MO0708TSPAVALI.000 [DIRS 182985]).
[c] Dose per unit concentration (mrem/yr)/(g/L) = (Specific Activity)∗(BDCF)∗(1E+12 pCi/Ci).

INTENTIONALLY LEFT BLANK

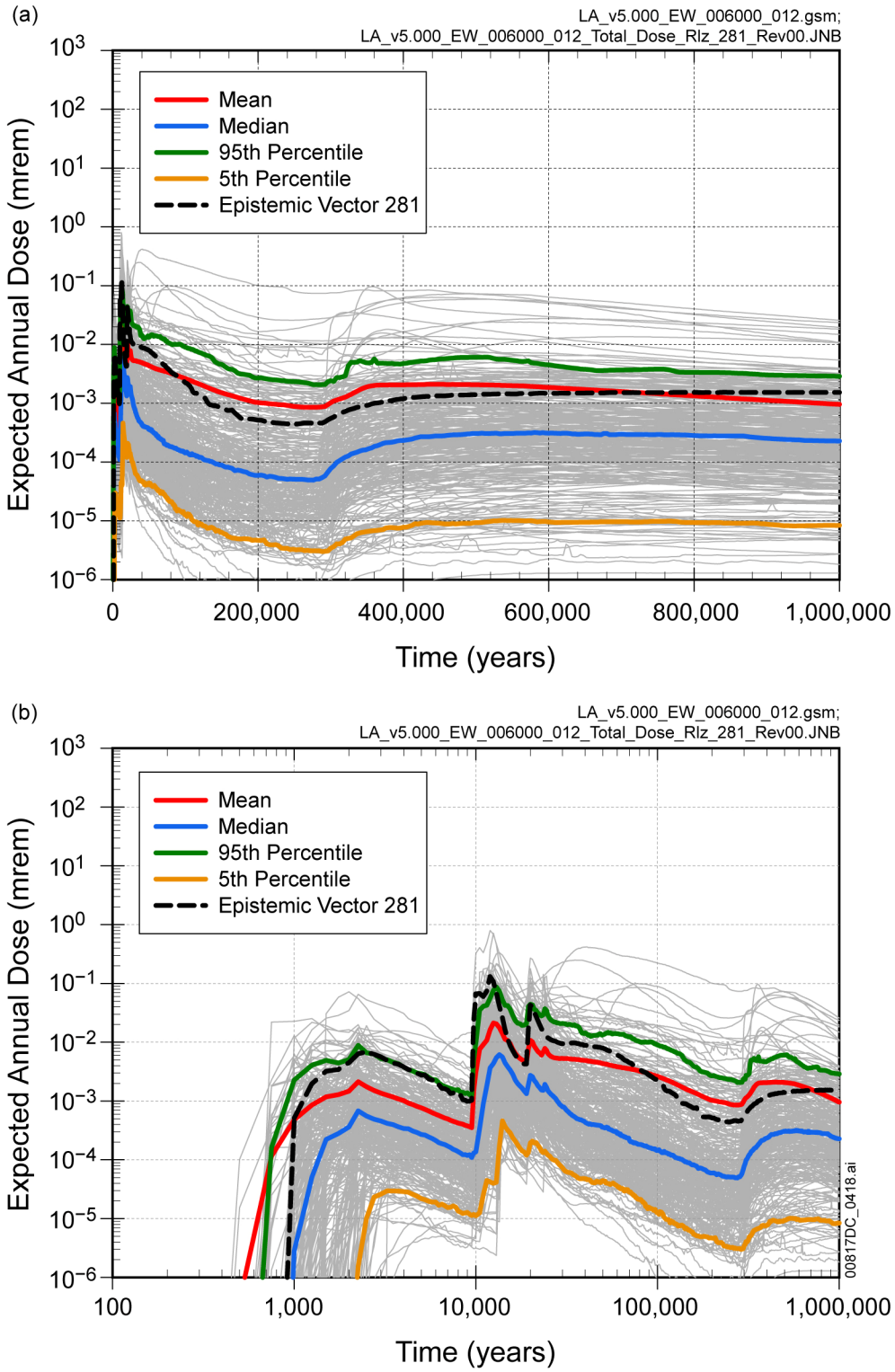

Source: Output DTN: MO0709TSPAREGS.000 [DIRS 182976].

Figure 7.7.1-1. Expected Annual Dose for the Waste Package Early Failure Modeling Case for the 1,000,000-Year Simulation after Repository Closure: (a) Linear Time and (b) Log Time

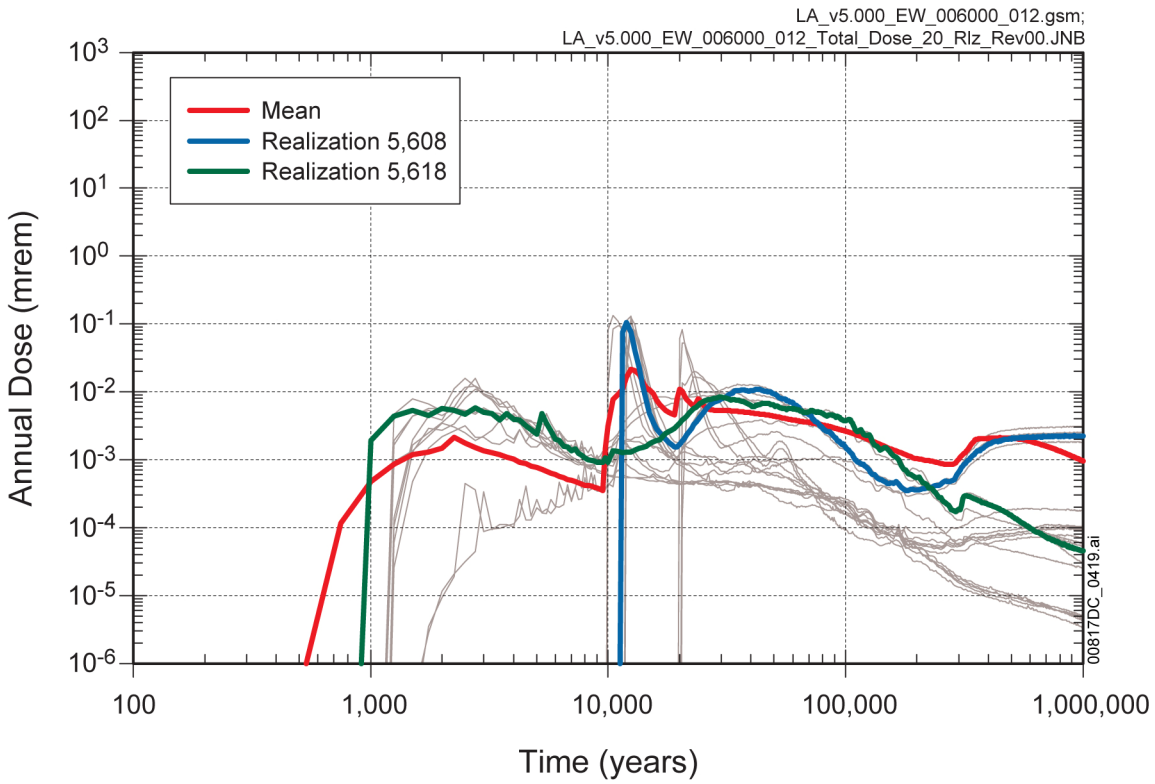

Source: Output DTN: MO0709TSPAREGS.000 [DIRS 182976].

Figure 7.7.1-2. Annual Dose from Realizations 5601 through 5620 of the Waste Package Early Failure Modeling Case for the 1,000,000-Year Simulation after Repository Closure

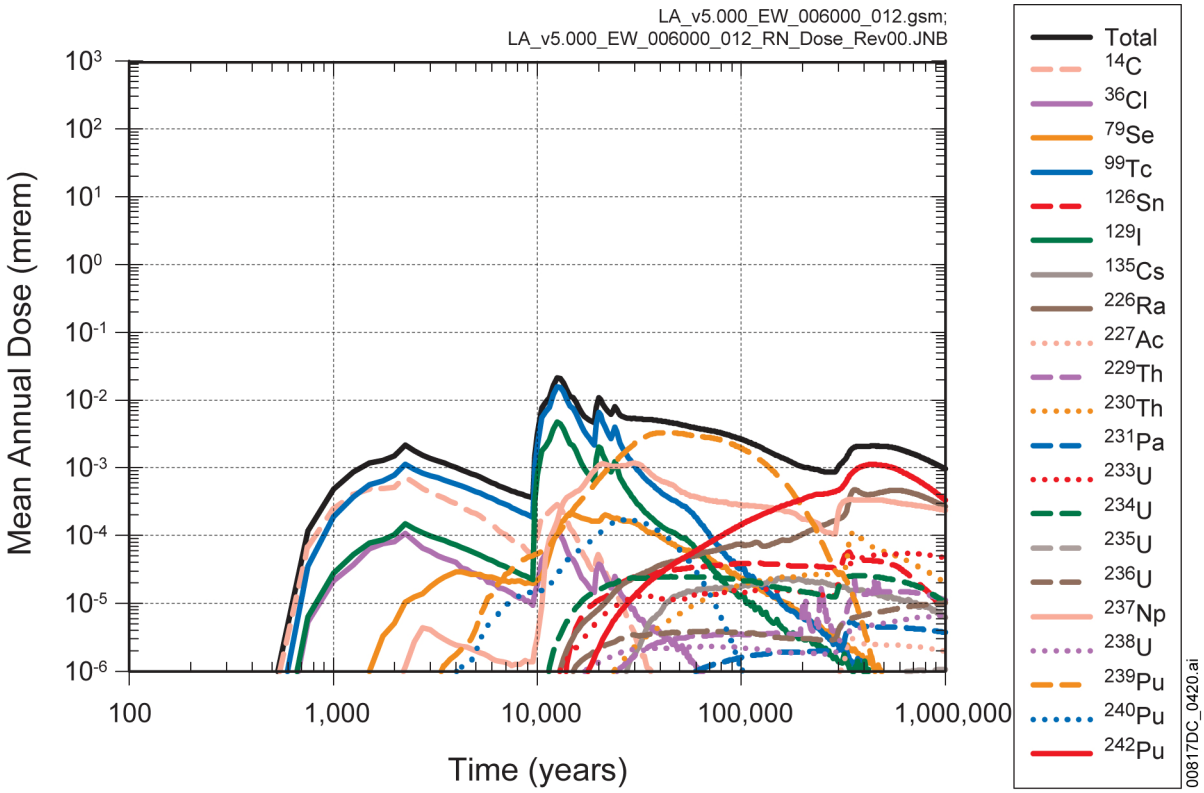

Source: Output DTN: MO0709TSPAREGS.000 [DIRS 182976].

NOTES: ^{226}Ra dose is the sum of ^{226}Ra and ^{210}Pb doses (secular equilibrium assumed).

Figure 7.7.1-3. Major Radionuclide Contributors to Mean Annual Dose for the Waste Package Early Failure Modeling Case for the 1,000,000-Year Simulation after Repository Closure

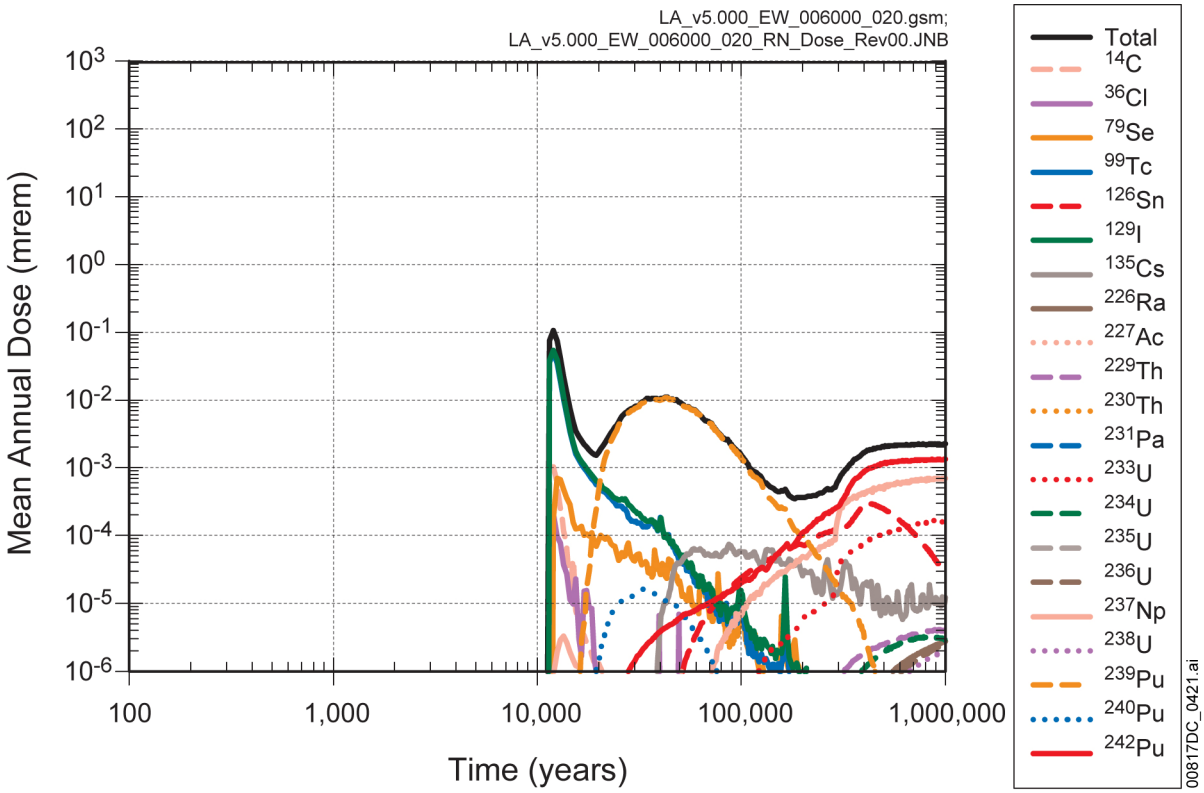

Source: Output DTN: MO0708TSPAVALI.000 [DIRS 182985].

NOTES: ^{226}Ra dose is the sum of ^{226}Ra and ^{210}Pb doses (secular equilibrium assumed).

Figure 7.7.1-4. Major Radionuclide Contributors to Mean Annual Dose for Realization 5608 of the Waste Package Early Failure Modeling Case for the 1,000,000-Year Simulation after Repository Closure

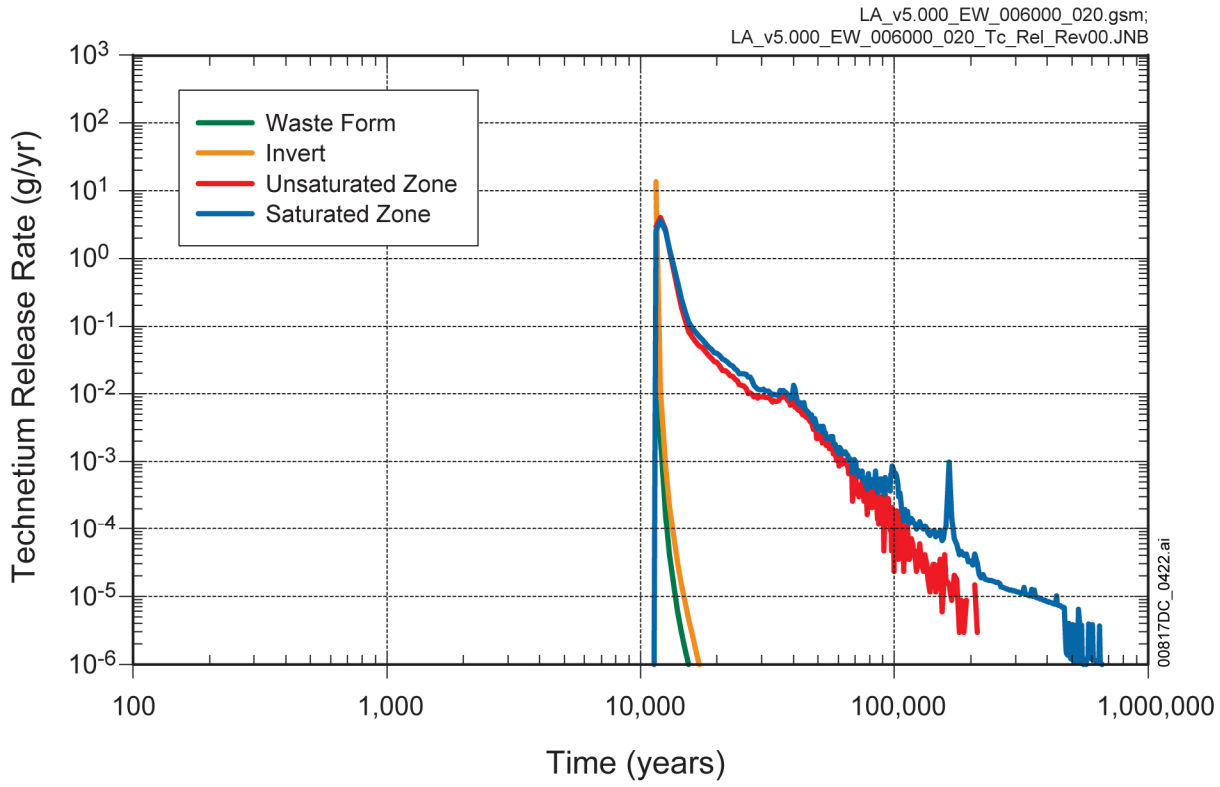

Source: Output DTN: MO0708TSPAVALI.000 [DIRS 182985].

Figure 7.7.1-5. Release Rates of Technetium from the Waste Form, EBS, Unsaturated Zone, and Saturated Zone for Realization 5608 of the Waste Package Early Failure Modeling Case for the 1,000,000-Year Simulation after Repository Closure

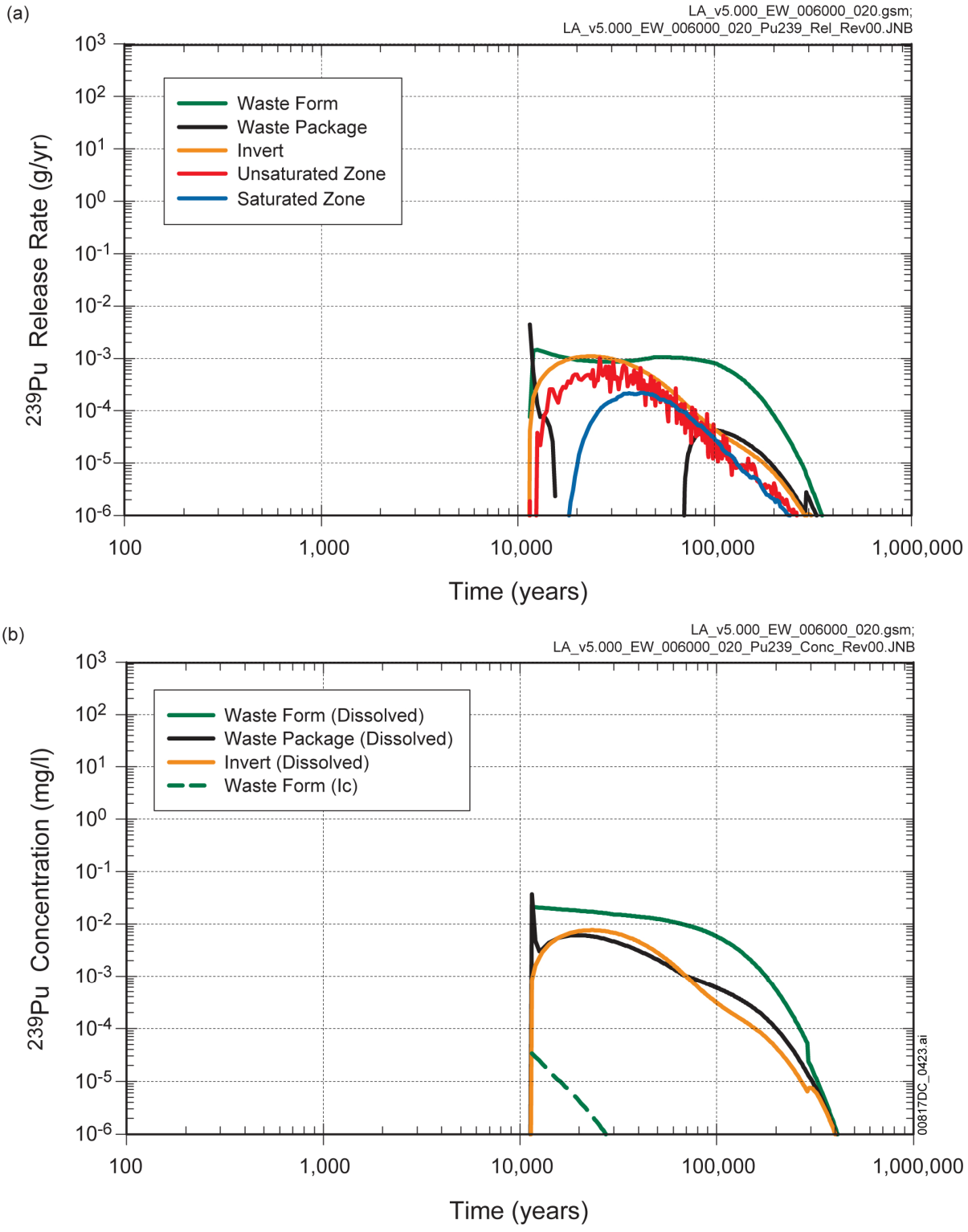

Source: Output DTN: MO0708TSPAVALI.000 [DIRS 182985].

Figure 7.7.1-6. (a) Release Rates and (b) Concentration of ^{239}Pu for Realization 5608 of the Waste Package Early Failure Modeling Case for the 1,000,000-Year Simulation after Repository Closure

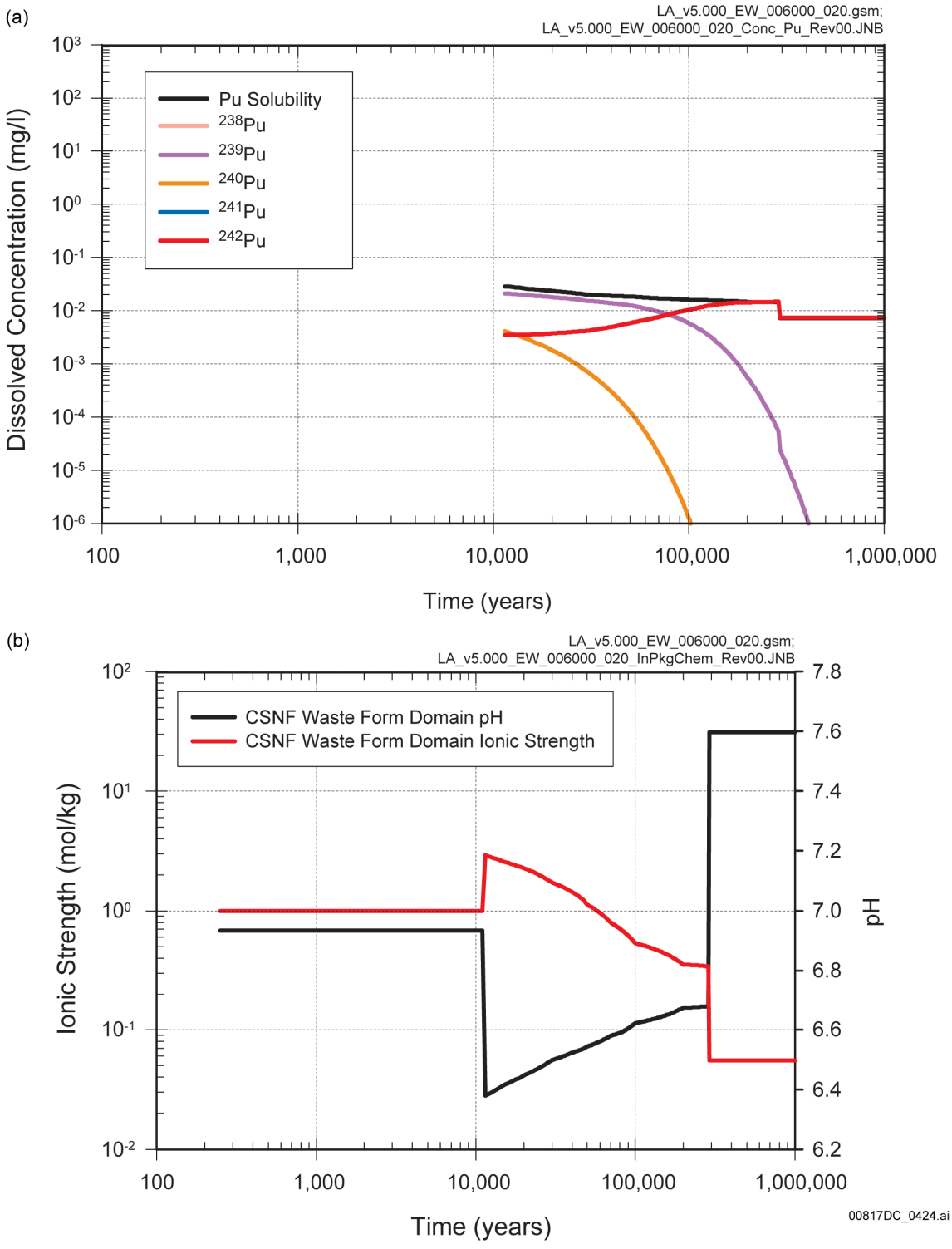

Source: Output DTN: MO0708TSPAVALI.000 [DIRS 182985].

Figure 7.7.1-7. (a) Dissolved Concentrations of Plutonium in the CSNF Waste Form Domain for Realization 5608 and (b) CSNF Waste Form Domain Chemistry for Realization 5608 of the Waste Package Early Failure Modeling Case for the 1,000,000-Year Simulation after Repository Closure

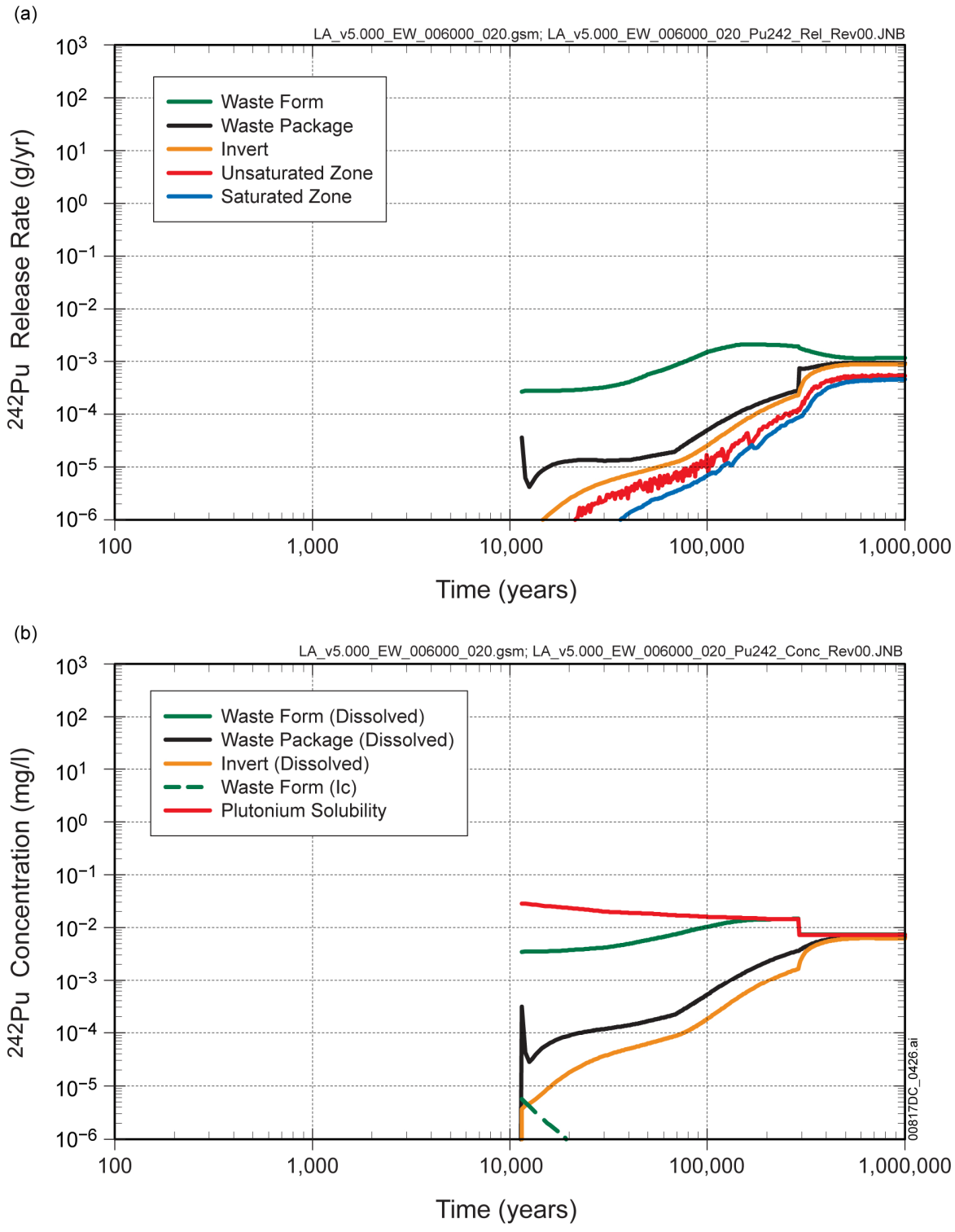

Source: Output DTN: MO0708TSPAVALI.000 [DIRS 182985].

Figure 7.7.1-8. (a) Release Rates and (b) Concentration of ^{242}Pu for Realization 5608 of the Waste Package Early Failure Modeling Case for the 1,000,000-Year Simulation after Repository Closure

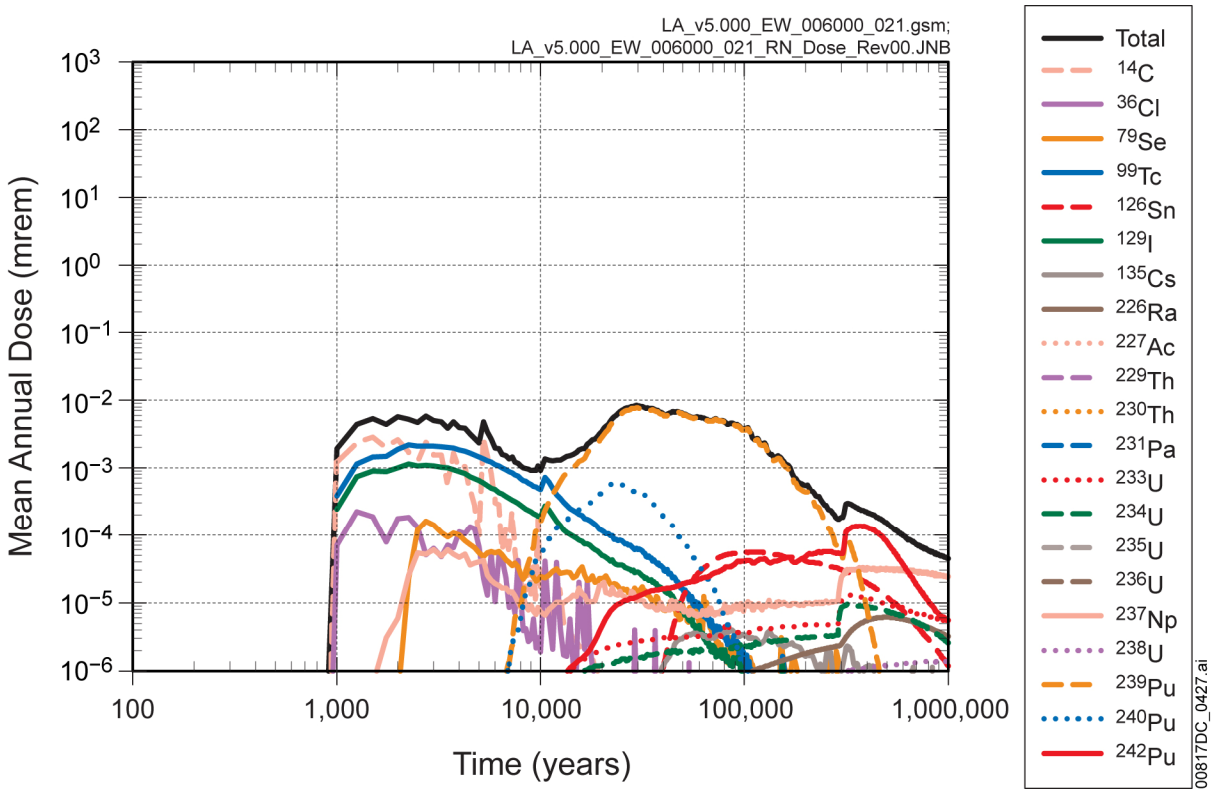

Source: Output DTN: MO0708TSPAVALI.000 [DIRS 182985].

NOTES: ^{226}Ra dose is the sum of ^{226}Ra and ^{210}Pb doses (secular equilibrium assumed).

Figure 7.7.1-9. Major Radionuclide Contributors to Mean Annual Dose for Realization 5618 of the Waste Package Early Failure Modeling Case for the 1,000,000-Year Simulation after Repository Closure

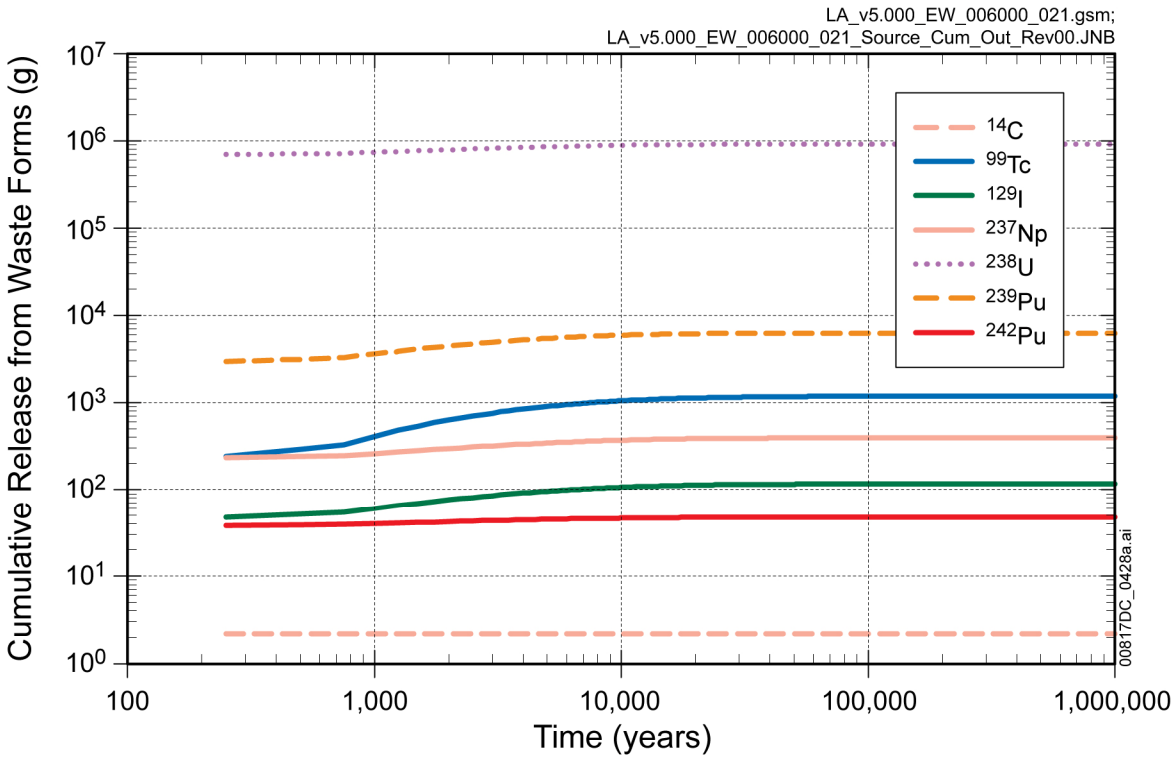

Source: Output DTN: MO0708TSPAVALI.000 [DIRS 182985].

Figure 7.7.1-10. Cumulative Release from HLW and DSNF Waste Forms for Realization 5618 of the Waste Package Early Failure Modeling Case for the 1,000,000-Year Simulation after Repository Closure

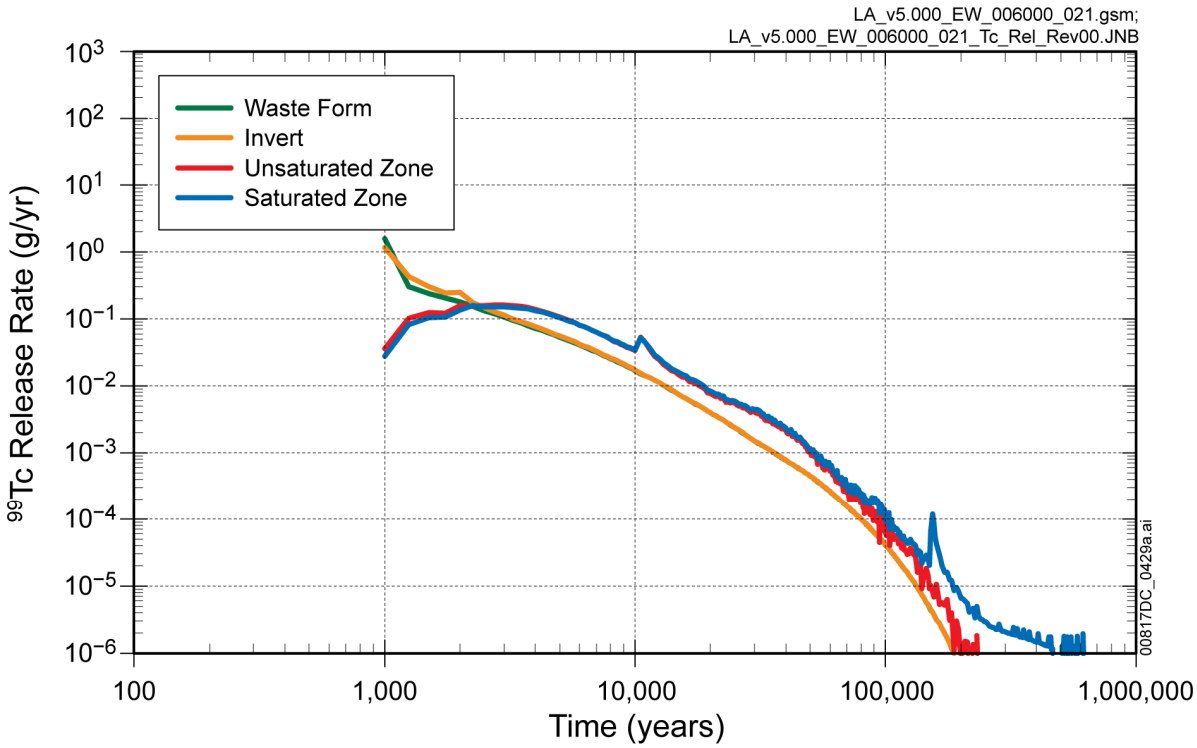

Source: Output DTN: MO0708TSPAVALI.000 [DIRS 182985].

Figure 7.7.1-11. Release Rates of ^{99}Tc from the Waste Form, EBS, Unsaturated Zone, and Saturated Zone for Realization 5618 of the Waste Package Early Failure Modeling Case for the 1,000,000-Year Simulation after Repository Closure

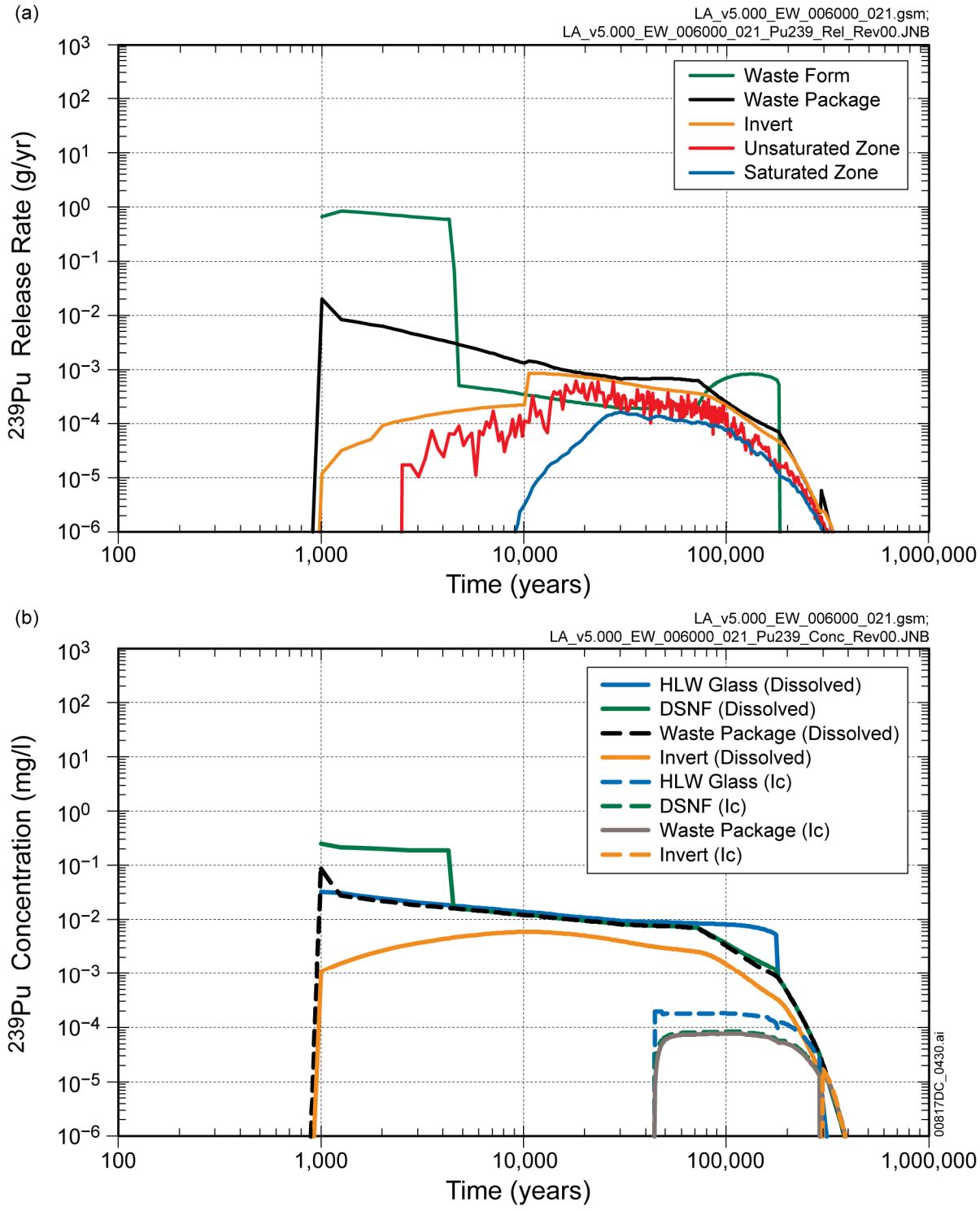

Source: Output DTN: MO0708TSPAVALI.000 [DIRS 182985].

Figure 7.7.1-12. (a) Release Rates and (b) Concentration of ^{239}Pu for Realization 5618 of the Waste Package Early Failure Modeling Case for the 1,000,000-Year Simulation after Repository Closure

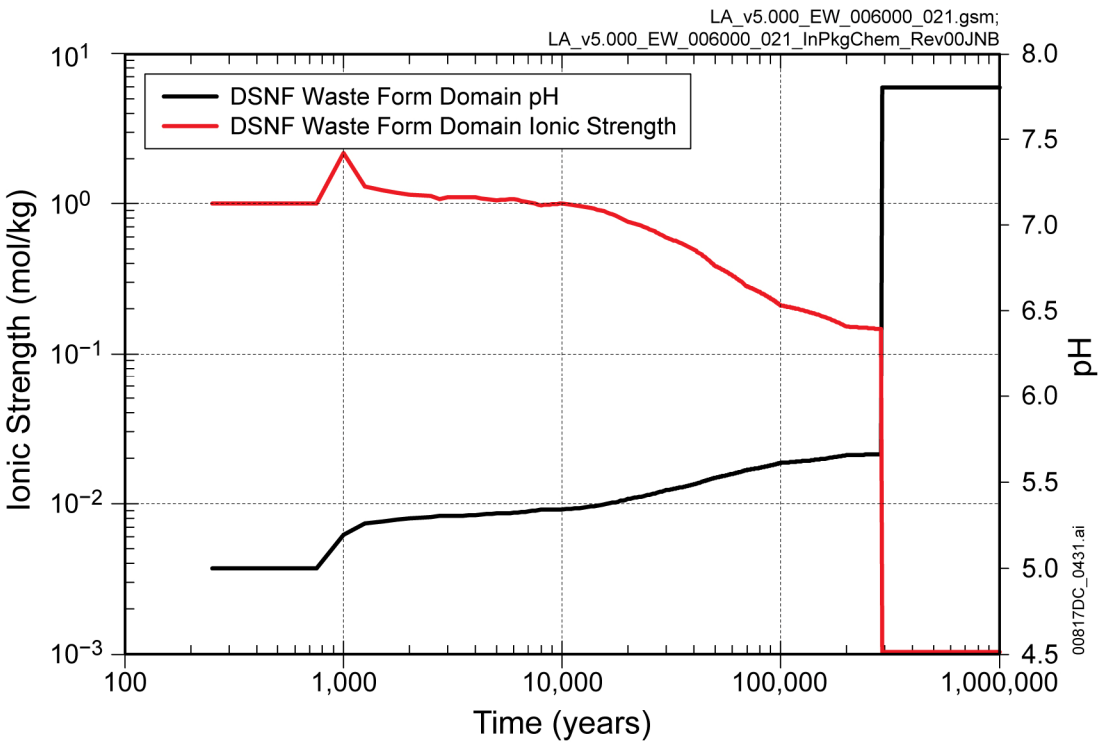

Source: Output DTN: MO0708TSPAVALI.000 [DIRS 182985].

Figure 7.7.1-13. DSNF Waste Form Domain Chemistry for Realization 5618 of the Waste Package Early Failure Modeling Case for the 1,000,000-Year Simulation after Repository Closure

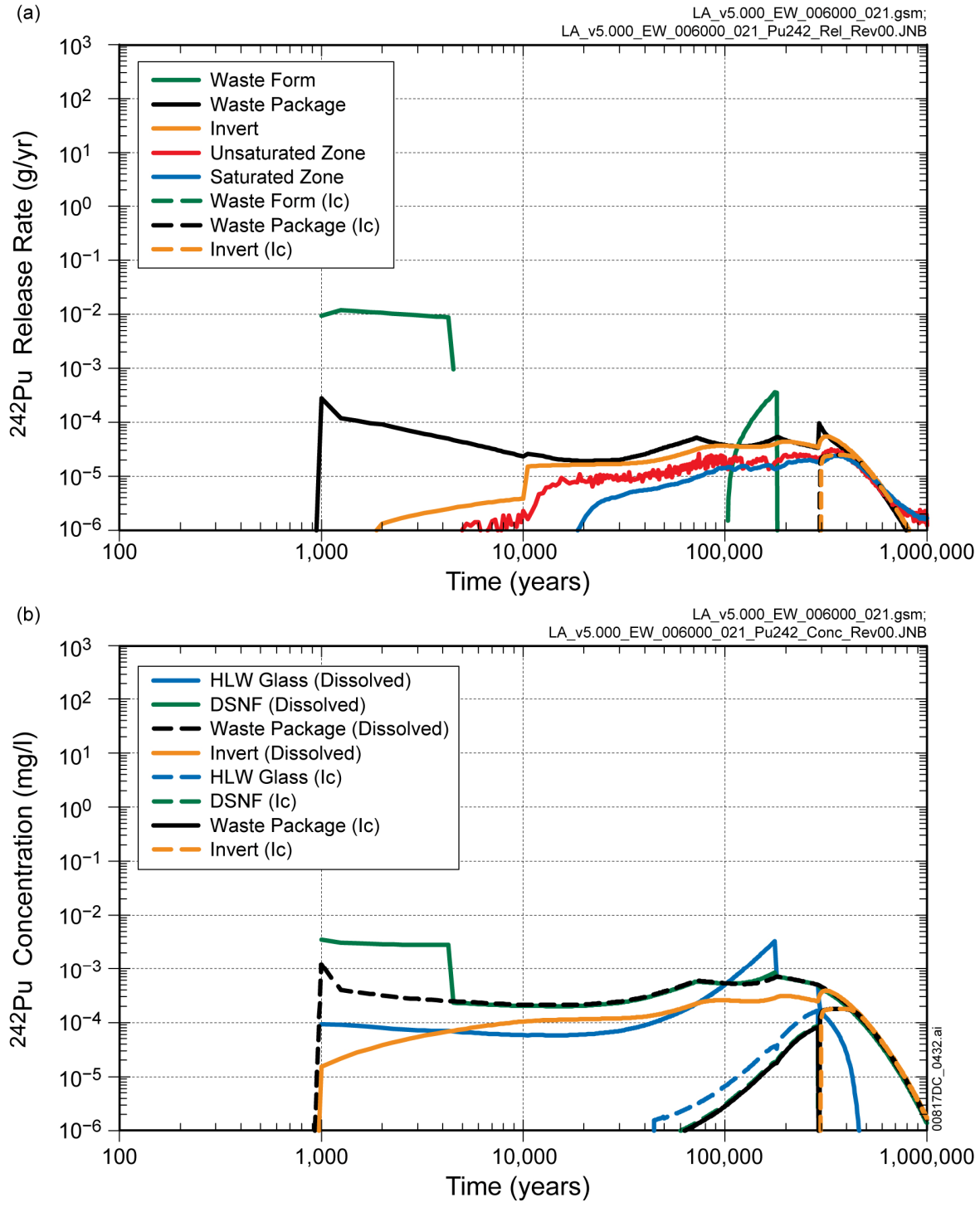

Source: Output DTN: MO0708TSPAVALI.000 [DIRS 182985].

Figure 7.7.1-14. (a) Release Rates and (b) Concentration of ^{242}Pu for Realization 5618 of the Waste Package Early Failure Modeling Case for the 1,000,000-Year Simulation after Repository Closure

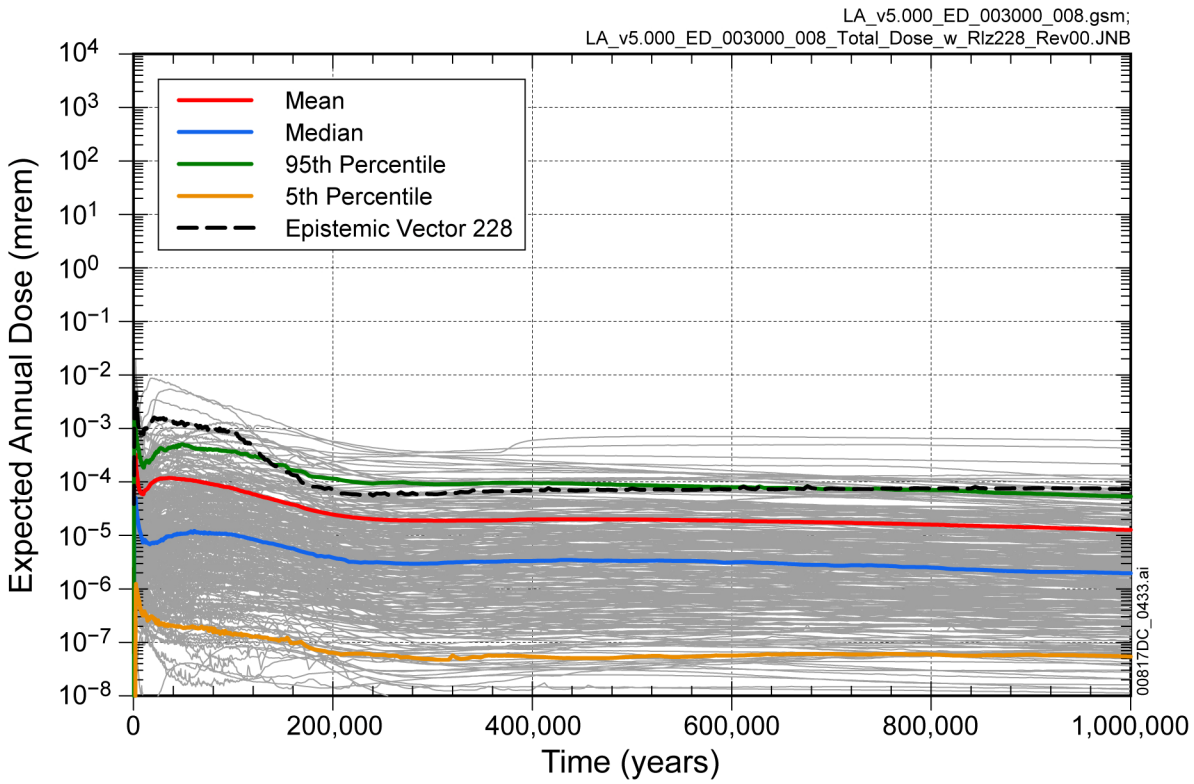

Source: Output DTN: MO0709TSPAREGS.000 [DIRS 182976].

NOTES: ^{226}Ra dose is the sum of ^{226}Ra and ^{210}Pb doses (secular equilibrium assumed).

Figure 7.7.1-15. Comparison of Expected Annual Dose for all Realizations along with that from Realization 228 (Epistemic Uncertainty Vector) of the Drip Shield Early Failure Modeling Case for the 1,000,000-Year Simulation after Repository Closure

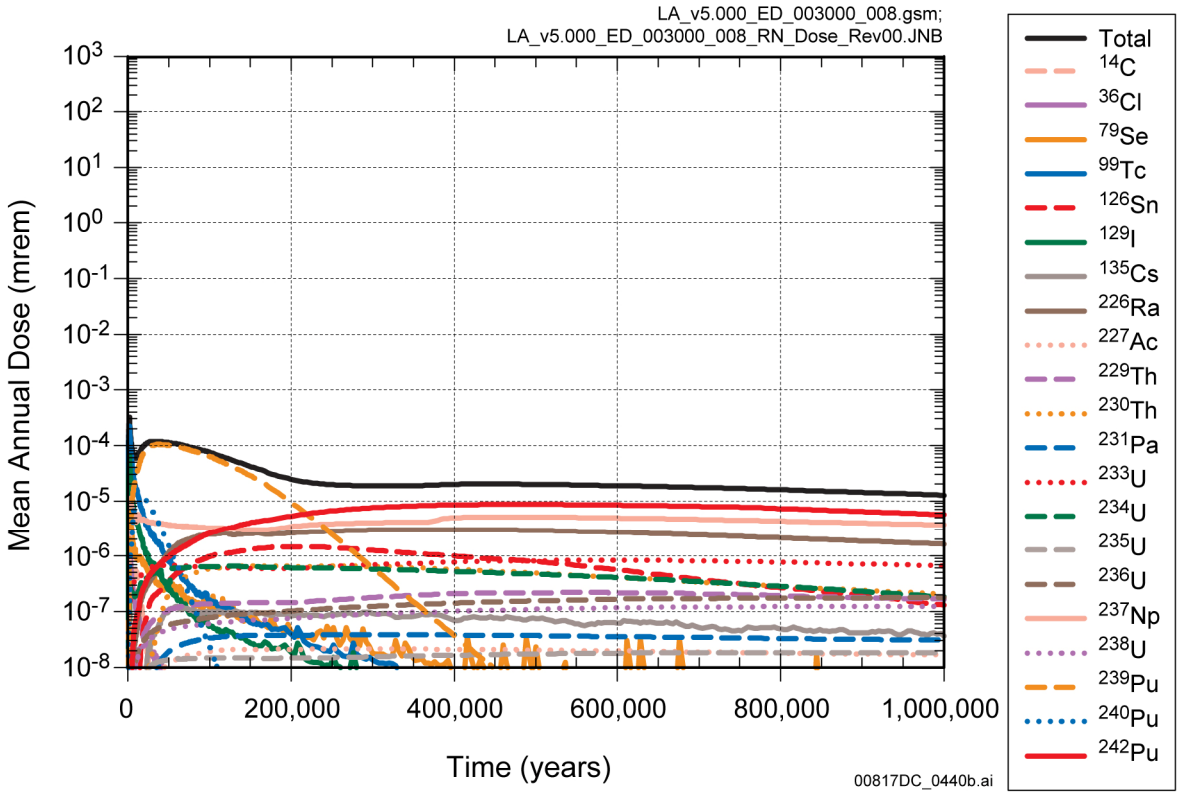

Source: Output DTN: MO0709TSPAREGS.000 [DIRS 182976].

NOTES: ^{226}Ra dose is the sum of ^{226}Ra and ^{210}Pb doses (secular equilibrium assumed).

Figure 7.7.1-16. Major Radionuclide Contributors to Mean Annual Dose for the Drip Shield Early Failure Modeling Case for the 1,000,000-Year Simulation after Repository Closure

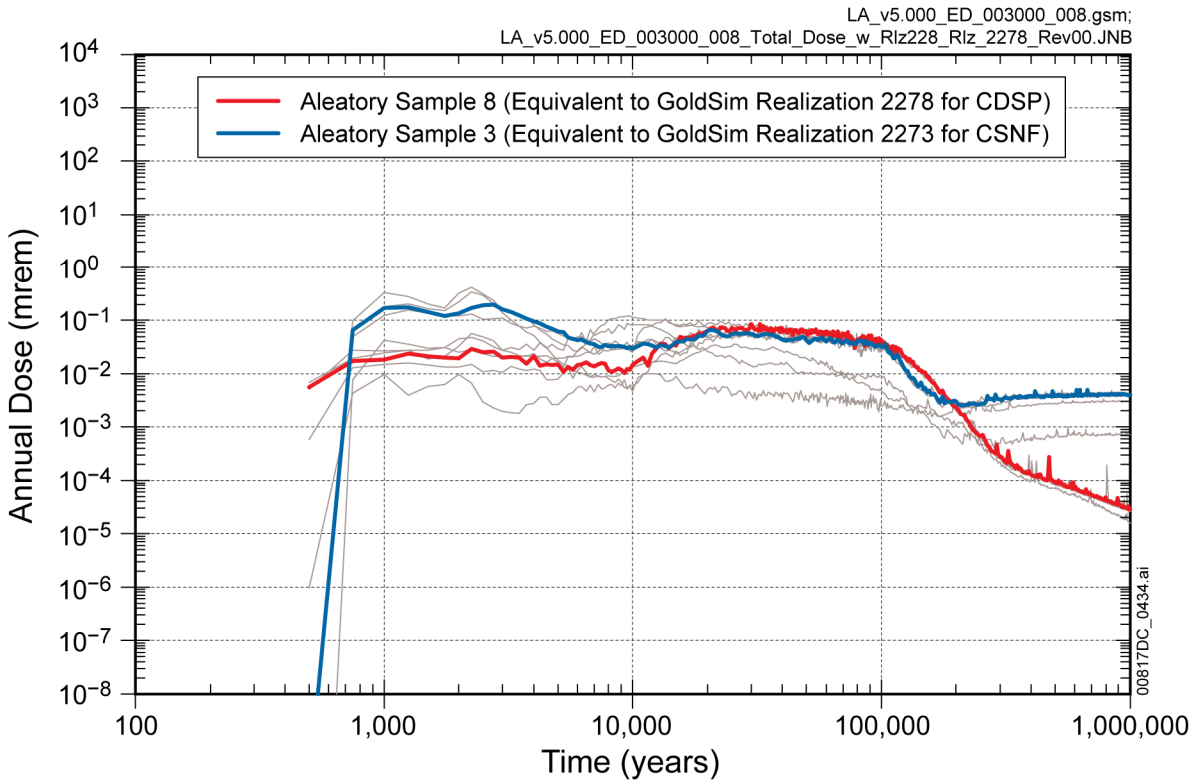

Source: Output DTN: MO0709TSPAREGS.000 [DIRS 182976].

Figure 7.7.1-17. Annual Dose for Ten Aleatory Uncertainty Realizations (vectors) for the Epistemic Uncertainty Realization 228 of the Drip Shield Early Failure Modeling Case for the 1,000,000-Year Simulation after Repository Closure

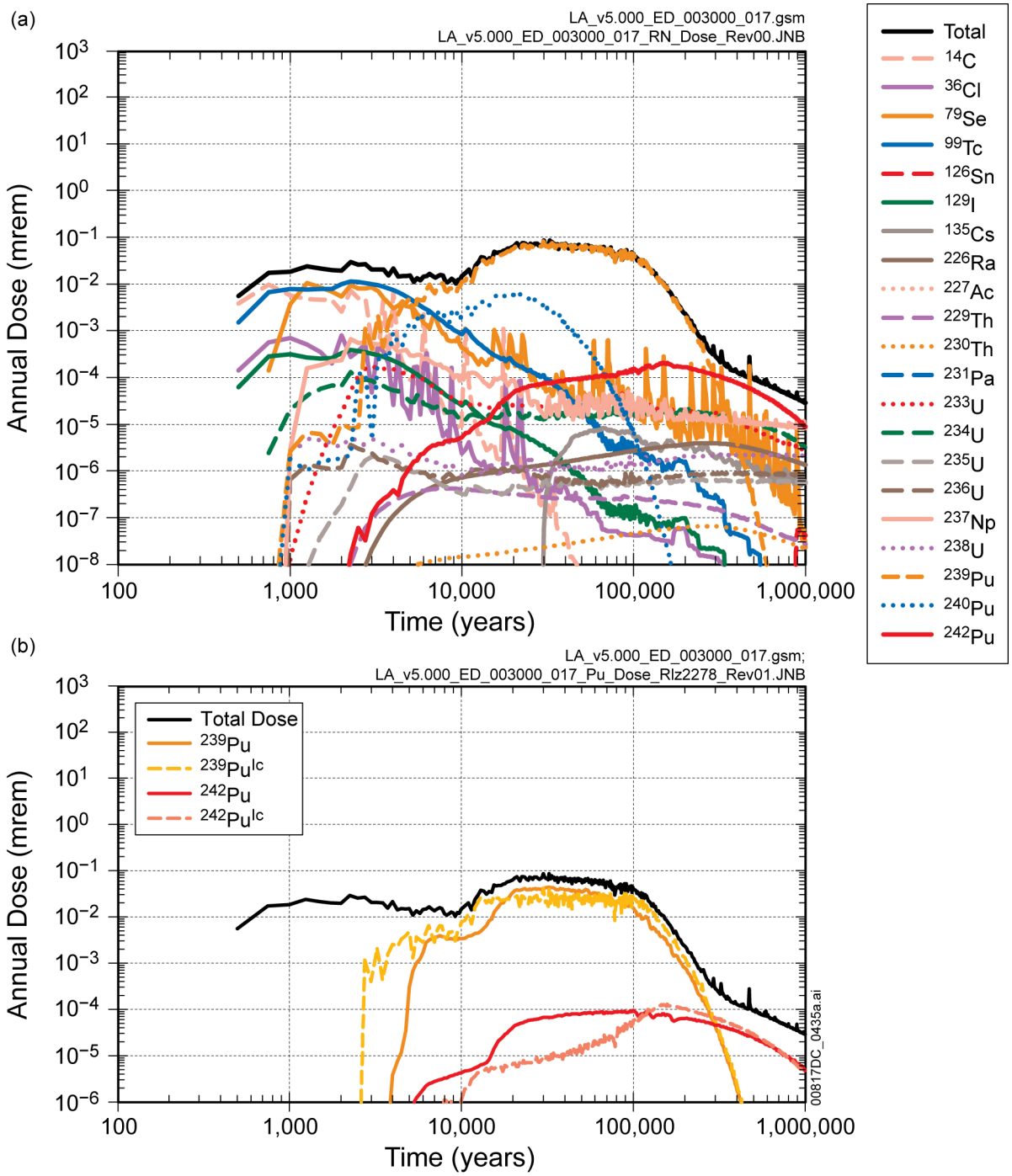

Source: Output DTN: MO0708TSPAVALI.000 [DIRS 182985].

NOTES: ^{226}Ra dose is the sum of ^{226}Ra and ^{210}Pb doses (secular equilibrium assumed).

Figure 7.7.1-18. (a) Annual Dose along with Major Radionuclide Dose Contributors and (b) Contribution of Dissolved ^{239}Pu and ^{242}Pu and that Associated Irreversibly with Colloids (Denoted by Superscript Ic) for Realization 2278 of the Drip Shield Early Failure Modeling Case for the 1,000,000-Year Simulation after Repository Closure

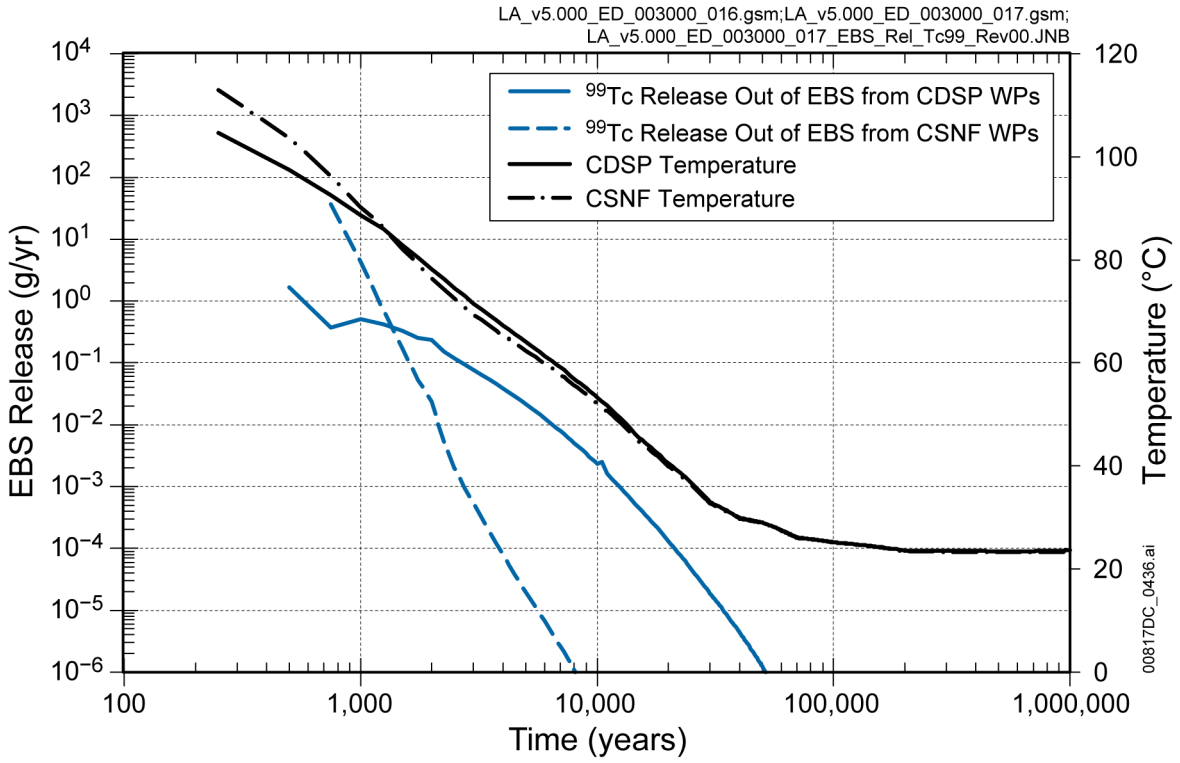

Source: Output DTN: MO0708TSPAVALI.000 [DIRS 182985].

Figure 7.7.1-19. EBS Release Rates of ^{99}Tc Along with Waste Package Temperatures for the Two Selected Realizations of Drip Shield Early Failure Modeling Case for the 1,000,000-Year Simulation after Repository Closure

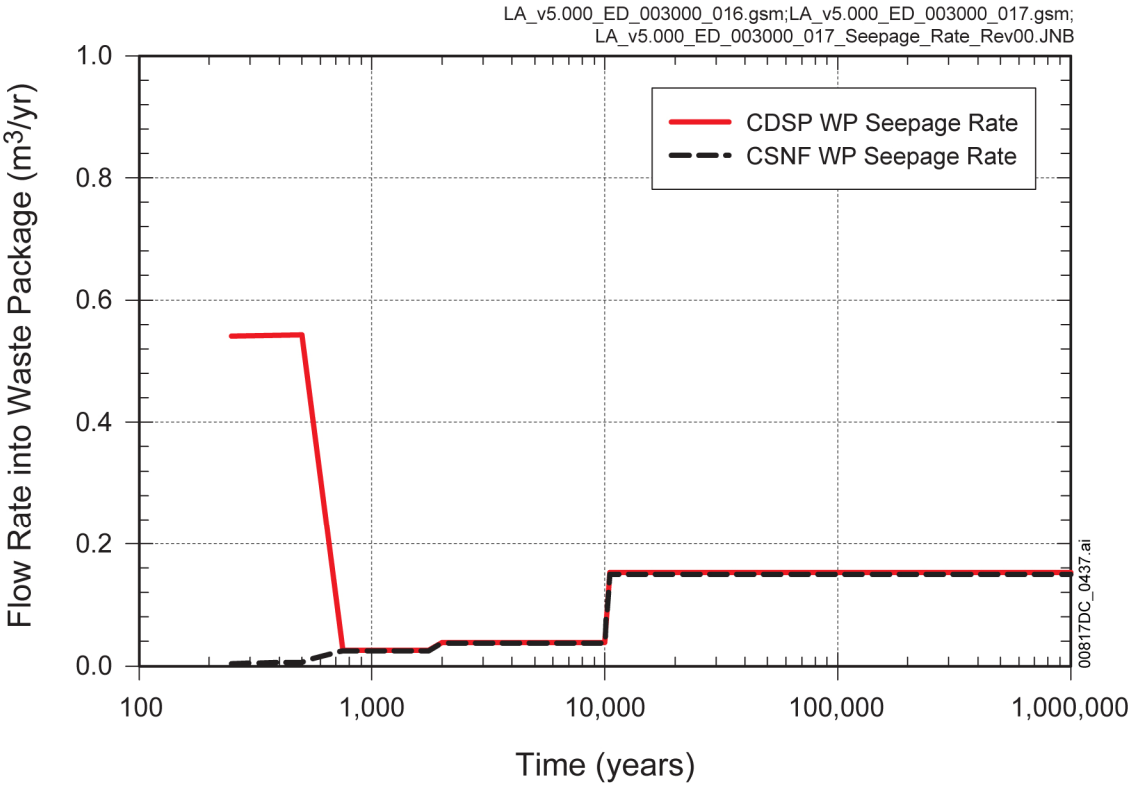

Source: Output DTN: MO0708TSPAVALI.000 [DIRS 182985].

Figure 7.7.1-20. Seepage Rate Incident on the Waste Package Showing the Effects of Drift Wall Condensation and Climate Change for the Two Selected Realizations of the Drip Shield Early Failure Modeling Case for the 1,000,000-Year Simulation after Repository Closure

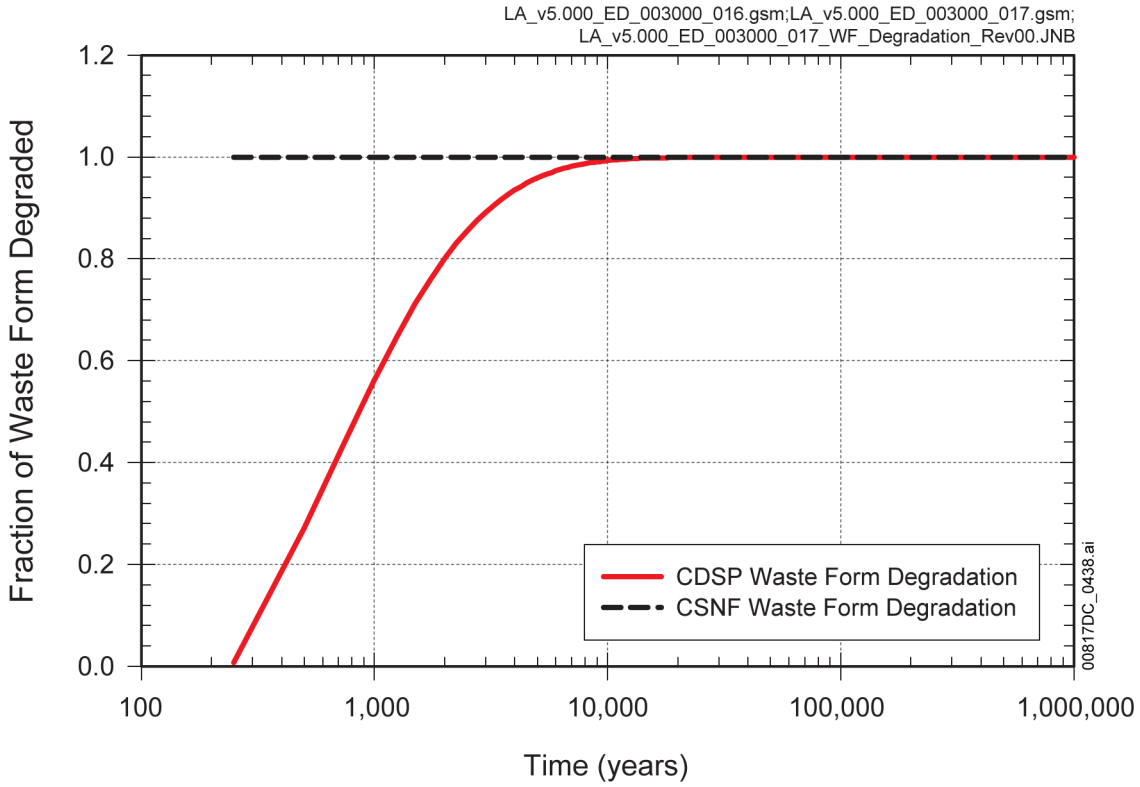

Source: Output DTN: MO0708TSPAVALI.000 [DIRS 182985].

Figure 7.7.1-21. Fraction of CSNF and CDSP Waste Form Degraded for the Two Selected Realizations of the Drip Shield Early Failure Modeling Case for the 1,000,000-Year Simulation after Repository Closure

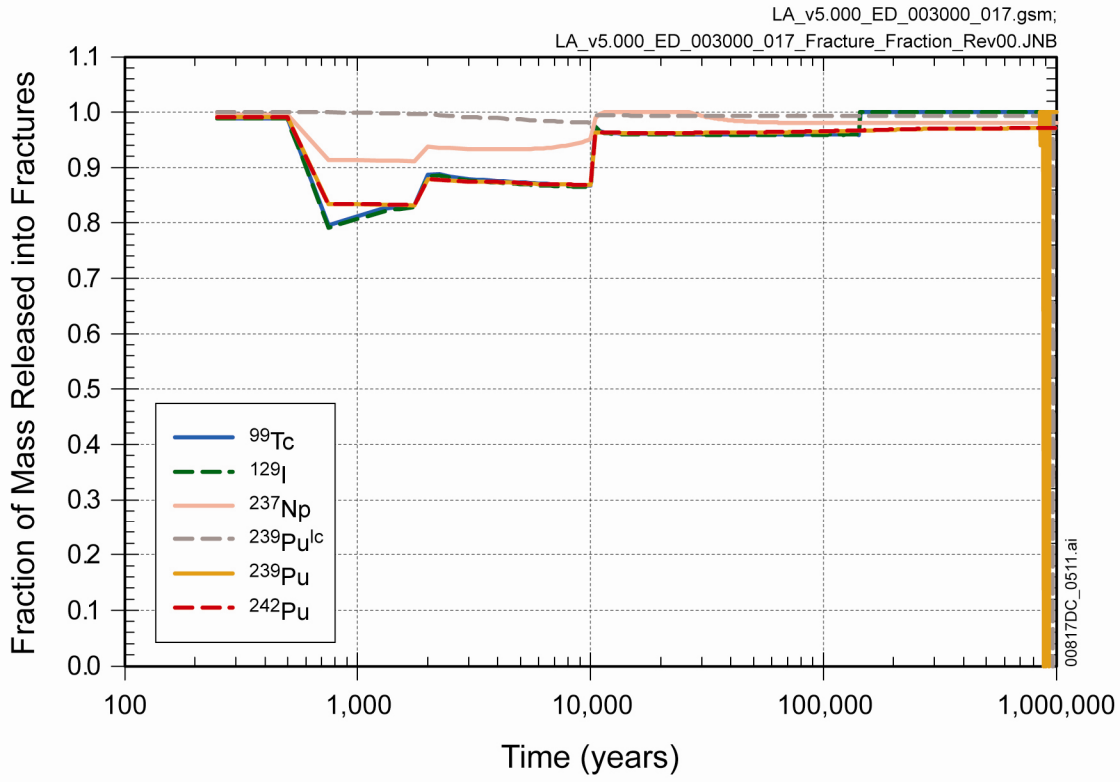

Source: Output DTN: MO0708TSPAVALI.000 [DIRS 182985].

NOTES: The GoldSim realization 2278 represents a CDSP WP in percolation subregion 3.

Figure 7.7.1-22. Fraction of EBS Mass Flux Released into Unsaturated Zone Fractures for Selected Radionuclides for Realization 2278 of the Drip Shield Early Failure Modeling Case for the 1,000,000-Year Simulation after Repository Closure

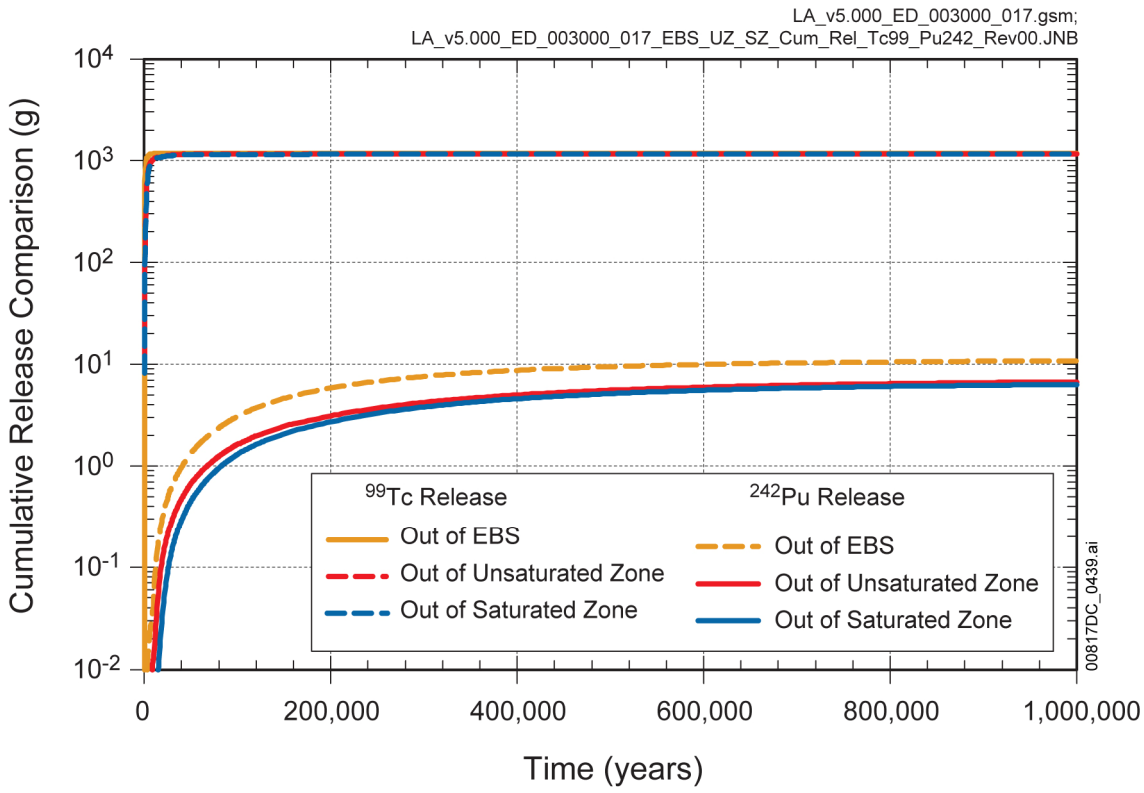

Source: Output DTN: MO0708TSPAVALI.000 [DIRS 182985].

Figure 7.7.1-23. Cumulative Mass Release of ^{99}Tc and ^{242}Pu from the EBS, Unsaturated Zone, and Saturated Zone for Realization 2278 of the Drip Shield Early Failure Modeling Case for the 1,000,000-Year Simulation after Repository Closure

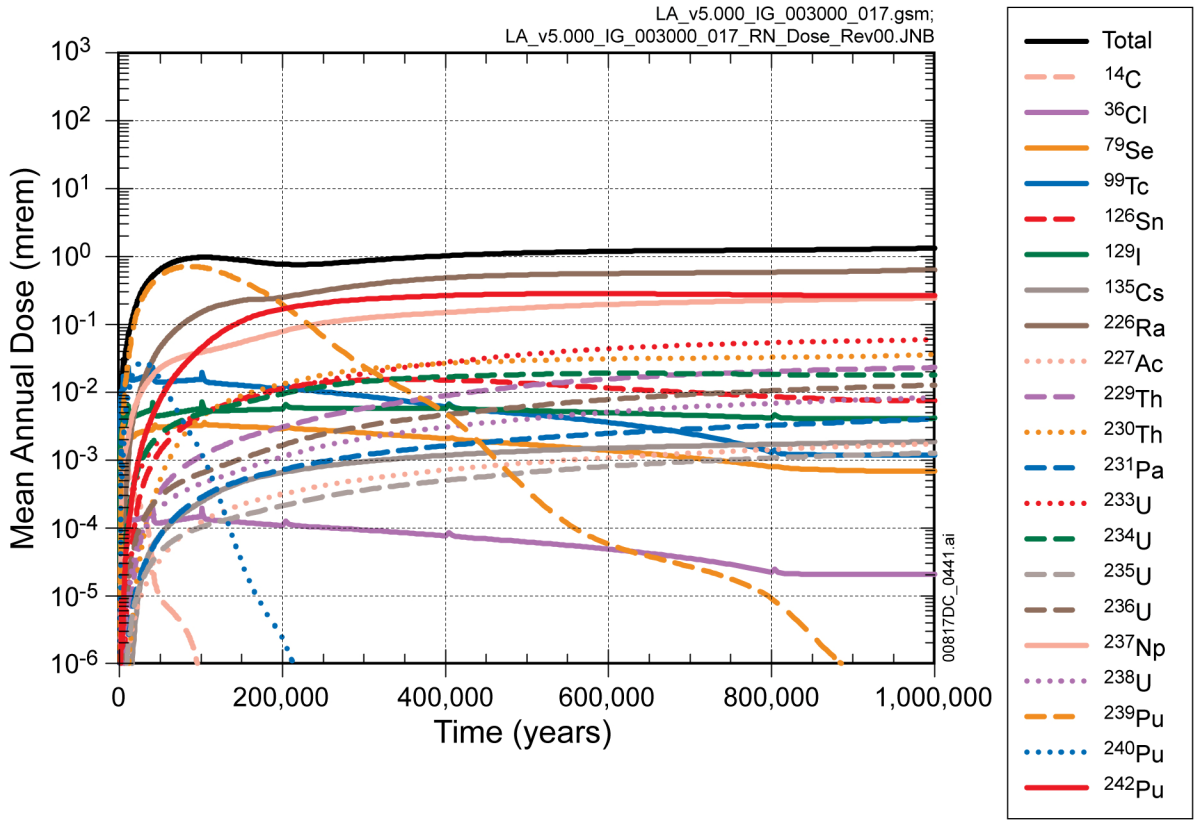

Source: Output DTN: MO0709TSPAREGS.000 [DIRS 182976].

NOTES: ^{226}Ra dose is the sum of ^{226}Ra and ^{210}Pb doses (secular equilibrium assumed).

Figure 7.7.1-24. Major Radionuclide Contributors to Mean Annual Dose for the Igneous Intrusion Modeling Case for the 1,000,000-Year Simulation after Repository Closure

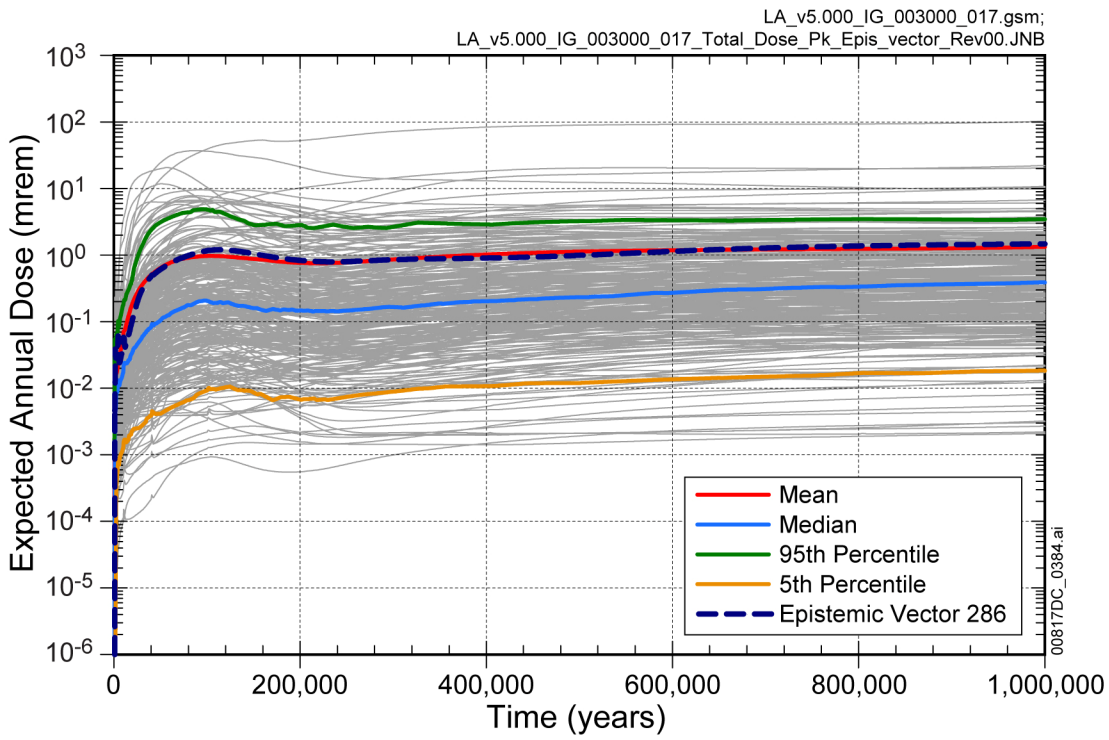

Source: Output DTN: MO0709TSPAREGS.000 [DIRS 182976].

NOTES: ^{226}Ra dose is the sum of ^{226}Ra and ^{210}Pb doses (secular equilibrium assumed).

Figure 7.7.1-25. Expected Annual Dose from the 300 Epistemic Vectors Along with their Quantiles and Expected Dose from Epistemic Uncertainty Vector #286 for the Igneous Intrusion Modeling Case for the 1,000,000-Year Simulation after Repository Closure

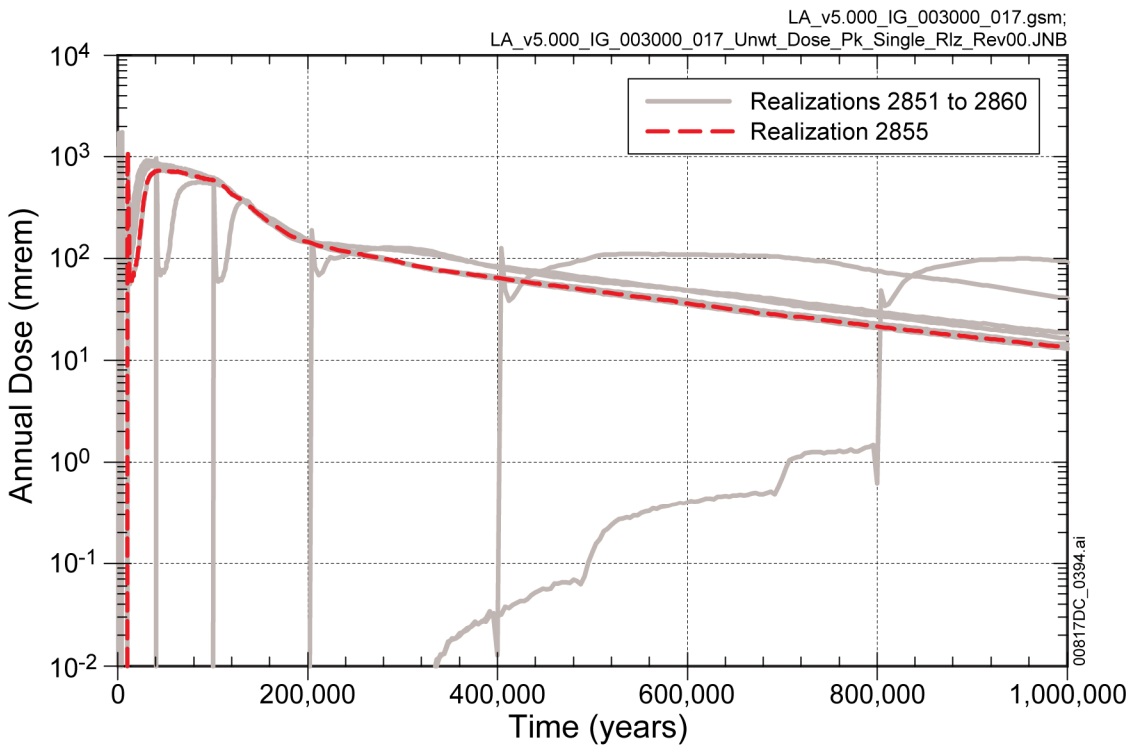

Source: Output DTN: MO0709TSPAREGS.000 [DIRS 182976].

Figure 7.7.1-26. Annual Dose for Realizations 2851 through 2860 (representing Epistemic Uncertainty Vector 286) along with Selected Realization 2855 of the Igneous Intrusion Modeling Case for the 1,000,000-Year Simulation after Repository Closure

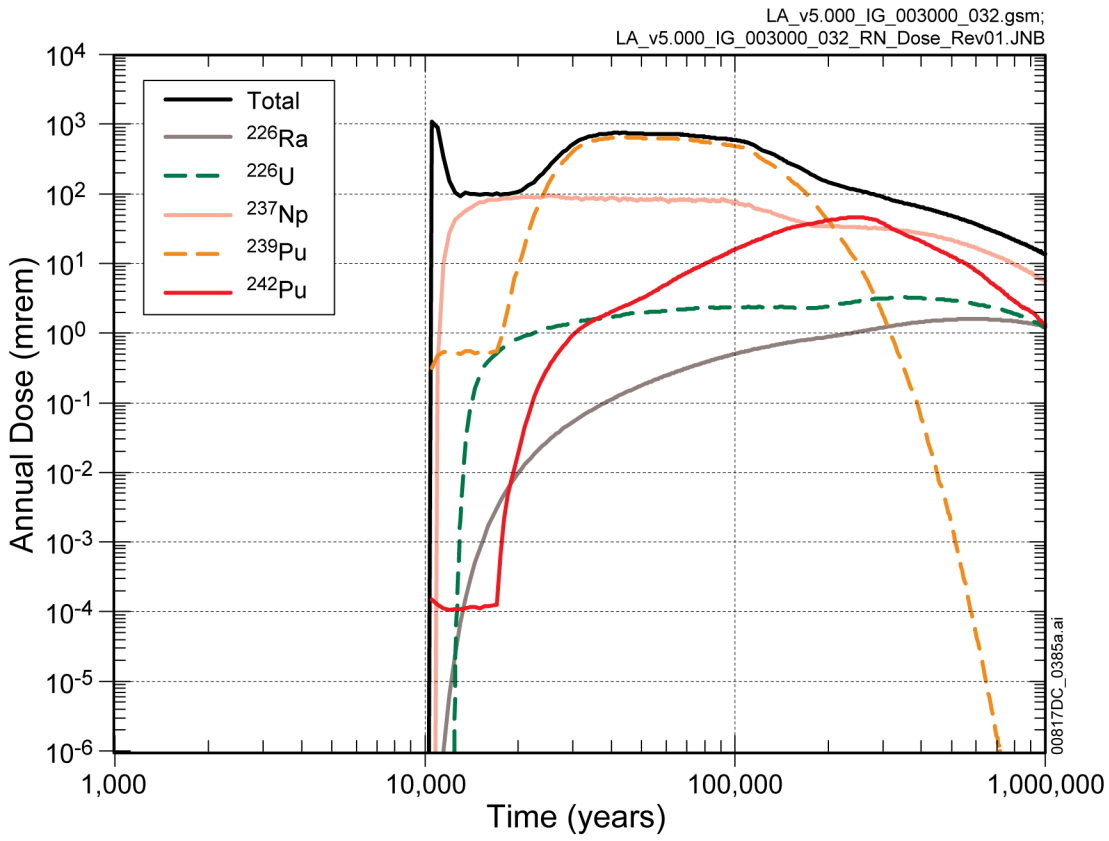

Source: Output DTN: MO0708TSPAVALI.000 [DIRS 182985].

NOTES: ^{226}Ra dose is the sum of ^{226}Ra and ^{210}Pb doses (secular equilibrium assumed).

Figure 7.7.1-27. Annual Dose along with Major Radionuclide Dose Contributors for Realization 2855 of the Igneous Intrusion Modeling Case for the 1,000,000-Year Simulation after Repository Closure

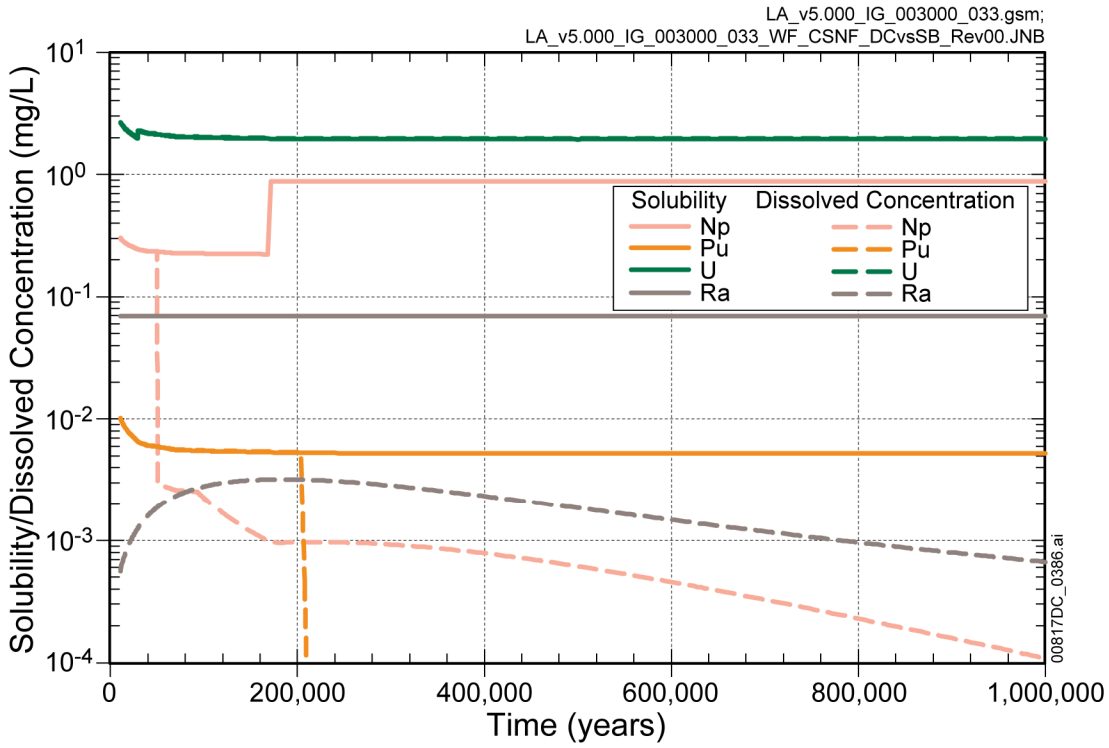

Source: Output DTN: MO0708TSPAVALI.000 [DIRS 182985].

Figure 7.7.1-28. Dissolved Concentrations and Solubility Limits of Neptunium, Plutonium, Uranium, and Radium in the CSNF Waste Form Domain for Percolation Subregion 3 Dripping Environment for Realization 2855 of the Igneous Intrusion Modeling Case for the 1,000,000-Year Simulation after Repository Closure

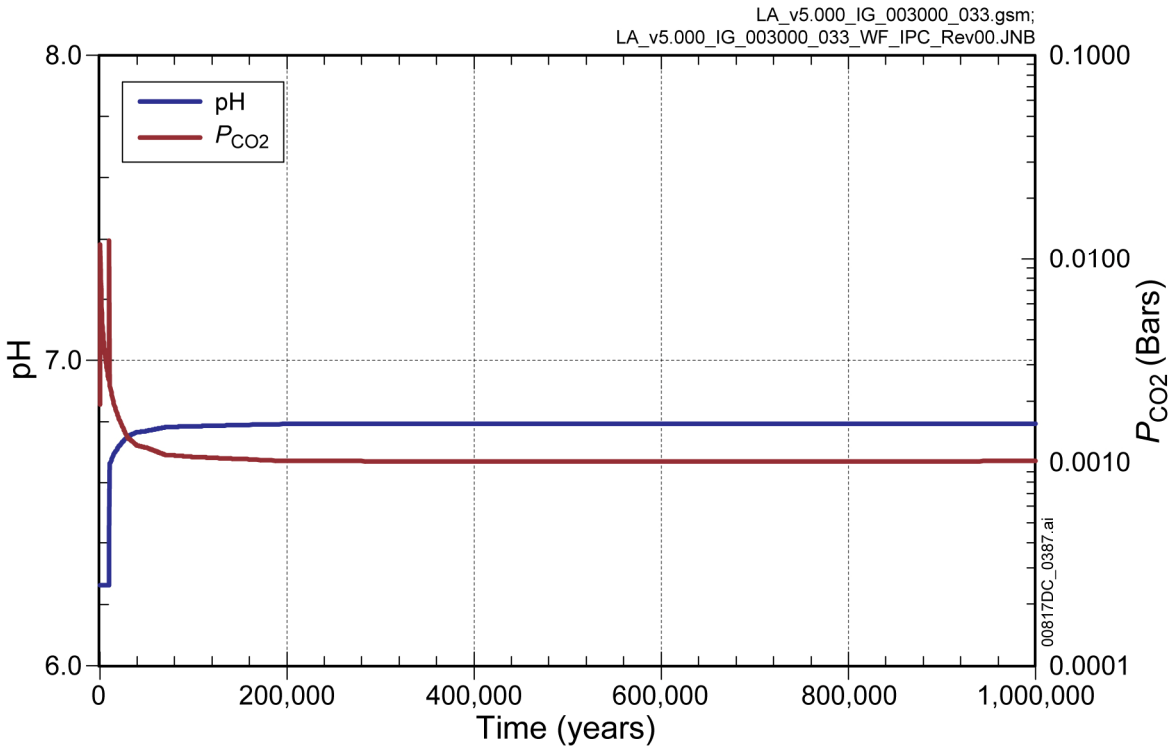

Source: Output DTN: MO0708TSPAVALI.000 [DIRS 182985].

Figure 7.7.1-29. In-Package pH and P_{CO2} in the Waste Form Domain for Percolation Subregion 3 Dripping Environment for Realization 2855 of the Igneous Intrusion Modeling Case for the 1,000,000-Year Simulation after Repository Closure

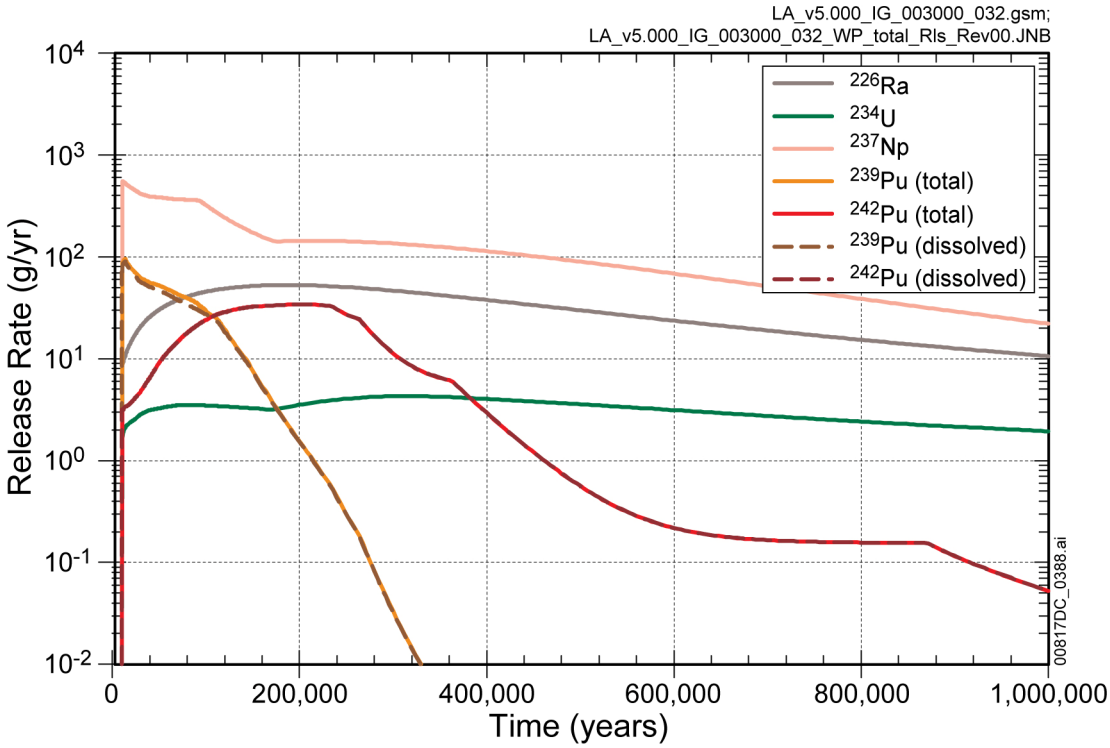

Source: Output DTN: MO0708TSPAVALI.000 [DIRS 182985].

Figure 7.7.1-30. Release Rate of Major Radionuclides from all WPs for Realization 2855 of the Igneous Intrusion Modeling Case for the 1,000,000-Year Simulation after Repository Closure

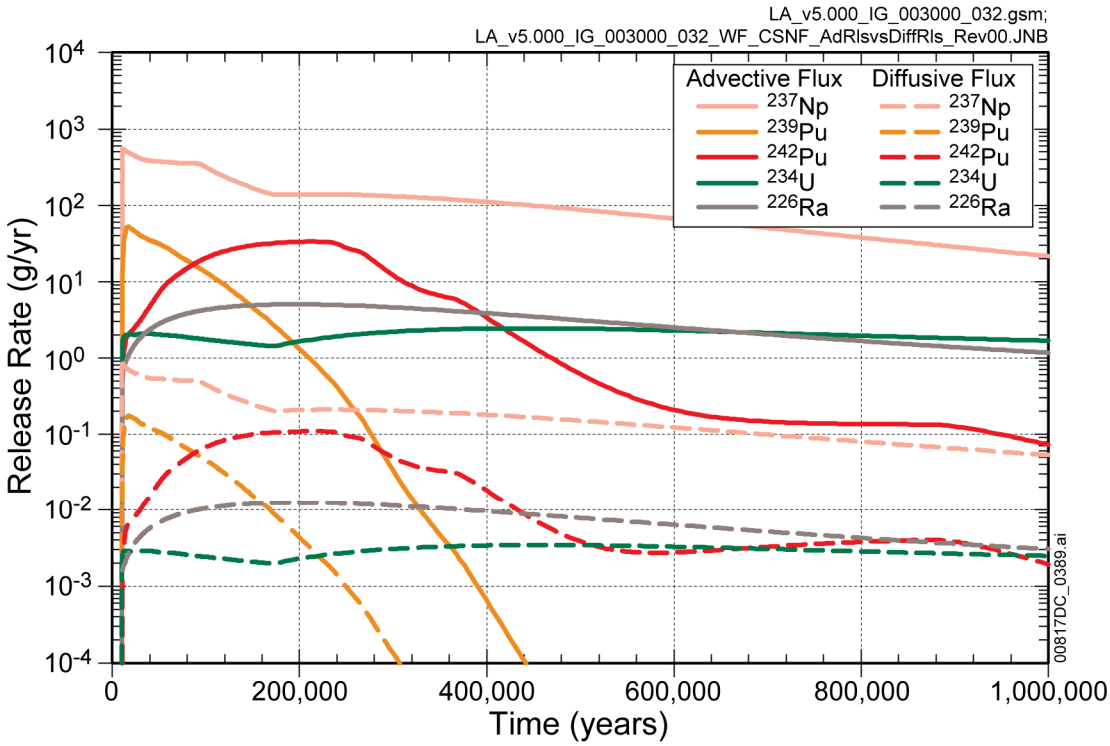

Source: Output DTN: MO0708TSPAVALI.000 [DIRS 182985].

Figure 7.7.1-31. Advective and Diffusive Release Rates of Major Radionuclides from the CSNF WPs for Realization 2855 of the Igneous Intrusion Modeling Case for the 1,000,000-Year Simulation after Repository Closure

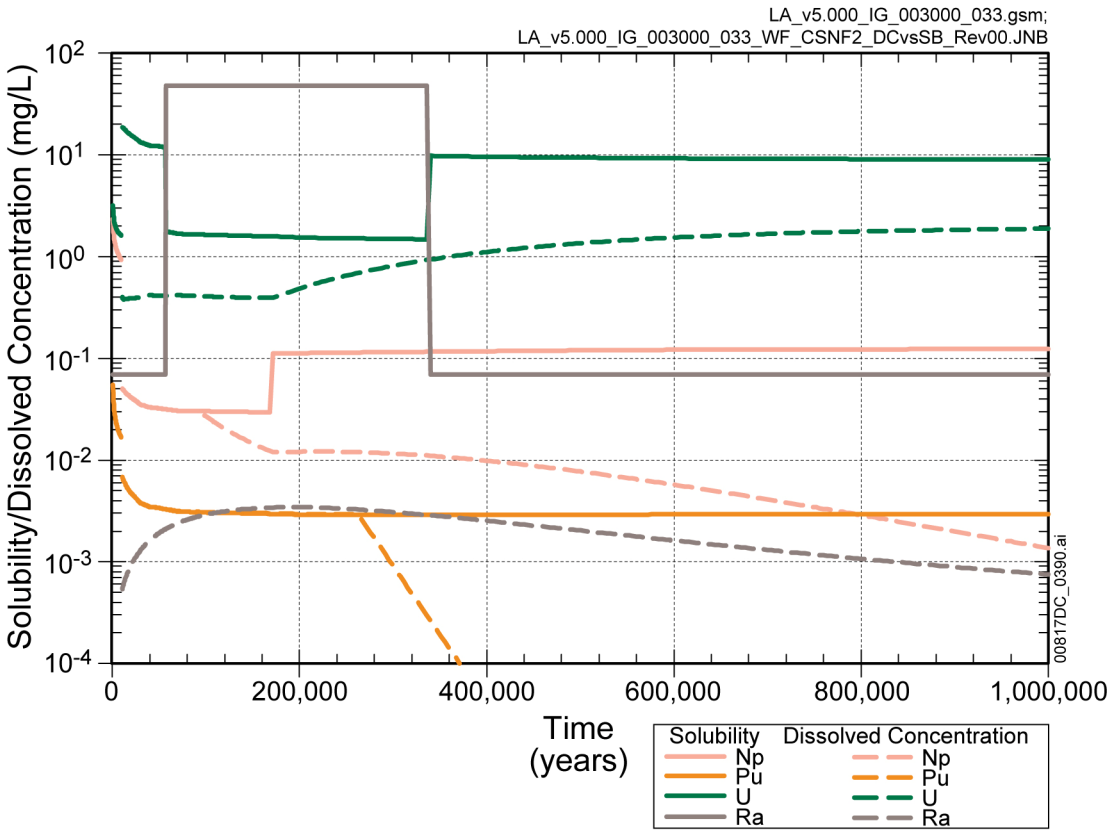

Source: Output DTN: MO0708TSPAVALI.000 [DIRS 182985].

Figure 7.7.1-32. Total Dissolved Concentrations and Solubility Limits of Neptunium, Plutonium, Uranium, and Radium in the Corrosion Products Domain of CSNF WP Located in Percolation Subregion 3 Dripping Environment for Realization 2855 of the Igneous Intrusion Modeling Case for the 1,000,000-Year Simulation after Repository Closure

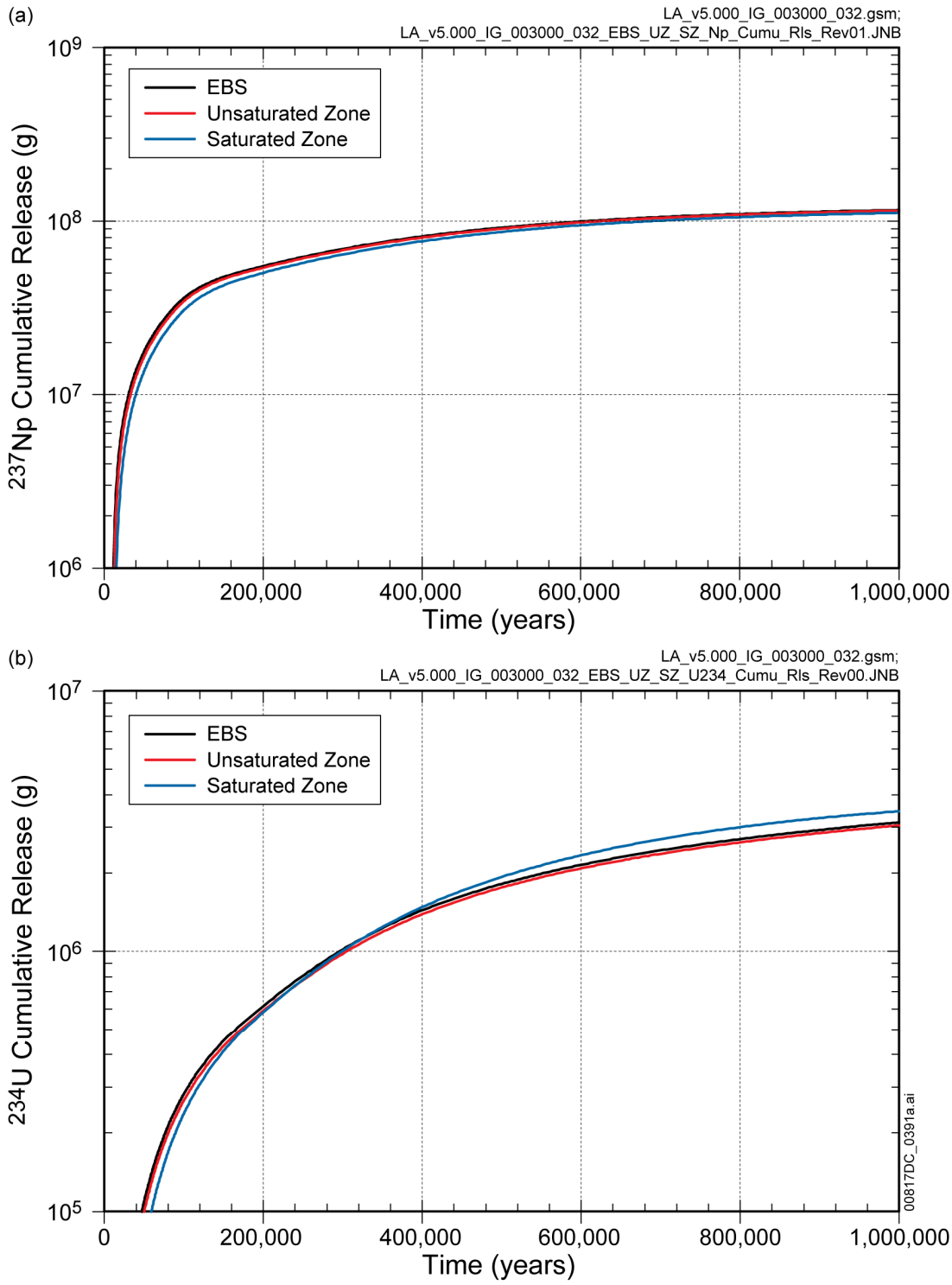

Source: Output DTN: MO0708TSPAVALI.000 [DIRS 182985].

Figure 7.7.1-33. Cumulative Releases of: (a) ^{237}Np, (b) ^{234}U, (c) ^{242}Pu, and (d) ^{226}Ra from the EBS, Unsaturated Zone, and Saturated Zone for Realization 2855 of the Igneous Intrusion Modeling Case for the 1,000,000-Year Simulation after Repository Closure

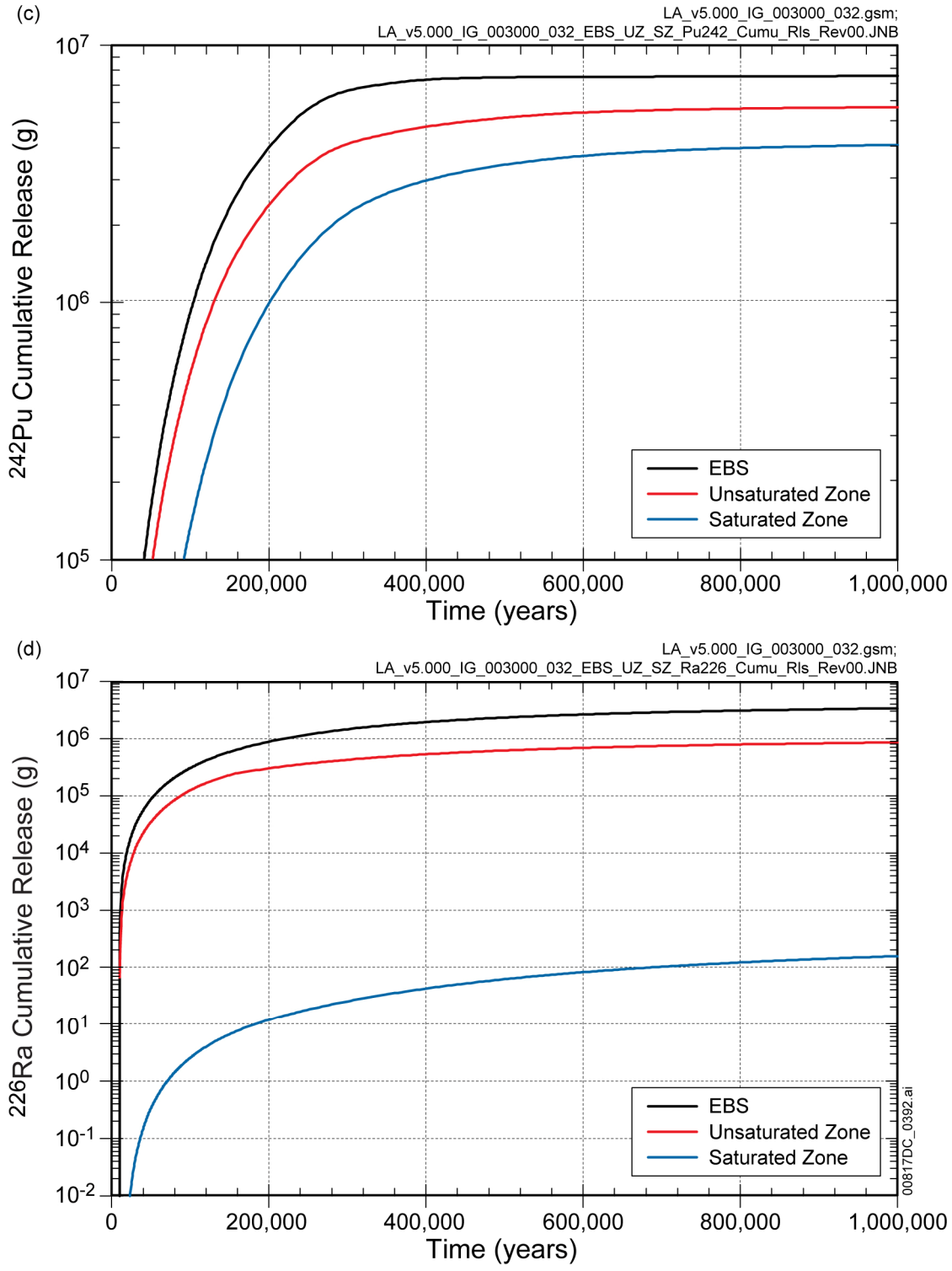

Source: Output DTN: MO0708TSPAVALI.000 [DIRS 182985].

Figure 7.7.1-33. Cumulative Releases of: (a) ^{237}Np, (b) ^{234}U, (c) ^{242}Pu, and (d) ^{226}Ra from the EBS, Unsaturated Zone, and Saturated Zone for Realization 2855 of the Igneous Intrusion Modeling Case for the 1,000,000-Year Simulation after Repository Closure (Continued)

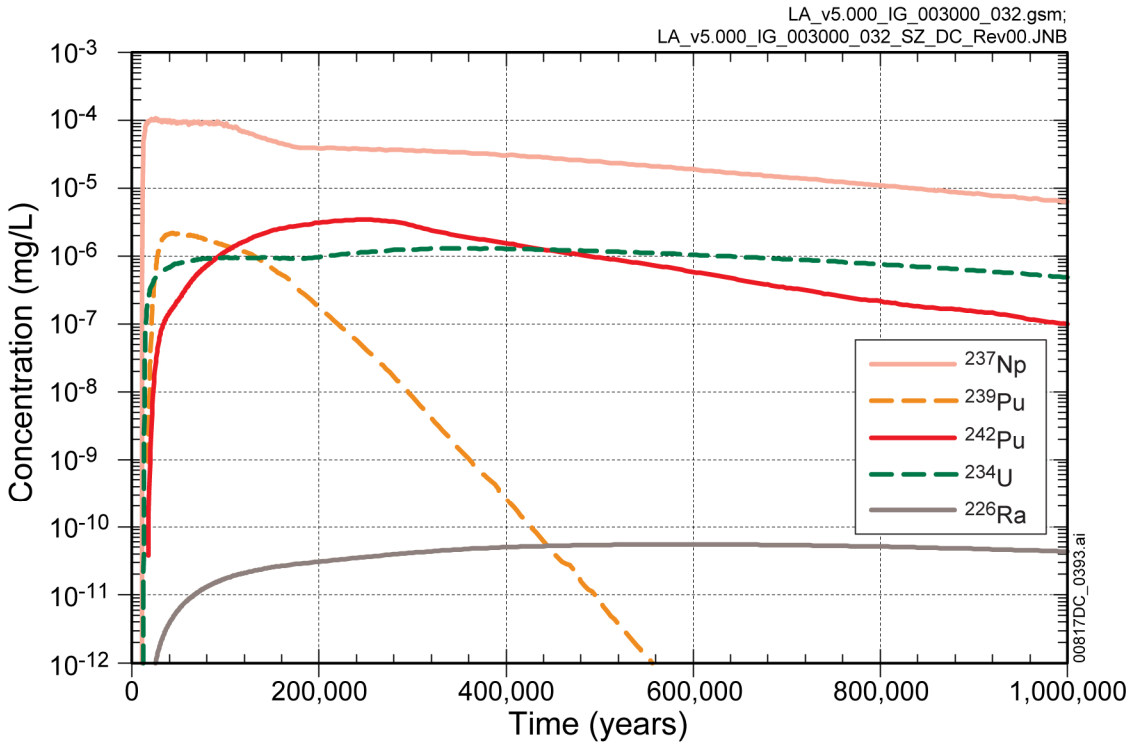

Source: Output DTN: MO0708TSPAVALI.000 [DIRS 182985].

NOTE: The saturated zone concentrations shown on this figure are obtained by dividing the annual releases of radionuclides from the saturated zone by the 3,000 acre-ft/yr annual water usage, as required by regulations.

Figure 7.7.1-34. Concentrations of Major Radionuclides at the RMEI Location for Realization 2855 of the Igneous Intrusion Modeling Case for the 1,000,000-Year Simulation after Repository Closure

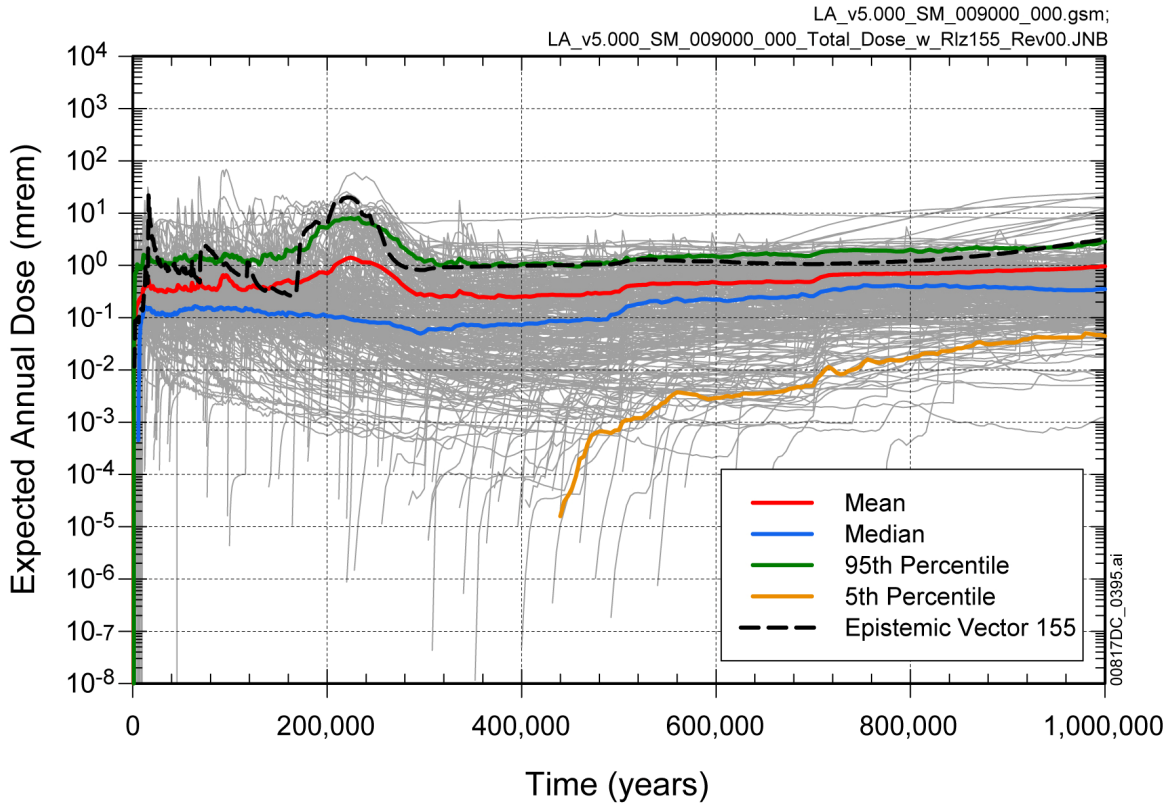

Source: Output DTN: MO0709TSPAREGS.000 [DIRS 182976].

NOTE: ^{226}Ra dose is the sum of ^{226}Ra and ^{210}Pb doses (secular equilibrium assumed).

Figure 7.7.1-35. Expected Annual Dose from the 300 Epistemic Uncertainty Realizations (Vectors) Along With their Quantiles and Expected Dose from Epistemic Uncertainty Vector #155 for the Seismic Ground Motion Modeling Case for the 1,000,000-Year Simulation after Repository Closure

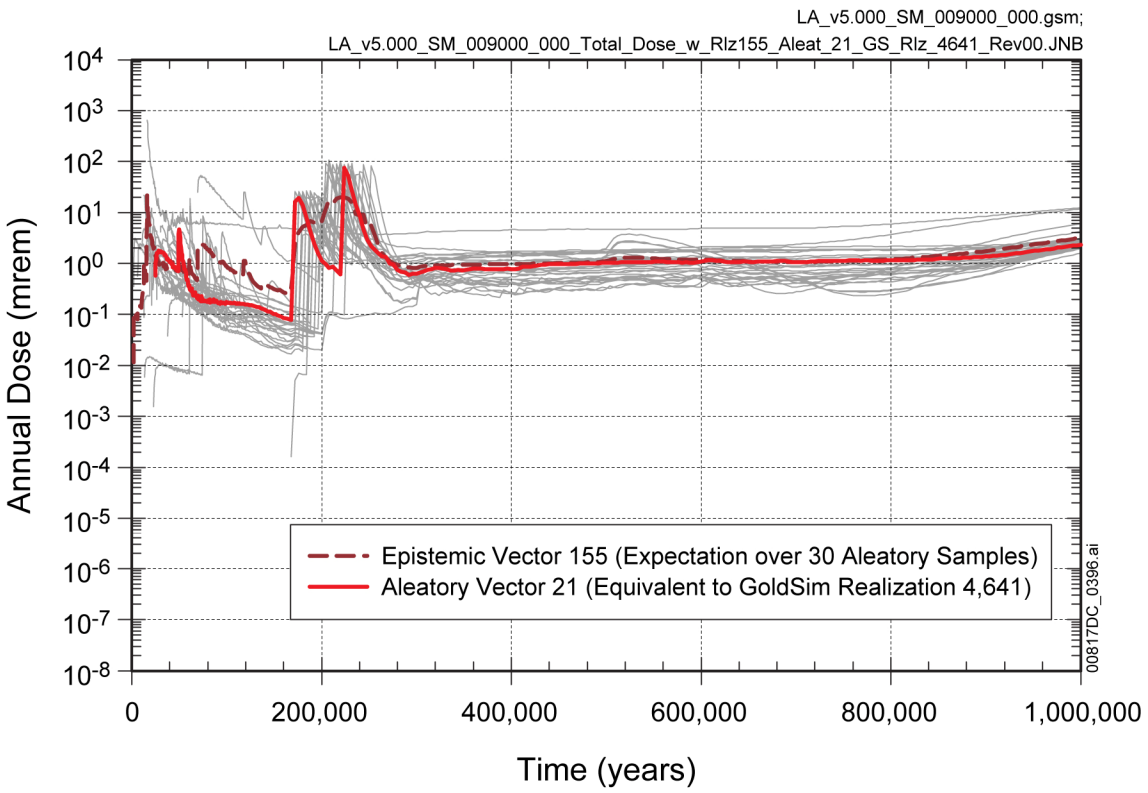

Source: Output DTN: MO0709TSPAREGS.000 [DIRS 182976].

NOTE: The dashed line is the expected annual dose for epistemic uncertainty vector 155 by taking expectation over the thirty aleatory vectors. The solid red line is the annual dose from aleatory vector 21, which is equivalent to GoldSim realization 4641.

Figure 7.7.1-36. Annual Dose from the Thirty Aleatory Vectors (Seismic Event Sequences) Associated with the Epistemic Vector 155 for the Seismic Ground Motion Modeling Case for the 1,000,000-Year Simulation after Repository Closure

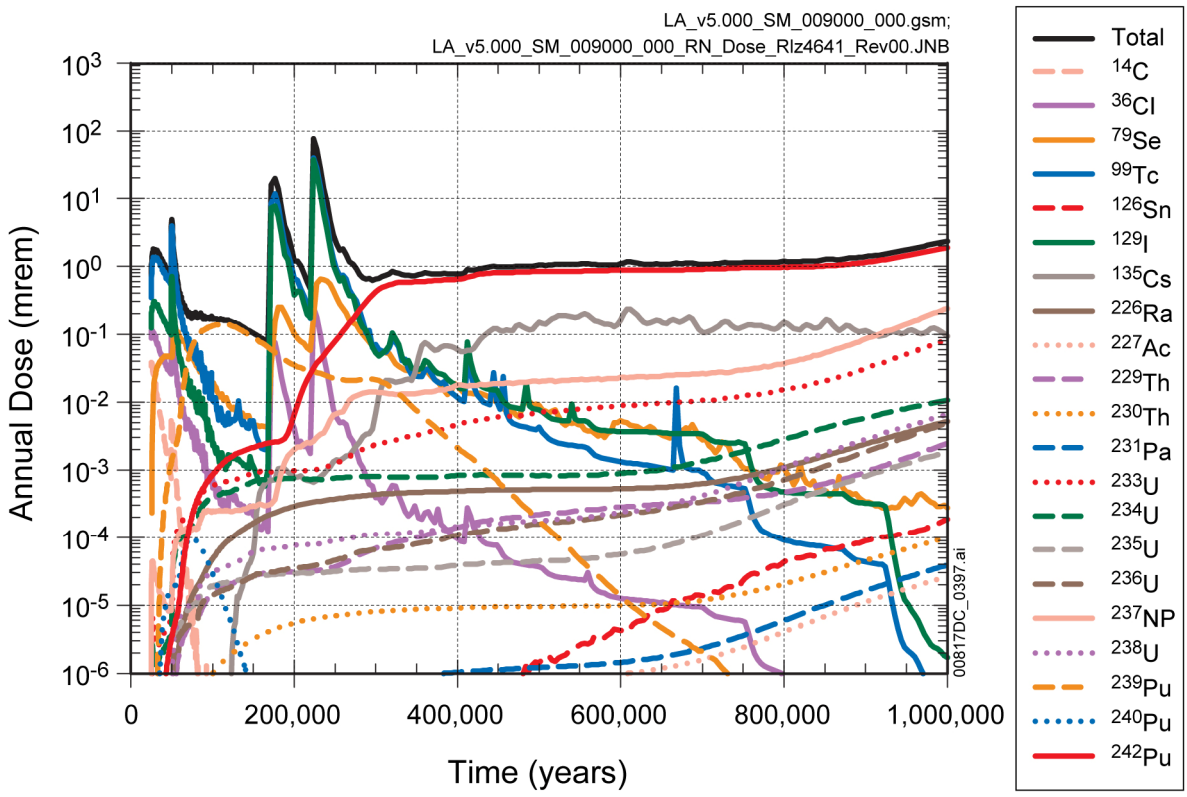

Source: Output DTN: MO0709TSPAREGS.000 [DIRS 182976].

NOTE: ^{226}Ra dose is the sum of ^{226}Ra and ^{210}Pb doses (secular equilibrium assumed).

Figure 7.7.1-37. Annual Dose along with Major Radionuclide Dose Contributors for Realization 4641 of the Seismic Ground Motion Modeling Case for the 1,000,000-Year Simulation after Repository Closure

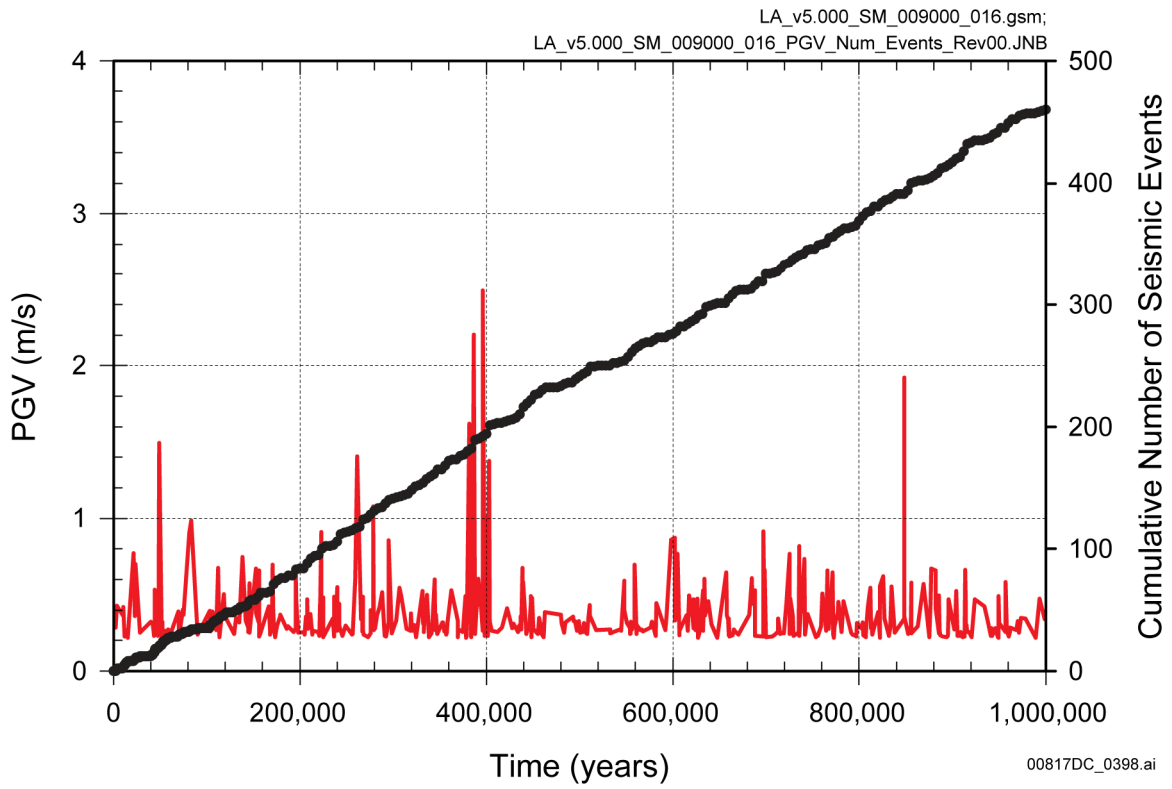

Source: Output DTN: MO0708TSPAVALI.000 [DIRS 182985].

Figure 7.7.1-38. Number of Seismic Events and the Peak Ground Velocity Time History for Realization 4641 of the Seismic Ground Motion Modeling Case for the 1,000,000-Year Simulation after Repository Closure

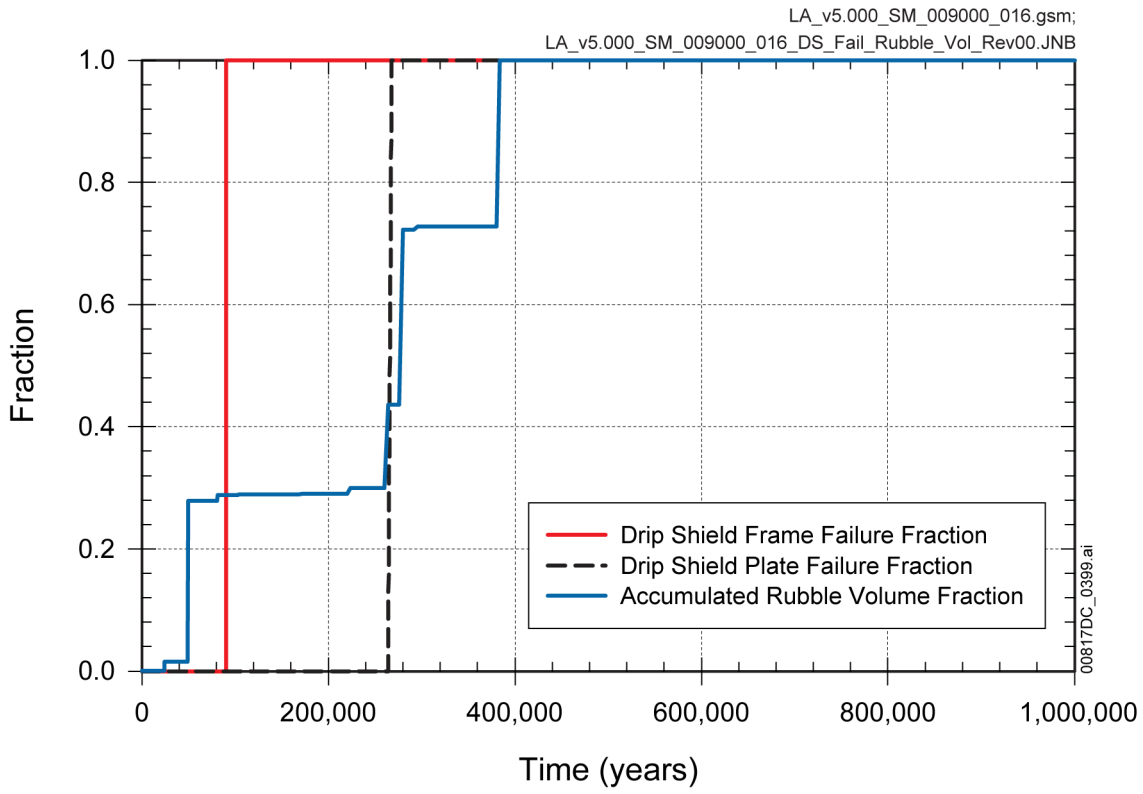

Source: Output DTN: MO0708TSPAVALI.000 [DIRS 182985].

Figure 7.7.1-39. Failure Fraction for the Drip Shield Plate and Framework and the Rubble Fill Fraction in the Drift (Lithophysal Zone) for Realization 4641 of the Seismic Ground Motion Modeling Case for the 1,000,000-Year Simulation after Repository Closure

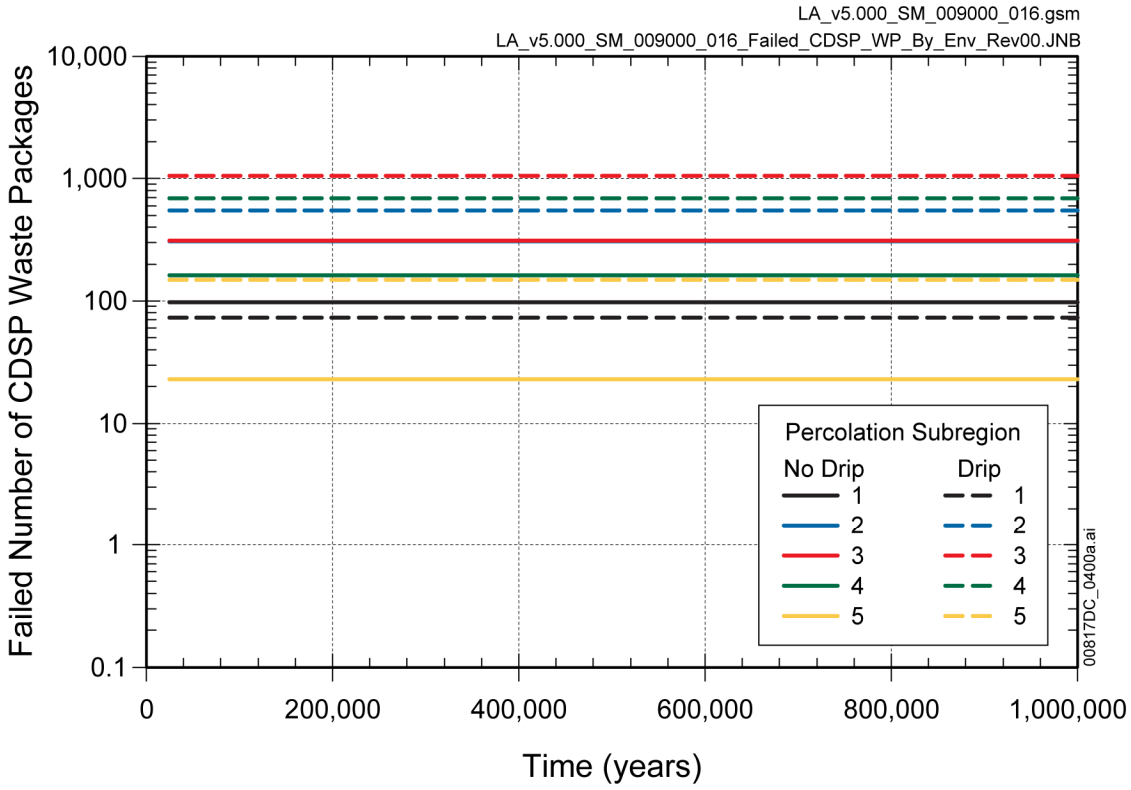

Source: Output DTN: MO0708TSPAVALI.000 [DIRS 182985].

Figure 7.7.1-40. CDSP WP Failure History in all Five Percolation Subregions for Both Dripping and Non-Dripping Environments for Realization 4641 of the Seismic Ground Motion Modeling Case for the 1,000,000-Year Simulation after Repository Closure

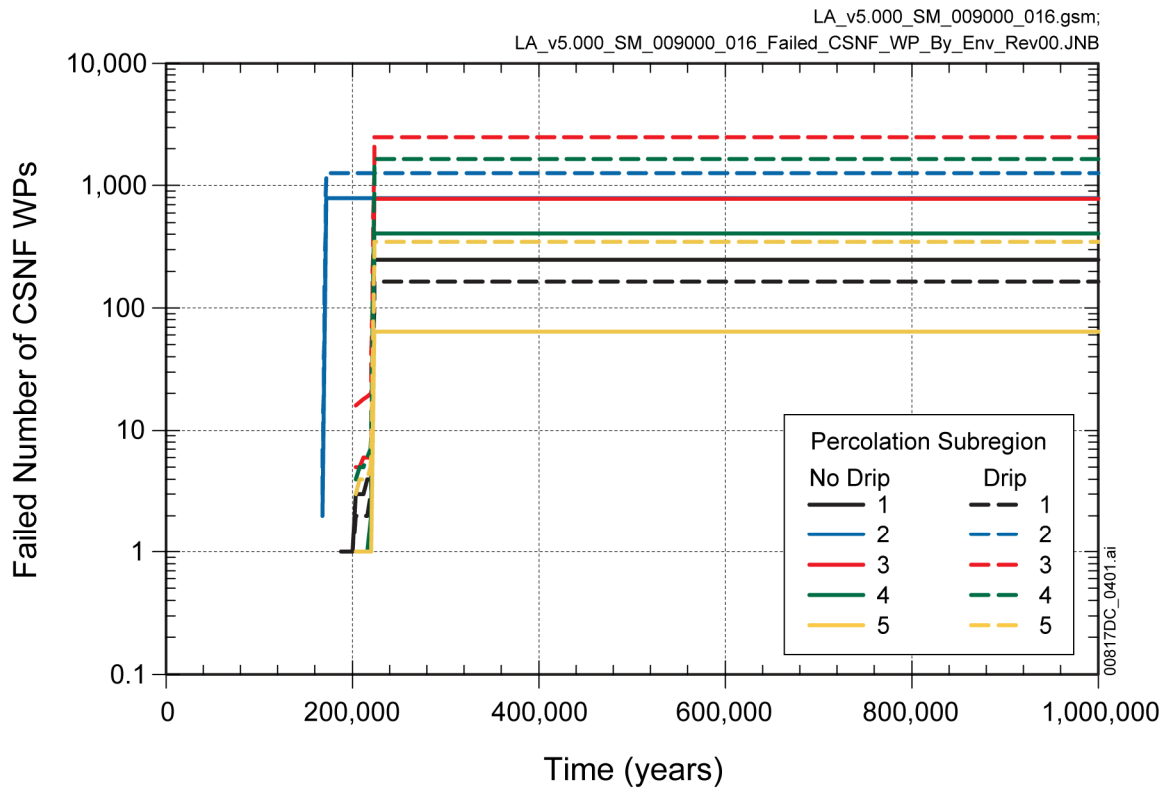

Source: Output DTN: MO0708TSPAVALI.000 [DIRS 182985].

Figure 7.7.1-41. CSNF WP Failure History for Each Percolation Subregion for Both Dripping and Non-Dripping Environments for Realization 4641 of the Seismic Ground Motion Modeling Case for the 1,000,000-Year Simulation after Repository Closure

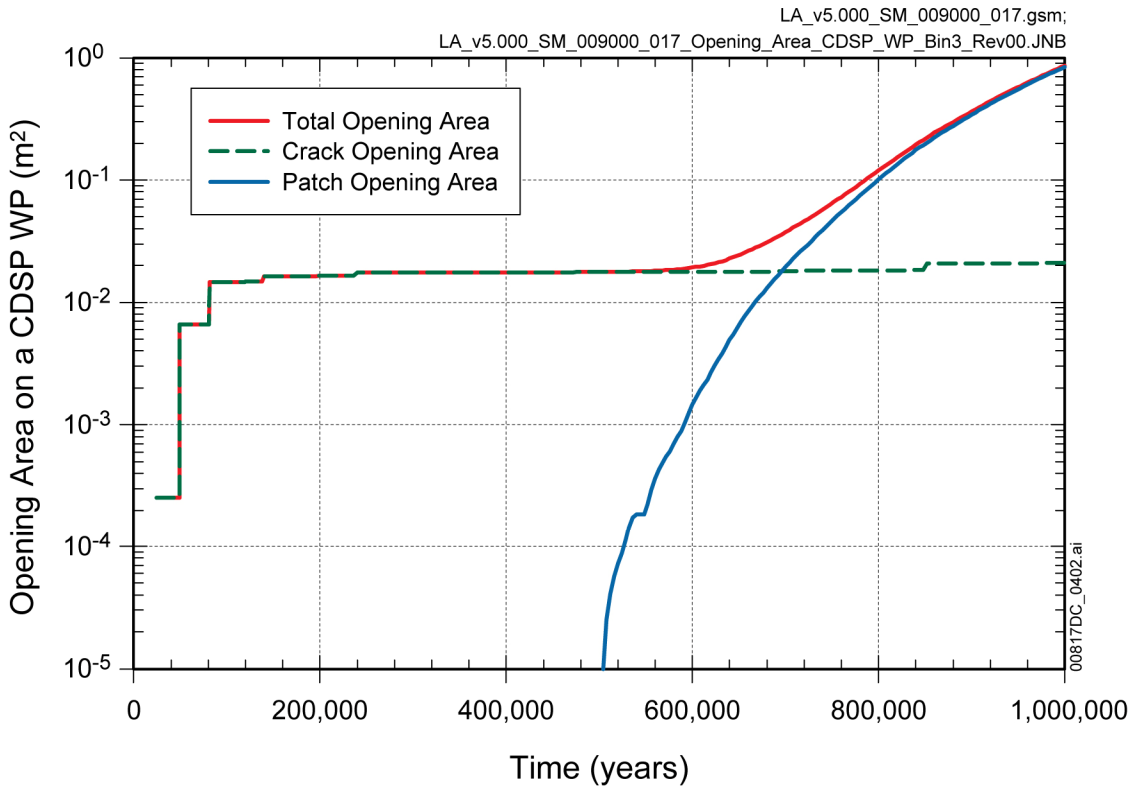

Source: Output DTN: MO0708TSPAVALI.000 [DIRS 182985].

Figure 7.7.1-42. CDSP WP Opening Area after Failure for Percolation Subregion 3 from Crack and Patches for Realization 4641 of the Seismic Ground Motion Modeling Case for the 1,000,000-Year Simulation after Repository Closure

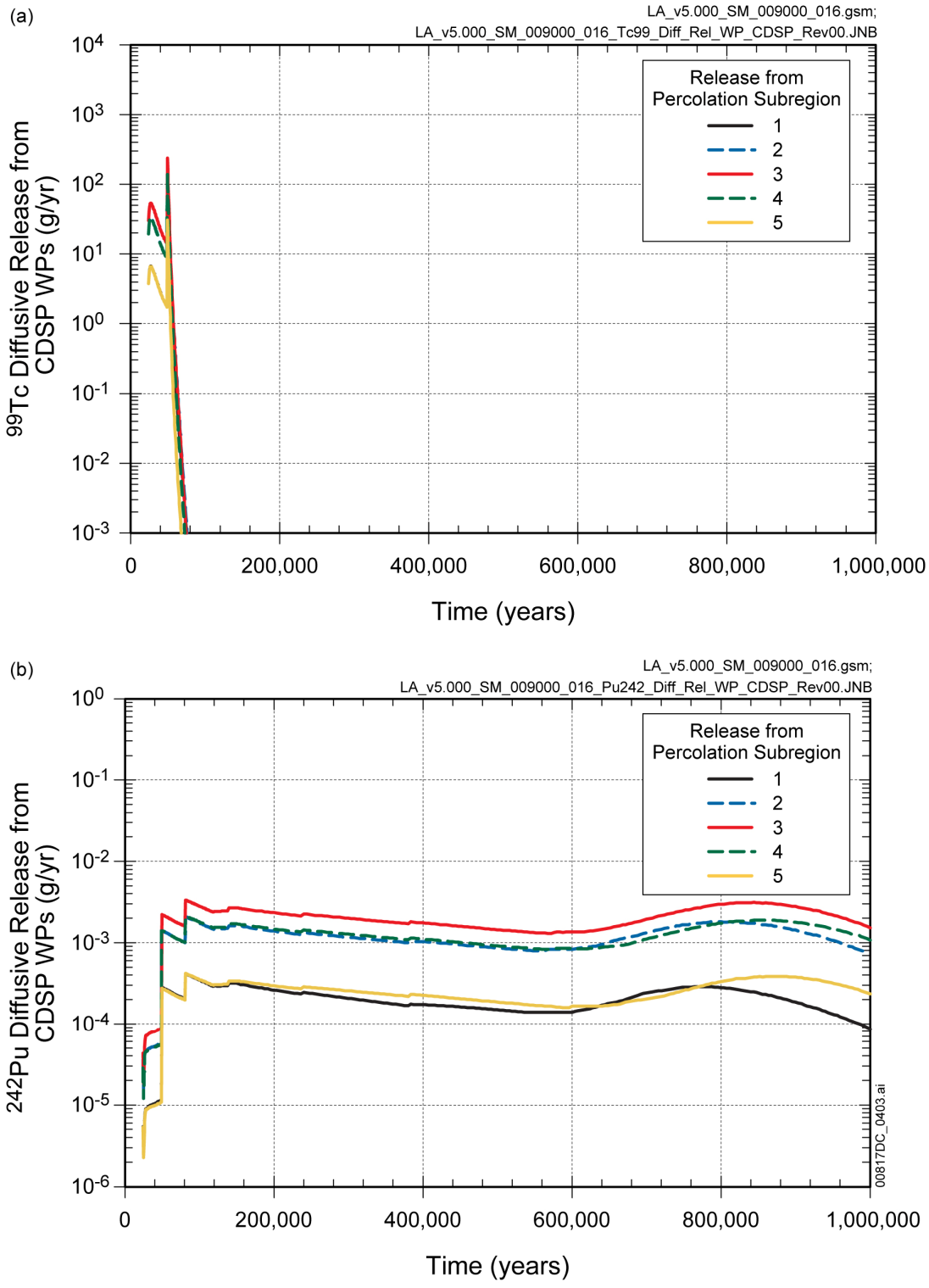

Source: Output DTN: MO0708TSPAVALI.000 [DIRS 182985].

Figure 7.7.1-43. Diffusive Release Rates of: (a) ^{99}Tc and (b) ^{242}Pu from CDSP WPs from each Percolation Subregion for Realization 4641 of the Seismic Ground Motion Modeling Case for the 1,000,000-Year Simulation after Repository Closure

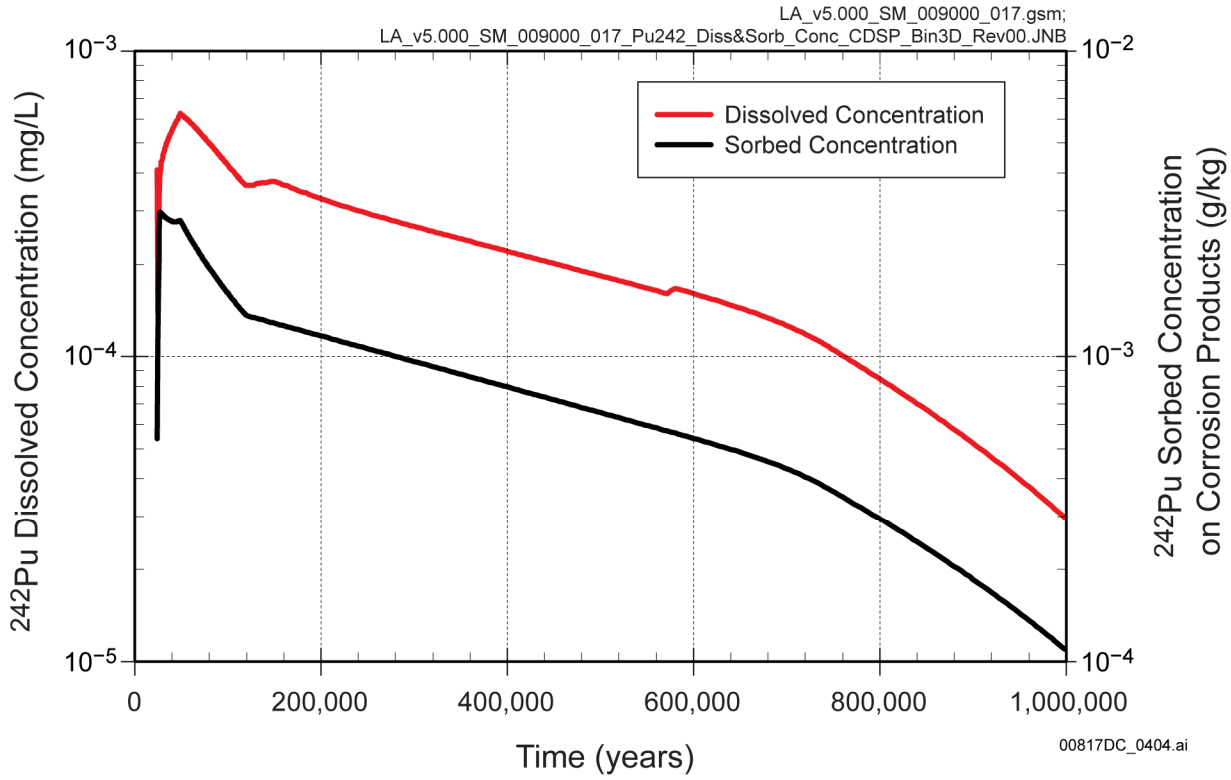

Source: Output DTN: MO0708TSPAVALI.000 [DIRS 182985].

Figure 7.7.1-44. Dissolved Concentration of ^{242}Pu in the Corrosion Products Domain Compared to the Sorbed Concentration on Corrosion Products for CDSP Percolation Subregion 3 Dripping Environment for Realization 4641 of the Seismic Ground Motion Modeling Case for the 1,000,000-Year Simulation after Repository Closure

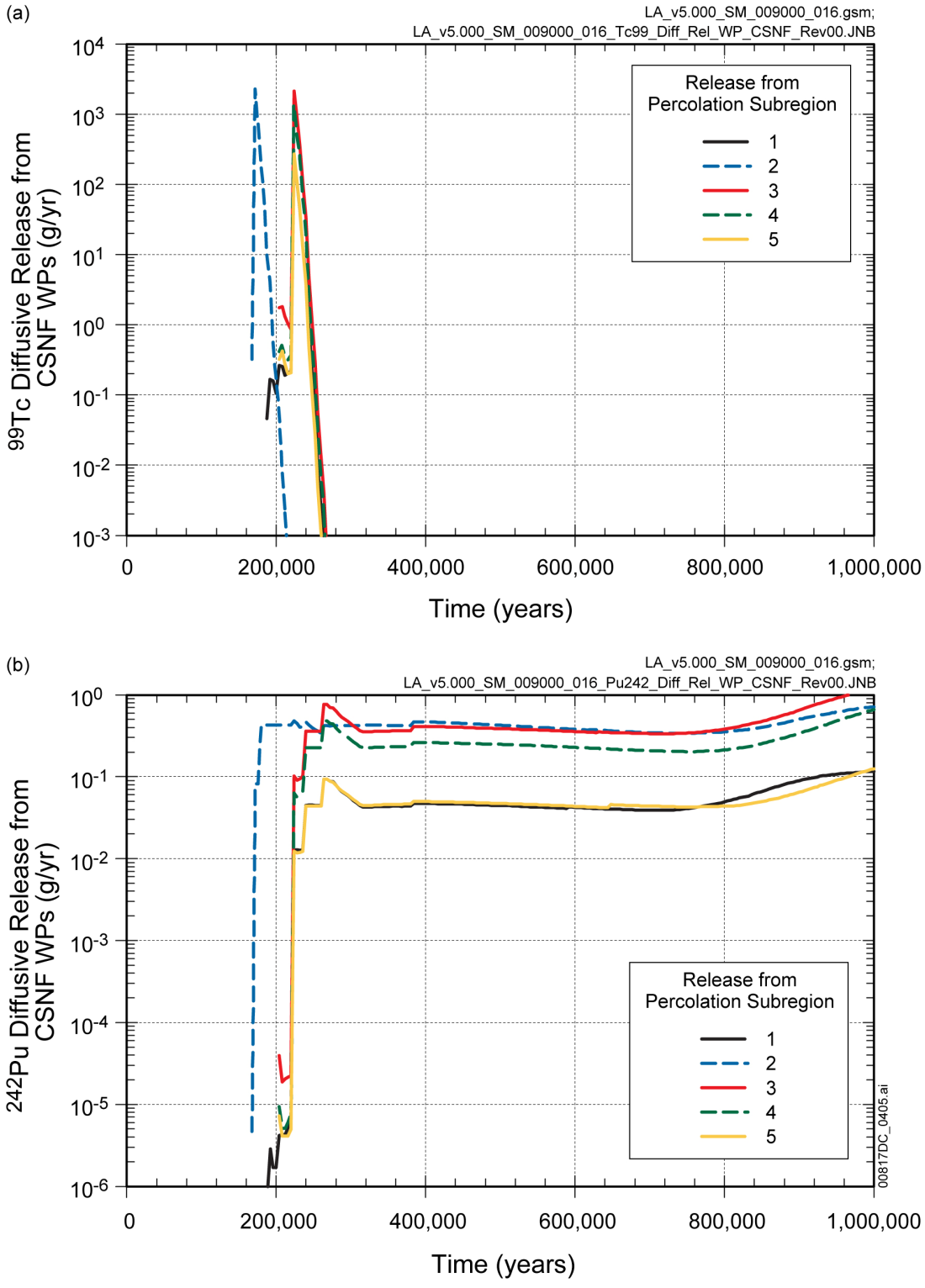

Source: Output DTN: MO0708TSPAVALI.000 [DIRS 182985].

Figure 7.7.1-45. Diffusive Release Rates of: (a) ^{99}Tc and (b) ^{242}Pu from CSNF WPs from each Percolation Subregion for Realization 4641 of the Seismic Ground Motion Modeling Case for the 1,000,000-Year Simulation after Repository Closure

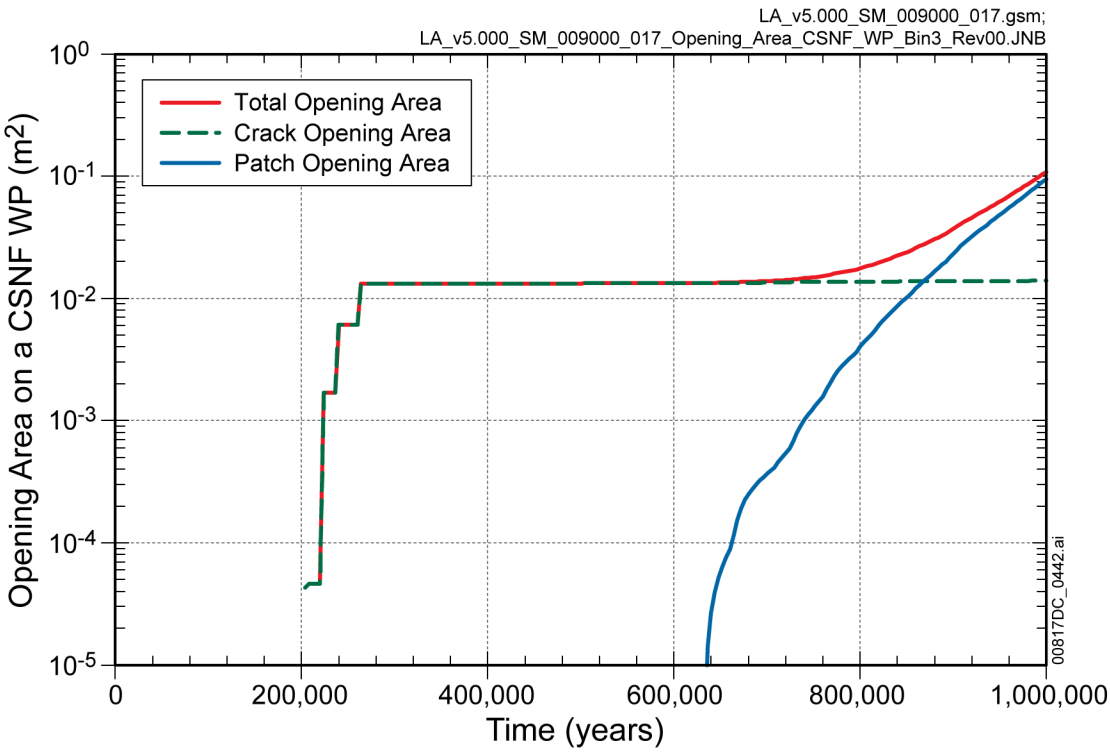

Source: Output DTN: MO0708TSPAVALI.000 [DIRS 182985].

Figure 7.7.1-46. CSNF WP Opening Area after Failure for Percolation Subregion 3 from Cracks and Patches for Realization 4641 of the Seismic Ground Motion Modeling Case for the 1,000,000-Year Simulation after Repository Closure

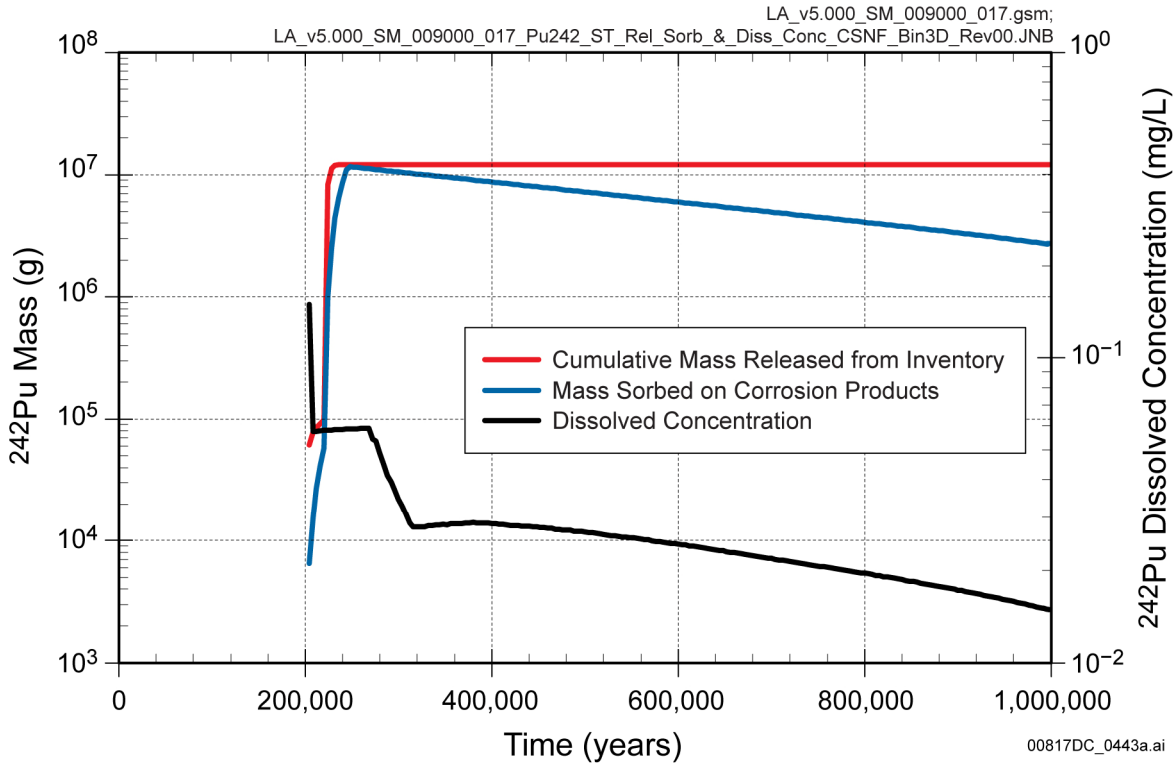

Source: Output DTN: MO0708TSPAVALI.000 [DIRS 182985].

Figure 7.7.1-47. Comparison of ^{242}Pu Cumulative Mass Released from the Inventory, Mass Sorbed on Corrosion Products, and the Dissolved Concentration in the Corrosion Products Domain for CSNF Percolation Subregion 3, Dripping Environment for Realization 4641 of the Seismic Ground Motion Modeling Case for the 1,000,000-Year Simulation after Repository Closure

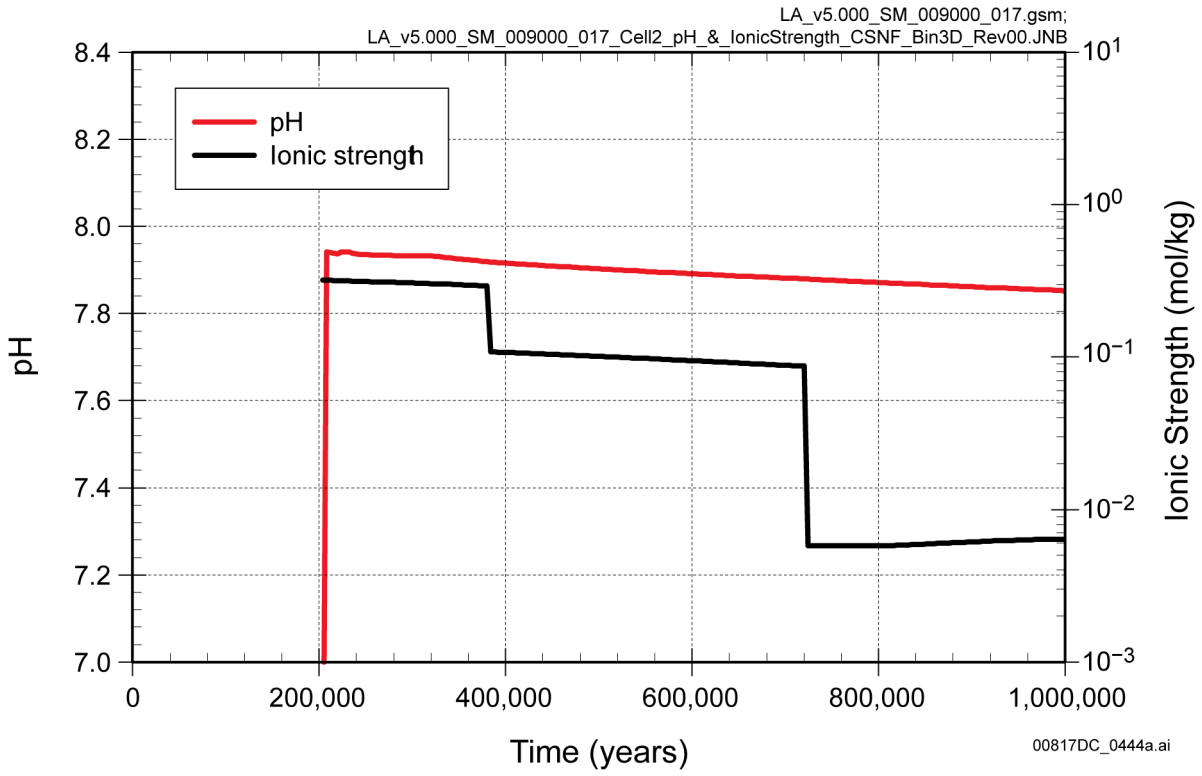

Source: Output DTN: MO0708TSPAVALI.000 [DIRS 182985].

Figure 7.7.1-48. pH and Ionic Strength Profile in the Corrosion Products Domain for CSNF Percolation Subregion 3, Dripping Environment for Realization 4641 of the Seismic Ground Motion Modeling Case for the 1,000,000-Year Simulation after Repository Closure

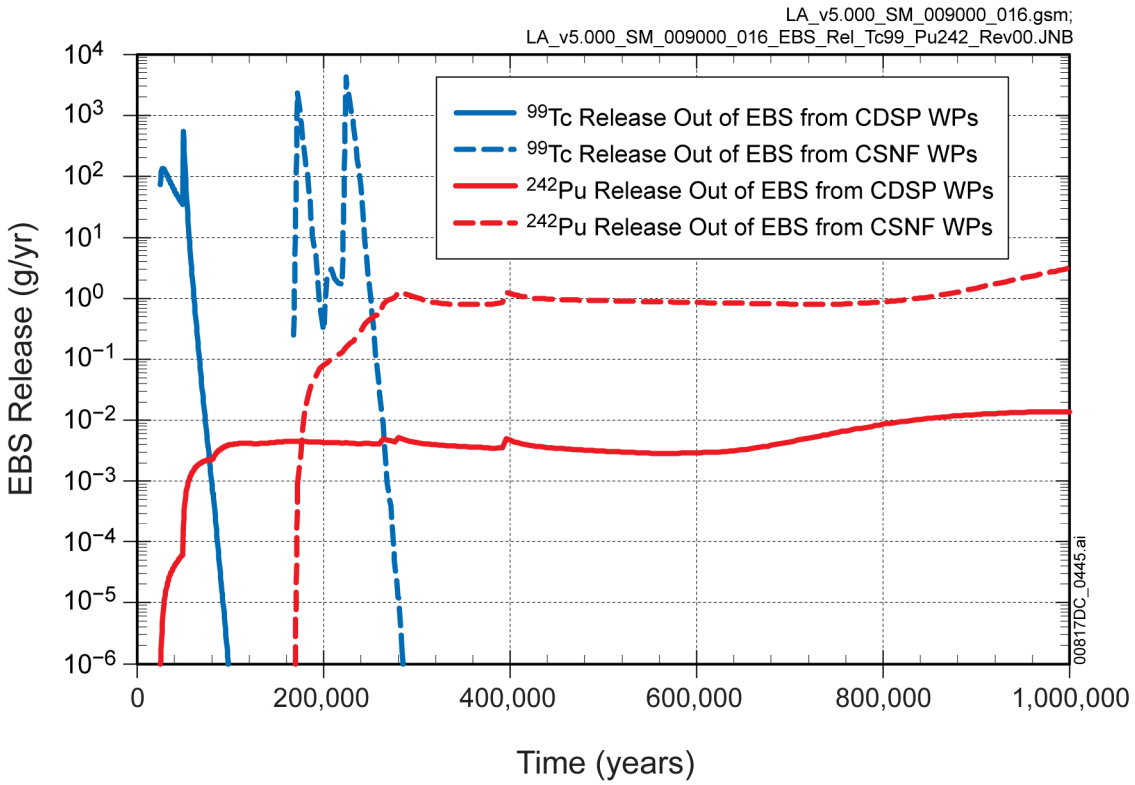

Source: Output DTN: MO0708TSPAVALI.000 [DIRS 182985].

Figure 7.7.1-49. EBS Release Rates from CSNF and CDSP WPs (All Percolation Subregions) for Realization 4641 of the Seismic Ground Motion Modeling Case for the 1,000,000-Year Simulation after Repository Closure

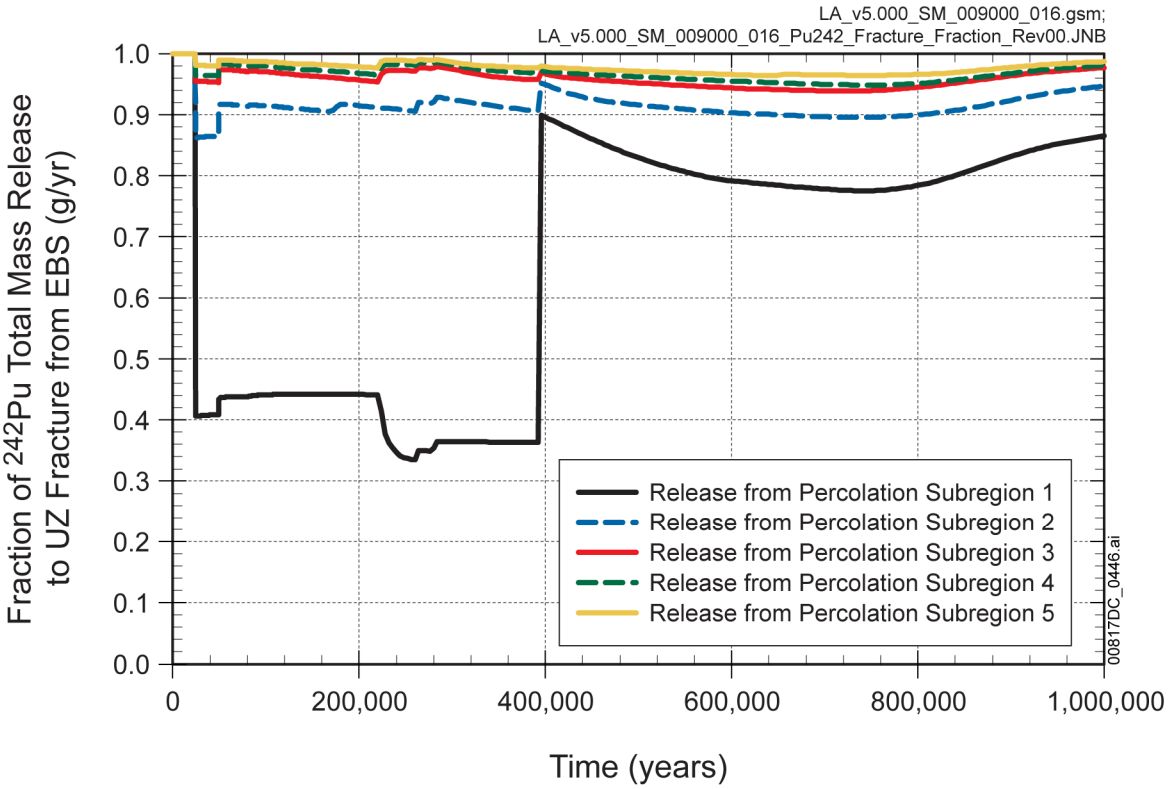

Source: Output DTN: MO0708TSPAVALI.000 [DIRS 182985].

Figure 7.7.1-50. Fraction of ^{242}Pu Mass Going to Unsaturated Zone Fractures as Compared to the Unsaturated Zone Matrix at the Repository Horizon for Realization 4641 of the Seismic Ground Motion Modeling Case for the 1,000,000-Year Simulation after Repository Closure

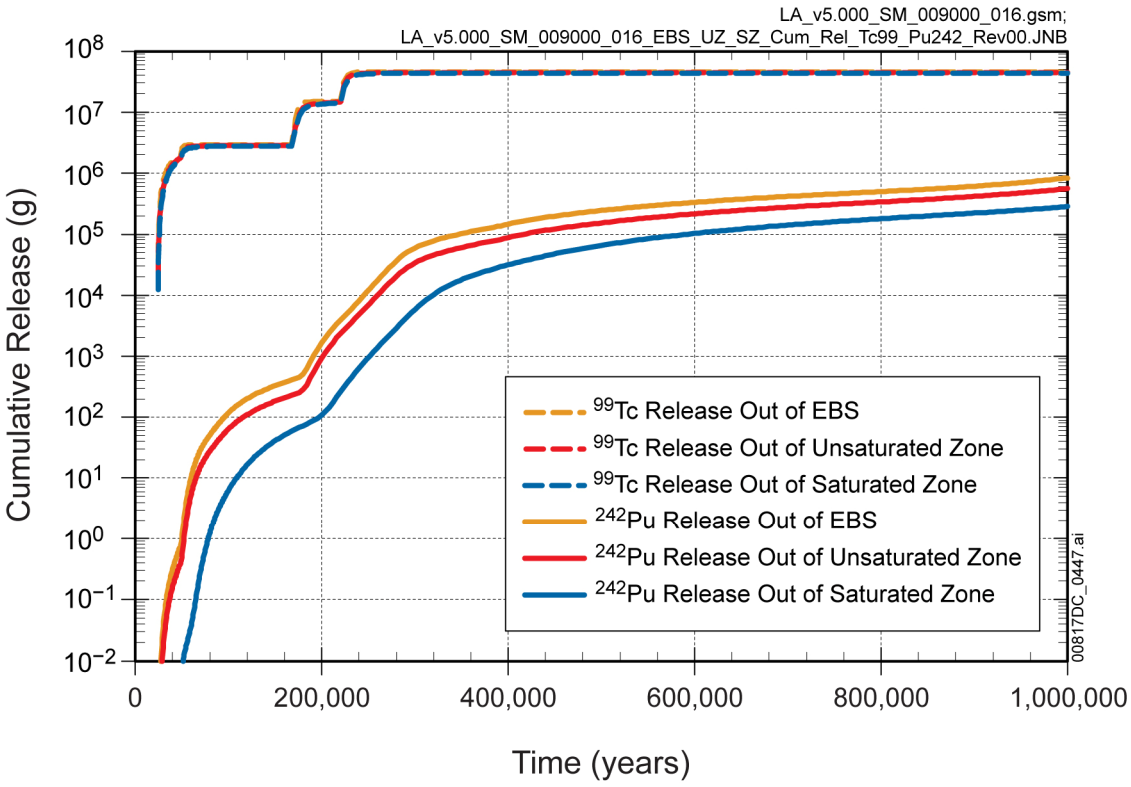

Source: Output DTN: MO0708TSPAVALI.000 [DIRS 182985].

Figure 7.7.1-51. Cumulative Mass Release of ^{99}Tc and ^{242}Pu from the EBS, Unsaturated Zone, and Saturated Zone for Realization 4641 of the Seismic Ground Motion Modeling Case for the 1,000,000-Year Simulation after Repository Closure

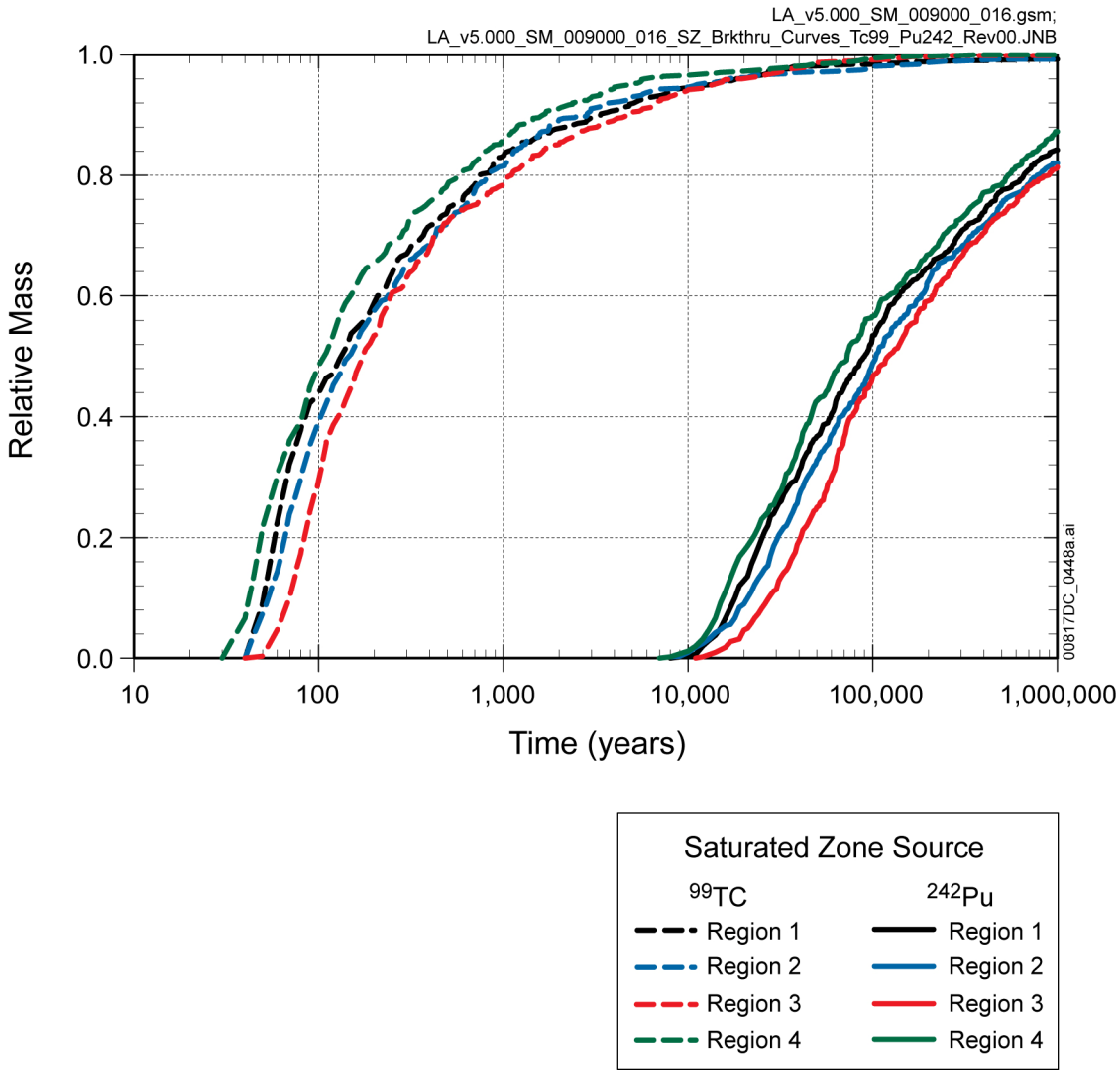

Source: Output DTN: MO0708TSPAVALI.000 [DIRS 182985].

NOTE: The SZ breakthrough curve #122 is used in Realization 4641.

Figure 7.7.1-52. Comparison of Saturated Zone Breakthrough Curves for ^{99}Tc and ^{242}Pu for All Four Saturated Zone Regions for Realization 4641 of the Seismic Ground Motion Modeling Case for the 1,000,000-Year Simulation after Repository Closure

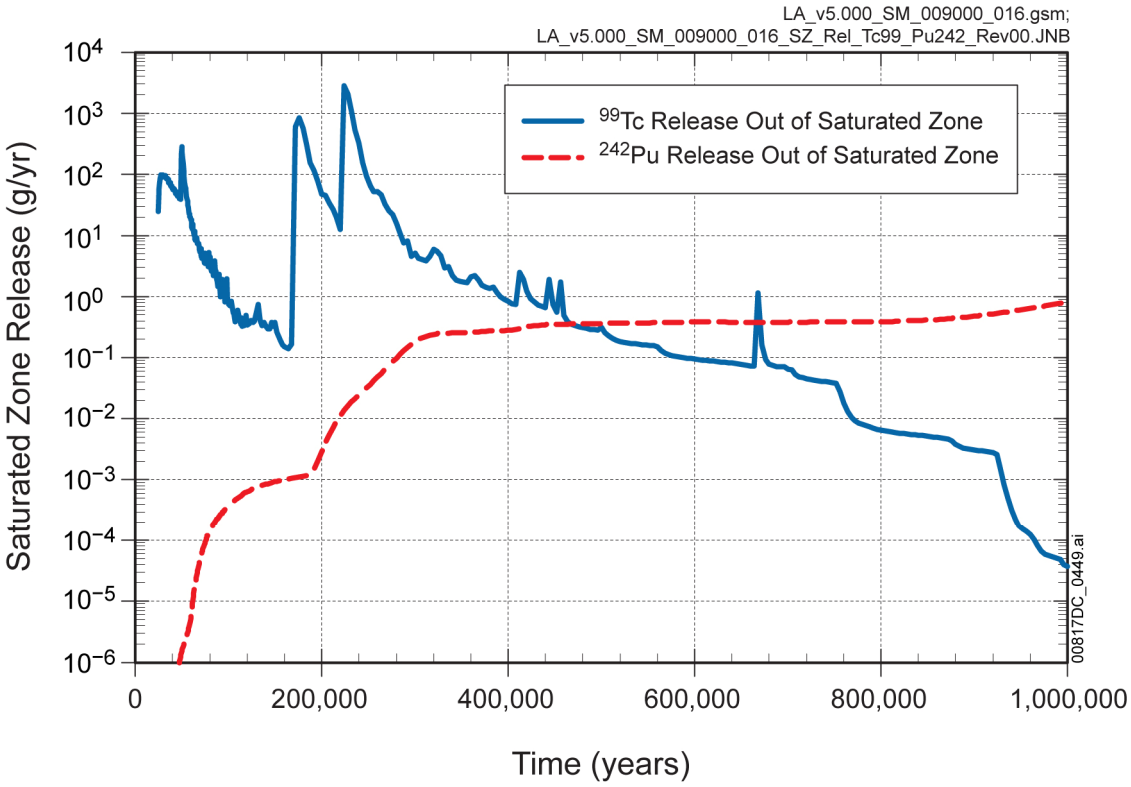

Source: Output DTN: MO0708TSPAVALI.000 [DIRS 182985].

Figure 7.7.1-53. Saturated Zone Release to the Biosphere for ^{99}Tc and ^{242}Pu for Realization 4641 of the Seismic Ground Motion Modeling Case for the 1,000,000-Year Simulation after Repository Closure

7.7.2 Comparison with Simplified TSPA Analysis

The TSPA-LA Model, presented in Chapter 6, describes the models and submodels used to calculate spatially varying radionuclide mass transfer rates from the EBS, the UZ, and the SZ. The mass flux exiting the SZ is then used to determine the annual dose to a RMEI. A complex numerical model is required to appropriately solve the coupled differential equations that describe repository performance while taking into account the spatial variability in properties and processes.

A Simplified Analysis has been developed to evaluate repository performance utilizing simplified representations of the mathematical equations that describe radionuclide mass transfer rates. This analysis, called Simplified TSPA Analysis (also referred herein as Simplified Analysis) is described in detail in Appendix L, and is being used to build confidence and corroborate the TSPA-LA Model presented in Chapter 6 and the results it generates that are shown in Chapter 8. The Simplified TSPA Analysis was developed as a stand-alone computer program written in FORTRAN 90 and compiled/linked using Compaq Visual Fortran as unqualified software. Unqualified software can be used to corroborate analysis or calculation results per Section 6.2.1 M of SCI-PRO-006, *Model.*

Overall, the Simplified TSPA Analysis is a higher-level abstraction than the TSPA-LA Model. In general, it includes the same FEPs that are considered in the TSPA, but the manner in which they are modeled is much simpler. Some FEPs have not been included in the Simplified TSPA Analysis based on a qualitative assessment of their importance in past TSPA models. For those FEPs that are included, the simplification primarily involves removing a considerable amount of detail included in the TSPA-LA to capture spatial and temporal variability and treating the repository system with a more "average" representation. In addition, many of the process level modeling results are further abstracted for inclusion in the Simplified TSPA Analysis.

The Simplified TSPA Analysis has its bases in the process- and abstraction-level modeling captured in the supporting Analysis and Model reports. Thus, it represents the same conceptualization of the repository system and its underlying technical bases are identical to those of the TSPA-LA Model. However, the Simplified TSPA Analysis is different than the TSPA-LA Model both in its structure and computational method. A summary of the key differences between the TSPA-LA Model and the Simplified TSPA Analysis is provided in Table 7.7.2-1, which summarizes those FEPs that were not included in the Simplified TSPA Analysis and the differences in the treatment of the FEPs between the Simplified TSPA Analysis and the TSPA-LA Model.

The largest degree of simplification was in the modeling of radionuclides within the UZ and SZ. A simple one-dimensional radionuclide transport model was developed using average properties for each hydrologic unit in the UZ and SZ. This simplified approach reflects the general behavior of the breakthrough curve, rather than the detailed behavior of ground water flow and radionuclide transport within the UZ and SZ.

A more complex, but still simplified, analysis was developed to model radionuclide transport within the EBS. The relative complexity of this portion of the Simplified TSPA Analysis, as compared to the UZ and SZ models, was necessary to appropriately model the rate that

radionuclides are released from the EBS, or the source term. This model included submodels that calculated the rate and manner that the WPs degrade, the rate the waste form degrades, and the rate radionuclides are transported through the engineered barriers.

The Simplified TSPA Analysis, as an auxiliary analysis of the overall repository system, is a different system-level mathematical model and its results can be used to build confidence in the TSPA-LA Model, its results, and the conclusions drawn from those results. Despite the differences in level of detail, the basic results of the two models (i.e. dose over time and contribution to dose of dominant radionuclides) can be compared for individual modeling cases. If the comparison between the Simplified TSPA Analysis and the TSPA-LA Model demonstrates that the two models produce results that are similar in magnitude with similar trends, then the comparison supports the verification that the TSPA-LA Model produces reasonable results.

Models of the degradation of the engineered barriers were developed for the nominal, seismic ground motion, and igneous intrusion conditions. This was done to allow for comparisons with the modeling cases evaluated with the TSPA-LA Model.

The Simplified TSPA Analysis described in Appendix L was used to simulate four modeling cases that were analyzed using the TSPA-LA Model over a 1,000,000 year period. These are:

- Waste Package EF Modeling Case: This case evaluated repository performance considering only those WPs that experience early failure. In this case, no failure of the WPs is considered to occur due to general corrosion, SCC, or seismic mechanical damage.

- Nominal Modeling Case: This scenario considered degradation of the WPs and DSs from corrosion processes only. Early WP failure was not considered in this scenario and mechanical damage of the DS and WP was not considered in this scenario. Seismic induced rockfall and its subsequent effects on seepage were also not considered.

- Seismic GM Modeling Case: This scenario considered degradation of the WPs and DS from corrosion processes. The effects of seismic ground motion were also considered including mechanical damage to the WPs and DS, and seismic induced rockfall. Aleatory and epistemic uncertainty were randomly sampled in each realization. Seismic events of varying magnitude were assumed to occur randomly following a Poisson process. The subsequent effects on rockfall, DS damage, and WP damage were then calculated.

- Igneous Intrusion Modeling Case: This scenario considered the degradation of the engineered barriers as a result of an intruding magma dike. Degradation of the WPs and DS due to corrosion processes, seismic mechanical damage, and early WP failure were not considered. Aleatory and epistemic uncertainty were randomly sampled in each realization. A single igneous intrusion was assumed to occur randomly over the simulation period resulting in the failure of all DS and WPs.

7.7.2.1 Waste Package Early Failure Modeling Case

A 500 realization simulation of the Waste Package EF Modeling Case was conducted over a 1,000,000 year period using the Simplified TSPA Analysis. Key aspects of this simulation case are:

- The number of early CSNF and CDSP WP failures was determined using the approach described in Section L.2.8.2. In summary, the number of CSNF and CDSP WPs that experience early failure, in a given realization, is sampled from a Poisson distribution. Several realizations do not result in any early WP failures.

- It is assumed that the entire surface of any of the WPs that experience early failure is degraded.

- DS degradation occurs only due to general corrosion following the approach presented in Section L.2.7.1. Radionuclide transport within and out of the WP is via diffusive processes until the DS fail due to general corrosion

- All WPs that experience early failure are assumed to be in a region of the repository that experiences seepage.

Figure 7.7.2-1 presents the annual dose histories for the Waste Package EF Modeling Case using the Simplified TSPA Analysis. This mean annual dose history takes into account the probability of early WP failure through the Poisson sampling discussed above and in Section L.2.8.2. Figure 7.7.2-1 also shows the contribution to mean annual dose from radionuclides that contribute most strongly to the mean annual dose for the Waste Package EF Modeling Case using the Simplified TSPA Analysis

The results shown on Figure 7.7.2-1 indicate that the mean annual dose and the individual radionuclide mean annual dose are similar in magnitude to those obtained for the WP Early Failure Modeling Case simulated over a 1,000,000 year period with the TSPA-LA Model shown on Figure 8.2-6. In addition, the most significant radionuclides are also similar with the mobile radionuclides ^{99}Tc and ^{129}I and moderately mobile radionuclide ^{237}Np initially dominating, then by ^{239}Pu until approximately 200,000 years after repository closure, then ^{242}Pu and ^{229}Th. The TSPA-LA results shown in Figure 8.2-6 also show that the mobile and soluble radionuclides (^{99}Tc, ^{129}I, and ^{14}C) dominating first with the solubility limited and less mobile radionuclides (^{239}Pu, ^{242}Pu, ^{237}Np, and ^{226}Ra), becoming important later.

The overall trends are very similar except for ^{229}Th being a key radionuclide at later times in the Simplified TSPA Analysis while the TSPA-LA Model shows ^{226}Ra being a key radionuclide. Two factors contribute to the increased importance of ^{229}Th in the Simplified TSPA Analysis relative to the TSPA-LA Model.

- Both models assume ^{226}Ra is in secular equilibrium with ^{230}Th at the receptor well. As discussed in Section L2.16, the Simplified TSPA Analysis uses a very rough approximation to handle chain decay in the UZ and SZ. The UZ is divided into three layers to represent the Topopah Spring, Calico Hills, and Prow Pass units while the SZ is

divided into two fractured-volcanic segments and one alluvial segment. The chain decay approach implemented in the Simplified TSPA Analysis calculates how much mass of a parent radionuclide breaks through a UZ layer or SZ segment both without and with decay. The difference is assumed to be the daughter radionuclide and is introduced at the beginning of the next UZ layer or SZ segment. This approach does not allow for decay of the daughter in the layer where it is formed. Because of this, the Simplified TSPA Analysis adds a bit more of a daughter to the top of layers than would be present with a more explicit method as is used in the TSPA-LA Model. Since ^{229}Th has roughly an order of magnitude shorter half-life than ^{230}Th, the Simplified TSPA Analysis effectively "adds more" ^{229}Th relative to ^{230}Th, artificially increasing its importance as compared to the TSPA-LA Model.

- ^{229}Th is a daughter product of ^{233}U and builds in both the engineered and natural systems. ^{229}Th that is released from the EBS is transported throughout the natural barrier system with the properties of thorium. However, when ^{229}Th is created in one of the components of the natural system (UZ layer or segment of the SZ) in the Simplified TSPA Analysis, it is assumed to transport through that component with the properties of uranium until it exits that component. Thorium travels much more slowly through the natural barriers than uranium because it has a higher sorption coefficient. Thus, the modeling approach for the natural barrier system in this simplified analysis leads to artificially high transport rates for thorium and results in higher annual doses as is seen for ^{229}Th in this modeling case.

An estimate of the uncertainty in the annual dose for the WP Early Failure Modeling case using the Simplified TSPA Analysis is shown on Figure 7.7.2-2. The estimates of annual dose shown on Figure 7.7.2-2 takes into account uncertainties in the various submodels of this modeling case in addition to sampling the number of CSNF and CDSP WPs that experience early failure. These uncertainties are addressed in terms of probability distributions for parameters of the submodels (i.e., adsorption coefficients for transport of radionuclides in the UZ, the uncertainty term added for actinide solubilities). These uncertainties along with uncertainty in the number of WPs that experience early failure are addressed in the estimate of mean annual dose by evaluating 500 realizations with each realization providing an annual dose that results from one set of values representing the uncertainty and the sampled number of WPs that experience early failure. The mean annual dose at a given time is the average for the 500 annual dose values. The range of uncertainty in the annual dose is represented by the 5th and 95th percentiles of the annual dose values for each of the 500 realizations.

These 5th, 50th, and 95th percentile annual dose histories are shown, along with the mean annual dose, on Figure 7.7.2-2. However, approximately 60 percent of the realizations sample no early WP failures, resulting in 5th and 50th percentile annual dose histories of zero. Comparing Figure 7.7.2-2 and Figure 8.2-5 shows that the Simplified TSPA Analysis yields higher mean annual total and individual radionuclide doses than does the TSPA-LA Model. The higher mean annual dose is due to higher mean individual radionuclide doses for ^{239}Pu and ^{242}Pu as a result of the simplified approach used for modeling radionuclide transport in the EBS.

A comparison of the Simplified TSPA Analysis results considering all realizations and the TSPA-LA Model results for this modeling case at 200,000 years, 400,000 years 600,000 years,

800,000 years, and 1,000,000 years following repository closure, is shown on Figure 7.7.2-3. This comparison shows that the Simplified TSPA Analysis results in annual doses that are similar in magnitude to, but higher, than those of the TSPA-LA.

7.7.2.2 Nominal Modeling Case

The Nominal Modeling Case accounts for the WPs that fail under nominally expected conditions because of general corrosion and SCC and for the DSs that fail under nominally expected conditions because of general corrosion.

Figure 7.7.2-4 presents the mean annual dose histories for the Nominal Modeling Case using the Simplified TSPA-LA Analysis. Figure 7.7.2-4 also shows the contribution to mean annual dose from the radionuclides that contribute most strongly to the mean annual dose for the Nominal Modeling Case using the Simplified TSPA-LA Analysis.

The results shown on Figure 7.7.2-4 indicate that the mean annual dose and the individual radionuclide mean annual dose are similar in magnitude to those obtained for the Nominal Modeling Case simulated over a 1,000,000 year period with the TSPA-LA Model, as shown on Figure-8.2-2. In addition, the most significant radionuclides are also similar with the soluble and mobile radionuclides ^{129}I and ^{99}Tc dominating, and the less mobile radionuclide ^{135}Cs to a lesser extent. The mean annual dose of solubility limited radionuclides (i.e., ^{237}Np and ^{242}Pu) is shown to be steadily increasing out to 1,000,000 years in both models. These trends are consistent with those of the TSPA-LA Model shown on Figure 8.2-2.

An estimate of the uncertainty in the annual dose for the Nominal Modeling Case using the Simplified TSPA Analysis is shown on Figure 7.7.2-5. The estimate of mean annual dose shown on Figure 7.7.2-5 takes into account uncertainties in the various submodels of this scenario. These uncertainties are addressed in terms of probability distributions for parameters of the submodels. These uncertainties are addressed in the estimate of mean annual dose by evaluating 500 realizations with each realization providing an annual dose that results from one set of values representing the uncertainty. The mean annual dose at a given time, is the average for the 500 annual dose values. The range of uncertainty in the annual dose is represented by the 5th and 95th percentiles of those annual dose values.

The annual dose results shown on Figure 7.7.2-5 for the Simplified TSPA Analysis are lower than those from the TSPA-LA Model shown in Figure 8.2-1. This is further illustrated on Figure 7.7.2-6 which shows a comparison of the Simplified TSPA Analysis results and the TSPA-LA Model results for this modeling case at 200,000 years, 400,000 years, 600,000 years, 800,000 years, and 1,000,000 years following repository closure. The Simplified TSPA Analysis results in mean annual doses that are around an order of magnitude lower than the TSPA-LA results until about 800,000 years following repository closure. The mean annual dose calculated by the Simplified TSPA Analysis is approximately a factor of two lower than that calculated by the TSPA-LA at 1,000,000 years. This difference is attributed to differences in the rate and manner that the WPs fail between the Simplified TSPA Analysis and the TSPA-LA Model.

The general corrosion rate of the WP outer barrier material is dependent on temperature in both the Simplified TSPA Analysis and the TSPA-LA Model. General corrosion failure of the WP

outer barrier occurs in three percent of the realizations in the Simplified TSPA Analysis, all occurring after 800,000 years following repository closure. As discussed in Section 8.2.1, by 1,000,000 years, approximately 10 percent of the WPs are projected to be failed by general corrosion breaches.

The Simplified TSPA Analysis results in SCC occurring in approximately 50 percent of the realizations. The earliest failures due to SCC occur around 300,000 years following repository closure in the Simplified TSPA Analysis, whereas the earliest failures due to SCC occur around 100,000 years in the TSPA-LA Model. Approximately 50 percent of the realizations of the Simplified TSPA Analysis result in no WP failure due to stress corrosion, and no resultant dose, within a 1,000,000 year period. Over 95 percent of the realizations of the TSPA-LA Model result in SCC of the WPs within a 1,000,000 year period. This difference is shown in Figure 7.7.2-6 in the comparison of the mean values of the annual dose between the two models. The difference in the time that SCC begins between the Simplified TSPA Analysis and the TSPA-LA Model results in the difference in the annual dose histories. In a sense, the annual dose from the Simplified TSPA Analysis are translated outward in time by a few hundred thousand years.

The general trend in the annual dose between the two models is very similar and the peak mean annual dose calculated using the Simplified TSPA Analysis is within approximately half of an order of magnitude as that calculated by the TSPA-LA Model.

7.7.2.3 Seismic Ground Motion Modeling Case

The Seismic Ground Motion Modeling Case evaluates repository performance for those WPs that fail due to the ground motion damage associated with the seismic event. This case begins with the Nominal Modeling Case discussed above and includes the effect of seismic events over a 1,000,000 year period. The occurrence of seismic events is modeled using the approach presented in Section L.2.1. The effects of seismic events on rockfall/drift degradation and seepage are modeled as presented in Sections L.2.2 and L.2.5 respectively. The effects of seismic ground motion on the performance of the DS and WP is modeled as presented in Sections L.2.7.2 and L.2.8.3 respectively.

Figure 7.7.2-7 presents the mean annual dose histories for the Seismic GM Modeling Case using the Simplified TSPA-LA Analysis. Figure 7.7.2-8 also shows the contribution to mean annual dose from the radionuclides that contribute most strongly to the mean annual dose for the Seismic GM Modeling Case using the Simplified TSPA-LA Analysis.

The results shown in Figure 7.7.2-7 indicate that the mean annual dose is similar in magnitude to that obtained for the Seismic GM Modeling Case simulated over a 1,000,000 year period with the TSPA-LA Model shown on Figure 8.2-12. The most significant radionuclides for the Simplified TSPA Analysis initially are ^{129}I and ^{99}Tc, followed by ^{239}Pu dominating until about 300,000 years following repository closure. After 300,000 years ^{242}Pu becomes the dominant radionuclide contributing to the mean annual dose with ^{129}I, ^{99}Tc, ^{237}Np, ^{135}Cs, and ^{229}Th also contributing.

Comparing the results from this Simplified TSPA Analysis shown on Figure 7.7.2-7 with those of the TSPA-LA Model shown on Figure 8.2-12 indicates that the trend in the mean annual dose for the key radionuclides are similar although the magnitude may be slightly different. For example, the TSPA-LA Model results show ^{129}I and ^{99}Tc as the primary contributors to the mean annual dose over a 1,000,000 year period with ^{79}Se, ^{239}Pu, ^{242}Pu, ^{226}Ra, and ^{237}Np contributing to a lesser degree. The Simplified TSPA Analysis results also show ^{129}I and ^{99}Tc as the primary contributors, but ^{229}Th, ^{239}Pu, ^{242}Pu, and ^{237}Np are shown to contribute more to the mean annual dose than is shown in the TSPA-LA Model results. The increased importance of the actinide radionuclides in the Simplified TSPA Analysis is attributed to the simplified treatment of radionuclide transport within the EBS, UZ, and SZ (e.g., neglecting matrix diffusion). In addition, the simplified treatment of radionuclide decay chains leads to an artificially high annual dose from ^{229}Th as discussed in Section 7.7.2.1. These simplifications result in somewhat higher transport of solubility limited and less mobile radionuclides through both the engineered and natural barrier systems and lead to slightly more rapid releases and slightly larger doses for this modeling case as compared to the TSPA-LA Model. However, in general the trends are similar with the mobile radionuclides (^{129}I and ^{99}Tc) being important over the entire 1,000,000 year period with the importance of the less mobile, solubility limited actinides becoming more important at later times.

An estimate of the uncertainty in the annual dose for the Seismic GM Modeling Case using the Simplified TSPA Analysis is shown on Figure 7.7.2-8. The estimate of mean annual dose shown on Figure 7.7.2-8 takes into account uncertainties in the various submodels of this scenario. These uncertainties are addressed in terms of probability distributions for parameters of the submodels. These uncertainties are addressed in the estimate of mean annual dose by evaluating 500 realizations with each realization providing an annual dose that results from one set of values representing the uncertainty. The mean annual dose at a given time is the average for the 500 annual dose values. The range of uncertainty in the annual dose is represented by the 5th and 95th percentiles of those annual dose values for each of 500 realizations.

The mean annual dose results shown on Figure 7.7.2-8 for the Simplified TSPA Analysis are similar to, but slightly higher than those from the TSPA-LA Model shown in Figure 8.2-11. This is further illustrated on Figure 7.7.2-9 which shows a comparison of the Simplified TSPA Analysis results and the TSPA-LA Model results for the Seismic GM Modeling Case at 200,000 years, 400,000 years, 600,000 years, 800,000 years, and 1,000,000 years following repository closure. This is again due to the simplifications applied in the Simplified TSPA Analysis that result in slightly larger EBS releases when WPs are breached, and subsequently higher dose rates.

The Simplified TSPA Analysis results show no annual dose at the 5th percentile whereas, the TSPA-LA Model results for the Seismic GM Modeling Case show doses occurring. In addition, the median annual dose from the Simplified TSPA Analysis shown on Figure 7.7.2-8 is significantly lower than that shown on Figure 8.2-11 for the TSPA-LA Model. This is due to differences in sampling between the two models.

The sampling technique used in the TSPA-LA Model effectively and efficiently takes into account both epistemic and aleatory uncertainty associated with characteristics of future seismic events. The Simplified TSPA Analysis combines aleatory and epistemic uncertainty within the

500 realizations sampled. Thus, the Simplified TSPA Analysis sample size of 500 realizations is not sufficiently large to resolve the 5th and 50th (median) percentiles. However, a sample size of 500 realizations is sufficient to estimate the mean annual dose for the purposes of comparison with that from the TSPA-LA.

In addition, as discussed in Section 7.7.2.2, the WP outer barrier general corrosion rate is lower in the Simplified TSPA Analysis as compared to the TSPA-LA Model. This results in WPs that tend to be more durable under seismic loadings. The predominant mechanism causing damage to the CDSP and CSNF WPs in both the Simplified TSPA Analysis and the TSPA-LA Model, consisted of small cracks that result in releases from the WPs by diffusion. Diffusive transport of dissolved radionuclides through the cracks is high enough to contribute significantly to the mean annual dose.

The sampling technique used in the Simplified TSPA Analysis and the lower rate of general corrosion results in 40 percent of the realizations having no WP failures over the 1,000,000 year simulation period. This is also further illustrated in Figure 7.7.2-9.

Both models demonstrate that the mean annual dose is strongly affected by realizations that cause higher annual doses. This is evident because the mean annual dose is within an order of magnitude of the 95th percentile annual dose.

7.7.2.4 Igneous Intrusion Modeling Case

The Igneous Intrusion Modeling evaluates repository performance for the disruptive event where a volcanic dike intersects the repository. A 1,000,000 year simulation was conducted where a single igneous intrusion event was assumed to randomly occur over the simulation period in each of 500 realizations. All WPs are assumed to be completely failed when the event occurs.

Figure 7.7.2-10 presents the mean annual dose for the Igneous Intrusion Modeling Case using the Simplified TSPA Analysis. Figure 7.7.2-10 also shows the contribution to mean annual dose associated with the radionuclides that contribute most strongly to the mean annual dose for the Igneous Intrusion Modeling Case using the Simplified TSPA-LA Analysis.

The results shown on Figures 7.7.2-10 indicate that the mean annual dose is similar in magnitude to that obtained for the Igneous Intrusion Modeling Case simulated over a 1,000,000 year period with the TSPA-LA Model shown on Figure 8.2-8. The most significant radionuclides for the Simplified TSPA Analysis are ^{129}I, ^{99}Tc, and ^{237}Np for approximately the first 10,000 years following repository closure, followed by ^{239}Pu dominating until about 200,000 years following repository closure, then ^{237}Np and ^{242}Pu, and ^{229}Th. The TSPA-LA Model shows the same trends, but has ^{229}Th being of lesser importance and ^{226}Ra being of greater importance after 200,000 years following repository closure. As discussed in Section 7.7.2.1 above, the increased importance of ^{229}Th is attributed to how its transport in the natural system is being modeled in the Simplified TSPA Analysis.

An estimate of the uncertainty in the distribution of the probability-weighted annual dose for the Igneous Intrusion Modeling Case using the Simplified TSPA Analysis is shown on Figure 7.7.2-11. The estimate of mean annual dose shown on Figure 7.7.2-11 takes into account uncertainties in the various submodels of this scenario in addition to the random sampling of the

time that the intrusion event occurs. These uncertainties are addressed in terms of probability distributions for parameters of the submodels. These uncertainties are addressed in the estimate of mean annual dose by evaluating 500 realizations with each realization providing an annual dose that results from one set of values representing the uncertainty and the sampled number of WPs that experience early failure. Each realization is then weighted by the overall probability of an igneous intrusion event occurring during the 1,000,000 year simulation period. The product of the probability of one igneous intrusion event and the annual dose is termed the probability-weighted annual dose. The mean annual dose at a given time is the average of the 500 probability-weighted annual dose values. The range of uncertainty in the distribution of the probability-weighted annual dose is represented by the 5th and 95th percentiles of those annual dose values for each of 500 realizations.

The results shown on Figure 7.7.2-11 are similar in magnitude as those generated by the TSPA-LA Model shown on Figure 8.2-7 with the Simplified TSPA Analysis yielding slightly higher mean and 95th percentile probability-weighted annual doses. The range of uncertainty is also very similar. The results of both models indicate that the mean annual dose is skewed towards the 95th percentile probability-weighted annual dose. The sampling technique used in the Simplified TSPA Analysis results in only two events being sampled in the 10,000 year period whereas the TSPA-LA approach has much greater resolution during this period. These differences are further illustrated on Figure 7.7.2-12 which shows a comparison of the Simplified TSPA results and the TSPA-LA Model results for this modeling case at 200,000 years, 400,000 years, 600,000 years, 800,000 years, and 1,000,000 years following repository closure.

INTENTIONALLY LEFT BLANK

Table 7.7.2-1. Summary of Modeling Approaches Used for TSPA-LA Model and the Simplified TSPA Analysis

Component Model	TSPA-LA Model		Simplified TSPA Analysis	
	Section	Approach	Section	Approach
Climate	6.3.1	Four climate states, present-day (600 year), monsoon (1,400 year duration), glacial-transition (8,000 year duration), post-10,000 years.	L2.3	Four climate states, present day (600 year), monsoon (1,400 year duration), glacial-transition (8,000 year duration), post-10,000 years.
Infiltration	6.3.1	Four infiltration cases for each climate state with each case weighted.	L2.4	Four infiltration cases for each climate state with each case weighted.
UZ Flow	6.3.1	Three-dimensional flow fields and percolation rate maps at the repository horizon for each infiltration rate and climate state.	L2.4 and L2.16.1	Percolation flux distribution and average percolation rates at the repository horizon.
Emplacement Drift Seepage	6.3.3	Calculates seepage at each of 3,264 repository subdomains. Uses percolation flux at those locations where percolation flux depends on climate state and infiltration rate case. Samples fracture permeability, capillary strength, and flow focusing factor for each subdomain. Uses results to determine seepage rate and seepage fraction for CSNF and CDSP WPs in each of five percolaton subregions. Considers intact and collapsed drift conditions and adjusts seepage rate for drift degradation.	L2.5	Calculates average seepage fraction and seepage rate over the entire repository horizon. Uses percolation flux distribution to determine localized flux at 100 'locations' over the repository horizon. Samples fracture permeability and capillary strength from distributions representing uncertainty and applies them over the entire repository horizon. Samples flow focusing factor at each of 100 'locations'. Considers intact and collapsed drift conditions and adjusts seepage rate for drift degradation.
Drift Wall Condensation	6.3.3	Calculates a probability of condensation occurrence on the drift walls at a WP location and, if condensation occurs, a rate of condensation after all locations in the drift are below the boiling temperature.		Not included.

Table 7.7.2-1. Summary of Modeling Approaches Used for TSPA-LA Model and Simplified TSPA Analysis (Continued)

Component Model	TSPA-LA Model		Simplified TSPA Analysis	
	Section	Approach	Section	Approach
EBS Thermal-Hydrologic Environment	6.3.2	Time histories of • WP temperature • Invert temperature • Drift wall temperature • WP relative humidity • Invert relative humidity • Invert liquid flux (vertical component) • Invert saturation at 3,264 repository subdomains for four different infiltration rate cases •Three levels of host rock thermal conductivity (low, medium, high) • CSNF and CDSP representative WPs. These are categorized into five percolation subregions.	L2.6.1	Considers only WP temperature, determined for one infiltration rate case. To account for spatial variability, the WP temperature time histories for each 3,264 subdomains were used to develop a distribution of WP temperature time history over the entire repository area for the CSNF and CDSP representative WPs and for three levels of host rock thermal conductivity. The average CSNF and CDSP WP temperature histories were also determined for each host rock thermal conductivity.
EBS Chemical Environment	6.3.4	Calculates the time-dependent pCO_2 in the gas phase in the drift above the invert and pH and ionic strength conditions in the invert for each of five percolation subregion. Calculates the chemistry (pH, $[Cl^-]$, and $[NO_3^-]$) of the seepage water from the crown of the drift for the localized corrosion initiation analysis.	L2.6.2	Assumes constant pCO_2 and a range of invert pH over the entire repository, neither change with time.
Drip Shield Degradation - General Corrosion	6.3.5	Calculates DS degradation rate by sampling general corrosion rates for the top- and under-side of the DS. Does not consider spatial variability across DS or on the surface of individual DSs.	L2.7.1	Calculates DS degradation rate by sampling general corrosion rates for the top- and under-side of the DS. Does not consider spatial variability across DS or on the surface of individual DSs.
Drip Shield Degradation - Drip Shield Early Failure	6.4	Samples rate of early DS failure and uses a Poisson distribution to determine the number of DSs that experience early failure. A DS early failure removes the DS as a barrier to seepage at the time of repository closure and allows the full volume of seepage to contact the WP.		Not included.

Table 7.7.2-1. Summary of Modeling Approaches Used for TSPA-LA Model and Simplified TSPA Analysis (Continued)

Component Model	TSPA-LA Model		Simplified TSPA Analysis	
	Section	Approach	Section	Approach
Waste Package Degradation - General Corrosion	6.3.5	Calculates general corrosion penetration on individual CSNF and CDSP WPs within each percolation subregion. The general corrosion rate is sampled and assumed to vary spatially over the surface of the WP. The general corrosion rate also is temperature dependent and a unique WP temperature history is applied to each WP. Samples MIC enhancement factor that increases the general corrosion rate after the relative humidity in the drift exceeds a threshold. A unique WP relative humidity history is applied to each WP. Determines the fraction of WPs that are initially breached as a function of time due to general corrosion and the average number of general corrosion breaches present on breached WPs in each percolation subregion.	L2.8.1.1	Calculates general corrosion penetration on CSNF and CDSP WPs at 100 'locations' over the entire repository area. The general corrosion rate is sampled and assumed to vary over the surface of the WP. The 100 'locations' cover the range of WP temperature histories and the WP temperature at each 'location' is used to determine the temperature dependent general corrosion rate. Samples MIC enhancement factor that increases general corrosion rate after the relative humidity in the drift exceeds a threshold. The relative humidity threshold is assumed to be exceeded at the same time over the entire repository and depends on the WP type (CSNF or CDSP). The host rock thermal conductivity determines the fraction of WPs that are initially breached as a function of time and the average number of general corrosion breaches present on each breached WP over the entire repository.

Table 7.7.2-1. Summary of Modeling Approaches Used for TSPA-LA Model and Simplified TSPA Analysis (Continued)

Component Model	TSPA-LA Model		Simplified TSPA Analysis	
	Section	Approach	Section	Approach
Waste Package Degradation - Stress Corrosion Cracking	6.3.5	Considers both incipient crack initiation and pre-existing (manufacturing defect) weld flaws, the stress conditions (that drive the crack initiation and propagation), the stress threshold (that defines the crack initiation), the threshold stress intensity factor (that defines propagation of both initiated incipient cracks and weld flaws), and the crack growth model (based on the slip dissolution-film rupture theory) that determines the crack growth rate. Calculates whether SCC will occur at individual locations over the circumference of the closure lid weld region for individual locations within each percolation subregion. Samples uncertain parameters associated with SCC (uncertainty in stress conditions and crack growth rate). Applies general corrosion rate model discussed above that accounts for spatial variability in the general corrosion rate over the circumference of the closure lid and spatial variability in the WP temperature. Calculates SCC penetrations that occur on individual WPs within each percolation flux subregion. Determines the fraction of WPs that are initially breached as a function of time due to SCC and the average number of SCC breaches present on breached WPs in each percolation sub-region.	L2.8.1.2	Considers incipient crack initiation, the stress conditions (that drive the crack initiation and propagation), the stress threshold (that defines the crack initiation), the threshold stress intensity factor (that defines propagation of both initiated incipient cracks and weld flaws), and the crack growth model (based on the slip dissolution-film rupture theory) that determines the crack growth rate. Calculates conditions where stress corrosion occurs for average conditions over the circumference of the closure lid weld region. Determines average depth that must be removed by general corrosion before SCC can initiate and propagate. Applies general corrosion model discussed above to determine when SCC occurs. Determines the fraction of WPs that are initially breached as a function of time due to SCC and the average number of SCC breaches present on breached WPs over the entire repository.
Waste Package Degradation - Localized Corrosion	6.3.5	Determines if environmental conditions on the WP outer surface will initiate localized corrosion and lead to WP failure for each repository percolation subregion and WP type.		Not included.
Waste Package Degradation - Waste Package Early Failure	6.4	The uncertain rate of WP early failures was abstracted to a log-normal distribution. For any particular value of the rate of WP early failures, the number of WP early failures is described by a Poisson distribution because WP early failure is independent between packages. Assumes complete failure of the WP, with respect to radionuclide containment, at the time of repository closure.	L2.8.2	The uncertain rate of WP early failures was abstracted to a log-normal distribution. For any particular value of the rate of WP early failures, the number of WP early failures is described by a Poisson distribution because WP early failure is independent between packages. Assumes complete failure of the WP, with respect to radionuclide containment, at the time of repository closure.

Table 7.7.2-1. Summary of Modeling Approaches Used for TSPA-LA Model and Simplified TSPA Analysis (Continued)

Component Model	TSPA-LA Model		Simplified TSPA Analysis	
	Section	Approach	Section	Approach
EBS Flow	6.3.6	Complete diversion of seepage around the WP until the DSs fail, then all seepage contacts the WP. Calculates the fraction of seepage that flows through breaches in WP as a function of the number of general corrosion breaches.	L2.13	Complete diversion of seepage around the WP until the DSs fail, then all seepage contacts the WP. All water flowing through the breached DS is assumed to be diverted around the WP until the first general corrosion breach occurs. Then all water flowing through the breached DS is assumed to flow through the breached WP.
In-Package Chemistry	6.3.7	Quantifes the temporal evolution of values of the aqueous chemistry variables pH, ionic strength, and ΣCO_3 for four different abstraction conditions representing CSNF and CDSP WPs that have water flow through them and CSNF and CDSP WPs that do not have water flow through them in each percolation sub-region.	L2.9	Does not include ionic strength. The in-package pH is sampled and assumed to be constant with time and applicable to both CSNF and CDSP WPs. Calculates ΣCO_3 as a function of time using a constant pCO_2, the sampled pH and the average CSNF WP temperature history.
Cladding Degradation	6.3.7	The cladding of all CSNF and DSNF is assumed to be failed upon arrival at the repository.	L2.11	The cladding of all CSNF and DSNF is assumed to be failed upon arrival at the repository.
CSNF Waste Form Degradation	6.3.7	The instantaneous release fraction is computed as the fraction of cesium, iodine, technetium, and strontium in the total inventory in CSNF fuel that is instantly available for release once cladding is degraded. Calculates the specific or absolute dissolution rate as a function of four independent variables, which vary spatially in the repository: WP temperature in degrees Kelvin, aqueous pH, ΣCO_3, and oxygen fugacity according to the rate law. The four independent variables are determined in each percolation subregion. This results in a time-dependent CSNF waste form degradation rate in each percolation sub-region.	L2.12.1	The instantaneous release fraction is computed as the fraction of cesium, iodine, technetium, and strontium in the total inventory in CSNF fuel that is instantly available for release once cladding is degraded.Calculates the specific or absolute dissolution rate as a function of four independent variables, which do not vary spatially in the repository: WP temperature in degrees Kelvin, aqueous pH, ΣCO_3, and oxygen fugacity according to the rate law. The four independent variables are determined for average repository conditions. This results in a time-dependent CSNF waste form degradation rate representative of repository average conditions.
DSNF Waste Form Degradation	6.3.7	Releases the entire per package DSNF inventory for solubilization and mobilization from the CDSP WPs when the WPs are breached.	L2.11	Releases the entire per package DSNF inventory for solubilization and mobilization from the CDSP WPs when the WPs are breached.

Table 7.7.2-1. Summary of Modeling Approaches Used for TSPA-LA Model and Simplified TSPA Analysis (Continued)

Component Model	TSPA-LA Model		Simplified TSPA Analysis	
	Section	Approach	Section	Approach
DHLW Waste Form Degradation	6.3.7	The rate equation requires the specification of three parameter values: k_E, η, and E_a, and the two model variables, temperature and pH. The parameters kE, h, and Ea are different for acidic and alkaline conditions. Temperature histories are determined in each percolation subregion and pH is determined for dripping and non-dripping conditions in each percolation subregion. The DHLW degradation rate is determined for both acidic and alkaline conditions as a function of time and the maximum of the two is taken as the DHLW degradation rate. This results in a time-dependent DHLW waste form degradation rate in each percolation subregion.	L2.12.2	The rate equation requires the specification of three parameter values: k_E, η, and E_a, and the two model variables, temperature and pH. The parameters k_E, h, and Ea are different for acidic and alkaline conditions. The average CDSP WP temperature history and the sampled pH is determined. The DHLW degradation rate is determined for both acidic and alkaline conditions as a function of time and the maximum of the two is taken as the DHLW degradation rate. This results in a time-dependent DHLW waste form degradation rate representative of repository average conditions.
Dissolved Concentration Limits	6.3.7	The solubility models for americium, neptunium, plutonium, protactinium, thorium, tin, and uranium are in the form of look-up tables with pH and log pCO_2 as the independent variables. Two uncertainty terms accounting for uncertainties associated with thermodynamic properties and variations in water chemistry are also included for this group of elements. Since pH and log pCO_2 vary both spatially and temporally, the dissolved concentration limits also vary spatially (each percolation subregion) and temporally.The remaining elements (technetium, carbon, iodine, cesium, chlorine, selenium, and strontium) are considered highly soluble and no solubility-controlling solids are expected to form under repository conditions.		The solubility models for americium, neptunium, plutonium, protactinium, thorium, tin, and uranium are in the form of look-up tables with pH as the independent variable assuming a constant log pCO_2. A single uncertainty terms accounting for uncertainties associated with thermodynamic properties is also included for this group of elements. Since pH and log pCO_2 are assumed to be constant both spatially and temporally, the dissolved concentration limits do not vary spatially (each percolation sub-region) and temporally.The remaining elements (technetium, carbon, iodine, cesium, chlorine, selenium, and strontium) are considered highly soluble and no solubility-controlling solids are expected to form under repository conditions.
Colloids	6.3.7	Calculates the formation, stability, and concentration of radionuclide bearing colloids in the waste form and WP, as well as sorption of dissolved radionuclides.	L2.15	Not included.

Table 7.7.2-1. Summary of Modeling Approaches Used for TSPA-LA Model and Simplified TSPA Analysis (Continued)

Component Model	TSPA-LA Model		Simplified TSPA Analysis	
	Section	Approach	Section	Approach
EBS Radionuclide Transport	6.3.8	The four EBS transport one-dimensional continuum form mass balance equations are approximated and solved using a finite difference approach: • Transport of dissolved radionuclide species and radionuclide species that are reversibly sorbed onto three types of colloids: iron oxyhydroxide, waste form, and groundwater. • Transport of kinetically (and irreversibly) sorbed radionuclide species on iron oxyhydroxide colloids. • Kinetic sorption of radionuclide species onto stationary corrosion products in the WP. • Transport of embedded (irreversibly sorbed) radionuclide species in waste form colloids. The domains considered are: • CSNF: CSNF Waste Form, CSNF Corrosion Product, Invert underlying CSNF WPs • CDSP: DHLW Waste Form, DSNF Waste Form, DHLW Corrosion Product, Invert underlying CDSP WPs. These domains are represented as cell networks in each percolation subregion for dripping and non-dripping conditions. The number of cell pathways in the finite difference network and the discretization of the cells are chosen to capture the physical and chemical properties of the EBS components with respect to radionuclide transport. Both advective and diffusive transport mechanisms are explicitly represented. Linking of cells results in a coupled system of differential equations that is mathematically equivalent to a finite difference network.	L2.15	The EBS transport one-dimensional continuum form mass balance equation for dissolved radionuclide species is approximated and solved using a simplified explicit-in-time approach for a each domain: • CSNF: CSNF Waste Form, CSNF Corrosion Product, Invert underlying CSNF WPs • CDSP: DHLW Waste Form (DSNF inventory assumed to be in DHLW), DHLW Corrosion Product, Invert underlying CDSP WPs. These domains are represented as cell networks in a single representation of repository average conditions for seeping and non-seeping conditions. Advective and diffusive transport mechanisms are approximately represented. Key differences between the TSPA-LA Model and the Simplified TSPA Analysis are: • No radionuclide sorption onto stationary corrosion products. • No relative humidity threshold for radionuclide transport within the CSNF waste form cells • All EBS media are assumed to be fully saturated.

Table 7.7.2-1. Summary of Modeling Approaches Used for TSPA-LA Model and Simplified TSPA Analysis (Continued)

Component Model	TSPA-LA Model		Simplified TSPA Analysis	
	Section	Approach	Section	Approach
UZ Transport	6.3.9	Utilizes a three-dimensional dual-continuum model that includes a numerical grid of fracture cells representing the fracture continuum and a grid of matrix cells representing the matrix continuum, with each fracture cell connected to a corresponding matrix cell. The following processes are simulated: • Advective transport of dissolved and colloidal-bound radionuclides in the fracture and matrix continua utilizing three-dimensional flow fields • Longitudinal dispersion • Sorption of dissolved radionuclides to the matrix continuum (linear, equilibrium sorption model) • Matrix diffusion • Retardation of irreversible and reversible colloids in the fracture continuum • Colloid filtration at interfaces between rock-matrix units • Colloid size exclusion at fracture matrix continua interfaces • Radioactive decay and ingrowth • Climate change and its effect on fluid flow rates in the UZ • Climate change and associated rise in water table elevation and its effect on radionuclide release to the SZ.	L2.16.1	Utilizes a simplified one-dimensional solution of the advective-dispersive transport for radionuclides transported in the rock matrix. Assumes rapid transport of radionuclides in the fracture continuum. Discretizes the UZ underneath the repository into three layers with average properties. Determines the fraction of radionuclides transported in the matrix and fractures using the average percolation flux over the repository horizon. Includes the following processes: • Advective transport of dissolved and colloidal-bound radionuclides in the fracture and matrix continua utilizing a simplified approach • Longitudinal dispersion in the matrix continuum • Sorption of dissolved radionuclides to the matrix continuum (linear, equilibrium sorption model) • Radionuclide decay and ingrowth Processes not included are: • Matrix diffusion • Colloids are not included • UZ fluid flow rates for post-10,000 year climate state only • Change in water table elevation
SZ Transport	6.3.10	Utilizes the results of three-dimensional SZ flow and transport modeling to calculate the flow and transport through the SZ to the accessible environment for individual radionuclides important to dose. The output from the three-dimensional SZ Flow and Transport Process Model is developed in the form of unit source radionuclide breakthrough curves that are combined with the time varying radionuclide sources from the UZ using a convolution integral technique to quantify radionuclide transport to the accessible environment.Utilizes a one-dimensional SZ Flow and Transport Model to calculate the radioactive decay, ingrowth, and transport for four decay chains.	L2.16.2	Utilizes a simplified one-dimensional solution of the advective-dispersive transport for radionuclides transported in the SZ. This approach is identical to that used to model UZ radionuclide transport.

Table 7.7.2-1. Summary of Modeling Approaches Used for TSPA-LA Model and Simplified TSPA Analysis (Continued)

Component Model	TSPA-LA Model		Simplified TSPA Analysis	
	Section	Approach	Section	Approach
Biosphere	6.3.11	Utilizes BDCF distributions for the present-day climate state.	L2.17	Utilizes BDCF distributions for the present day climate state.
Igneous Intrusion	6.5	Utilizes the nominal scenario model with the following modifications: • All DSs and WPs are failed when the igneous intrusion event occurs • Local seepage rate equals the local percolation flux.	L2.18	Utilizes the nominal scenario model with the following modifications: • All DSs and WPs are failed when the igneous intrusion event occurs • The seepage rate equals the average seepage rate for collapsed drift conditions.
Seismic Mechanical Damage	6.6	Utilizes the nominal scenario model with the following additional models included: • Rockfall - the amount of rock that falls into the emplacement drifts is determine as a function of the peak ground velocity for the seismic event • Seepage - the amount of rock that accumulates in the emplacement drifts determines whether intact or collapsed drift seepage conditions are used • DS damage - determines whether the DSs fail either due to failure of the DS plates or DS frame structure. Failure of the DS in response to a seismic event renders all DSs failed as a barrier to seepage DS damage - determines the state of damage to the WP outer barrier due to vibrational ground motion or due to rockfall (when the DS fails). Calculates the area of the WP outer barrier damaged due to SCC.	L2.1 L2.2 L2.7.2 L2.8.3	Utilizes the nominal scenario model with the following additional models included: •Rockfall - the amount of rock that falls into the emplacement drifts is determined as a function of the peak ground velocity for the seismic event •Seepage - the amount of rock that accumulates in the emplacement drifts determines whether intact or collapsed drift seepage conditions are used •DS damage - determines whether the DSs fail either due to failure of the DS plates or DS frame structure. Failure of the DS in response to a seismic event renders all DSs failed as a barrier to seepage DS damage - determines the state of damage to the WP outer barrier due to vibrational ground motion or due to rock fall (when the DS fails). Calculates the area of the WP outer barrier damaged due to SCC. Simpler approaches are used to determine seismic consequences as compared to the TSPA-LA

INTENTIONALLY LEFT BLANK

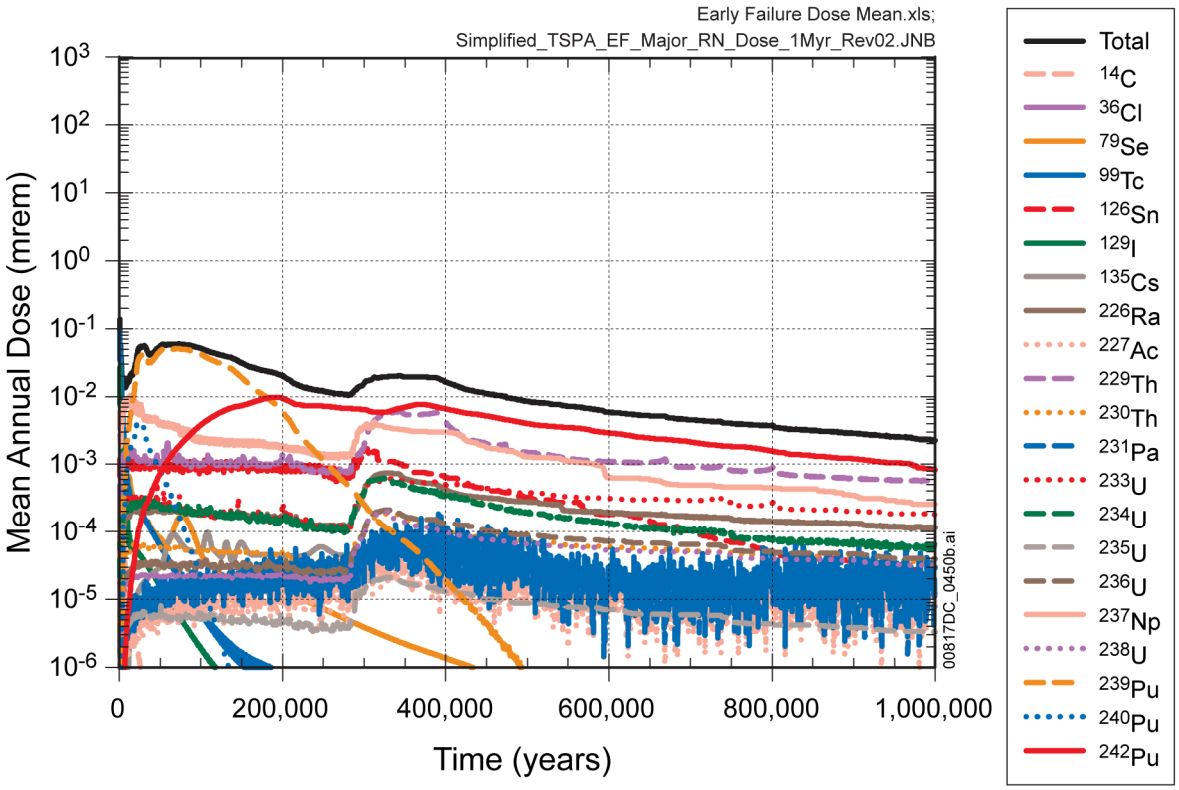

Source: Corroborative DTN: MO0708SIMPLIFI.000 [DIRS 182980].

Figure 7.7.2-1. Mean Annual Dose and Annual Dose for Individual Radionuclides for the Simplified TSPA Analysis Waste Package Early Failure Modeling Case for 1,000,000 Years after Repository Closure

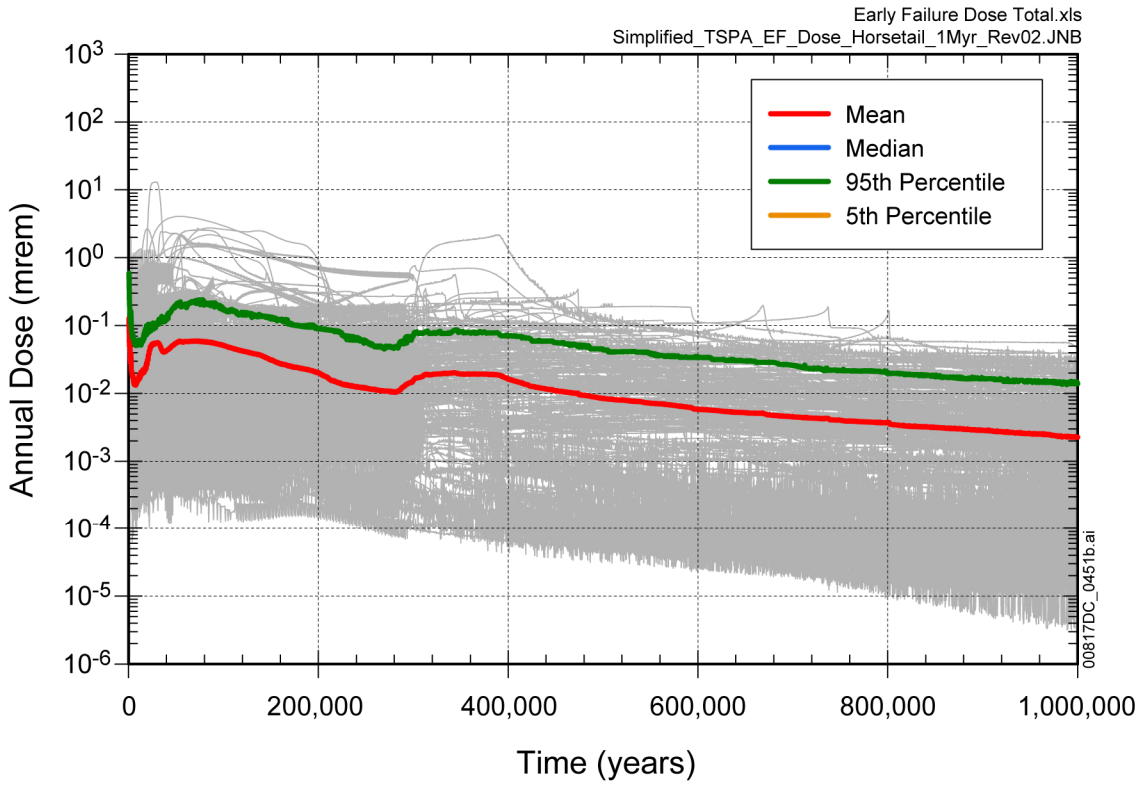

Source: Corroborative DTN: MO0708SIMPLIFI.000 [DIRS 182980].

Figure 7.7.2-2. Annual Dose for the Simplified TSPA Analysis Waste Package Early Failure Modeling Case for All Realizations for 1,000,000 Years after Repository Closure

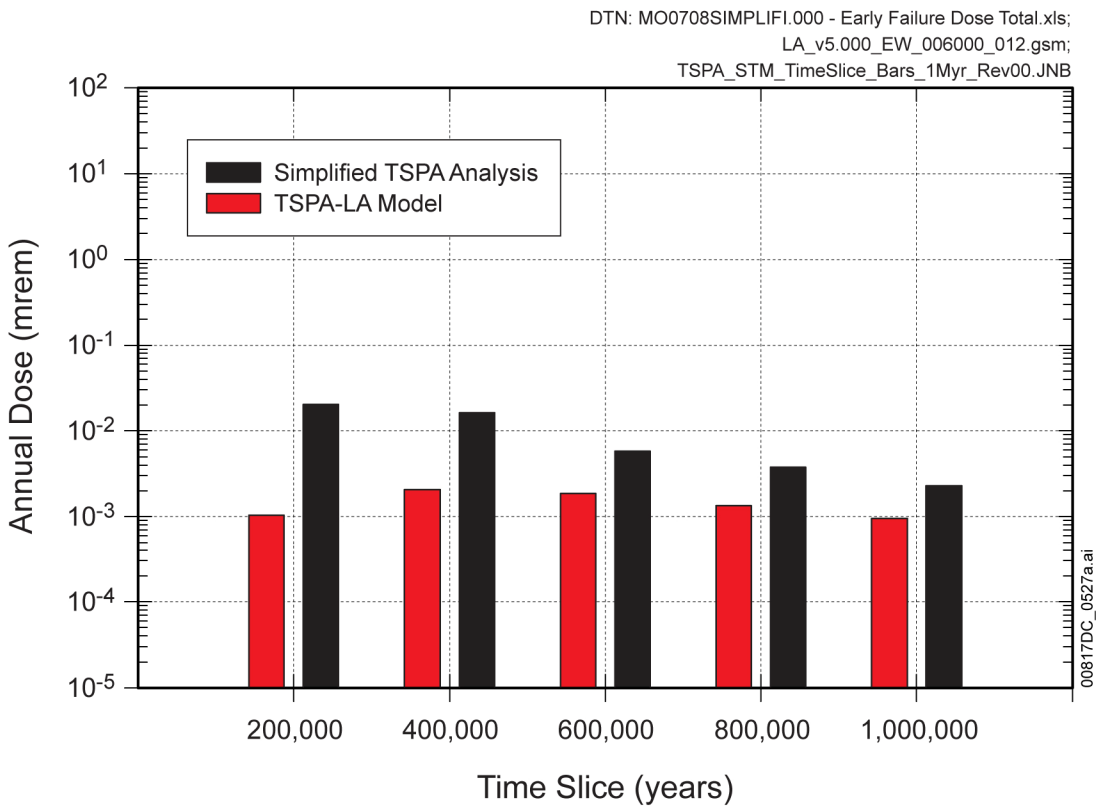

Source: Corroborative DTN: MO0708SIMPLIFI.000 [DIRS 182980]; and Output DTN: MO0709TSPAREGS.000 [DIRS 182976].

Figure 7.7.2-3. Time-Slice Comparison of the Simplified TSPA Analysis Results against the TSPA-LA Model Results for the Waste Package Early Failure Modeling Case

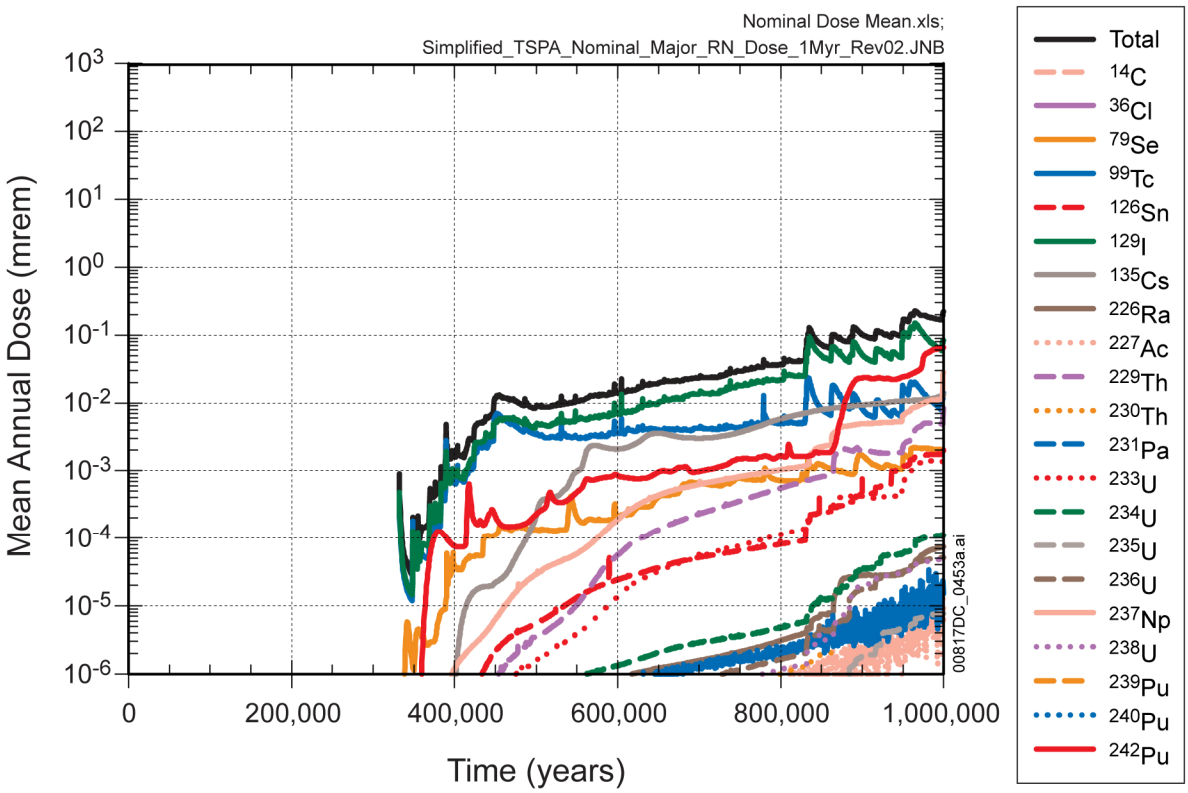

Source: Corroborative DTN: MO0708SIMPLIFI.000 [DIRS 182980].

Figure 7.7.2-4. Mean Annual Dose and Annual Dose for Individual Radionuclides for the Simplified TSPA Analysis Nominal Modeling Case

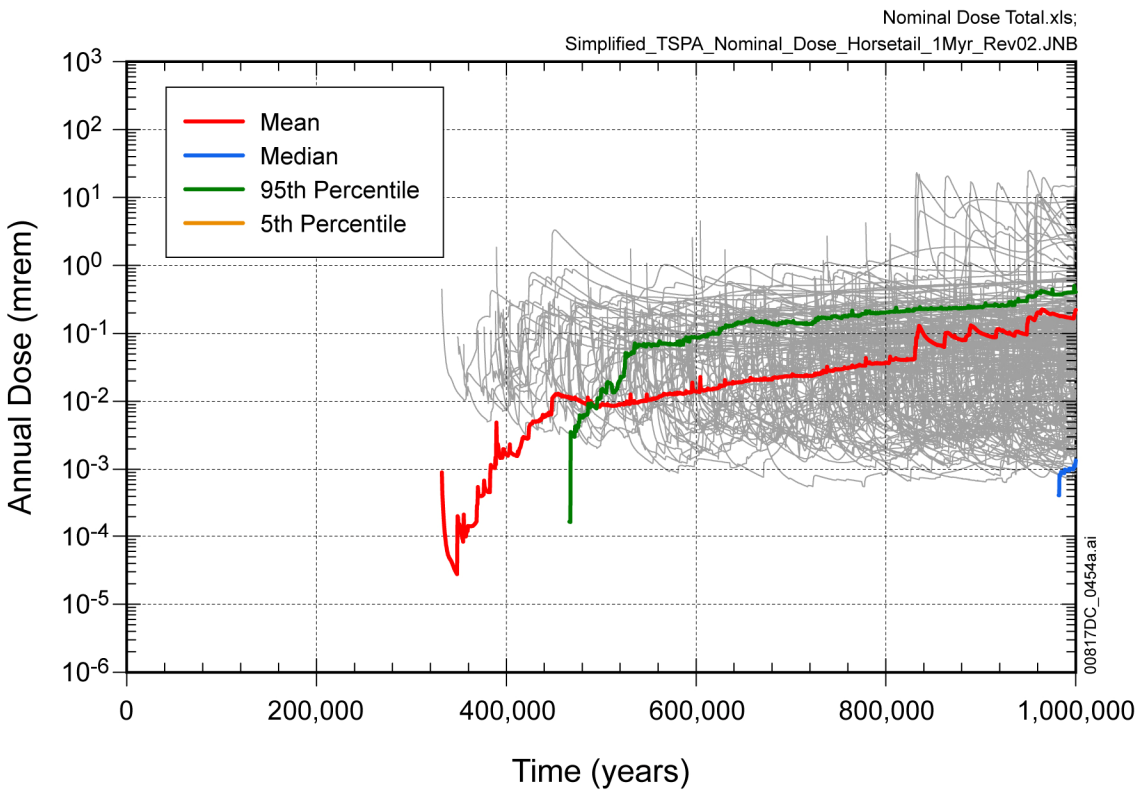

Source: Corroborative DTN: MO0708SIMPLIFI.000 [DIRS 182980].

Figure 7.7.2-5. Annual Dose for the Simplified TSPA Analysis Nominal Modeling Case

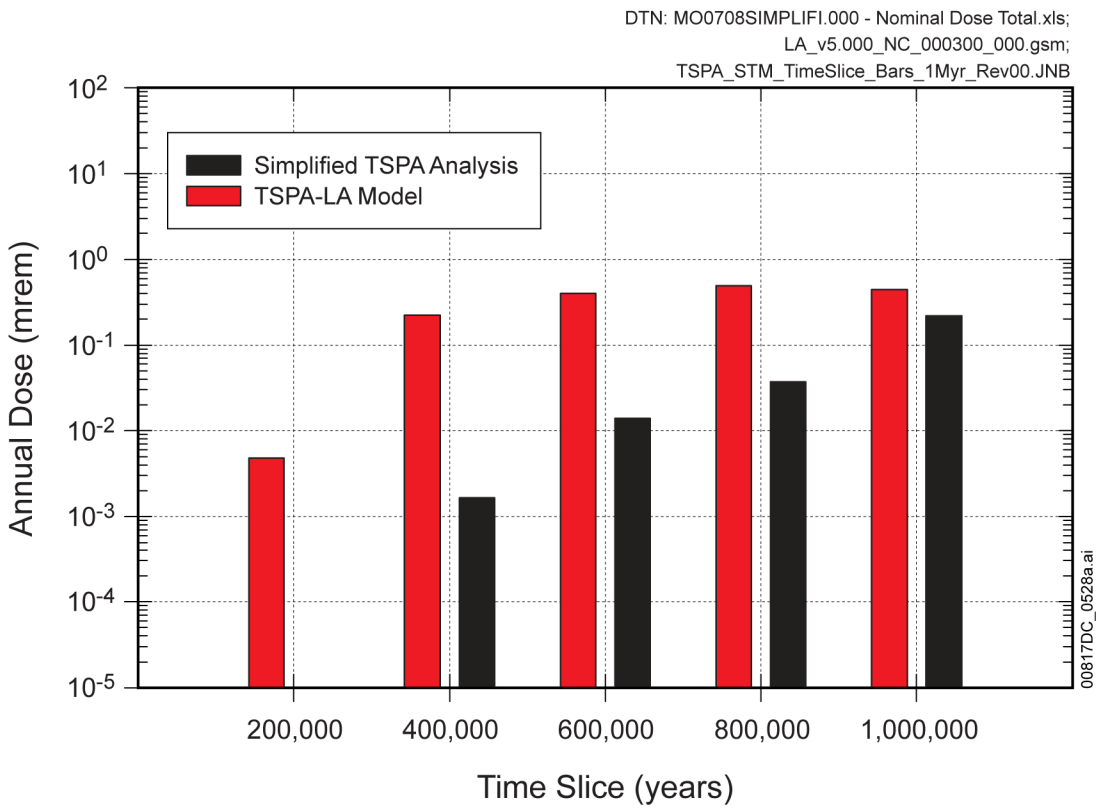

Source: Corroborative DTN: MO0708SIMPLIFI.000 [DIRS 182980]; and Output DTN: MO0709TSPAREGS.000 [DIRS 182976].

Figure 7.7.2-6. Time-Slice Comparison of the Simplified TSPA Analysis Results against the TSPA-LA Model Results for the Nominal Modeling Case

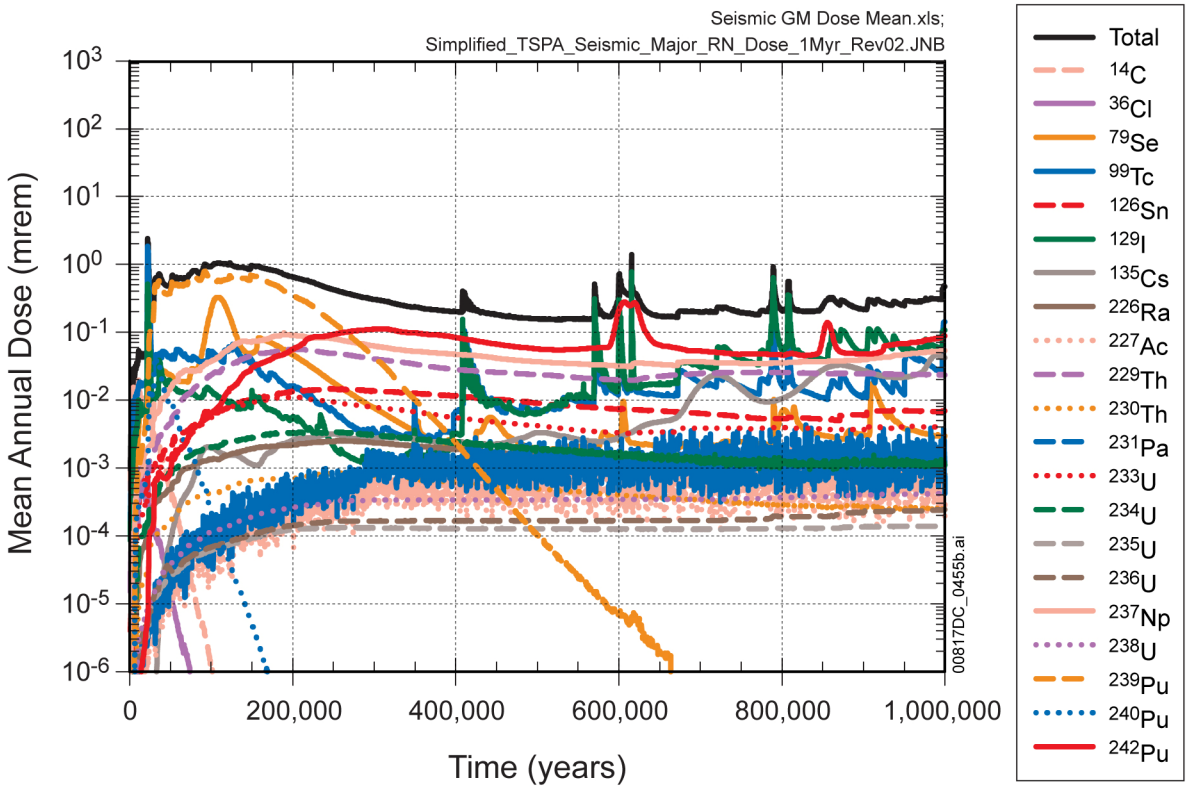

Source: Corroborative DTN: MO0708SIMPLIFI.000 [DIRS 182980].

Figure 7.7.2-7. Mean Annual Dose and Annual Dose for Individual Radionuclides for the Simplified TSPA Analysis Seismic Ground Motion Modeling Case for 1,000,000 Years after Repository Closure

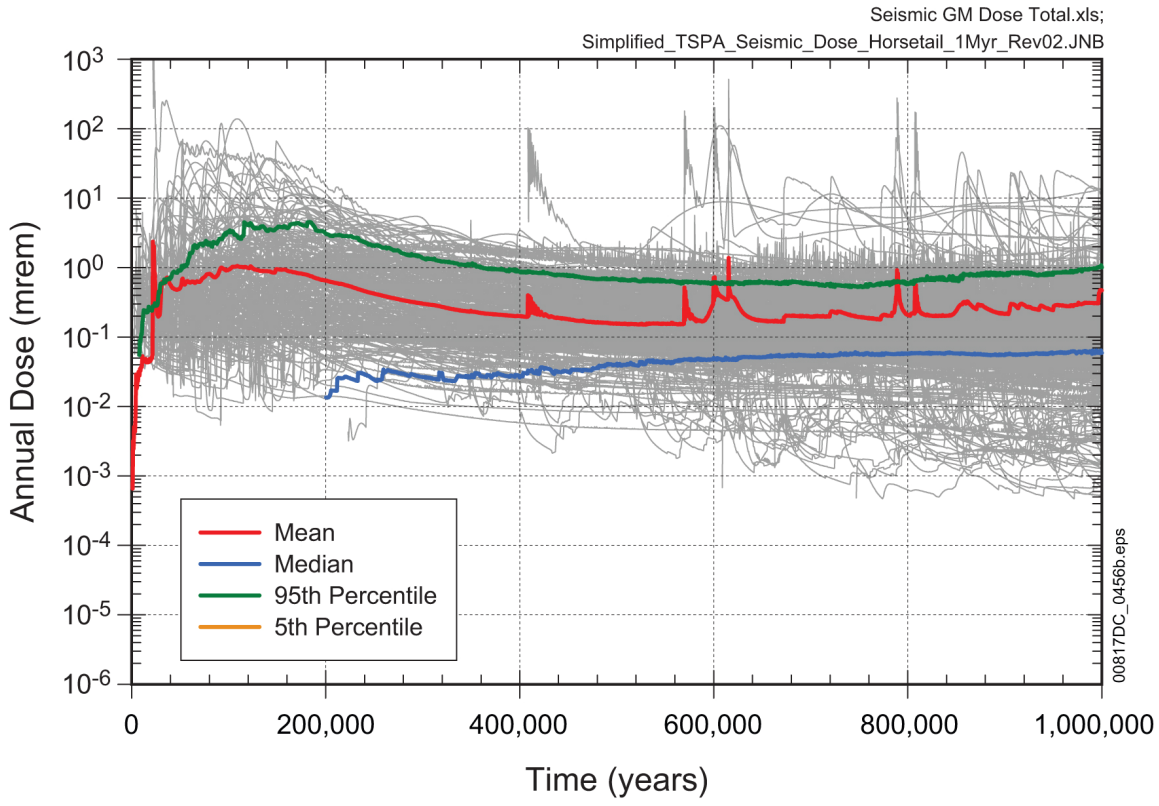

Source: Corroborative DTN: MO0708SIMPLIFI.000 [DIRS 182980].

Figure 7.7.2-8. Mean Annual Dose and Annual Dose for Individual Radionuclides for the Simplified TSPA Analysis Seismic Ground Motion Modeling Case for 1,000,000 Years after Repository Closure

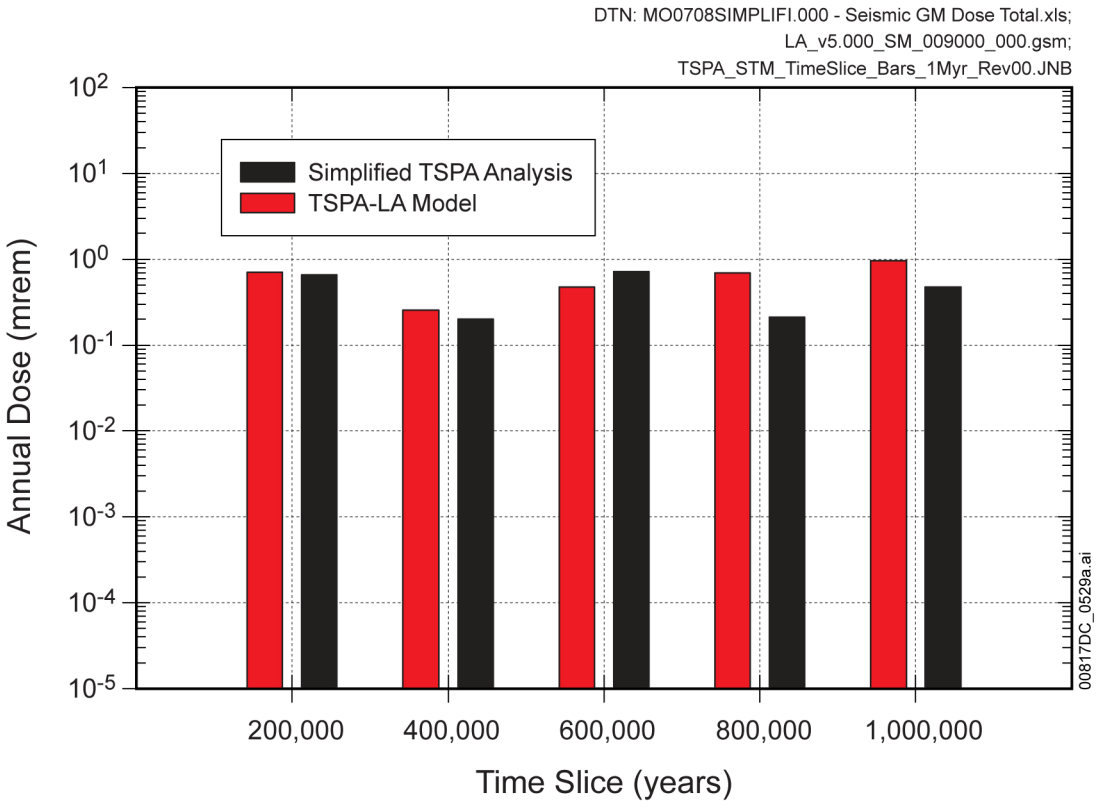

Source: Corroborative DTNs: MO0708SIMPLIFI.000 [DIRS 182980]; and Output DTN: MO0709TSPAREGS.000 [DIRS 182976].

Figure 7.7.2-9. Time-Slice Comparison of the Simplified TSPA Analysis Results against the TSPA-LA Model Results for the Seismic Ground Motion Modeling Case

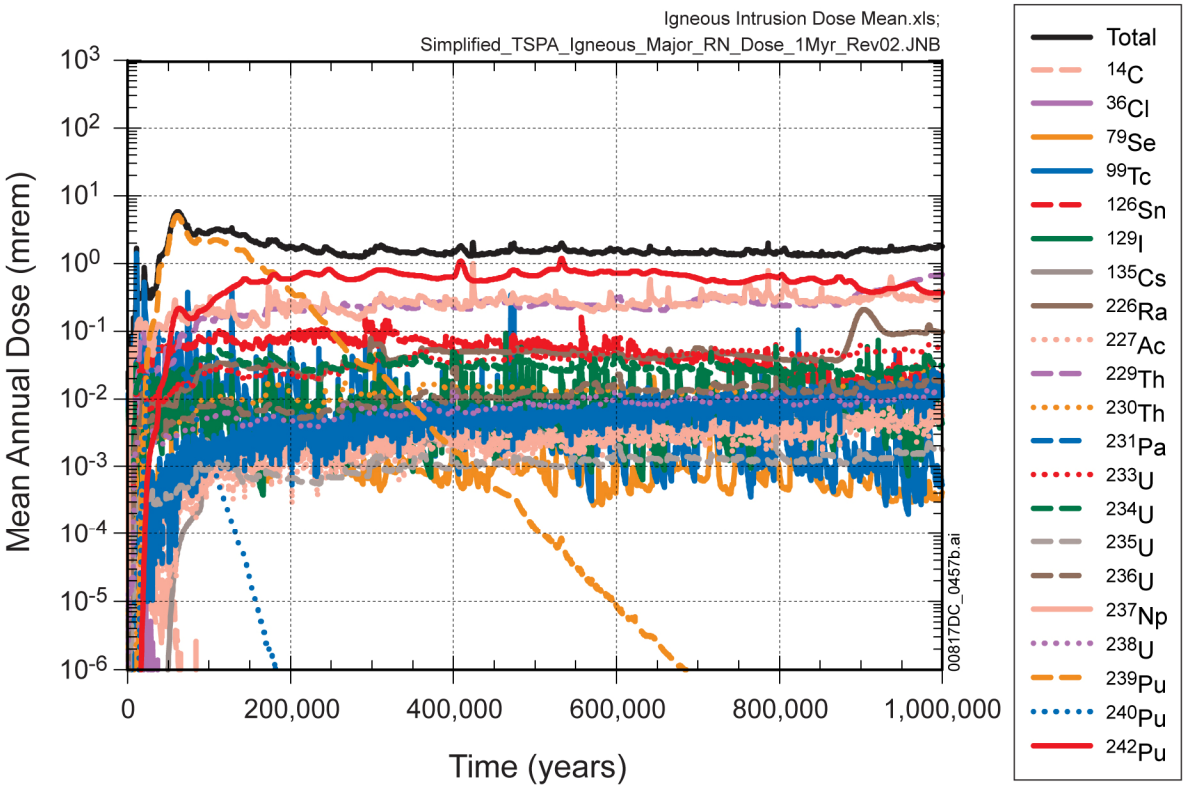

Source: Corroborative DTN: MO0708SIMPLIFI.000 [DIRS 182980].

Figure 7.7.2-10. Mean Annual Dose and Annual Dose for Individual Radionuclides for the Simplified TSPA Analysis Igneous Intrusion Modeling Case for 1,000,000 Years after Repository Closure

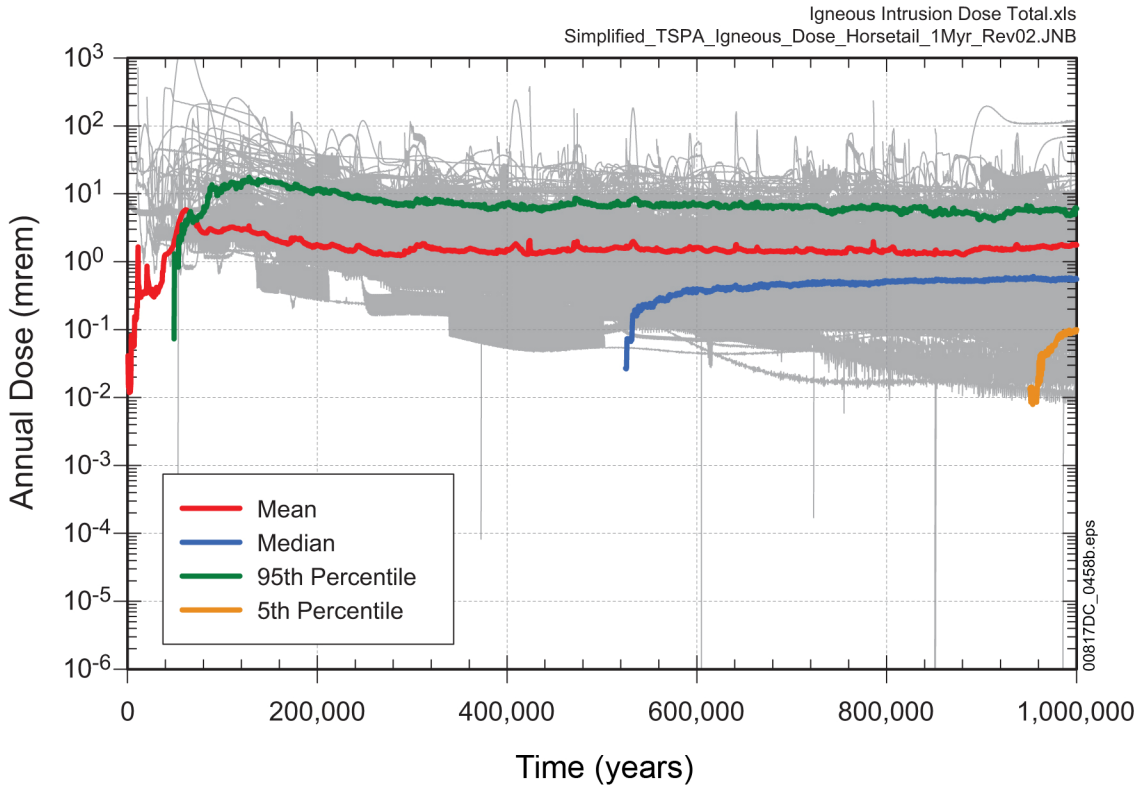

Source: Corroborative DTN: MO0708SIMPLIFI.000 [DIRS 182980].

Figure 7.7.2-11. Mean Annual Dose and Annual Dose for Individual Radionuclides for the Simplified TSPA Analysis Igneous Intrusion Modeling Case for 1,000,000 Years after Repository Closure

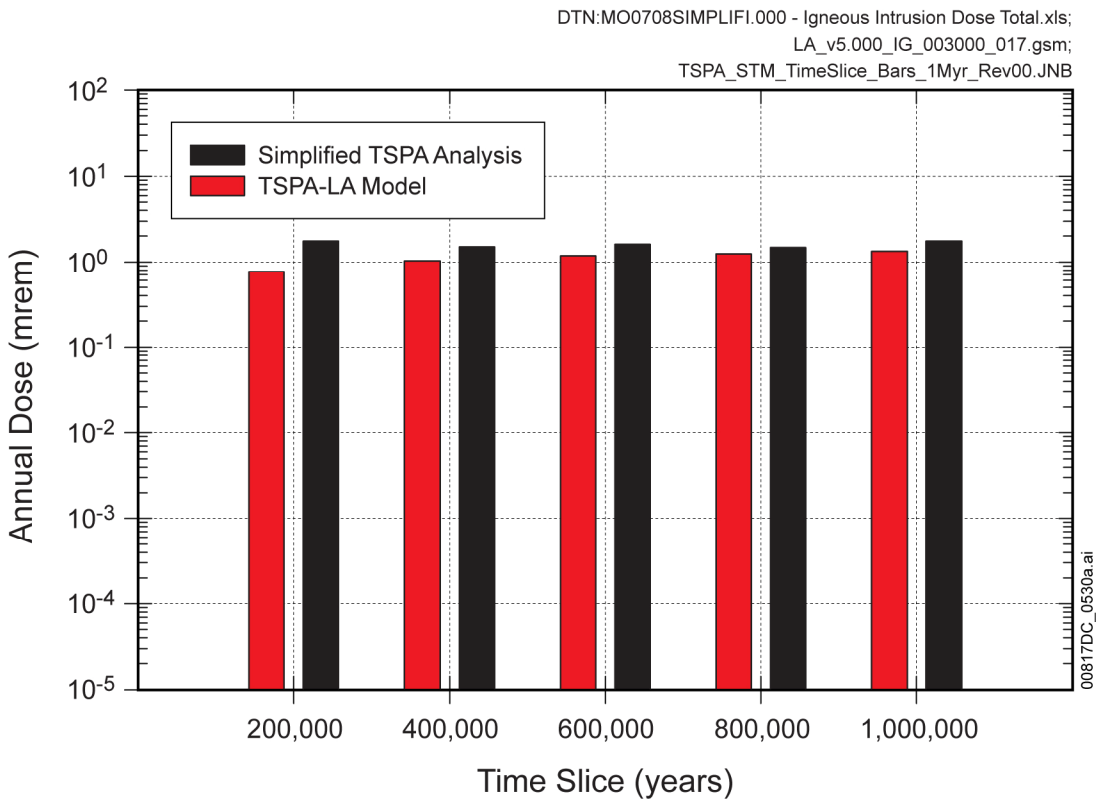

Source: Corroborative DTNs: MO0708SIMPLIFI.000 [DIRS 182980]; and Output DTN: MO0709TSPAREGS.000 [DIRS 182976].

Figure 7.7.2-12. Time-Slice Comparison of the Simplified TSPA Analysis Results against the TSPA-LA Model Results for the Igneous Intrusion Motion Modeling Case

7.7.3 Comparison with Electric Power Research Institute Analysis

7.7.3.1 Introduction and Purpose

The Electric Power Research Institute (EPRI) has been conducting assessments of the total system performance of the candidate radioactive waste repository at Yucca Mountain, Nevada (Apted and Ross 2005 [DIRS 182229]). The objective of the EPRI's TSPA Analysis is to provide an independent third-party assessment of key technical and scientific issues associated with the proposed geologic repository at Yucca Mountain. The EPRI TSPA Analysis was developed by an independent organization, based on independently developed methodology and its own total systems performance code, IMARC (Kozak and Kessler 2005 [DIRS 178580]).

This section gives a summary of the comparison between the EPRI TSPA Analysis and the TSPA-LA Model. The purpose of the comparison is to use the EPRI model as another auxiliary analysis to satisfy the post-development validation criterion related to auxiliary analyses. This section includes a general overview of the EPRI TSPA and briefly describes the main features of the different model components, which are presented in more detail in Appendix M. The main results in terms of dose history curves from the EPRI and TSPA-LA Model are compared and apparent differences are discussed. The main features of the computed dose release curves for the nominal scenario in the EPRI TSPA Analysis compare reasonably well with the TSPA-LA Model, and differences can be related to different treatment of seepage, inventory, and EBS failure characteristics.

These differences are mostly due to the fact that the EPRI TSPA does not incorporate the most recent updates of analysis and/or model reports which are included in the TSPA-LA Model. That is, most of the input to the EPRI TSPA Analysis corresponds to an earlier version of the TSPA Model. As a result, a direct comparison between the results from the EPRI TSPA Analysis and from the TSPA-LA Model is not possible. However, the overall features of the dose history curves can be compared and, together with evaluating the apparent differences, provides a validation of the general methodology and strategy used in the TSPA-LA Model.

7.7.3.2 Overview of the TSPA Models

The overall conceptual approach of the IMARC and the basic elements of the analysis method are similar to the TSPA-LA approach as depicted on Figure 6.1.5-9 in Section 6.1.5. The differences between IMARC and the TSPA-LA Model are in the details of the implementation and the specifics of the assumptions, models, parameters, and couplings used. The EPRI TSPA Analysis has evolved over the years updating to the Yucca Mountain regulations, the disposal system design, and conceptual understanding of the proposed repository. However, most of the input into the EPRI TSPA Analysis corresponds to that used in the earlier version of the TSPA-LA Model.

The EPRI TSPA Analysis represents a more simplified implementation of the various process models and associated uncertainties compared to the TSPA-LA Model. The EPRI TSPA Analysis implemented a logic-tree approach and the TSPA-LA approach uses a Monte-Carlo sampling approach, which represent two ends of a spectrum of TSPA analysis methods. The EPRI TSPA Analysis uses a logic-tree approach for quantifying the impacts of model and

parameter uncertainty in the TSPA calculations. Logic-tree analysis is used for uncertainty propagation of parameters, which are described using a limited number of probable states (e.g., high, medium, and low values), and their likelihoods (Kozak and Kessler 2005 [DIRS 178580], Figure 2-3). In addition, the Monte Carlo simulation method is used to generate cumulative probability distributions for WP and DS degradation and for BDCFs.

The TSPA-LA Model accounts for the epistemic uncertainty of parameters, model components, and/or assumptions by sampling uncertainty distributions of large numbers of parameters or model inputs using Monte Carlo simulations. Furthermore, the TSPA-LA Model accounts for aleatory uncertainty associated with spatial variability of infiltration and seepage and timing of igneous and seismic events. The spatial variability in infiltration and seepage is represented by different percolation subregions).

The EPRI TSPA Analysis does not consider aleatory uncertainty. The EPRI TSPA Analysis assumes fixed times for the occurrence of igneous and seismic events. The EPRI TSPA Analysis does not account for spatial variability of infiltration, but assumes spatially uniform infiltration and accounts for uncertainty in infiltration rates in the logic-tree analysis, using high, medium, and low infiltration rates, each having a different probability.

Similar to TSPA-LA Model, the EPRI TSPA Analysis considers different scenarios, which include nominal, igneous, a seismic scenario and a human intrusion scenario, although the human intrusion scenario has only been studied in a preliminary fashion. Both the EPRI TSPA Analysis and TSPA-LA Model account for corresponding model components, which are summarized in Table 7.7.3-1.

The focus of the comparison described here between the EPRI TSPA Analysis and TSPA-LA Model is on the Nominal Scenario Class. The following sections summarize the implementation of the different model components in the EPRI TSPA Analysis for comparison with the TSPA-LA Model, which is described in detail in Section 6. Given the differences in the TSPA approaches implemented in the EPRI TSPA Analysis and in the TSPA-LA, it builds confidence when the two approaches yield similar results, or if the differences in the results can be explained based on the different assumptions and models underlying the two TSPAs.

7.7.3.3 Unsaturated Zone Flow

In the EPRI TSPA Analysis, the UZ flow above the repository is not represented by a process model as in the TSPA-LA Model, but is represented via lumped parameters incorporating time history of infiltration accounting for different climate states, flow focusing factor accounting for focused flow along fractures, and seepage into the repository. Infiltration rates for the different climate states used in the EPRI TSPA Analysis (Table M-1) compare reasonably well with the weighted mean infiltration rates used in the TSPA-LA Model (Table M-2). The seepage rates used in the EPRI TSPA Analysis (Table M-3a) are based on computed seepage and fraction of the repository experiencing flowing water summarized in *Abstraction of Drift Seepage* (CRWMS M&O 2001 [DIRS 154291], Table 16). A comparison of the seepage rates given in Table M-3a with those given in the recent analysis and/or model report (Table M-3b) indicates that the seepage rates used in the EPRI TSPA Analysis are significantly lower than those in the TSPA-LA Model (Figure 7.7.3-1).

7.7.3.4 Engineered Barrier System Environment

The EPRI TSPA Analysis neglects thermal effects on water flow, release, and migration of radionuclides for the nominal scenario. It is assumed that there is little to no liquid water present to facilitate radionuclide mobilization and migration until temperatures have decreased to near the local boiling point of water. However, failure distributions generated for each of the three main engineering barrier system components, (i.e., DS, WP, and cladding) do take into account thermal history within the drift and drift stability due to thermal stresses.

7.7.3.5 Waste Package and Drip Shield Degradation

The EBS Corrosion Model is used in the EPRI TSPA Analysis to compute failure distributions for the different components of the EBS, which comprises three versions for the nominal, seismic, and igneous scenarios. The EBS Corrosion Model accounts for various failure mechanisms and uncertain parameters that are sampled using Monte Carlo simulations to produce mean failure distribution curves for the DS, WP, and cladding. These mean failure distribution curves are used as input in the near-field model, which is described in greater detail in Appendix M. The current TSPA-LA Model does not take credit for cladding; that is, radionuclides can be released as soon as the WP starts to fail. The EPRI TSPA Analysis accounts for cladding failure for dripping and non-dripping conditions following WP failure.

The computed failure distributions curves for the nominal scenario for the DS and WP are shown on Figure 4-5 in Apted and Ross (2005 [DIRS 182229]). In comparison, the mean WP and DS failure curves for the TSPA-LA Nominal Scenario Class (Figure 7.7.3-2) indicate a later failure onset but a steeper curve, where 6,256 WPs failed after one-million years. The EPRI TSPA Analysis only considers 8,160 CSNF WPs, of which about 5,304 WPs fail after one-million years.

The EPRI TSPA Analysis accounts for early failure whereby one WP and one DS are assumed to fail initially from a manufacturing defect. The probability of a joint failure of a WP and a DS at the same location is not considered, due to an extremely low probability.

7.7.3.6 Waste Form Degradation and Mobilization

Waste form degradation and mobilization is computed as part of the near-field radionuclide release and transport submodel COMPASS (Compartment Model for Partially Saturated Repository Source Terms) in IMARC, which is described in greater detail in Appendix M. Radionuclides dissolve into water congruently with waste form degradation rate subject to the cladding failure rate. Uncertainty in waste form degradation rates is accounted for in the logic-tree analysis; using alteration times of 1,000 years, 3,000 years, and 5,000 years and associated probabilities of 0.05, 0.9, and 0.05 respectively (Kozak and Kessler 2005 [DIRS 178580], Figure 2-3).

The EPRI TSPA Analysis accounts for gradual cladding failure whereby the fraction of radionuclides, in the gap and grain boundaries of the spent fuel, dissolve instantaneously into water. For specific radionuclides bound in the waste form, the release of radionuclides in water is constrained by solubility limits. The ranges in solubility limits used in TSPA-LA Model and in the EPRI TSPA Analysis are summarized in Table M-4. In the EPRI TSPA Analysis, the

uncertainty in the solubility limits represented by low, moderate, and high values is linked to the probabilities for the alteration times of the waste form degradation. Overall, the median solubility limits used in the EPRI TSPA Analysis fall within the range of those used in the TSPA-LA Model, except for neptunium which is slightly below the range given in TSPA-LA Model (Table M-4).

The EPRI TSPA Analysis only considers CSNF WPs and the associated inventory, whereby the inventory is based on that given in *Initial Radionuclide Inventories* (SNL 2007 [DIRS 180472], Table 7-1). Furthermore, the EPRI TSPA Analysis considers only 12 radionuclides which were identified to have a significant contribution to total dose. The inventory used in the EPRI TSPA Analysis in comparison with that used in the current TSPA-LA Model (Table M-5) indicates that the total inventory per WP compares well with that for CSNF in the TSPA-LA Model. The inventory for DSNF and HLW, which is not considered in the EPRI TSPA Analysis, amounts to about 12.5 percent of the inventory of a CSNF WP. The EPRI TSPA Analysis accounts for 8,160 CSNF WPs, whereas the TSPA-LA Model considered 8,203 CSNF WPs and 3,413 CDSP WPs containing DSNF and HLW.

7.7.3.7 Engineered Barrier System Flow and Transport

In the EPRI TSPA Analysis, radionuclides are transported by diffusion and advection through the near-field, which is comprised of a series of compartments including waste, corrosion products, a pallet or basalt layer, and invert, and the near-field rock matrix and fracture (Table 7.7.3-1). The radionuclide transport in the EBS is computed in the near-field radionuclide release and transport submodel. The computed radionuclide release rates from the near-field to the far-field UZ is then used as boundary conditions for the unsaturated-zone submodel simulating radionuclide transport in the UZ below the repository. The EBS flow and transport implemented in the TSPA-LA Model is described in detail in Section 6.3.6 and 6.3.8.

7.7.3.8 Unsaturated Zone Transport

The EPRI TSPA Analysis flow and transport of the UZ below the repository is simulated by the IMARC submodel 'UZ-code' which is represented by several one-dimensional vertical columns approximating spatial variations of repository releases and different lengths corresponding to spatial and temporal variations in the water table. The vertical discretization distinguishes the main UZ layers, which are each discretized in greater detail. The model accounts for variations in saturations associated with variations in permeability, capillary pressure, porosity, and fracture spacing for both fractures and matrix in each geologic layer. Transport of radionuclides accounts for dispersion, decay, diffusion, and sorption. Uncertainty in sorption in the UZ is represented in the logic tree approach as retardation (Kozak and Kessler 2005 [DIRS 178580], Figure 2-3) which includes sorption in the SZ. In the EPRI TSPA Analysis, sorption coefficients (K_d) are defined for specific radionuclides for volcanic rocks in the UZ and SZ and for the alluvium in the SZ. Only for neptunium are sorption coefficients given for individual layers and as low, median, and high values represented in the logic-tree analysis. A comparison of the K_d values used in the EPRI TSPA Analysis and in the TSPA-LA Model is given in Table M-6. Median K_d values for uranium, plutonium, and thorium are significantly lower in the EPRI TSPA Analysis compared to the median values in the TSPA-LA Model, whereas the Kd value for neptunium is only slightly greater.

7.7.3.9 Saturated Zone Transport

The SZ submodel in the EPRI TSPA Analysis (SZ code) consists of two segments, representing the fractured tuff (15 km downgradient) and the other subsequent alluvial segment (5 km), which is 2 km beyond the location of the RMEI. For transport simulation in the tuff, the model considers steady-state groundwater flow in the fracture only. Boundary conditions for the transport simulation include prescribed mass fluxes from the UZ model along the footprint of the repository, and infiltration (boundary condition Type III, Cauchy condition) is prescribed along the entire water table. Similar to the UZ model, transport is affected by fracture flow and sorption in the tuff and in the alluvium. Uncertainty in the K_d values in the SZ is included in the logic-tree analysis that is combined with the UZ Kds. A comparison of the sorption coefficients between those used in the EPRI TSPA Analysis and those used in TSPA-LA Model are summarized in Table M-7. In general, median K_d values are similar for both fractured volcanic rocks and alluvium between the EPRI TSPA Analysis and TSPA-LA Model.

7.7.3.10 Biosphere

The conversion of radionuclide concentration to dose is through the BDCFs for the RMEI living approximately 18 km downstream of the repository. For this, a representative volume of 3,000 acre-feet per year for consumption by the RMEI is assumed. The BDCFs used in the EPRI TSPA Analysis and those used in the TSPA-LA Model are compared in Table M-8. Overall, the EPRI BDCFs are higher than those used in TSPA-LA Model, which would result in higher doses in the EPRI TSPA Analysis for the same concentration.

7.7.3.11 Mean Annual Dose Comparison—Nominal Case

The computed mean radionuclide doses for the EPRI nominal scenario is given on Figure 5-10 in Apted and Ross (2005 [DIRS 182229]). In comparison, the results from the TSPA-LA Model for the computed mean annual doses for the combined Nominal Scenario Modeling Case and the Waste Package EF Modeling Case are shown on Figure 7.7.3-3. The results indicate a similar pattern for the nominal scenario characterized by a significant increase in dose after 100,000 years. The early failure dose is represented by the dose increase after about 1,000 years in the TSPA-LA Model (Figure 7.7.3-3), which is somewhat delayed in the EPRI TSPA Analysis (Apted and Ross 2005 [DIRS 182229], Figure 5-10). The mean annual dose in the EPRI TSPA Analysis is about 2.0×10^{-2} mrem/yr compared to about 4.0×10^{-1} mrem/yr in the TSPA-LA Model after one-million years. The main contributor to mean annual dose at late time is ^{129}I in both cases.

The differences between the EPRI TSPA Analysis and the TSPA-LA Model results can be accounted for by differences in:

- Seepage rates through the repository
- Early-failure representation and EBS failure curves
- Inventory, both in terms of waste type and individual radionuclides
- Solubility limits and sorption characteristics in the UZ and SZ.

As shown in Figure 7.7.3-1, seepage rates used in the EPRI TSPA Analysis are significantly lower than the corresponding rates used in the TSPA-LA Model, whereby the seepage rates in the EPRI TSPA Analysis are based on previous analysis and/or model report results. This causes a delay in radionuclide release from the EBS.

The EPRI TSPA Analysis only accounts for CSNF waste and considers failure of DS, WP, and cladding, whereas the TSPA-LA Model accounts for CSNF, DSNF, and HLW WPs, but does not take credit for cladding in CSNF WPs. Consequently, the overall dose release in the EPRI TSPA Analysis is delayed both during early failure case and for the nominal case, where the WP failure curve indicates that only about 5,300 CSNF packages failed after one-million years, whereas the TSPA-LA Model indicates that on average about 50 percent of WPs have failed.

The EPRI TSPA Analysis only considers 12 radionuclides compared to 26 radionuclides in the TSPA-LA Model (Table M-4). During early failure ^{14}C is shown to contribute significantly to total dose in the TSPA-LA Model, which is not considered in the EPRI TSPA Analysis. At late time, the dominant radionuclides contributing to mean annual dose include ^{129}I, ^{99}Tc, ^{135}Cs, ^{79}Se, ^{242}Pu, and ^{237}Np in the TSPA-LA Model. The dominant radionuclides in the EPRI TSPA Analysis include ^{129}I followed by ^{237}Np, ^{233}U, and ^{229}Th. However, the EPRI TSPA Analysis does not consider ^{135}Cs and ^{79}Se.

Solubility limits used in the EPRI TSPA Analysis indicate significantly lower values for neptunium, plutonium, and thorium compared to the range given in the TSPA-LA Model. On the other hand, sorption characteristics used in the EPRI TSPA Analysis for the UZ are significantly lower for uranium and plutonium compared to those in the TSPA-LA Model. However, this does not affect ^{129}I, ^{99}Tc, and ^{135}Cs, which represent the main contributors to mean annual dose in the TSPA-LA Model.

In general, the main features of the dose release curves for the nominal scenario compares reasonably well with the TSPA-LA Model. The differences can be related mostly to differences in seepage and in different implementation of the inventory and EBS failure characteristics. This is partly due to the fact that the EPRI TSPA Analysis uses earlier analysis and/or model report results.

Table 7.7.3-1. Model Components and Processes Represented in the TSPA-LA Model and the EPRI TSPA Analysis

TSPA-LA Model[1]	EPRI TSPA Analysis
Unsaturated Zone Flow	**Climate, Net Infiltration, and Percolation** Parametric representation of: Time-history of infiltration rate Flow focusing factor Seepage fraction
Engineered Barrier System Environment Waste Package and Drip Shield Degradation	**Engineered Barrier System Degradation** Degradation processes represented by mean failure curves for: Drip shield Waste-Packages Cladding
Waste Form Degradation and Mobilization Engineered Barrier System Flow and Transport	**Near-field Model and Coupling** *Compartment model to: compute mass transfer across the different near-field components:* *Waste* *Corrosion Products* *Pallet/Basalt* *Invert* *Nearfield rock matrix/fractures*
Unsaturated Zone Transport	**Lower Unsaturated Zone Model and Coupling** UZ-Code: 1-D unsaturated-zone flow and transport, representing four unsaturated horizons: tsw35, tsw38, ch1Vl, Ch2Ze.
Saturated Zone Transport	**Saturated Zone Model and Coupling** SZ-Code: 2-D saturated flow and transport representing fractured tuff segment and alluvial segment
Biosphere	**Biosphere Model and Coupling** Determination of radionuclide-specific set of Biosphere Dose Conversion Factors for the Reasonably Maximally Exposed Individual based on assessment of relevant radiation exposure media

[1]Relevant processes used in the TSPA-LA Model are described in Section 6.

INTENTIONALLY LEFT BLANK

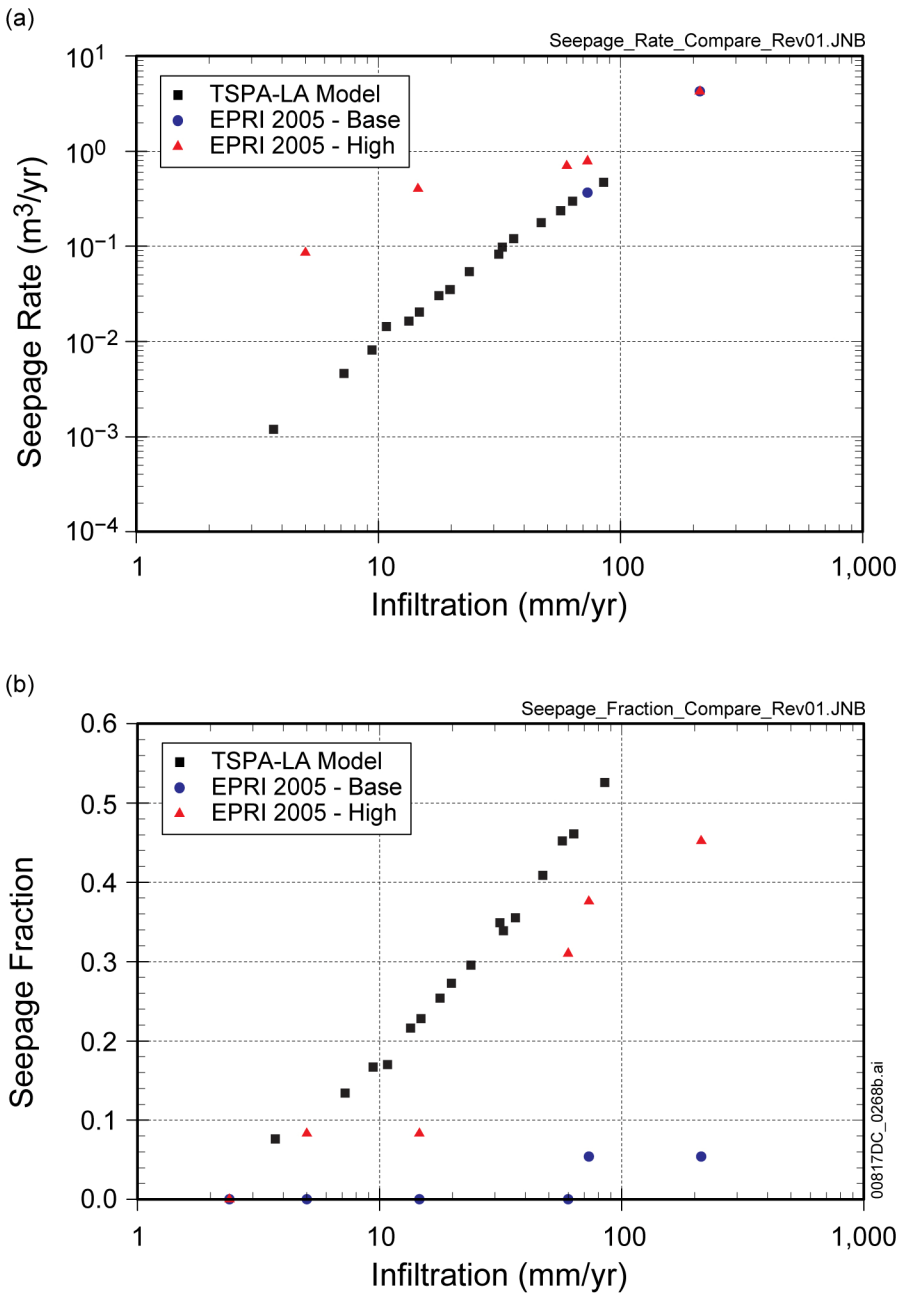

Sources: Kozak and Kessler 2005 [DIRS 178580], Table 3-2; CRWMS M&O 2001 [DIRS 154291], Table 4.3.1-1; and SNL 2007 [DIRS 181244], Tables 6-5[a] and 6-6[a].

Figure 7.7.3-1 Comparisons of (a) Seepage Rate and (b) Seepage Fraction versus Infiltration Rates as Used in the EPRI Analysis and the TSPA-LA Model

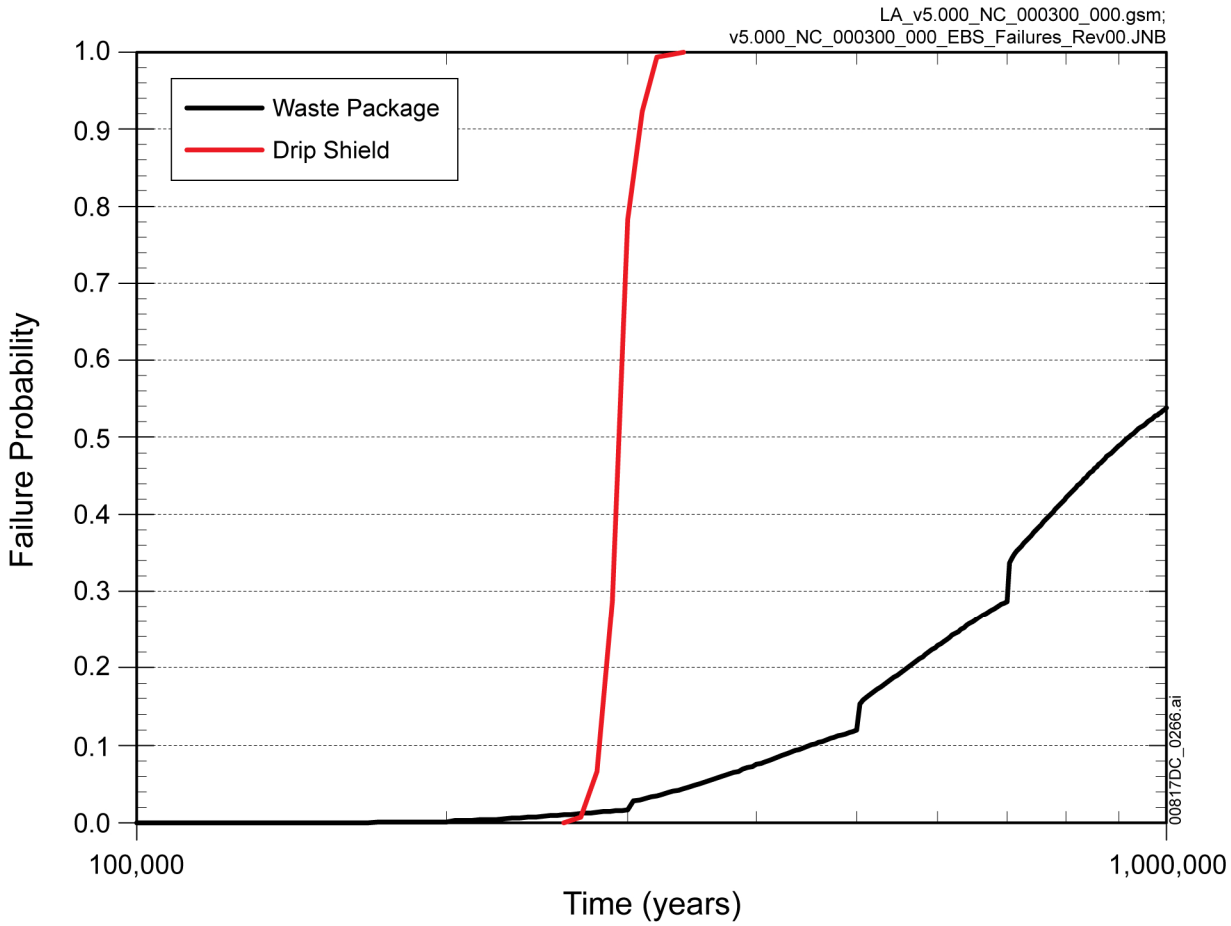

Source: Output DTN: MO0709TSPAREGS.000 [DIRS 182976].

Figure 7.7.3-2. TSPA-LA Nominal Scenario Class Mean Failure Curves for the Drip Shield and Waste Package

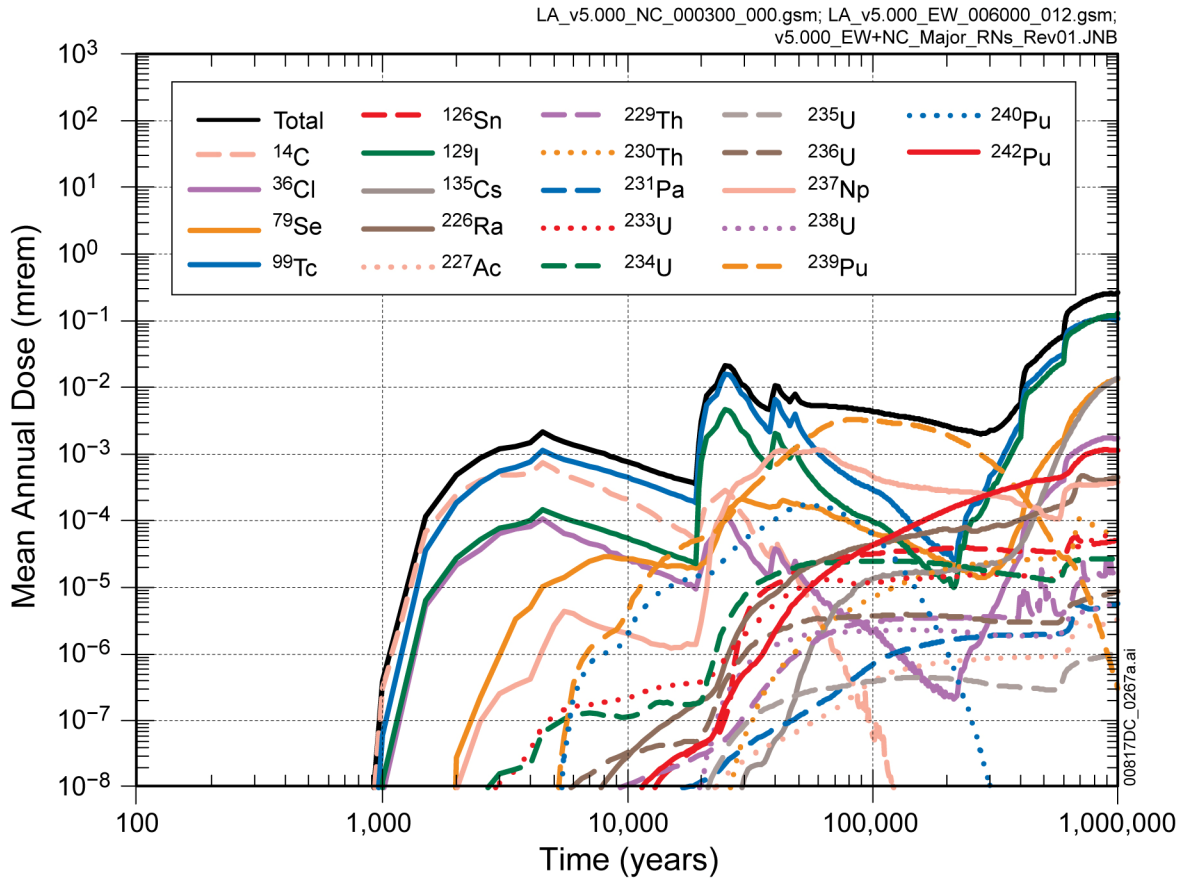

Source: Output DTN: MO0709TSPAREGS.000 [DIRS 182976].

Figure 7.7.3-3. TSPA-LA Mean Dose Histories for Major Radionuclides for the Combined Early Failure and Nominal Scenario Classes

INTENTIONALLY LEFT BLANK

7.7.4 Performance Margin Analysis

The judicious use of reasonable conservative assumptions, play an important role in the development of the TSPA-LA Model, and building confidence in the TSPA-LA results. Conservative assumptions were introduced in the formulation of the TSPA submodels and in selected submodel parameters to compensate for epistemic uncertainties, but more importantly, to ensure that the potential radiological risks would not be underestimated. Individual conservatisms introduced at the submodel level, however, can be attenuated differently to the system level performance measures, i.e., total mean annual dose. Consequently, it was necessary to carefully and quantitatively evaluate the significant explicit and implicit conservatisms of the type discussed in Section 6.3. More specifically, the selected conservatisms were evaluated to:

1. Confirm that, when propagated individually through the TSPA-LA Model, they are conservative with respect to the total system performance measures (e.g., total mean annual dose)

2. Quantify the extent to which the conservatisms, individually and collectively, overestimate the total mean annual dose, relative to the model projections presented in the performance demonstration described in Section 8.0

3. Assess that evaluated conservatisms did not introduce any inappropriate risk dilution in the TSPA-LA results presented in support of the LA (e.g., reduce the peak total mean annual doses).

To perform these evaluations, a separate set of TSPA calculations were conducted and referred to as the Performance Margin Analysis (PMA). The PMA calculations paralleled those of the TSPA-LA Model (Section 8.0), but focused on scrutinizing the impact of select conservatisms embedded in TSPA model components and submodels and utilized by the modeling cases to calculate annual doses. In addition, the PMA was intended to gauge the collective impact of the conservatisms, and thereby give a perspective on the potential performance margin embedded in the TSPA-LA dose-risk projections.

Most of the conservatisms in the TSPA-LA Model were introduced during submodel development and/or derivation of parameter uncertainty characterizations as discussed in Section 6.3. For the most part, these conservatisms are implemented to bound the effects of processes that promote radionuclide release and transport. Other conservatisms were also introduced as a result of not taking credit for processes or conditions, which may potentially enhance containment and isolation. Additional submodels were developed for inclusion in the PMA for the specific purpose of evaluating implicit conservatisms. It is important to state, however, that while these additional submodels and data have been through the required quality assurance (QA) process, in some cases they have a limited technical foundation and/or may use an unqualified software (Section C3), and are only used as a quantitative tool for the PMA.

The PMA was conducted by first modifying selected submodels and parameters of the TSPA-LA Model, including the additional submodels and parameters for the PMA, and then repeating a select set of modeling cases that were run for the TSPA-LA. The total mean annual dose was recalculated replacing the selected set of TSPA-LA modeling cases with PMA results. The

collective impact of the major assumptions was quantified by comparison of the total mean annual dose (for example Figure 7.7.4-2). The PMA results are compared to the mean annual dose results of the TSPA-LA Model. Thus, the PMA is one aspect of the validation work supporting the TSPA-LA Model. The detailed PMA are presented in Volume III, Appendix C.

Changes to the TSPA-LA submodels necessary to conduct the PMA are embedded in the following principal model components defined in Section 6.0 and Figure 6-1:

- Drift-Scale UZ Flow (C6.2)
  - Reduction of seepage flux to WP based on a reduced hydrologic cross-section for the representation of collapsed drift geometry (Drift Seepage Submodel)
- Waste Package and Drip Shield Degradation (C6.3)
  - Modification of corrosion rates based on fluoride ion concentration threshold instead of fixed and pervasive condition of aggressive corrosion
  - Implementation of a lower WP Alloy 22 (UNS N06022) general corrosion rate based on weight loss coupon data instead of conservative crevice corrosion data
  - Implementation of SCC of Alloy 22 using a less conservative representative yield stress threshold
  - Inclusion of a mechanistic approach to the calculated distribution of breached area as a result of localized corrosion on the WP outer barrier
- EBS Flow (C6.4)
  - Inclusion of a detailed in-package water balance to more accurately account for the mass fluxes of water through the WPs
- Waste Form Degradation and Mobilization (C6.5)
  - Modification of In-Package Chemistry Model that accounts for the extent of material degradation and the availability of water inside a WP
  - Inclusion of long-term degradation rate models for CSNF and HLW glass waste forms
  - Inclusion of credit for initial clad failure fractions in place of conservatively assuming all cladding is failed at time of emplacement; applied to first 20,000 years only
  - Reduction of uncertainties for thermodynamic properties of neptunium, uranium, and plutonium
- UZ Flow and Transport Submodel (C6.6)

  - Enhanced matrix diffusion effects on radionuclide transport
  - Addition of colloid diversity model and retardation of irreversibly sorbed radionuclides
  - Addition of detailed model for water table rise
- SZ Transport Submodel (C6.7)
  - Addition of discrete interface for redistribution of the diffusive mass released from the UZ matrix to SZ fractures
  - Addition of colloid diversity model and retardation of reversible and irreversibly sorbed radionuclides
  - Addition of enhanced radionuclide sorption in potential reducing zone
  - Implementation of less conservative distribution for flowing interval porosity
  - Inclusion of correlation between flowing interval porosity and groundwater specific discharge
- Seismic Scenario Class (C6.8)
  - Inclusion of an alternative conceptual model for the crack-area density model in the Seismic Damage Abstraction.

Discussion of each change and how they were addressed in terms of modifications to the above submodels is presented in Volume III, Appendix C.6, PMA Model Description.

7.7.4.1 Projections of the TSPA-LA Performance Margin

In the PMA the postclosure performance was analyzed over a select set of modeling cases to evaluate the changes listed above. The objective of the PMA is to carefully and quantitatively evaluate the significance of the major explicit and implicit conservatisms which would be otherwise very difficult to address given the range of uncertainties and long-term projections inherent in a model of this magnitude.

Scenario Classes and Modeling Cases Considered

The TSPA-LA demonstration of performance for the individual protection standard is based on the total mean annual dose summed over seven scenario modeling cases: (1) Nominal, (2) Waste Package EF, (3) Drip Shield EF, (4) Igneous Intrusion, (5) Volcanic Eruption, (6) Seismic GM, and (7) Seismic FD (Section 8.1). As required by the disposal standards, for the TSPA-LA the postclosure performance is quantified for time periods of 10,000-years and 1,000,000-years after closure. Likewise the PMA was conducted over the 10,000 year and 1,000,000 year postclosure periods for comparison with the TSPA-LA. Drawing from the evaluation presented in Section 8.0, the PMA was exercised using five modeling cases (the Seismic GM Modeling Case

includes the effects of the nominal processes when run for 1,000,000-years postclosure). The Volcanic Eruption Modeling Case was not evaluated in the PMA, because none of the changes included in the PMA have any impact on the Volcanic Eruption Modeling Case.

In addition, a sensitivity analysis was conducted to evaluate the use of weight-loss Alloy 22 general corrosion data (as noted above). This analysis was conducted for two additional simulations: a Seismic GM and a Nominal Modeling Case were run for a period of 1,000,000 years after repository closure. These simulations are documented in Volume III, Appendix C, Section C.7.1.2.

In summary, the performance margin demonstration for the TSPA-LA Model considered projections of radionuclide releases for five modeling cases for the time period of 10,000 years and for the time period after 10,000 years and through the period of geologic stability.

Calculation of Total Mean Annual Dose

The PMA total mean annual dose was calculated replacing the selected set of TSPA-LA modeling cases (identified above) with PMA results. The TSPA-LA results for the Volcanic Eruption Modeling Cases were combined with the PMA results to calculate the PMA total mean annual dose. A detailed discussion of the method used to calculate the total mean annual doses for the TSPA-LA and the PMA, is presented in Appendix J. The total mean annual dose was evaluated to assess the potential performance margin embedded in the TSPA-LA Model results (presented in Section C7).

Performance Margin in the Total Mean Annual Dose for 10,000-years Postclosure

The main result of the simulation process is a set of expected annual dose histories shown on Figure 7.7.4-1, along with curves for the mean, median, 5th- and 95th-percentiles. The total mean annual dose history, which is plotted as the red curve, was computed by taking the 'arithmetic average' of the 300 expected annual dose values, for individual time planes along the curves (Appendix J). A comparison of the total mean annual dose history for the PMA and the TSPA-LA is shown on Figure 7.7.4-2. The peak total mean annual dose to the RMEI is estimated by the PMA to be about 0.02 mrem for the 10,000-year disposal period. Important performance margin insights can be gained by comparison of the total mean annual dose curves between the PMA and the TSPA-LA, which are shown on Figure 7.7.4-2 over the 10,000-years postclosure period. From those dose curves, the following general observations can be drawn about the performance margin demonstration:

- The PMA total mean annual doses are generally lower by nearly an order of magnitude over the first 10,000 years compared with the total mean annual dose from the TSPA-LA Model.

- The peak PMA total mean annual doses calculated over 10,000 years are lower by over an order of magnitude over the largest total mean annual dose from the TSPA-LA Model.

- Total mean annual doses calculated for 10,000 years are dominated by projected releases for the Igneous Intrusion Modeling Case (Appendix C, Figure C7-7).

The radionuclides which contribute the most to the total mean annual dose depend on time frame being evaluated, i.e., 10,000-years or 1,000,000-years after closure, because of the effect of decay on activities. From dose curves shown on Figure 7.7.4-3(b), the principal contributors to the peak total mean annual dose in the PMA for 10,000 years, ranked from highest to lowest, are: ^{99}Tc, ^{129}I, ^{14}C, ^{237}Np, ^{239}Pu, ^{240}Pu, and ^{234}U. Though the relative importance is different, collectively, the dominant radionuclides shown in the PMA results are the same dominant radionuclides that are found in the TSPA-LA Model total mean dose. The similarity between the dominant radionuclides in the PMA and the TSPA-LA Model indicates that the EBS and Natural System components are behaving the same, but the lower total mean annual dose for the PMA would suggest that the reduction in the conservative assumptions embedded in these component models as the primary factor accounting for the lower dose and are responsible for the margin in the TSPA-LA results.

Performance Margin in the Total Mean Annual Dose after 10,000 years through the Period of Geologic Stability

The set of expected annual dose histories for the time period after 10,000 years and through the period of geologic stability are shown on Figure 7.7.4-4. The peak total mean annual dose to the RMEI after 10,000 years, but within the period of geologic stability, is estimated by the PMA to be about 1.1 mrem. Comparison of the total mean annual dose curves between the PMA and the TSPA-LA is shown on Figure 7.7.4-5 for the 1,000,000-year time period. From this comparison plot, the following general observations can be drawn about the performance margin demonstration:

- The PMA total mean annual doses are generally lower by nearly an order of magnitude over the first 200,000 years compared with the total mean annual dose from the TSPA-LA Model.

- The peak PMA total mean annual doses calculated over 1,000,000 years are lower by a factor of two over the largest total mean annual dose from the TSPA-LA Model.

In general, the radionuclides in the nuclear waste that dominate the calculation of annual doses typically have a combination of unique characteristics such as: (1) large initial inventories in the nuclear waste, (2) moderately to highly soluble, (3) very long half-lives (e.g., $\geq 10^5$ yrs), and (4) low sorbing to non-sorbing properties. The important radionuclides vary according to time frame, i.e., 10,000 years or 1,000,000 years after closure, because of the effect of decay on activity. From dose curves shown on Figure 7.7.4-6(b), that the principal contributors to the peak total mean dose in the PMA for 1,000,000 yrs, ranked from highest to lowest, are: ^{226}Ra, ^{242}Pu, ^{237}Np, ^{129}I, ^{233}U, ^{135}Cs, ^{99}Tc, ^{229}Th and ^{230}Th. Through their relative importance changes, these PMA dominant radionuclides are the same dominant radionuclides that are found in the TSPA-LA Model total mean dose. This similarity between dominant radionuclides indicates that the EBS and Natural System components behave in an analogous manner. Moreover, the lower peak total mean annual dose projected for the PMA demonstrates the impact of this reduction in the degree of conservatism.

Scenario Specific Insights to the Performance Margin

Additional important insights to the performance margin can be gained by disaggregating the total mean annual dose into the total mean annual dose curves for the individual modeling cases and conducting a systematic evaluation of the effects of the changes incorporated into the PMA. This detailed analysis is included in Appendix C and the following general observations can be drawn about the PMA results:

- Total mean annual doses calculated for both 10,000 years and 1,000,000 years are dominated by projected releases for the Igneous Intrusion Modeling Case.

- Total mean annual dose projected for Seismic GM Modeling Case is on the order of 10^{-1} mrem or less and is the second largest contributor to the calculated total mean annual dose 1,000,000-years after closure.

- Total mean annual dose projected for Waste Package EF Modeling Case is on the order of 10^{-3} mrem or less and is the second largest contributor to the calculated total mean annual dose calculated until 10,000-years after closure.

- Total mean annual doses for the Drip Shield EF, Seismic FD, and Volcanic Eruption Modeling Cases are relatively small and are estimated to be on the order of 10^{-4} mrem or less for both 10,000-years and 1,000,000-years after closure.

A comparison between the observations listed above for the PMA and the TSPA-LA results yields some notable differences. With regards to the TSPA-LA results, the Seismic GM Modeling Case dominates the total mean annual dose for the 10,000-year time period, whereas for 1,000,000 years the Seismic GM and Igneous Intrusion Modeling Cases contribute equally to the total mean annual dose to the RMEI (Section 8.1.1.2). However, in the PMA results, the Igneous Intrusion Modeling Case dominates the total mean annual dose for the time period of 10,000 years. For the time period after 10,000 years and through the period of geologic stability the Igneous Intrusion Modeling Case dominates the total mean annual dose with a small contribution from the Seismic GM Modeling Case beginning around 225,000 years. This difference is primarily due to a lower incidence of WP failure (Appendix C6.8 and C.7.2) and WP cracking during a seismic event for the PMA (Appendix C6.8 and C.7.2). The remaining cases combined, have a negligible contribution for both the PMA and TSPA-LA total mean annual dose results.

7.7.4.2 Summary of the TSPA-LA Performance Margin

The differences in the relative contributions to the total mean annual dose from each of the scenario modeling cases between the PMA and the TSPA-LA Model indicates that the reduction in the selected conservative assumptions embedded in these TSPA-LA component models exposed a larger performance margin for the Early Failure and Seismic Scenario Classes than that may be contained within the Igneous Scenario Class. With respect to the specified objectives of the PMA:

1. The PMA results confirm that submodel conservatisms propagated through the TSPA-LA Model, are also conservative with respect to the total system performance measures (e.g., total mean annual dose).

2. Relative to the TSPA-LA Model results, the peak PMA total mean annual dose is lower by over an order of magnitude for the 10,000 year time period and lower by a factor of two for the time period after 10,000 years.

3. The evaluated conservatisms did not introduce any inappropriate risk dilution in the TSPA results presented in support of the LA as demonstrated by the absence of higher peak mean annual doses in the PMA results for both the probabilistic projections of the total dose histories and the comparison of the projected total mean dose history for the PMA relative to the TSPA-LA.

The collective impact of the major assumptions was quantified by comparison with the TSPA-LA results. The assessment of the potential performance margin embedded in the TSPA-LA Model results is presented in detail in Volume III, Appendix C.

INTENTIONALLY LEFT BLANK

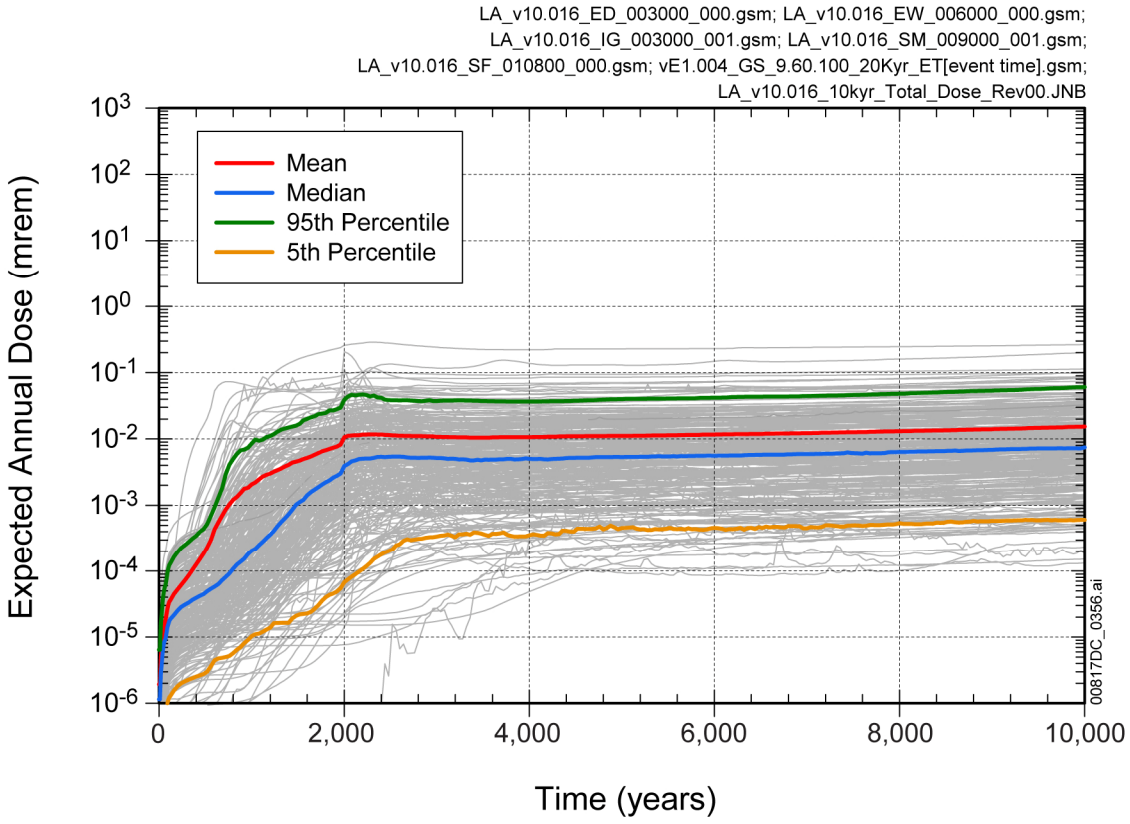

Source: Corroborative DTN: MO0709MARGANAL.000 [DIRS 182978]; and Output DTN: MO0709TSPAREGS.000 [DIRS 182976].

Figure 7.7.4-1. Total Expected Annual Dose for the Performance Margin Analysis for 10,000 Years after Repository Closure

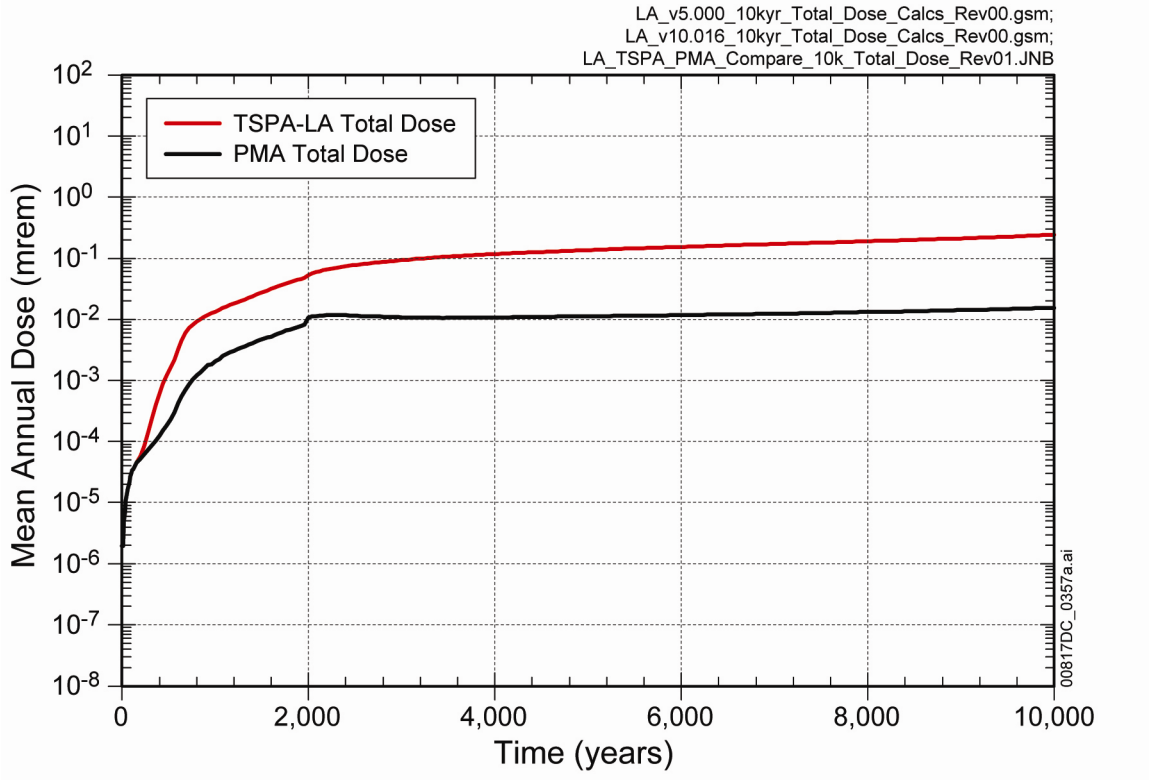

Source: Output DTN: MO0709TSPAPLOT.000 [DIRS 183010]; and Corroborative DTN: MO0709MARGANAL.000 [DIRS 182978].

Figure 7.7.4-2. Comparison of the Total Mean Annual Dose for the TSPA-LA Model to the Performance Margin Analysis 10,000 Years after Repository Closure

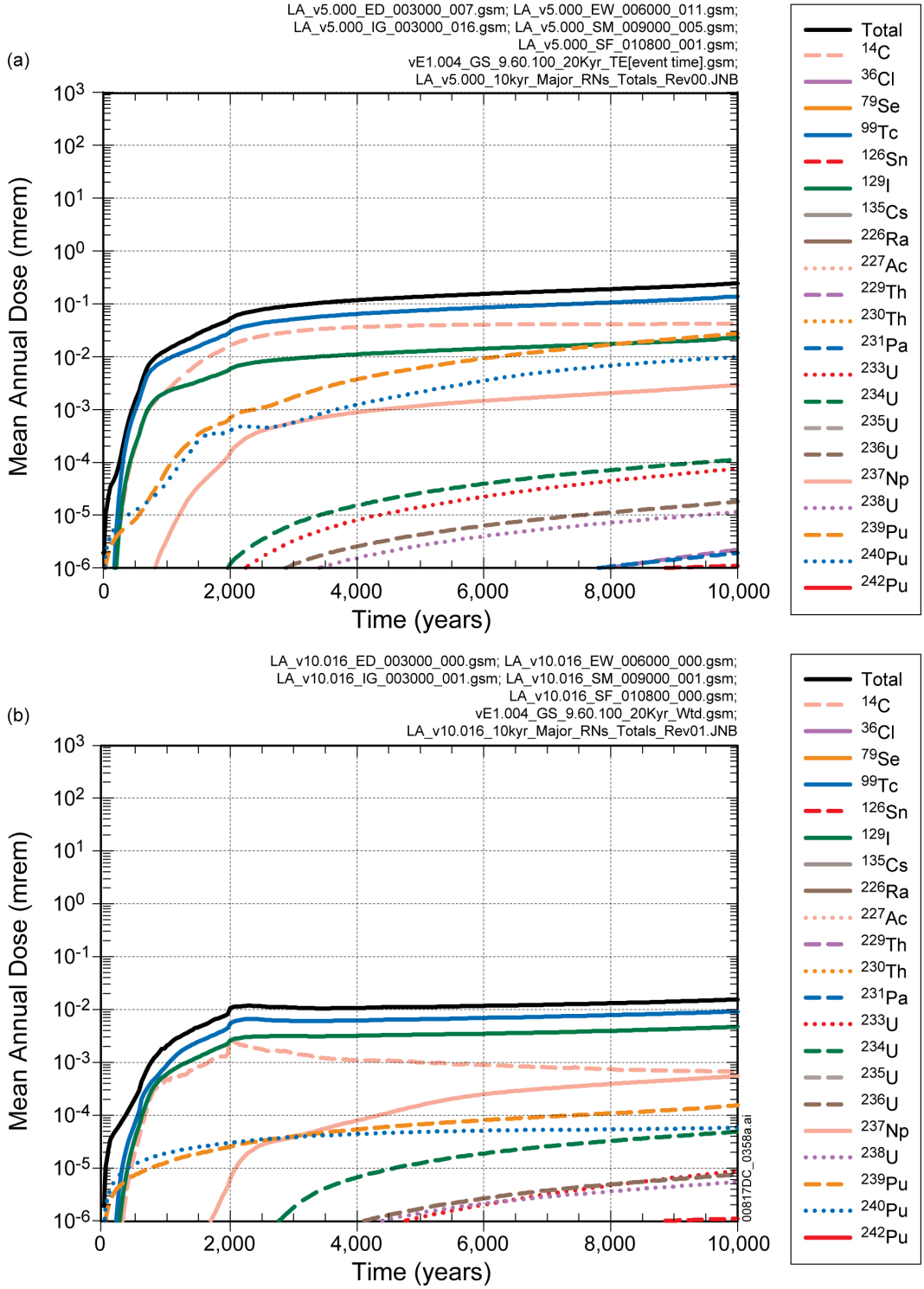

Source: Output DTN: MO0709TSPAREGS.000 [DIRS 182976]; and Corroborative DTN: MO0709MARGANAL.000 [DIRS 182978].

Figure 7.7.4-3. Contributions of Individual Radionuclides to Total Mean Annual Dose for (a) the TSPA-LA Model and (b) the Performance Margin Analysis 10,000 Years after Repository Closure

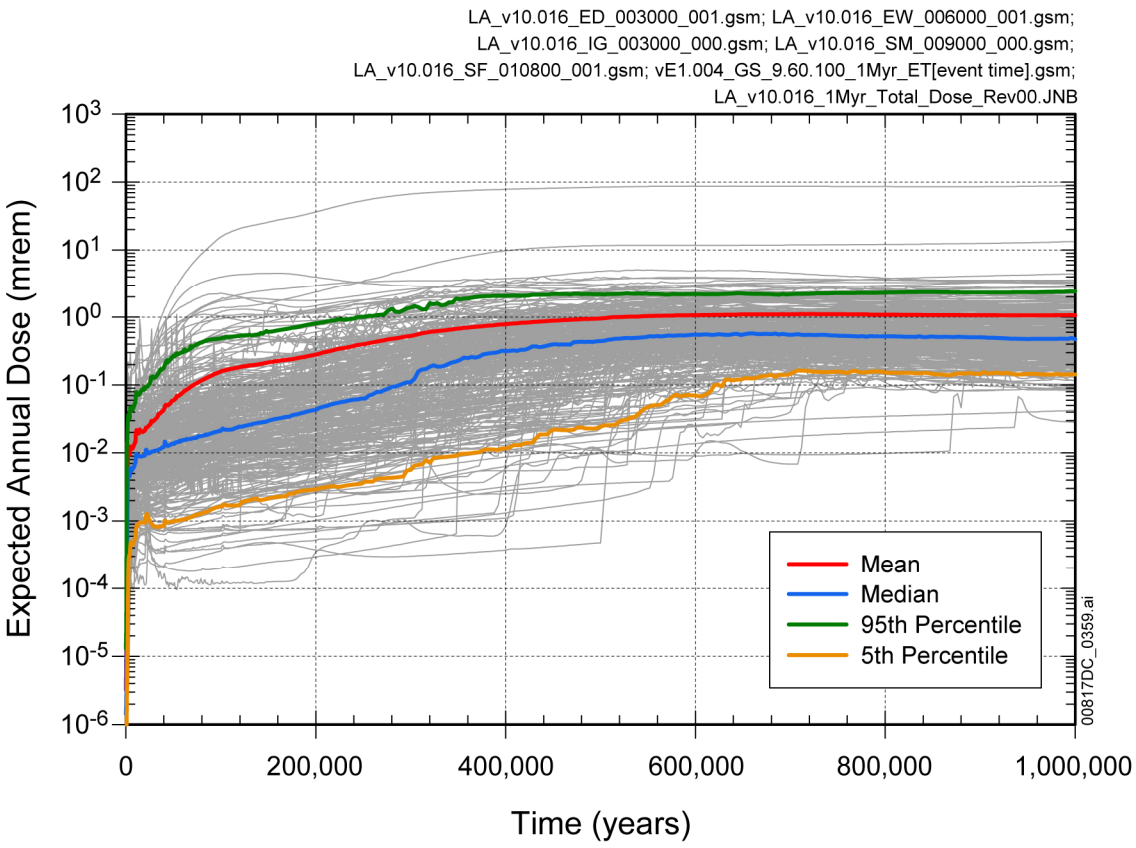

Source: Corroborative DTN: MO0709MARGANAL.000 [DIRS 182978]; and Output DTN: MO0709TSPAREGS.000 [DIRS 182976].

Figure 7.7.4-4. Total Expected Annual Dose for the Performance Margin Analysis for 1,000,000 Years after Repository Closure

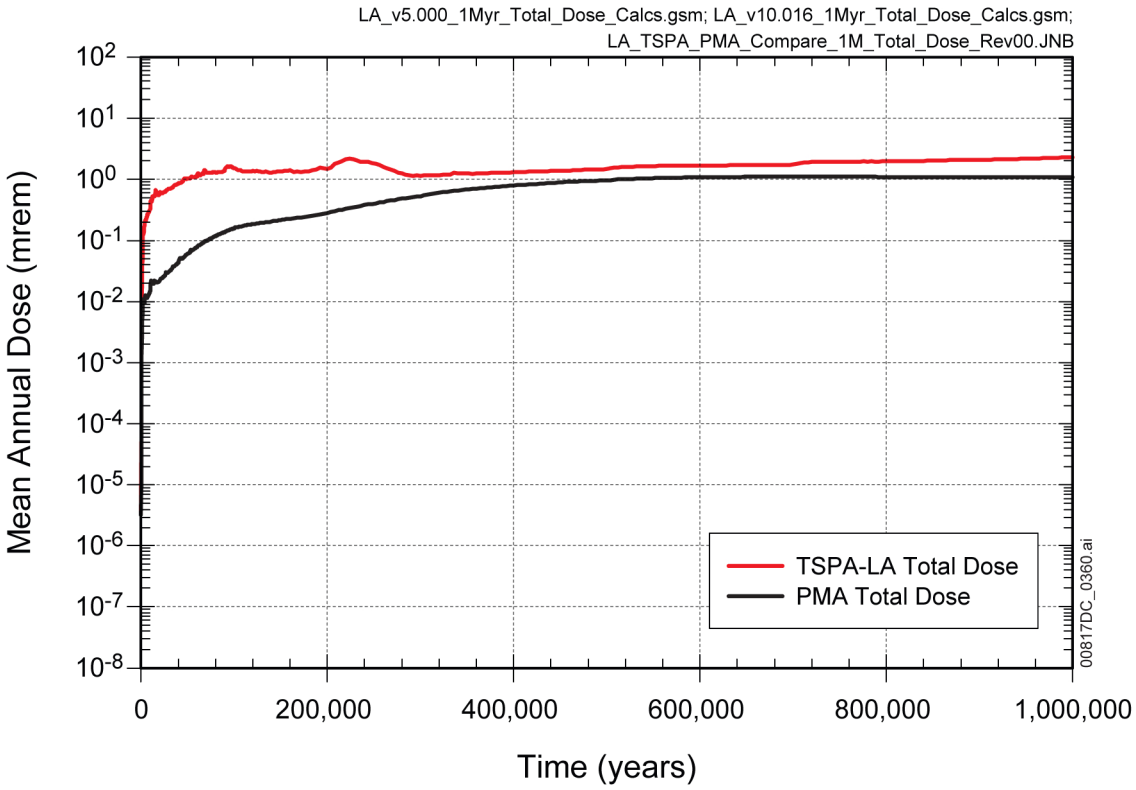

Source: Output DTN: MO0709TSPAPLOT.000 [DIRS 183010]]; and Corroborative DTN: MO0709MARGANAL.000 [DIRS 182978].

Figure 7.7.4-5. Comparison of the Total Mean Annual Dose for the TSPA-LA Model to the Performance Margin Analysis 1,000,000 Years after Repository Closure

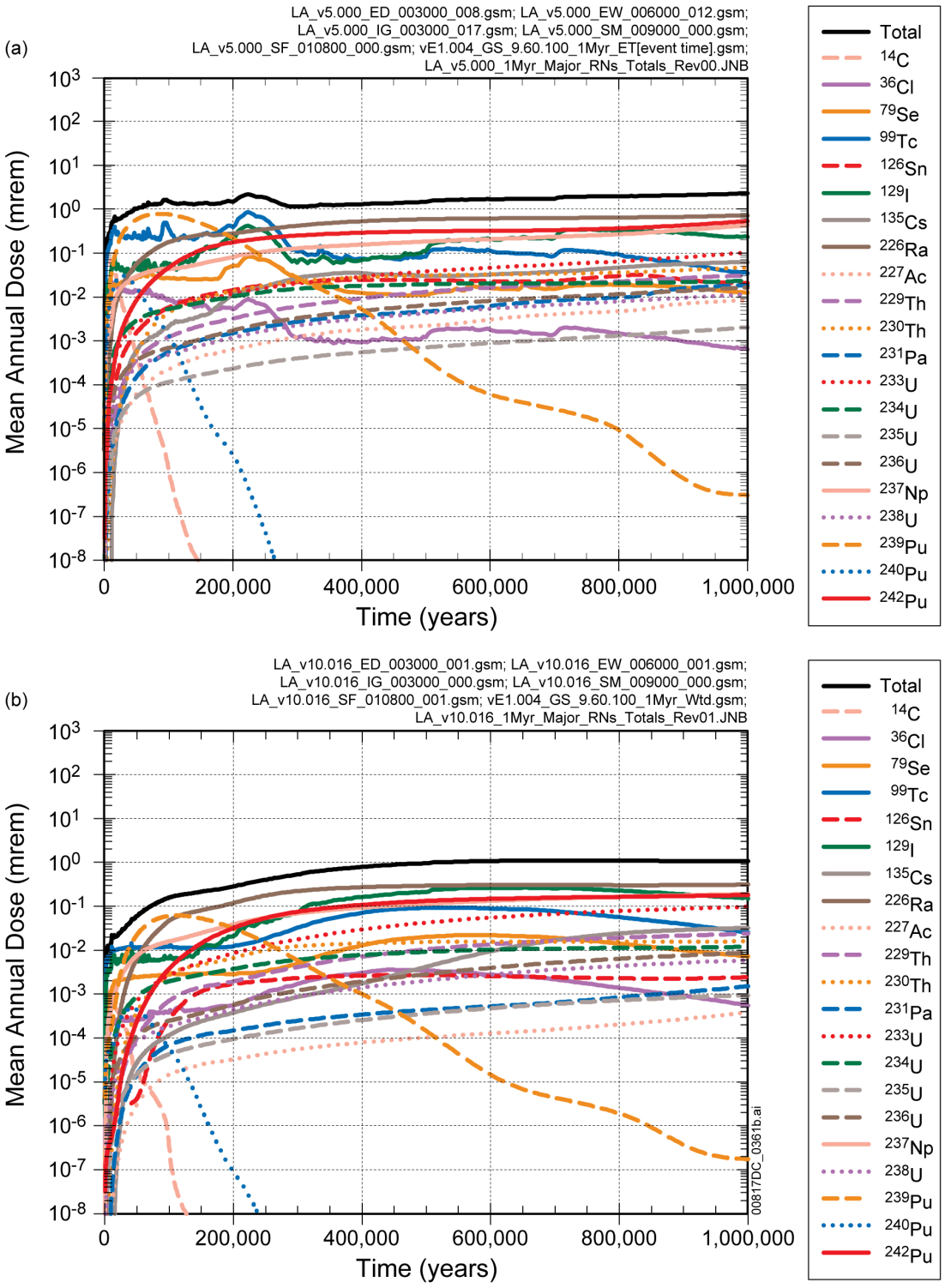

Source: Output DTN: MO0709TSPAREGS.000 [DIRS 182976]; and Corroborative DTN: MO0709MARGANAL.000 [DIRS 182978].

Figure 7.7.4-6. Contributions of Individual Radionuclides to Total Mean Annual Dose for (a) the TSPA-LA Model and (b) the Performance Margin Analysis 1,000,000 Years after Repository Closure

7.8 NATURAL ANALOGUES

The TSPA-LA Model accounts for the uncertainty in making long-term projections of the performance of the repository and simulates the performance of the Yucca Mountain repository for hundreds of thousands of years. Validation of the predicted performance of the repository at these time scales requires less than absolute proof because absolute proof is impossible to attain for disposal due to the uncertainty of projecting long-term performance (NRC Proposed Rule 10 CFR 63.304(1) [DIRS 180319]). Natural analogues to repository conditions and materials, both natural and anthropogenic, provide a means to compare repository conditions and materials to observed conditions and materials for time periods relevant to the lifetime of the repository. In the case of natural analogues, the National Research Council has endorsed the use of natural analogues as "natural test cases, geological settings in which naturally occurring radioactive materials have been subjected to environmental forces for millions of years" (National Research Council 1990 [DIRS 100061], p. 27). Analogues can provide quantitative and/or qualitative evidence to corroborate and assess expected repository performance covering geologic time scales. Analogues, although not the same as controlled laboratory or field experiments, can build confidence in the conceptual and numerical models that are used to represent processes and events that could affect repository performance.

Confidence in and corroboration of the predicted results of the TSPA-LA Model of the Yucca Mountain repository can be gained, in part, through comparison with natural and anthropogenic analogues to the processes, conditions, and materials affecting repository performance. The results of natural analogue analyses relevant to the long-term geologic storage of nuclear waste have served as corroborative input to several of the analysis and model reports that support the model components and submodels of the TSPA-LA Model. Natural analogues that are relevant to the assessment of the long-term performance of the Yucca Mountain repository are discussed in *Natural Analogue Synthesis Report* (BSC 2004 [DIRS 169218]). Some of the analogues to the process models and submodels of the TSPA-LA Model are summarized below. Following these discussions, Sections 7.8.1 and 7.8.2 describe two investigations of natural analogues that describe geologic processes that could possibly affect the performance of the Yucca Mountain repository. These analogues, which provide corroborative evidence for the TSPA-LA Model, are the simulation of the 1995 volcanic eruption at Cerro Negro, Nicaragua (Section 7.8.1), and the investigation of seepage and radionuclide transport at the Nopal I uranium deposit in the Sierra Peña Blanca in Chihuahua, northern Mexico (Section 7.8.2).

Drift Stability—The Nominal Scenario Class Modeling Case simulates the performance of the emplacement drifts as stable throughout the simulation period. The ability of underground openings, such as caves and engineered mines, to remain open and stable under ambient conditions depends on: (1) rock strength; (2) size, shape, and orientation of the opening; (3) orientation, length, and frequency of fractures; and (4) effectiveness of ground support. Cave and/or mine collapses are common occurrences but, depending on geology, natural caves and engineered mines and tunnels may remain stable and open for hundreds to thousands of years. Radiometric analyses of minerals found in cave floors indicate that natural openings, larger than those at Yucca Mountain, have remained stable and open for millions of years. Collapse of openings tends to occur where fracture density is high. Neolithic flint mines (approximately 4,000 to 3,000 B.C.), and Roman mines and aqueducts demonstrate that man-made underground openings can remain open and stable for thousands of years also, as summarized in *Natural*

Analogue Synthesis Report (BSC 2004 [DIRS 169218], Section 15.7.1). Stuckless (2000 [DIRS 151957]) provides examples of archeological analogues including enhanced caves, burial chambers, and underground temples that have been stable for several thousand years. The stability of structures like the Yucca Mountain repository, such as mines and tunnels, is individually dependent on geology, seismicity, quality of ground support, and local hydrogeology. There are no quantitative measures for these structures with respect to the repository.

Waste Form Degradation—The reaction path of the alteration of SNF at Yucca Mountain will be similar to that of geologically young lead-free uraninite, with schoepite and becquerelite forming as intermediate products, followed by uranyl silicates. Natural uraninite and its alteration products, found at the Nopal I uranium deposit at Peña Blanca, have these characteristics, making this deposit an appropriate analogue to the alteration of uranium oxide spent fuel. At Shinkolobwe, Zaire, more than 50 uranium phases were identified; however, because the deposit is 1.8 billion years old, lead-bearing phases have played a role in sequestering the uranium as shown in *Natural Analogue Synthesis Report* (BSC 2004 [DIRS 169218], Section 15.7.2).

The concentrations of fission products can be used as tracers in minerals precipitated in the rock matrix and in dissolved radionuclides in groundwater surrounding naturally occurring uraninite deposits. Geochemical analysis of these minerals and groundwater chemistries provides a means of estimating natural dissolution rates at some natural analogue sites. When this approach was used at the uranium ore deposits at Cigar Lake, Canada, and Koongarra, Australia, where these ore deposits are found under reducing and oxidizing conditions, respectively, the dissolution rate was found to be more rapid under the oxidizing conditions at Koongarra. Other lines of evidence from geochemical investigations concerning dissolution at the natural-analogue uraninite ore deposit at Oklo, Gabon, indicate that dissolution of the ore minerals has been slight over the past two billion years. Under radiolysis conditions occurring at the time of criticality at Oklo, the estimated mobilization of the original uranium for transport was only several percent as given in *Natural Analogue Synthesis Report* (BSC 2004 [DIRS 169218], Section 15.7.2). Uranium, plutonium, neptunium, and americium were retained in the reactor zone for almost two billion years in the reduced environment of the Oklo reactor zones. There has been limited migration of technetium, ruthenium, rhodium, and palladium, and there has been considerable migration of cesium, rubidium, strontium, and barium (the rare earth elements). Although conditions at Oklo's reactor zones are not like those expected at Yucca Mountain, study of the migration patterns for specific radionuclides give useful insights regarding the behaviors of these species in various environments (BSC 2004 [DIRS 169218], Section 15.7.2).

Although natural glasses are different in composition than borosilicate HLW glass, studies of natural glass alteration indicate that HLW glass will be stable in the Yucca Mountain repository environment. Natural geologic glasses tend to be more stable than archaeological glass, especially with regard to changing environments relative to humidity. In both natural and borosilicate glass, higher stability is favored by higher silica and alumina content and by lower alkali and water content. However, analogue studies have not considered radiation effects on glass over long time periods and, thus, cannot be used to confirm experimental results showing that radiation has little effect on HLW glass stability (BSC 2004 [DIRS 169218], Section 15.7.2).

WP Degradation—The analogues to common metals serve mainly to demonstrate that under ambient to slightly elevated temperatures, these metals can be stable for thousands of years, even under oxidizing conditions. The survival of metal archaeological artifacts over prolonged periods of time is related to the corrosion-resistant properties of metals and metal alloys, the development of protective passive film coatings with the onset of corrosion, and the location of artifacts in arid to semiarid environments. Such features were used in the selection of materials and design configuration to enhance the durability of WPs designed for the Yucca Mountain repository (BSC 2004 [DIRS 169218], Section 15.7.3).

Metal alloys similar to the alloys being considered for the WPs to be used at Yucca Mountain have few analogues found in nature. Some meteorites contain metal alloys that are analogues of WP materials (Johnson and Francis 1980 [DIRS 125291], Section 6.4). However, the composition of most meteorites is not analogous to the current suite of alloys being considered for use in the Yucca Mountain repository. Josephinite, a complex rock found in remnants of the earth's mantle in Josephine County, Oregon, contains several nickel-iron alloys. The survival of the naturally occurring ordered nickel-iron alloy in josephinite for millions of years, with only relatively minor amounts of surface oxidation, indicates that this material is highly resistant to oxidation and other forms of corrosion that occur in its geologic environment. Although the composition of the nickel-iron alloy in josephinite differs from Alloy 22 (UNS N06022) in that it does not contain chromium, molybdenum, or tungsten, it does provide evidence that a similar alloy can remain passive over prolonged periods of time under conditions similar to those expected at the Yucca Mountain repository (BSC 2004 [DIRS 169218], Section 15.7.3).

The instability of chromium-bearing materials is illustrated by the observed natural release of chromium from chromite in the Sierra de Guanajuato, in Guanajuato State, central Mexico, ultramafic rocks under ambient conditions. Corrosion was observed to be concentrated along exsolution rims, which are analogues to structural defects on metal surfaces. However, although the chromite has undergone some alteration, it has survived for more than 140 million years (BSC 2004 [DIRS 169218], Section 15.7.3).

EBS Components—Although the invert's crushed devitrified welded tuff does not have high concentrations of zeolite and clay minerals, the high surface area of crushed tuff is expected to provide sorption sites that will retard radionuclide transport. Adsorption of actinides in a gravel bed at Los Alamos, New Mexico, provides qualitative evidence of radionuclide retardation at the contact between an invert-like material and underlying bedrock as seen in *Natural Analogue Synthesis Report* (BSC 2004 [DIRS 169218], Section 15.7.4).

The Pocos de Caldas, Brazil, analogue illustrates that iron-bearing colloids may retard the transport of uranium and other spent-fuel components by forming colloids that are then filtrated from suspension at short distances. Degradation of steel structural elements in the EBS could conceivably contribute to this process (BSC 2004 [DIRS 169218], Section 15.7.4).

Drift Seepage—An important variable related to the preservation, or lack of preservation, of engineered materials in underground openings is relative humidity. If ventilation reduces the relative humidity in the emplacement drifts to less than 100 percent, seepage of liquid water will be reduced or completely suppressed. Most caves have close to, but less than, 100 percent humidity. Thus, the amount of seepage in caves found in ventilated and unsaturated

environments has been observed to be low. This would also be true at Yucca Mountain as long as ventilation is maintained (BSC 2004 [DIRS 169218], Section 15.7.5).

Analogues of the UZ support the hypothesis that most of the infiltrating water in the UZ is diverted around underground openings, and does not enter into these openings. The analogues show that this is true even for areas with much greater precipitation rates than those at Yucca Mountain. Although there are examples where large amounts of seepage can be observed, such as in the Mission Tunnel, California, and at Mitchell Caverns, California, and cave minerals formed by water are common in unsaturated environments, these hydrogeologic settings are very different from those at Yucca Mountain and, thus, are not appropriate analogues. However, for analogues that have some water, at least some of the water that enters underground openings does not drip but, rather, flows down the walls as can be seen at dwellings excavated in tuffs at Goreme, Cappadocia, Turkey, and in efflorescent salts found in the leaking vaulted construction in Building 810 at the Denver Federal Center, Colorado (BSC 2004 [DIRS 169218], Section 8.3). In the few instances where dripping has been noted in settings that are analogous to Yucca Mountain, the drips can be attributed to asperities in the surface of the roof and ceiling of the openings such as seen at Carlsbad Caverns, New Mexico (BSC 2004 [DIRS 169218], Section 8.3). Whether or not water flows on walls or drips depends on conditions affecting the variables that determine drop formation and drop detachment, such as surface tension, roughness angle, and saturation. Thus, although most water would most likely flow around emplacement drifts at Yucca Mountain, the analogue information indicates that the expected small amount of water that could occur would primarily flow down the walls of the drifts. In the few instances where dripping may occur, it would be expected to occur at asperities on emplacement drift walls (BSC 2004 [DIRS 169218], Section 15.7.5).

UZ Flow and Transport—The UZ Flow and the UZ Transport Model Components of the TSPA-LA Model contain submodels with modeling approaches that are corroborated by analogue investigations that build confidence in those approaches. This analogue information provides a body of data for validating the conceptual and numerical models incorporated in the TSPA-LA Model.

The quantitative analogue investigation using related data sets gathered at the Idaho National Laboratory (INL) provides confidence in the dual-permeability approach used for the Yucca Mountain UZ Flow Model. The INL test site is analogous to Yucca Mountain in hydrogeology, precipitation, infiltration, rock types, and perching horizons. Hydrographs of ponded water and ^{75}Se breakthrough curves measured during the pond-infiltration test conducted at INL were analyzed to determine parameters controlling unsaturated flow and transport. Analysis of this data involved building a numerical model using TOUGH2 in a dual-permeability modeling approach used to simulate flow and transport at Yucca Mountain (BSC 2004 [DIRS 169218], Section 9.1).

The UZ Flow Model Component (Table 6-1) at Yucca Mountain considers a range of infiltration rates that are then used to bound the range of percolation flux. The Paintbrush nonwelded unit (PTn) at Yucca Mountain has a damping effect on downward flow to the Topopah Spring welded unit (TSw). Although, the INL transport calculations predicted retardation factors for neptunium and uranium that are orders of magnitude higher than retardation factors for other radionuclides, radionuclide retardation is supported by radionuclide migration experiments under unsaturated

conditions conducted in a 30-cm block of Calico Hills nonwelded tuff from the Busted Butte Test Facility near Yucca Mountain (BSC 2004 [DIRS 169218], Section 10.1). The Calico Hills nonwelded tuff lies below the repository at Yucca Mountain. These studies indicated conservative transport of TcO_4^-, but retardation of Np^{+4} by a factor of three more than the conservative tracer used for field tests.

The Peña Blanca natural analogue site, described in Section 7.8.2, has conditions similar to those at Yucca Mountain. The Nopal I mine at Peña Blanca has groundwater chemistry that is analogous to the groundwater chemistry in the Yucca Mountain hydrogeologic system. Chemical analyses of samples of groundwater from beneath the ore deposit indicate that radionuclides leached from the deposit are mostly sorbed or re-precipitated in the rocks surrounding the ore deposit and that there is little UZ transport. Nopal I also displays discrete alteration zones in fractured rocks intersected by likely groundwater flow paths (BSC 2004 [DIRS 169218], Section 15.7.11). The application of information describing the Peña Blanca natural analogue with respect to validation of the TSPA-LA Model is described in Section 7.8.2.

Coupled Processes—Geothermal systems illustrate a variety of thermal-hydrologic-chemical (THC) processes that are relevant to Yucca Mountain. Yellowstone, Wyoming, and other geothermal systems in welded ash flow tuffs or other low-permeability rocks indicate that the fluid flow is controlled by interconnected fractures. Alteration in low-permeability rocks is typically focused along fracture flow pathways. Only a small portion of the fracture volume needs sealing by precipitated minerals to retard fluid flow effectively. The principal minerals predicted to precipitate in the near field of the Yucca Mountain repository are amorphous silica and calcite, which are also commonly found as sealing minerals in geothermal systems as in *Natural Analogue Synthesis Report* (BSC 2004 [DIRS 169218], Section 15.7.7).

Sealing in geothermal fields can occur over a geologically short time frame in the order of a few days to several years. The unsaturated conditions, lower temperatures, and much lower fluid-flow rates predicted for the Yucca Mountain system, in comparison to the conditions in geothermal systems, should result in less extensive water-rock interaction than is observed in geothermal systems. Fracturing and sealing occur episodically in geothermal systems. Most of the mineralization at Yucca Mountain is predicted to occur 1,000 to 2,000 years after waste emplacement, when temperatures would reach boiling in the vicinity of the emplacement drifts (BSC 2004 [DIRS 169218], Section 15.7.7).

Coupled processes are expected to have a much smaller effect on hydrogeologic properties at Yucca Mountain than are observed at Yellowstone. However, development of a heat pipe above emplacement drifts at Yucca Mountain under a higher temperature operating mode could lead to increased chemical reaction and transport in the near field. Condensate reflux and boiling of silica-bearing fluids within the near field at Yucca Mountain could cause fracture plugging and consequent changing of fluid flow paths. Geochemical modeling of fluid compositions has been used to successfully predict observed alteration mineral assemblages at Yellowstone. The THC simulations conducted to date for the Yucca Mountain repository suggest that only 1 to 3 percent reduction in fracture porosity and less than one order of magnitude reduction in permeability are expected to occur in the near field as a result of the precipitation of amorphous silica and calcite. Changes in permeability, porosity, and sorptive capacity are expected to be relatively minor at the mountain scale, where thermal perturbations will be reduced. This THC result applies to

both the higher and lower temperature sub-boiling operating conditions. These predicted changes in hydrogeologic properties should not negatively affect repository performance (BSC 2004 [DIRS 169218], Section 15.7.7).

Preliminary results from a one-dimensional THC dual-continuum model of the interaction of country rock with heat released from an intrusive complex emplaced above the water table demonstrated the possibility of forming opal-filled veins with the silica derived from the host-rock matrix. However, because of the irregularities caused by the kinetic barrier, effects associated with the geochemical reaction of glass (BSC 2004 [DIRS 169218], Section 15.7.7) provide information that compares and contrasts a number of different sites that provide general conclusions regarding mineral alteration. For example, the Marysvale hydrothermal uranium-molybdenum ore deposit in Utah, tuffaceous rocks in hydrothermal systems at the Long Valley caldera, California, and the Valles caldera, New Mexico, suggest that uranium was concentrated and was liberated from siliceous rocks in response to hydrothermal circulation and then concentrated in ferruginous and carbonaceous zones. The Valles and Long Valley studies indicate localized mobility of uranium and daughter products in tuff and underlying sedimentary rocks at temperatures comparable to those expected in a nuclear waste repository environment (BSC 2004 [DIRS 169218], Section 11.5).

SZ Transport—Some of the Uranium Mill Tailings Remedial Action Program sites may be useful in the evaluation of radionuclide transport in the alluvial portion of the Yucca Mountain flow system. The conclusions derived from an analysis of the Gunnison, Colorado, site are: (1) a fraction of the uranium originating at the site is transported in the alluvial aquifer at a rate similar to the rate at which a conservative constituent is transported and (2) there is little evidence for lateral dispersion of contaminants in the downgradient direction. For the New Rifle, Colorado site, the main conclusions are: (1) dilution occurs in the downgradient direction and (2) uranium is transported at almost the same rate as conservative constituents of natural groundwater. The conclusions regarding uranium transport distances relative to conservative constituents must be tempered by uncertainties regarding the presence of complexing agents (BSC 2004 [DIRS 169218], Section 15.7.8).

Although several natural analogue studies have demonstrated the effects of sorption and precipitation processes on fracture surfaces, none has been able to distinguish clearly between these processes or to provide quantitative information on retardation with respect to the transport of trace elements in natural waters. However, these studies do highlight which mineral phases are most active and provide useful information on the effect of the interaction between solutes and rock surfaces on fractures (BSC 2004 [DIRS 169218], Section 15.7.8).

In most studies of natural systems, a proportion of the total uranium, thorium, and rare earth elements in groundwater have been associated with colloids. Colloids can serve as sorbers of radionuclides and could be agents either of retardation or of fast transport. Unambiguous evidence from natural systems indicating colloidal transport over kilometer-scale distances is limited. Observations from Los Alamos, New Mexico, and the Nevada Test Site lend support to the concept that radionuclide transport in the SZ can be facilitated by colloids, but no natural analogue studies have been able to quantify the importance of this process (BSC 2004 [DIRS 169218], Section 15.7.8).

Biosphere—The Chernobyl, Ukraine, observations regarding hot-particle atmospheric dispersal and dust transport showed that radionuclides get attached to dust particles and are dispersed with these particles. Aspects of models of atmospheric contaminant dispersal, radionuclide fallout, radionuclide resuspension, and particle-size distributions may be relevant to constraining modeling for radionuclide resuspension affecting ash deposits that could result from a volcanic eruption through the Yucca Mountain repository.

The half-lives of radionuclides provide conservative estimates of radionuclide removal from soils in the Yucca Mountain Biosphere Model Component. An increase in the concentrations of radionuclides in soils during irrigation was observed in the southern Ukraine, a locality with environmental conditions more similar to those at Yucca Mountain than they are at Chernobyl. These increases in radionuclide concentrations confirm the concept of the radionuclide buildup factor used in the Yucca Mountain Biosphere Model Component (BSC 2004 [DIRS 169218], Section 15.7.9).

A literature survey regarding the behavior of radionuclides in soils, in the Chernobyl, Ukraine, area suggests that soil type influences the ecological half-life of radionuclides in the biosphere, both in regard to soil bioaccumulation factors, and with respect to advective and diffusive transport properties that limit radionuclide transfer to plant roots. Agricultural methods, including irrigation, tillage, and the types of crops that may play an important role in radionuclide resuspension, could have an effect on rural populations. Radionuclide resuspension is likely to increase the contamination of plant surfaces and would increase the inhalation dose for agricultural workers, especially for plutonium as given in *Natural Analogue Synthesis Report* (BSC 2004 [DIRS 169218], Section 15.7.9).

Estimated transport of groundwater from sources of contamination could result in radionuclide-contaminated water being used as a source for drinking water, irrigation, animal watering, and for domestic applications, thus increasing the likelihood of ingestion uptake of radionuclides by humans. Chernobyl observations showed that the ingestion pathway constitutes a small part of the total radiation dose, as the direct exposure to radiation is predominant within the Chernobyl Exclusion Zone. Chernobyl observations on the atmospheric distribution of contaminants, and their fallout and redistribution in soils and plants, may be considered as an analogue for the release of radionuclides caused by a volcanic eruption at Yucca Mountain. The Chernobyl observations are also useful in understanding the atmospheric dispersal of contaminants into the environment during posteruption ash fallout onto the land surface (BSC 2004 [DIRS 169218], Section 15.7.9).

Volcanism and Seismic Effects on Drifts—Natural analogue investigations are part of the effort to understand volcanism in the Yucca Mountain area. Analogues have been used to assess the probability of dike eruption, plausible eruption styles, eruption parameters, and magma compositions, factors that have been used to increase confidence in the use of the ASHPLUME model (SNL 2007 [DIRS 177431]), to simulate atmospheric dispersal following a theoretical eruption at Yucca Mountain (Section 7.8.1).

For seismic events, examples from observations of underground openings demonstrate that such openings are able to withstand ground shaking for peak ground acceleration as high as 0.4 G. The ability of underground openings to withstand ground shaking is increased by the thickness of

overburden, competence of the rock surrounding the opening(s), decreased earthquake magnitude, and increased distance of the opening(s) from the earthquake epicenter. The bulk of evidence from analogue examples of seismic impacts to underground openings, particularly in settings similar to Yucca Mountain, such as responses to the Little Skull Mountain earthquake, demonstrates that damage to repository drifts due to ground shaking during the postclosure period would be minimal or unlikely (BSC 2004 [DIRS 169218], Section 15.7.10).

Summary—The information from natural analogues has contributed to the understanding of drift stability, waste form and EBS degradation, seepage, UZ flow and transport, coupled processes, SZ transport, the biosphere, and disruptive events, such as igneous intrusions, volcanic eruption and seismic events. This information was used to develop the abstractions that are fed to the TSPA-LA Model through the analysis and model reports. The use of this information during the development of the TSPA-LA submodels ensures that the submodels are grounded in reality and provide confidence in the TSPA-LA Model results. In addition to the confidence provided by the examples of natural analogues on a qualitative basis, a performance comparison with two selected analogues, the Cerro Negro volcanic eruption and the Nopal I uranium mine at Peña Blanca, provides additional confidence in the TSPA-LA Model.

7.8.1 Performance Assessment Comparison with Ash Fall at Cerro Negro

The Cerro Negro volcano is one of a number of active basaltic volcanoes in a volcanic mountain range in Nicaragua. Cerro Negro is located on the Caribbean tectonic plate, and the volcanic activity expressed within this long volcanic mountain range, which extends from southern Mexico to Costa Rica, is directly related to subduction of the Pacific tectonic plate under the Caribbean tectonic plate. Volcanism at Cerro Negro has a 150-year history, with at least 22 documented eruptions. The eruption in 1995 produced a tephra volume of 0.004 km^3 (Hill et al. 1998 [DIRS 151040]), a volume similar to, but less than, the volume from the Lathrop Wells cone, which was approximately 0.07 km^3, as described in *Characterize Eruptive Processes at Yucca Mountain, Nevada* (SNL 2007 [DIRS 174260], Appendix C, Section C.7). The 1995 Cerro Negro eruption may be analogous to the type of eruption that could occur at the Yucca Mountain repository however, Cerro Negro's long history, shape, and magma-production rate suggest that it may represent a young composite volcano rather than a simple, long-lived cinder cone (McKnight and Williams 1997 [DIRS 162827]). Because of the uncertainties associated with the atmospheric and eruption conditions of the Cerro Negro event, comparison of ash-fall thicknesses between the observed distribution and the ASHPLUME result is qualitative. However, this comparison provides confidence that the ASHPLUME software code can give a reasonable representation of ash deposition for the type of eruption that could occur at Yucca Mountain.

The two-dimensional Advection-Dispersion Model of Suzuki (1983 [DIRS 100489]) is implemented by the ASHPLUME code. The following two versions of the code were used to simulate the Cerro Negro ash thickness measurements.

1. Version 1.4LV (STN: 10022-1.4LV-02 [DIRS 161296]) uses the volume and density of the ash to determine ash column height and mass, as described in *Atmospheric Dispersal and Deposition of Tephra from a Potential Volcanic Eruption at Yucca Mountain, Nevada* (SNL 2007 [DIRS 177431], Section 1.2.1).

2. Version 2.0 (STN: 10022-2.0-00 [DIRS 152844]) uses eruption power and event duration to determine column height and mass of ejecta (SNL 2007 [DIRS 177431], Section 1.2.1).

To evaluate the differences in the two ASHPLUME models and demonstrate that they can reasonably predict the ash fall distribution from the eruption of a basaltic cinder cone volcano, these two versions of ASHPLUME were used to simulate a Cerro Negro eruption, and the results were compared to Cerro Negro ash thickness measurements. A slightly different version, ASHPLUME_DLL_LA Version 2.1 (STN: 11117-2.1-00 [DIRS 181035]), was used for the TSPA-LA Model to calculate ash fall for the Volcanic Eruption Modeling Case. ASHPLUME_DLL_LA Versions 2.1 and ASHPLUME Version 2.0 are identical computationally. ASHPLUME_DLL_LA Version 2.1 only differs in its ability to interface with the Fortymile Wash Ash Redistribution code (FAR) for TSPA calculations.

Input parameter values from Hill et al. (1998 [DIRS 151040]), for each ASHPLUME version used in the Cerro Negro ash dispensing calculations, are compared in Table 7.8-1. The ASHPLUME_DLL_LA Version 2.0 [DIRS 152844] simulation was completed first, producing a value for the total mass of ash erupted, based on observed eruption parameters (e.g., total duration and ash column height). Next, the ASHPLUME_DLL_LA Version 1.4LV [DIRS 161296] simulation was performed using the same parameter set and a value for ash volume equal to the total mass of ash produced in the Version 2.0 [DIRS 181034] calculation as in *Atmospheric Dispersal and Deposition of Tephra from a Potential Volcanic Eruption at Yucca Mountain, Nevada* (SNL 2007 [DIRS 177431], Appendix L).

As shown on Figure 7.8-1, the ASHPLUME calculations compare well with the observed thicknesses for distances from the volcanic vent greater than 10 km. For distances less than 10 km, the ASHPLUME results give ash thickness values greater than the observed thicknesses. The lobe on the northern side of the map of measured ash thickness is interpreted to be a result of a variation in wind direction or speed, or both, that occurred during the eruption. This variation accounts for some of the discrepancy, because ASHPLUME assumes a constant wind speed and direction for a given simulation. Figure 7.8-1 compares ASHPLUME V1.4LV and ASHPLUME V2.0 to show the overall consistency between the two versions.

The results generally show that the ASHPLUME model can reasonably predict the ash-fall distribution and ash-fall thickness from the eruption of a basaltic cinder cone volcano similar to Cerro Negro. The Cerro Negro ash-fall calculation method was used to simulate eruptive releases of ash either near the Yucca Mountain repository or through the repository involving WP destruction and aerial distribution of radionuclides. Figure 7.8-2 provides a schematic illustration of the modeling elements that are included in the TSPA-LA Model for the Volcanic Eruption Modeling Case at Yucca Mountain.

ASHPLUME was used in two additional natural analogue studies performed for the Lathrop Wells Cone in Nevada and Cinder Cone in California, as documented in *Atmospheric Dispersal and Deposition of Tephra from a Potential Volcanic Eruption at Yucca Mountain, Nevada* (SNL 2007 [DIRS 177431], Sections 7.3.1.2 and 7.3.1.3). The comparisons of prehistoric ash thickness distribution with simulations using ASHPLUME V2.0 provide confidence that the ASHPLUME code can estimate ash thickness for simulated possible future volcanic eruptions involving the Yucca Mountain repository.

7.8.2 Nopal I Uranium Mine at Peña Blanca, Chihuahua, Mexico

The Peña Blanca natural analogue is a naturally occurring uranium ore deposit, Nopal I, that is analogous to the Yucca Mountain repository. The Nopal I site provides a means to estimate the fate of SNF when it is placed in a geologic repository. Hydrogeologic investigations accompanied by the installation of observation wells have provided opportunities to test the strength of the analogy between Nopal I and the repository, and attempt to provide confidence in the performance of the Yucca Mountain repository with respect to the fate and transport of radionuclides that could be released from the repository.

The Peña Blanca natural analogue Nopal I uranium mine, is located in the Sierra Peña Blanca range, approximately 50 km north of Chihuahua City, Chihuahua, Mexico (Murphy 1995 [DIRS 121310]). The Peña Blanca Nopal I uranium deposit is geologically, climatically, geochemically, and hydrologically analogous to Yucca Mountain, and its approximately 3 million years of exposure to oxidation (Murphy et al. 1991 [DIRS 151772]; and *Natural Analogue Synthesis Report* (BSC 2004 [DIRS 169218], Section 10.4) makes it temporally analogous to the more than one-million-year "period of geologic stability" of the Yucca Mountain repository defined in NRC Proposed Rule 10 CFR 63.302 [DIRS 178394] required for performance assessment in 10 CFR 63.342(c) [DIRS 178394]. Reports by Pickett and Murphy (1997 [DIRS 109989]); Murphy and Pearcy (1992 [DIRS 151773]); Leslie et al. (1993 [DIRS 101714]); Green et al. (1995 [DIRS 149528]); and Murphy (1995 [DIRS 121310]), describe the mineralogy and paragenesis of the uranium-bearing phases, as well as the source term for hydrochemical migration in the near-field area of the Nopal I ore body.

The Nopal I uranium deposit (Murphy and Codell, 1999 [DIRS 149529]) originally consisted of uraninite (uranium oxide) a mineral directly analogous to SNF, which is largely composed of uranium oxide. The essence of the analogue of Nopal I to Yucca Mountain, as described in *Uranium Mineralogy of the Nopal I Natural Site, Chihuahua, Mexico* (Pearcy et al. 1993 [DIRS 151774]); and *Natural Analogue Synthesis Report* (BSC 2004 [DIRS 169218], Section 10.4) is as follows:

- Climate—Nopal I and Yucca Mountain are located in arid to semi-arid regions. Annual rainfall at Nopal I is approximately 240 mm/year (Murphy et al. 1990 [DIRS 151772], p 271) and annual rainfall at Yucca Mountain between 100 and 300 mm/yr (BSC 2004 [DIRS 169734], Figure 7.6).

- Geology—The Peña Blanca district containing the Nopal I mine and Yucca Mountain are fault blocks in the Basin and Range structural geological province. The Nopal I mine and Yucca Mountain contain Tertiary volcanic rocks consisting of welded and non-welded ash-flow tuffs, and both overlie older carbonate rocks.

- Hydrogeology—The Nopal I mine and Yucca Mountain are located in the UZ under oxidizing conditions more than 100 m above the SZ.

- Geochemistry—The uraninite ore at the Nopal I mine has been altered to secondary uranium minerals such as the oxyhydroxide schoepite and uranyl silicates such as boltwoodite and uranophane. The SNF at Yucca Mountain will be primarily uranium

oxide, which is essentially uraninite, and the fuel is also expected to be altered to schoepite and uranyl silicates (Ebert et al. 2005 [DIRS 173071], Executive Summary).

7.8.2.1 Background

The Peña Blanca Nopal I ore deposit lies in high desert terrain in the Basin and Range geologic province shown on Figures 7.8-3 and 7.8-4 (Pearcy et al. 1993 [DIRS 151774]). The Nopal I ore body is located in the Peña Blanca uranium district on the southeast side of the Sierra Peña Blanca, which is named for the white color of oxidized mineral deposits in the range. Field observations indicate that the pre-mining land surface at the Nopal I deposit exposed a small portion of the ore body. The deposit lies in fractured, welded, and altered rhyolitic ash-flow tuffs analogous to the volcanic rocks at Yucca Mountain (George-Aniel et al. 1991 [DIRS 105636]).

When the Nopal I ore deposit was excavated and mined in the late 1970s and early 1980s, two prominent benches were cut across the ore body at the 0-m and +10-m levels (local, vertical mine coordinates). Two adits enter the mined area from land surface at the 0-m and 70-m levels, and the one principal shaft connects the 0-m adit with adits at the 20-m, 40-m, and 70-m levels, as shown on Figure 7.8-5 (Reyes-Cortes 1997 [DIRS 149533], Figure 25, p. 205). The total depth of the main mineshaft is approximately 110 m from the –20-m level.

The Nopal I ore deposit has been estimated to be approximately 32 ± 8 million years old (Fayek 2006 [DIRS 181367], p. 57). Examination of the weathering mineralogy of the ore body indicates that the deposit was stable and under reducing conditions until approximately 3 million years ago, when it was exposed to oxidizing groundwater, infiltration from precipitation, and weathering processes (Murphy and Codell 1999 [DIRS 149529]). Since that time, the oxidation of the uranium oxide ore proceeded through a progression of uranium minerals from schoepite to uranyl silicates dominated by uranophane (Pearcy et al. 1994 [DIRS 151774]; Murphy and Codell 1999 [DIRS 149529]).

The geologic characterization of the Nopal I ore body is described in *Geology of the Peña Blanca Uranium Deposits, Chihuahua, Mexico* (Goodell 1981 [DIRS 149484]), and shown on Figure 7.8-6. The ore deposit occurs in ignimbritic ash-flow tuffs similar to those found at the Yucca Mountain site (DOE 1998 [DIRS 100550]). The top 30 m of the deposit lie in the Nopal Formation, a fractured rhyolitic tuff, and the lower 70 m lies in the Coloradas Formation, a weakly welded, fractured, ignimbritic tuff. The deposit, and probably the lower several meters of the ore body, is underlain by 60 m of the Pozos Formation, a silicified, detrital conglomerate, composed principally of altered limestone clasts, which lies on Cretaceous limestone. A near vertical fault, with greater than 10 m of offset, intersects the hill containing the ore body and lies to the east of the deposit, but does not appear to cut the ore body. Minor faults and fractures are observed in the vertical walls of the open faces of the mine above the 0-m and 10-m levels.

The ore body can be approximately described as a roughly cylindrical, breccia-pipe-like form, approximately 18 m by 30 m in the horizontal plane and 100 m in the vertical dimension. The deposit is presently estimated to contain 333 metric tons of uranium (George-Aniel et al. 1991 [DIRS 105636]). Uranium comprises approximately 0.23 percent of the deposit by volume (George-Aniel et al. 1991 [DIRS 105636]). Using analyses of oxidized uranium minerals,

Pearcy et al. (1993 [DIRS 151774]); and Murphy and Codell (1999 [DIRS 149529]) estimated that the unoxidized ore body contained 408 metric tons of uranium as uranium oxide.

Elements of the site hydrogeology are presented in *Hydraulic Characterization of Hydrothermally Altered Nopal Tuff* (Green et al. 1995 [DIRS 149528]); and *Uranium Mineralogy of the Nopal I Natural Analog Site, Chihuahua, Mexico* (Pearcy et al. 1993 [DIRS 151774]). The Nopal I ore deposit lies in the UZ, and boreholes drilled in 2003 established that the water table is approximately 122 m below the ore deposit (BSC 2004 [DIRS 169218], Section 10.4). Green and Rice (1995 [DIRS 149485]), conducted an artificial recharge study at the Nopal I mine, and the field observations were used to estimate the hydraulic properties of the intact and oxidized portions of the ore body. Their investigations indicated that the porosity of the ore deposit ranged from 0.05 to 0.08 for unaltered rock, to 0.30 for altered rock. The saturated hydraulic conductivity ranged from 6×10^{-12} cm/s for the unaltered rock, to 1×10^{-7} cm/s for the altered rock.

Previous studies of the Nopal I deposit have focused on the geochemical aspects of the oxidation, transport, and reprecipitation of uranium mineral phases in the matrix and bedrock (Pearcy et al. 1993 [DIRS 151774]; Pickett and Murphy 1997 [DIRS 109989]; Pearcy 1994 [DIRS 149523]; Goldstein et al. 2003 [DIRS 168528]). These studies show that uranium, protactinium, and thorium have low groundwater concentrations. The analysis of rock samples collected from fractures exposed on the exposed 0.0 and +10 benches show that actinides released from the ore deposit precipitated in fracture filling minerals within a few tens of meters from the deposit (Goldstein et al. 2003 [DIRS 168528]).

Three boreholes were drilled at the Nopal I site in 2003. Borehole PB1 was drilled immediately adjacent to the ore body continuously cored to total depth approximately 20 m below the top of the SZ. Borehole PB2 was drilled approximately 50 m uphill from PB1 and borehole PB3 was drilled approximately 50 m downhill from PB1. The total well depths of these boreholes ranged from 243 m to 255 m, and they were all completed to approximately 20 m below the observed water table. The cuttings and core samples from the three boreholes were used to characterize the lithologic and hydrogeologic properties of the UZ. In addition, well PB4 located about 1.3 km southeast of the ore deposit was reconditioned to serve to measure the depth to the water table and collect water samples. Water samples have been collected from these four boreholes, and other wells in the area, since 2003. The locations of observation wells PB1 to PB4, and the Pozos Ranch windmill-operated, ranch-supply well, are shown on Figure 7.8-7 (BSC 2004 [DIRS 169218], Figure 10.4-4).

7.8.2.1.1 Climate/Infiltration

Precipitation infiltration has not been estimated at the Nopal I site, but the vegetation and soil of the area indicate that some infiltration is likely (Leslie et al. 1999 [DIRS 109967]). The climate of the Peña Blanca region is arid, with an estimated 250 mm/yr of precipitation (Pearcy et al. 1993 [DIRS 151774]). The presence of perched water in shot holes drilled into the open bench of the +10-m level indicates that precipitation infiltration occurs in the area of the Nopal I mine (Pickett and Murphy 1999 [DIRS 110009]). Because of the climatic similarity of Sierra Peña Blanca and the Yucca Mountain site, and because there have been no long-term infiltration

studies at the Nopal I mine site, the infiltration observations made at Yucca Mountain are considered to apply at the Nopal I site (CRWMS M&O 1998 [DIRS 100356]).

The physiography of the Peña Blanca district is similar to that of the Great Basin where long-term information on climate and precipitation patterns was assembled as part of the TSPA-LA, as summarized in *Yucca Mountain Site Description* (BSC 2004 [DIRS 169734], Sections 2.1.2 and 3.2.1, physiography, Sections 6.3 and 6.4, modern and past climate, respectively). Because of similarities in geography and physiography and the lack of local observations for the state of Chihuahua, the long-term infiltration patterns observed at Yucca Mountain and reported in the Yucca Mountain site description are considered to be adequate for the performance assessment analysis of the Peña Blanca natural analogue.

7.8.2.1.2 Unsaturated Zone

Ghezzehei et al. 2006 [DIRS 179134] conducted a passive seepage study that investigated the ore deposit's near-field UZ to examine patterns of responses to precipitation events. The investigation analyzed seepage in the mine adits using 240 water collectors installed in a gridded pattern. The results of the investigation indicated that there are very heterogeneous seepage volumes and arrival times after a precipitation event. The infiltration into the mine in the area of the ore body displayed slower seepage at a relatively constant rate. Faster flow paths and larger volumes of water were observed away from the ore body. Ghezzehei et al. 2006 ([DIRS 179134], p. 110) modeled the faster seepage locations as having discrete fracture flow and the slower seepage locations as indicative of matrix flow. The longer residence times at the slower seepage locations are consistent with higher uranium concentration and Uranium isotope disequilibrium observed in analyses of water samples collected at these locations.

The vertical UZ section of rock below the ore body is approximately 230-m thick based on the logs of the observation wells drilled in 2003. Figure 7.8-8 shows the stratigraphy of observation and sampling well PB1, as observed in core samples collected during drilling, as well as the results of geophysical logging in PB1 *Natural Analogue Synthesis Report* (BSC 2004 [DIRS 169218], Figure I-1). The UZ is composed both of the lower part of the tuff and volcanic conglomerate of the Pozos Formation and of the upper part of the Cretaceous limestone that underlies this region of northern Mexico. The UZ below the Nopal I deposit has heterogeneous hydrogeologic properties. Green and Rice (1995 [DIRS 149485]) calculated percolation flux based on measured hydrogeologic properties for samples of altered tuff and simulated water flow through partially saturated media in the upper part of the UZ. However, the heterogeneous nature of the UZ is illustrated by observations made during pumping of the three observation wells installed within 100 m of the ore deposit. The water levels in the three wells are not in agreement. Further, the inconsistent responses of the water levels in these wells that were observed during pumping to collect groundwater samples indicate that one of these wells, PB3, is not well connected to PB1 and PB2, despite their proximity to one another (Goldstein et al. 2006 [DIRS 181364], p. 218).

7.8.2.1.3 Saturated Zone

The SZ beneath the volcanic tuffs containing the uranium deposit at the Nopal I site lies near the base of the Pozos Conglomerate, from about 8 m to 20 m above the Cretaceous limestone as

reported in *Natural Analogue Synthesis Report* (BSC 2004 [DIRS 169218], Table 10.4-4, Figures I-1, I-4, and I-5). The water table is in the Cretaceous limestone in PB4. The water-table elevations of wells PB1 to PB4 are within 6 m of one another, with the highest elevation in PB1 and the lowest values in PB2 and PB4 (BSC 2004 [DIRS 169218], Table 10.4-5) Despite the apparent lower elevation in PB2, the data appear to indicate a flow gradient to the southeast.

The Nopal I ore deposit at the Peña Blanca natural analogue, in a manner similar to that at Yucca Mountain, could theoretically transport the water flowing through the ore deposit to the UZ, and any radionuclides released from the ore deposit and transported by water moving through the UZ would be passed to the SZ at the water table in a manner analogous to that expected beneath the Yucca Mountain repository (Sections 6.3.9.1 and 6.3.10.2). The estimated leachate from the Nopal I deposit would primarily contain uranium isotopes and potentially other radionuclides released from the ore deposit. The theoretically contaminated groundwater would flow eastward in the SZ through the Cretaceous limestone according to the hydraulic gradient (Green et al. 1995 [DIRS 149528], Figure 4.8).

7.8.2.1.4 Hydrogeology

The performance assessment analysis of Nopal I assumed the Peña Blanca area to be located in an area where there is lateral to vertically downward groundwater flow (Green et al. 1995 [DIRS 149528], Section 5, paragraph 1). The site of the Nopal I mine is in a recharge condition relative to the regional groundwater flow (Green et al. 1995 [DIRS 149528]). A significant playa, Playa Cuervo, exists east of the Sierra Peña Blanca, and is the likely regional discharge location for groundwater in the Peña Blanca area, and appears to be the local sink for groundwater flow in the Sierra Peña Blanca (Reyes-Cortes 1997 [DIRS 149533], Section I, pp. 24 to 27, Figure 6).

Although there is not sufficient water-level data from the region around the Peña Blanca district to provide an accurate direction of groundwater flow, the regional information indicates that, in general, flow is from west to east. Rodriguez-Piñeda et al. (2005 [DIRS 181366]) collected water-level data from the Encenillas Basin, immediately west of the Peña Blanca district, and these data indicate an overall higher water-table elevation in this basin compared to that in the El Cuervo Basin east of the Peña Blanca district. The regional water-level data (Figure 7.8-9) showed that the groundwater elevation is approximately 1,560 m above sea level (masl) in the Encinillas Basin, 1,240 to 1,243 masl at Nopal I, and 1,230 masl in the El Cuervo Basin. Therefore, if recharge to the Nopal I ore deposit mobilizes radionuclides from the deposit, it is likely that these radionuclides would be transported to the SZ and then eastward to the El Cuervo Basin.

7.8.2.2 Peña Blanca Analysis

The performance assessment analysis of the Nopal I ore deposit as a confidence-building analogue treats the original and present uraninite in the ore body as having been subject to oxidation and dissolution following the change from reducing to oxidizing conditions approximately 3 million years ago. The analogy is predicated on the supposition that alteration of the Nopal I ore deposit was followed by the release of uranium species, and that these

processes will be replicated in a manner similar to the degradation of the SNF waste forms in the WPs that will be placed in the Yucca Mountain repository. Past and recent investigations conducted at the Nopal I site support this conceptualization of the Peña Blanca natural analogue.

Pickett and Murphy (1997 [DIRS 109989]), and Pearcy et al. (1995 [DIRS 110223]) conclude that the Nopal I ore deposit has been exposed to oxidizing conditions over the last 3.2 to 3.4 million years (and indicate that uranium-mineral alteration of the Nopal I ore deposit has resulted in local-scale migration of uraniferous species involving precipitation of secondary uranium minerals and sorption of released uranyl species after tens of meters of lateral travel. Fayek et al. (2006 [DIRS 181367], p. 57) analyzed core samples obtained from the drilling of PB1 in 2003 as reported in *Natural Analogue Synthesis Report* (BSC 2004 [DIRS 169218], Section 10.4). These analyses provide age determinations for alteration minerals such as uranophane. However, the mineralogic analysis reveals a more complex sequence of mineral alteration and reprecipitation of uranium-bearing minerals, suggesting episodic alteration of the Nopal I ore deposit. The mineralogic analysis revealed that secondary uraninite was deposited under reducing conditions in the Pozos Conglomerate about 100 m beneath the main ore body and about 25 m above the present water table approximately 1.6 million years ago. Subsequently, this secondary deposit was subjected to continued oxidation resulting in the precipitation of schoepite and other uranium secondary minerals. Fayek et al. (2006 [DIRS 181367], p. 57-58) suggest that the secondary uraninite may have been precipitated under lower temperature conditions than were present when the main ore body was emplaced under hydrothermal conditions. Thus, this secondary uraninite zone could represent post ore-emplacement deposition of uranium mobilized under oxidative conditions. The work of Fayek et al. (2006 [DIRS 181367] p. 58) thus suggests that the Nopal I ore body has undergone a complex history of emplacement, oxidation, remobilization, and reprecipitation and that transport of much of the uranium in the original ore body has, despite mobilization, not been transported very far from the initial site of deposition.

The Peña Blanca analysis did not consider dose-to-receptor values as did the TSPA-LA Model analyses, because the goal of the investigation was to estimate concentrations in groundwater of uranium and other radionuclides at selected distances from the Nopal I mine. Radionuclides released from the ore body were reported in groundwater samples collected beneath the ore body and at approximately 50 m and approximately 1 km downgradient from the ore body (Goldstein et al. 2006 [DIRS 181364], Table1).

7.8.2.2.1 Source Term Dissolution and Radionuclide Inventory

The source term for the Peña Blanca natural analogue is a uranium mineral, primarily uraninite, ore body that has been the source for the alteration of the primary uraninite and the release of radionuclides since the ore body was exposed at or near land surface approximately three million years ago. Uranium-oxide degradation was the likely operating mechanism for degradation and dissolution of the Nopal I ore body. The sequence of uraninite alteration at Nopal I is similar to that of CSNF and the uranium-oxide fuel analyzed in the laboratory tests, and the corrosion products derived from the uranium-oxide fuel in the laboratory tests are the same mineral phases that are seen at Nopal I (BSC 2004 [DIRS 169987]). Wronkiewicz et al. (1996 [DIRS 102047], p. 92) compared the reaction paragenesis observed in laboratory experiments with the paragenesis of uranium minerals at Nopal I (Pearcy et al. 1994 [DIRS 100486], p 725).

Figure 7.8-10 illustrates these comparable paragenetic sequences. Wronkiewicz et al. (1996 [DIRS 102047], p. 94) conclude that SNF could be readily altered when exposed to moisture in an unsaturated repository and that, "The migration of fission products from a breached spent fuel package may be significantly retarded by the formation of secondary uranyl phases . . . ."

The approach for modeling CSNF waste form dissolution and release of radionuclides for the performance assessment of the Yucca Mountain repository was developed in *CSNF Waste Form Degradation: Summary Abstraction* (BSC 2004 [DIRS 169987]). The method consisted of using experimental measurements from flow-through dissolution rates for a set of specific spent fuels and for unirradiated uranium oxide for a range of controlled water chemistries and temperature. These measurements were used to develop a rate-law expression for the dependence of the corrosion rate on experimental factors. The dependent variables of the dissolution rate were determined to be pH, total carbonate concentration, temperature, and oxygen fugacity. The spent fuel dissolution rate model developed in *CSNF Waste Form Degradation: Summary Abstraction* (BSC 2004 [DIRS 169987]) is:

$$\text{Log (DR)} = a_0 + a_1 \times \text{IT} + a_2 \times \text{pCO}_3 + a_3 \times \text{pO}_2 + a_4 \times \text{pH} \qquad \text{(Eq. 7.8-1)}$$

where

DR is the dissolution rate

a_0, a_1, a_2, a_3, and a_4 are regression parameters and are considered to be uncertain in the Peña Blanca Analogue Model

IT is 1/temperature

pCO_3 is the negative log of total carbonate molar concentration (uncertain parameter)

pO_2 is the negative log of oxygen fugacity

pH is the negative log of hydrogen ion concentration (uncertain parameter).

Dissolution of the Nopal I ore body likely followed processes similar to that described by the CSNF dissolution equation used in the Yucca Mountain Performance Assessment (Equation 7.8-1). Because the Nopal I ore deposit has been at or near land surface for about 3 million years, the mineral alteration and transport of radionuclides has occurred at ambient temperature. An analogous alteration of the ore deposit would have occurred under similar conditions and using similar parameter values as were used for the corresponding fuel-dissolution rate calculation used for SNF in the Yucca Mountain performance assessment.

French et al. 2006 [DIRS 181362], examined transport of radionuclides from an isolated high-grade boulder that had been part of the high-grade ore stockpile placed near the Nopal I mine during operations in the 1980s. When the high-grade ore was removed from the mine site during the 1990s, an isolated boulder rolled off the stockpile and was left behind on unlined, previously undisturbed soil. The boulder provided a point source for radionuclides to be transported to the soil beneath and around the boulder within the last approximately 25 years. Gamma-ray characterization of soil samples revealed the presence of U-series radionuclides and

their intermediate daughters ^{210}Pb, ^{234}U, ^{234}Th, ^{230}Th, ^{226}Ra, ^{214}Pb, ^{214}Bi, and ^{234}Pa. French et al. (2006 [DIRS 181362], p. 68) conclude that the mobilization of radionuclides was due to leaching from precipitation and other weathering processes. Analysis of the concentrations and distribution of the radionuclides in the soil in the immediate vicinity of the boulder indicates that the boulder is the source of those radionuclides. Further, the investigations indicate that there has been multistage mobilization of radionuclides, and that they have not traveled far from the source before being fixed onto clays and organic material in the soil zone.

Another means by which radionuclides have been mobilized from the high-grade ore stockpile is through plant uptake. Leslie et al. 1999 [DIRS 109967] investigated radioactive plants that were growing on the high-grade ore stockpile under ambient conditions. The investigation of the vegetation residues from the plants growing on the high-grade stockpile together with radiochemical analyses of the ore from the Nopal I ore piles provided a radionuclide inventory of uranium species and some daughter products in the ore body. The inventory determined by the vegetation investigation found the uranium series radionuclides, including daughters such as thorium and protactinium, and the results agree with the data presented by French et al. (2006 [DIRS 181362]).

7.8.2.2.2 Water Sample Analyses

Figure 7.8-11 shows the observed concentrations of uranium reported for water samples collected from boreholes PB1, PB2, and PB3, from the mining camp supply well, PB4, and the Pozos Ranch well at the edge of the El Cuervo Basin to the east of the Nopal I mine. These chemical data are reported in Goldstein et al. (2006 [DIRS 181364], p. 217). The high initial concentrations of uranium in PB1, PB2, and PB3 are likely due to drilling contamination. The gradual decay of concentrations seen in these boreholes reflects post-drilling dilution by groundwater flow through the boreholes. Therefore, the late-time samples on Figure 7.8-11, as well as the concentrations at the Pozos Ranch well approximately 3.5 km east of Nopal I (Figure 7.8-7), are more representative of natural background concentrations. The uranium concentrations of less than 300 parts per billion at the distances of the Nopal I boreholes, 50 m from the ore body, show likely sorption or other sequestration of uranium. As shown on Figure 7.8-11, uranium concentrations at the mining-camp well PB4 about 1 km approximately downgradient, as shown on Figure 7.8-7, from the Nopal I ore deposit are negligible, potentially indicating very little downgradient transport of radionuclides from the ore body under active oxidation conditions. Although, PB4 is not directly east of PB1, PB2, and PB3, generally easterly flow from a large point source such as Nopal I, could be reasonably expected to produce a plume of concentration that would intersect PB4.

7.8.2.3 Summary and Discussion

Radionuclide transport by groundwater is the most likely off-site transport mechanism that could possibly affect the performance of the Yucca Mountain repository. Despite some uncertainty in the estimated direction and gradient of groundwater flow, the Peña Blanca natural analogue site offers a unique opportunity to examine the groundwater flow and transport of uranium and its daughter products in a climatic and geologic setting very similar to that of Yucca Mountain. Both sites are set in volcanic tuff in an oxidizing UZ, and they are in similar semi-arid

environments. The Peña Blanca natural analogue at the Nopal I uranium deposit displays the following contrasts and similarities with respect to the Yucca Mountain repository:

- A fully loaded Yucca Mountain repository will likely contain 154 times more uranium than the Nopal I mine (Murphy and Codell 1999 [DIRS 149529]).

- The time scale at Nopal I is on the order of 3 million years. The performance for the Yucca Mountain repository is 10,000 years for compliance with NRC Proposed Rule 10 CFR 63.342(b) [DIRS 178394], and project the performance assessment for the period of geologic stability of 1 million years postclosure per 10 CFR 63.342(c) [DIRS 178394].

- The hydrogeologic configuration of the Nopal I mine is relatively simple. The ore body is exposed at land surface with an approximately 200-m-thick UZ above the SZ. The SZ at Yucca Mountain is at a comparable distance below the repository, mainly in volcanic rocks underlain by Paleozoic carbonate rocks, whereas, at Nopal I, the SZ is primarily in the Cretaceous limestone found in and beneath the Sierra Peña Blanca.

- There are no naturally occurring radioactive ore deposits in the host rocks for the Yucca Mountain repository (BSC 2004 [DIRS 169734], Section 3.6.2), although there are occurrences of radioactive elements in minerals in the host rocks and fracture fillings. Thus, radionuclide transport calculations through the tuffs below the repository horizon are, of necessity, approximations of what could occur in the event that waste was emplaced at the repository. At Nopal I, the natural uranium from the ore body not only dissolves and migrates but also produces and transports its daughter products.

- The regional, surface-water-discharge location for the Nopal I ore deposit is approximately 10 km from the deposit, versus, an approximate 60 km to 80 km travel distance to the nearest surface-water discharge for the Yucca Mountain flow system at the Franklin Lake Playa (DOE 2000 [DIRS 155970], Section 5.3).

Observations at the Nopal I uranium-ore deposit at the Sierra Peña Blanca provide insight with which to estimate the migration and/or sequestration of uranium and other radionuclides from the Yucca Mountain repository. The paragenesis of uraninite at the Nopal I site parallels the paragenetic degradation sequence observed for uranium-oxide spent fuel in laboratory experiments simulating a moist unsaturated repository.

Studies regarding both large ore-bearing boulders and other uraniferous material removed from the Nopal I mine indicate that uranium and other radionuclides are mobile and can be transported in the soil and shallow bedrock or subject to plant uptake. The observations show that uranium leached from the ore deposit is apparently exchanging with uranium minerals that precipitate in fractures around the ore deposit. The analysis of water samples from observation wells at the Nopal I site show that despite the precipitation of radionuclides, there is sufficient uranium available for uranium and some of its daughter products to be transported through the Cretaceous limestone below the Sierra Peña Blanca. However, the observed groundwater concentrations are very low, probably due to reprecipitation and/or sorption of uranium and other radionuclides in the UZ and SZ.

The Nopal I mine was originally composed of uraninite, which is essentially the same material as SNF. Hydrogeologic and geochemical investigations at the Nopal I natural analogue indicate that there has been relatively little transport of the radionuclides from the ore deposit, and that few radionuclides have traveled very far from their sources. There are observed concentrations of uranium in the groundwater beneath the Nopal I ore body but the concentrations are relatively low. In addition, the original ore body composed of uranium oxide has been altered to relatively stable uranyl silicates that do not provide large amounts of radionuclides for transport. Geologic investigations of core samples indicate that oxidative leaching of the uraninite in the ore body was followed by a later lower-temperature precipitation of uraninite in the UZ above the SZ. The analysis of water samples collected from wells completed in the SZ beneath and downgradient from the ore deposit show that although there are radionuclides present in the groundwater, their concentrations are generally in the parts per billion range. In addition, the heterogeneous nature of the UZ provides opportunities for leached radionuclides to be naturally sequestered in mineralized fractures or the bedrock matrix. Analyses of soil and vegetation in the vicinity of stockpiles of high-grade uranium ore indicate that the leached radionuclides and radionuclides taken up in vegetation are sequestered and kept from transport.

The Peña Blanca Natural Analogue provides an example of the dissolution, fate, and transport of radionuclides released from the Nopal I mine through a UZ and SZ that are analogous to the Yucca Mountain repository site. The degradation and leaching of the Nopal I ore deposit is analogous to the expected fate of nuclear material to be emplaced at the Yucca Mountain repository. The Nopal I site indicates that material with a composition very similar to SNF has been subject to dissolution, but the leached material has been largely sequestered by paragenesis, mineral precipitation, or sorption onto clays or other minerals in the near vicinity of the ore body. Considering the analogous nature of the Nopal I site with respect to the Yucca Mountain repository, and that the Nopal I site is at land surface, the apparent immobilization and sequestering of uranium and other radionuclides leached from the ore deposit indicate that radionuclides released from the uranium deposit do not migrate far from their sources. Thus, the performance observed at the Nopal I Peña Blanca provides insight and confidence in the long-term performance of the Yucca Mountain repository.

INTENTIONALLY LEFT BLANK

Table 7.8-1. ASHPLUME Parameters Used for Cerro Negro Comparison

Parameter	Version 1.4LV	Version 2.0
Ash density (g/cm^3)	1.2	1.2
Particle shape factor	0.5	0.5
Air density (g/cm^3)	0.001293	0.001293
Air viscosity, g/cm-s	0.00018	0.00018
Constant C ($cm^2/s^{5/2}$)	400.0	400.0
Constant beta	10.0	10.0
Lower limit on column height (km)	0.001	0.001
Mean ash particle diameter (cm)	0.07	0.07
Particle diameter standard deviation	0.8	0.8
Wind speed (cm/s)	900.0	900.0
Initial eruption velocity (cm/s)	10,000.0	10,000.0
Eruption power (watts)	NA	7.34×10^9
Event duration (s)	NA	3.46×10^5
Eruption volume (km^3)	0.00288	NA

Source: SNL 2007 [DIRS 177431], Appendix L. Parameter values are from Hill et al. 1998 [DIRS 151040].

NOTE: NA = not applicable.

INTENTIONALLY LEFT BLANK

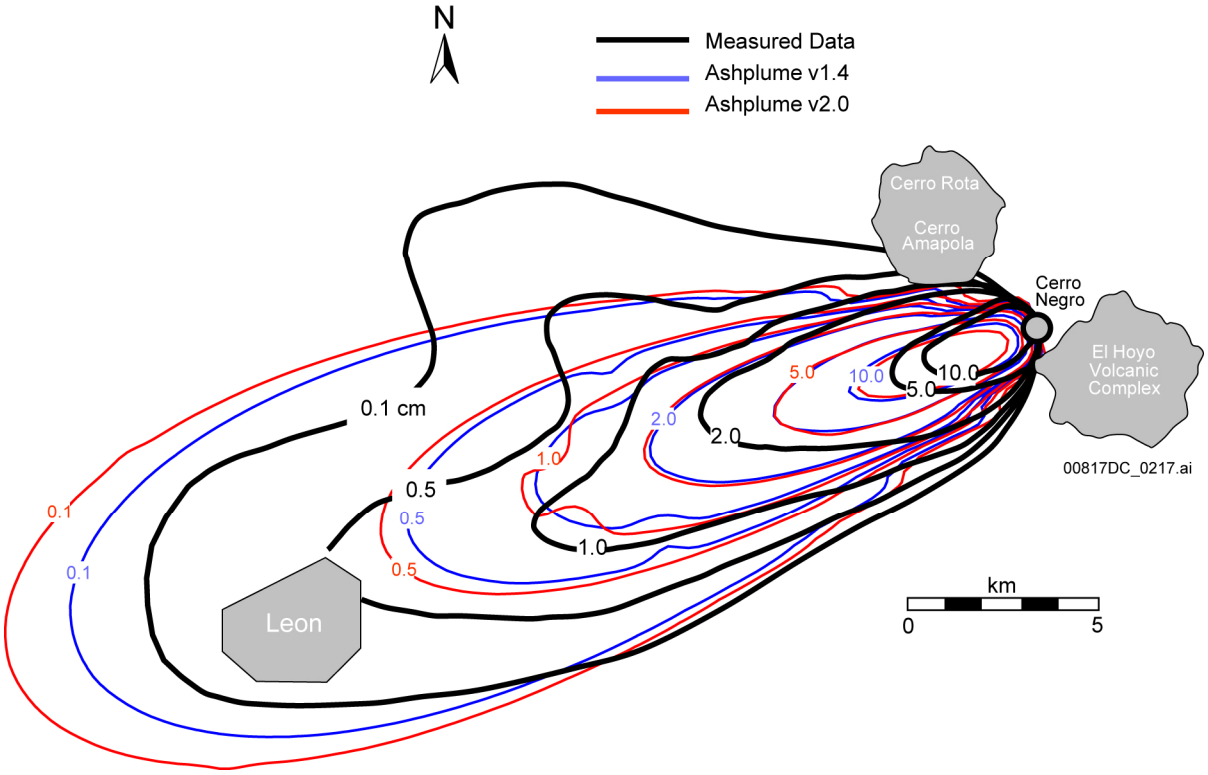

Source: SNL 2007 [DIRS 177431], Appendix L.

Figure 7.8-1. Comparison of Ash Fall at Cerro Negro with ASHPLUME Simulated Results

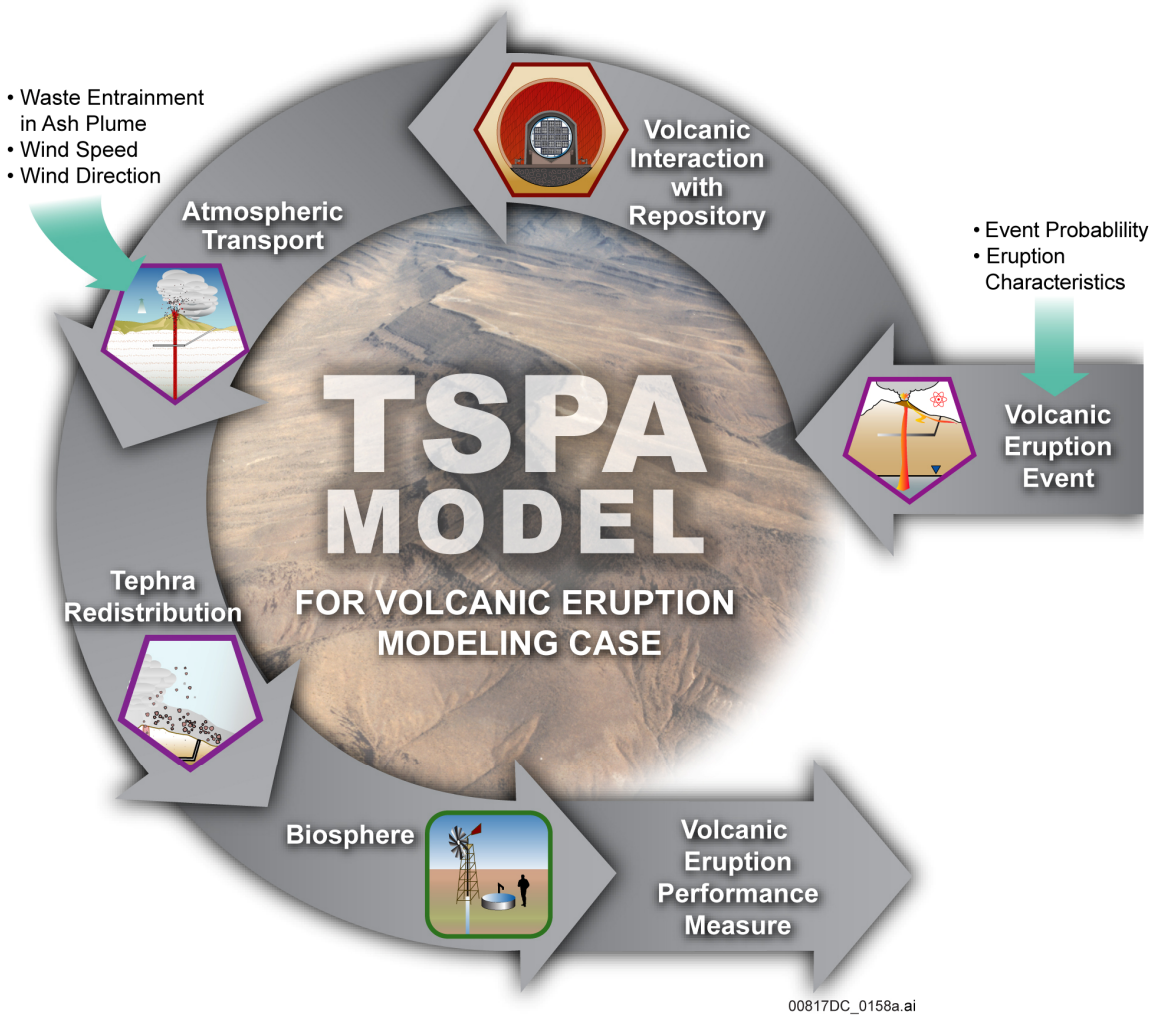

Figure 7.8-2. TSPA-LA Model for the Igneous Scenario Class Volcanic Eruption Modeling Case

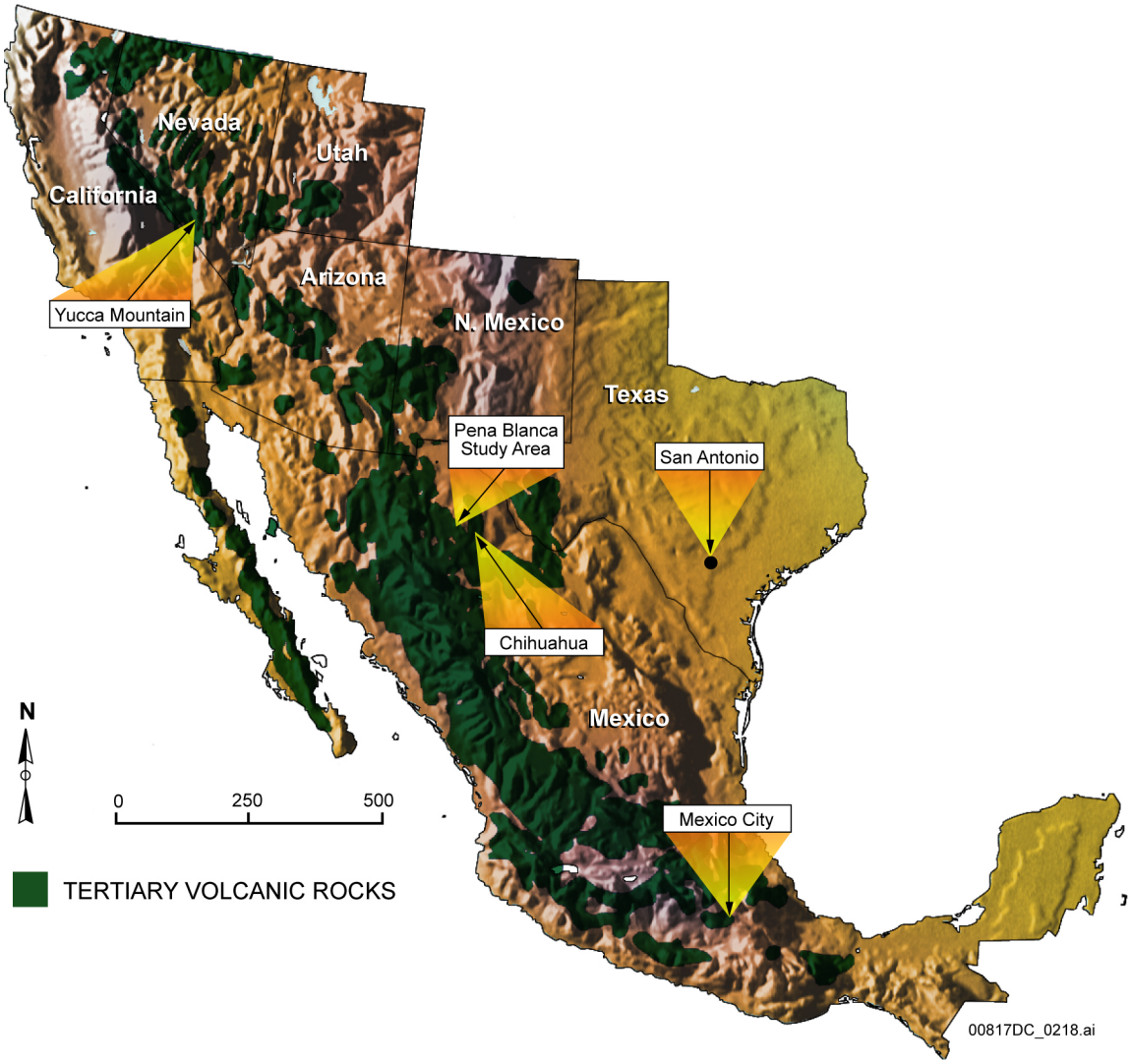

Source: Pearcy 1994 [DIRS 149523], pp. 1 and 2.

Figure 7.8-3. Location of Peña Blanca Study Area

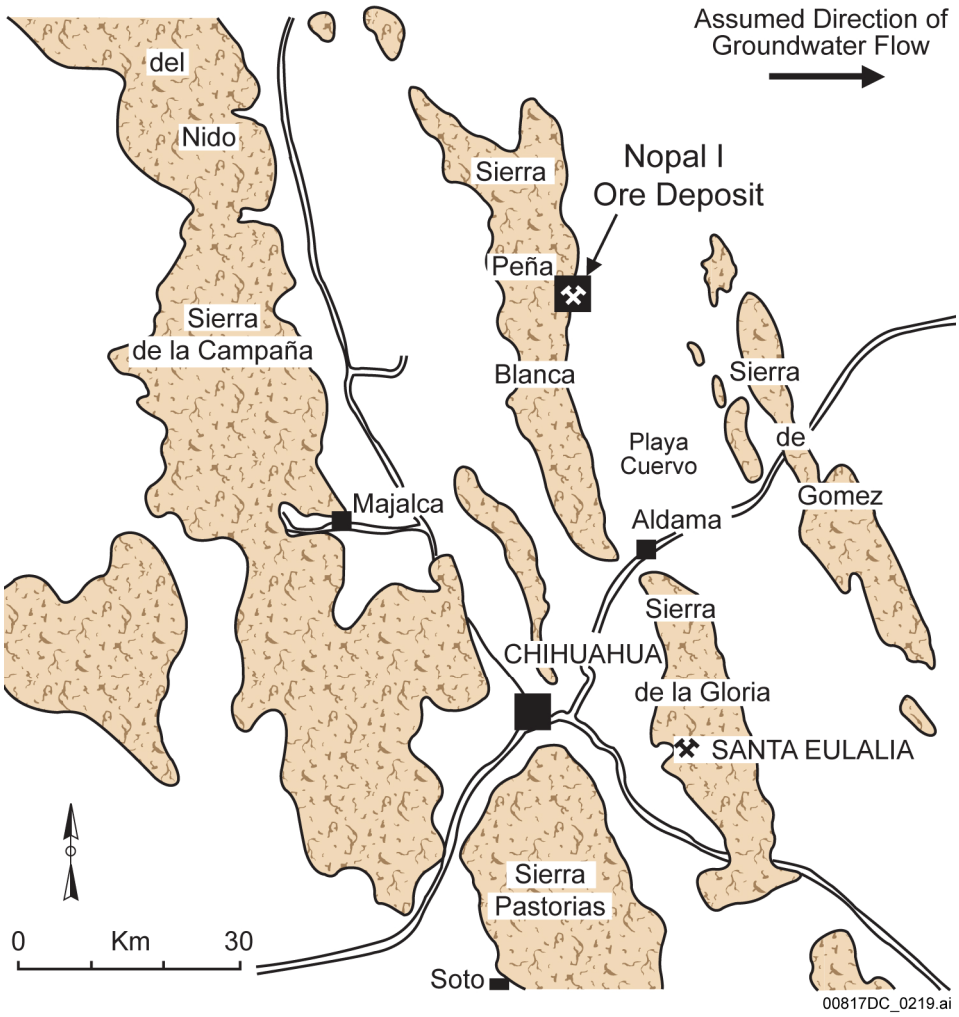

Source: Modified from George-Aniel et al. 1991 [DIRS 105636], Figure 1.

Figure 7.8-4. Location of Peña Blanca Nopal I Ore Deposit

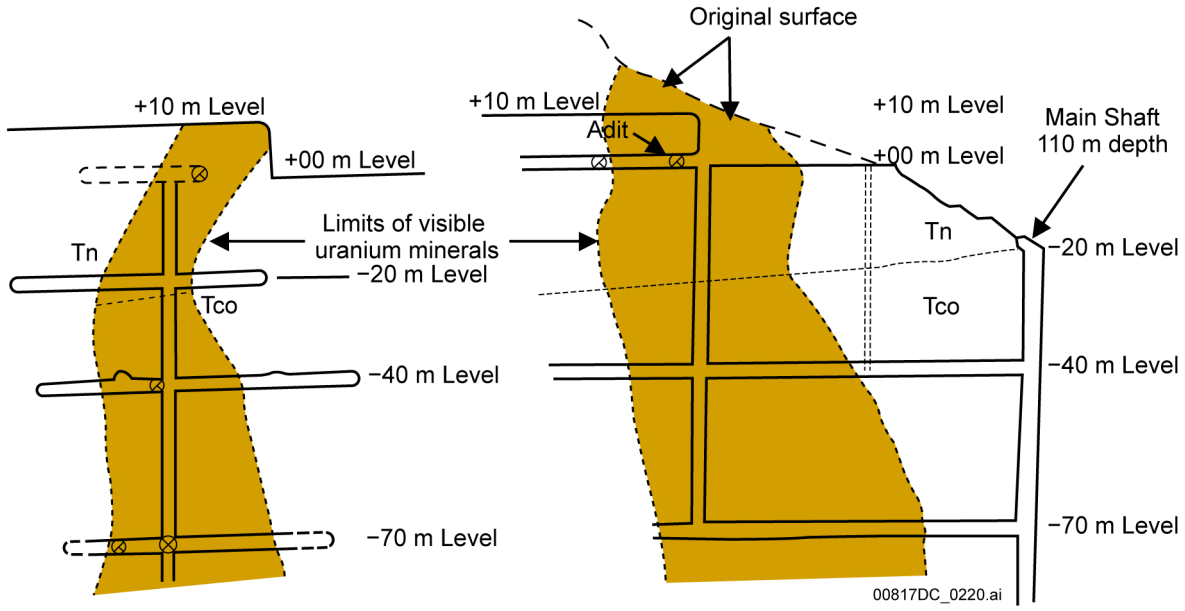

N 5120'E Section showing the accessible main adit at +00 level

N 3840'E Section showing +00 levels and the main shaft at −20 level

Source: Modified from Reyes-Cortes 1997 [DIRS 149533], Figure 25, p. 205.

Figure 7.8-5. Peña Blanca Mine Shaft Schematic

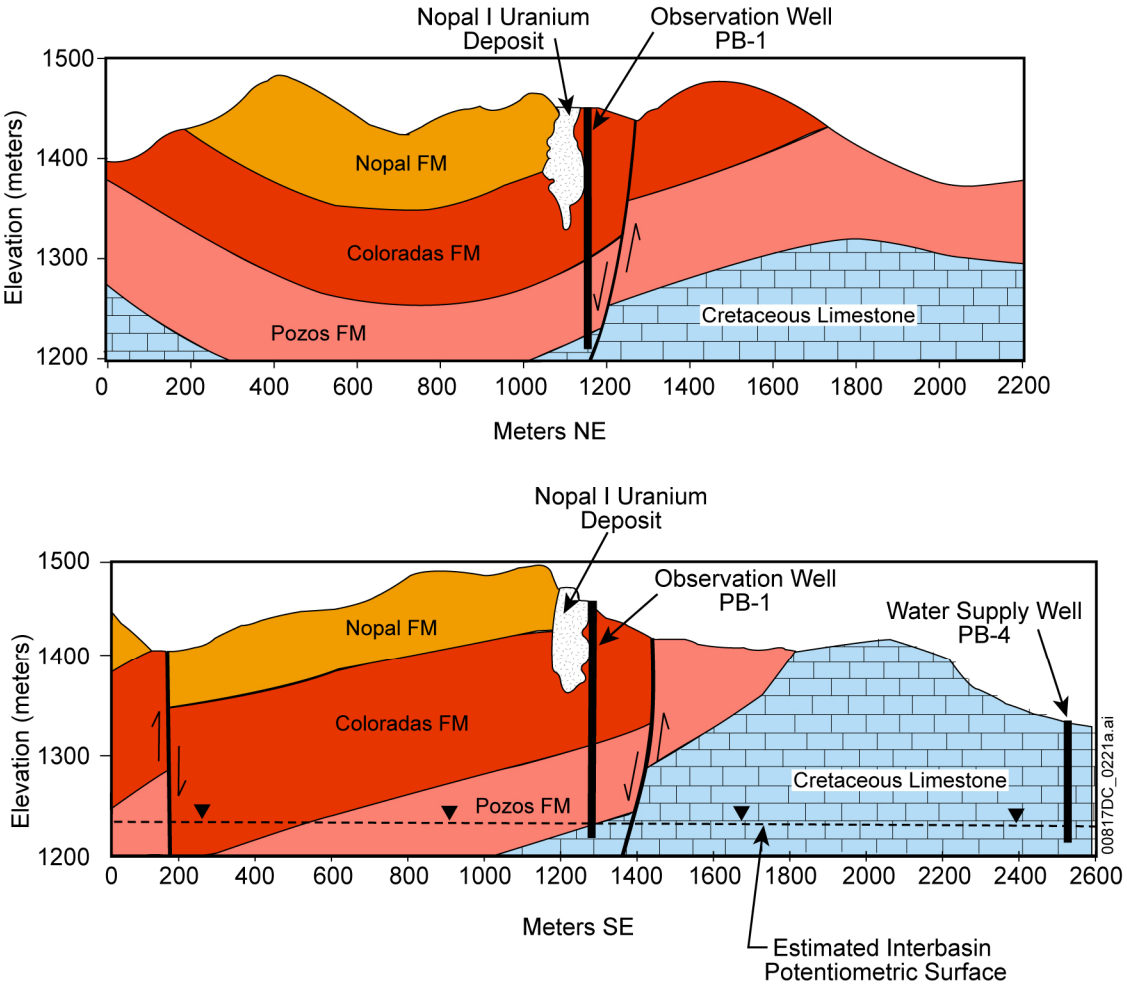

Source: Modified from Pearcy et al. 1993 [DIRS 151774], p. 1-4.

Figure 7.8-6. Geologic Characterization of Nopal I Ore Body

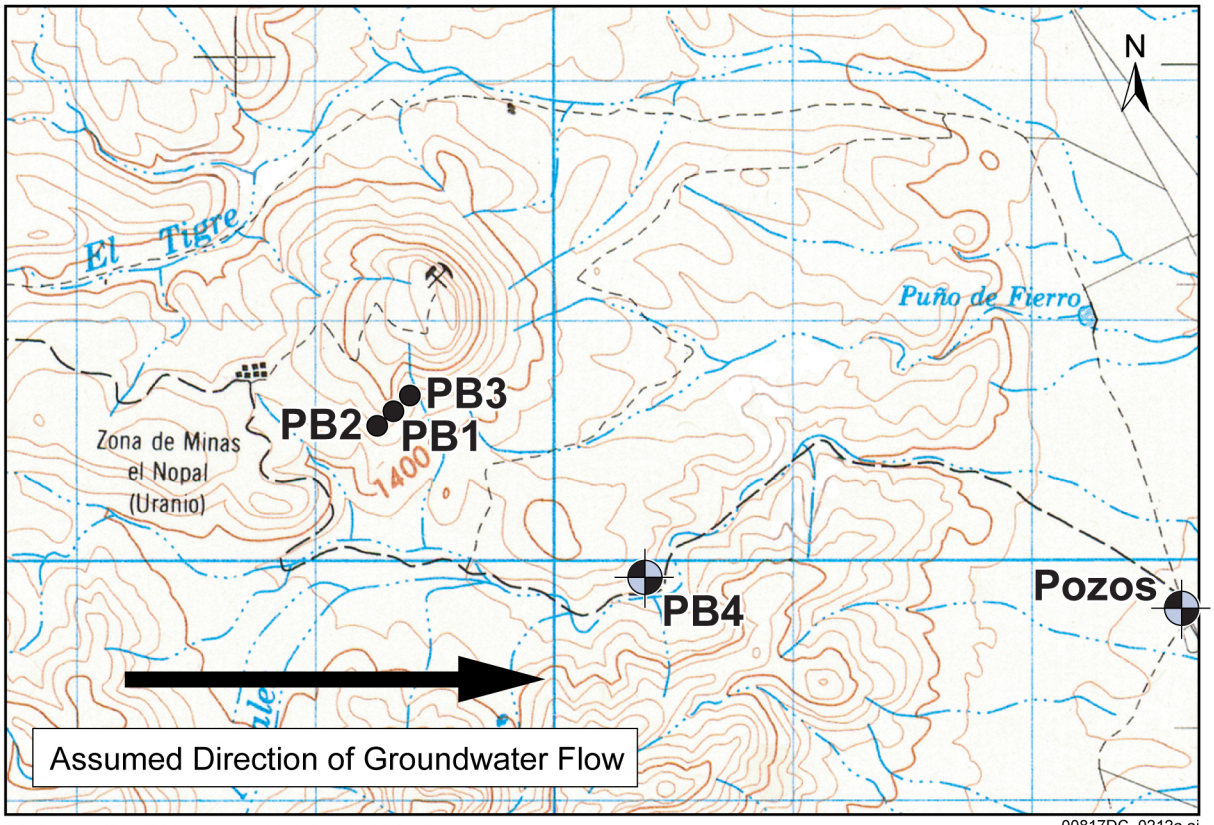

El Sauz 1:50,000 Topographic Map (H13C46)
North American 1927 datum

Legend
- Existing Wells
- New Peña Blanca Boreholes

Source: Modified from BSC 2004 [DIRS 169218], Figure 10.4-4.

NOTE: PB1, PB2, and PB3 were drilled in 2003. PB1 was cored continuously to total depth. PB4 is a former water supply well drilled in the early 1980s.

Figure 7.8-7. Location of Observation Wells at the Nopal I Mine in the Peña Blanca Uranium District

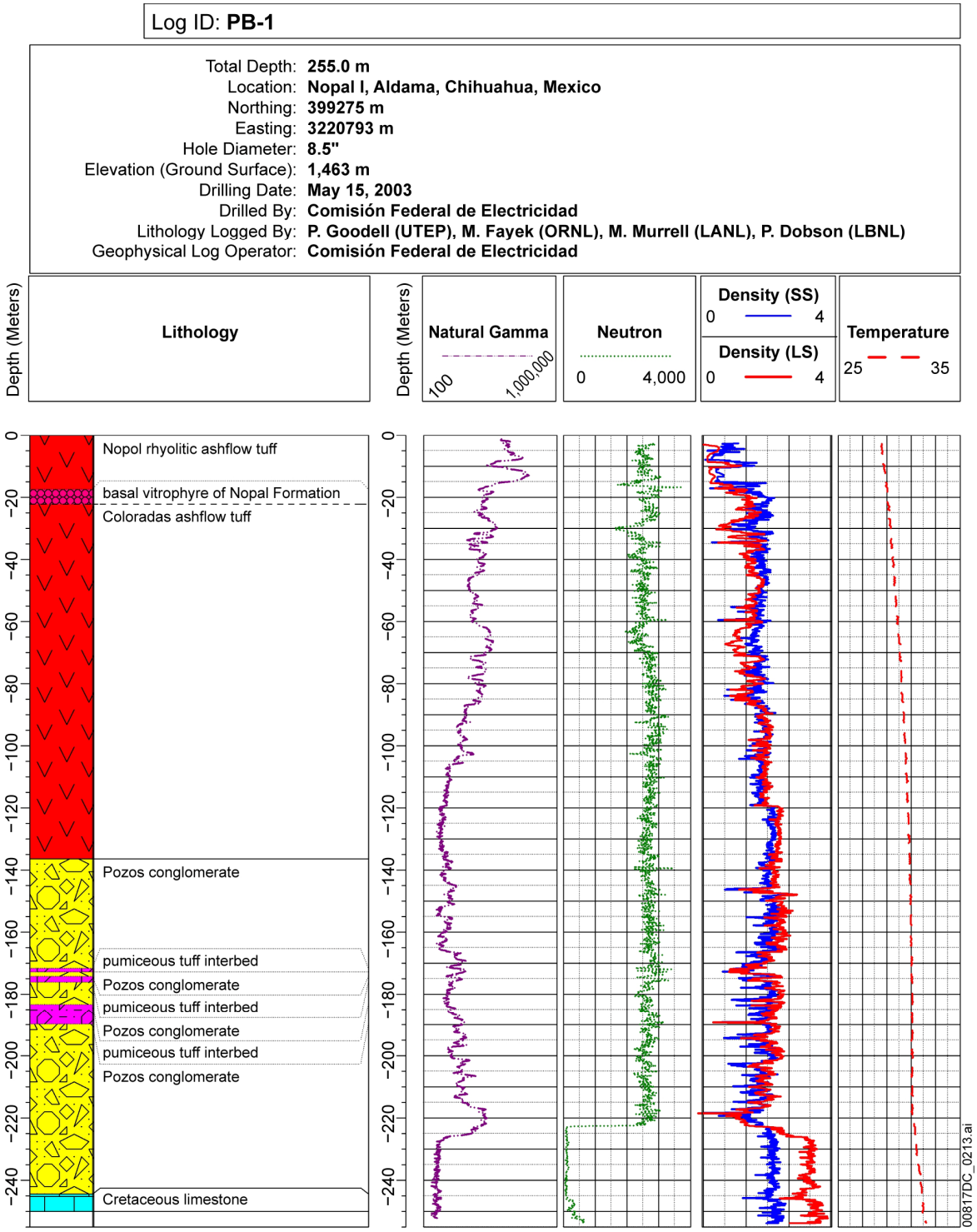

Source: BSC 2004 [DIRS 169218], Figure I-1.

Figure 7.8-8. Geophysical and Geologic Logs of Observation Well PB1

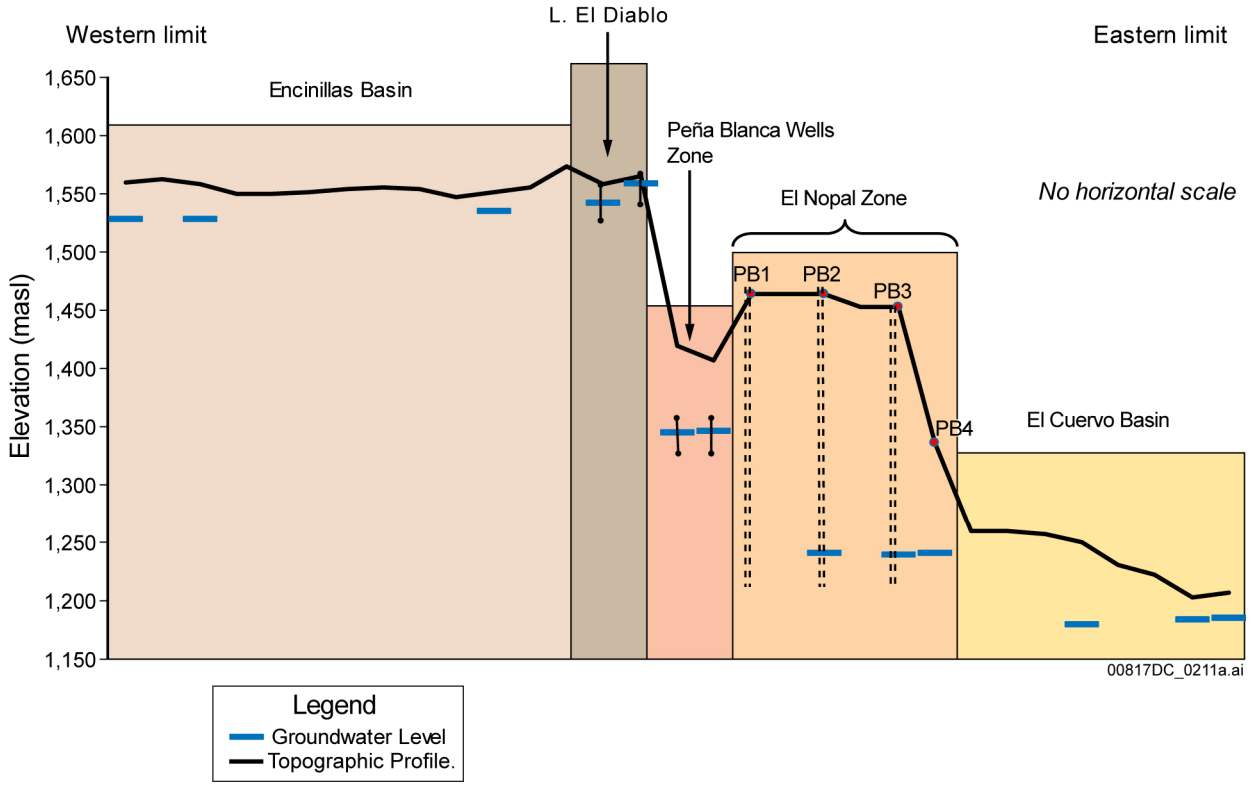

Source: Based on Geological Society of America 2005 [DIRS 181366].

Figure 7.8-9. Schematic Northwest to Southeast Cross Section of the Sierra Peña Blanca Showing the Relative Position of the Water Table in the Encinillas Basin, the Nopal I District, and the El Cuervo Basin

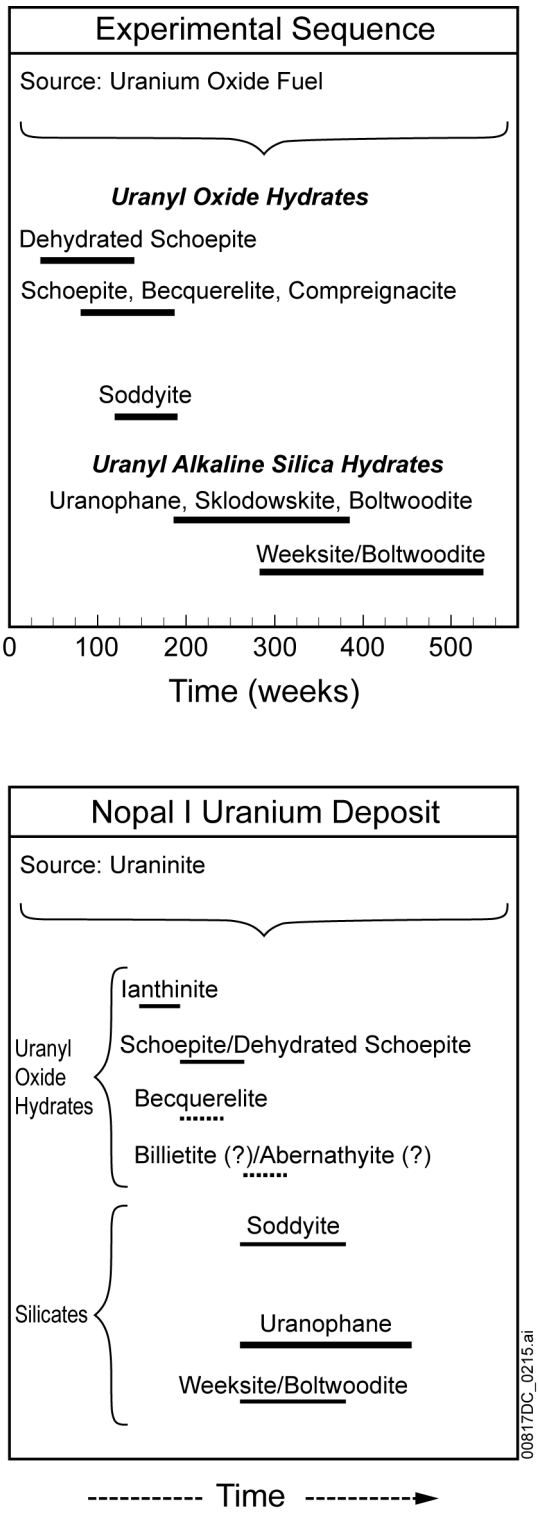

Source: Modified from Wronkiewicz et al. 1996 [DIRS 102047].

Figure 7.8-10. Comparative Reaction Paragenetic Sequences for Uranium Alteration Phases

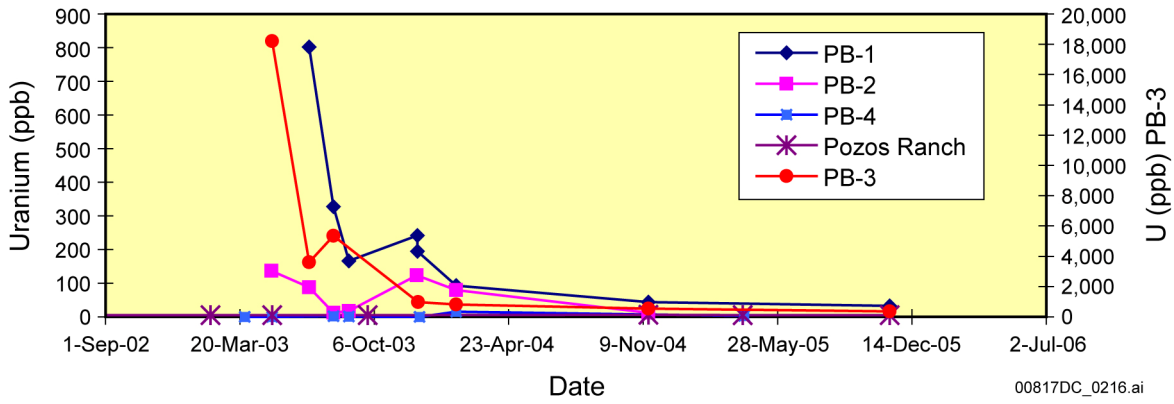

Source: Data from Goldstein et al. 2006 [DIRS 181364], p. 217.

Figure 7.8-11. Uranium Concentration Determined in Groundwater Samples from Wells at and Near the Nopal I Ore Deposit

INTENTIONALLY LEFT BLANK

7.9 TECHNICAL REVIEWS SUMMARY

Section 7.9 summarizes the empanelled technical reviews that were performed by the YMP during the last decade on its TSPA methodology-development approach for producing valid models. These reviews, conducted by teams of experts, were undertaken in order to ensure that the TSPA Model produced by the YMP applying the methodology was credible, defensible to the regulatory authorities, and respected by the technical community. The following sections chronologically describe the reviews, which are the cumulative results that supported the development of the TSPA-LA Model documented in this model report.

Section 7.9.1 addresses the first of these three reviews, namely the peer review of the TSPA-VA, which was completed in 1999. This review was conducted to evaluate whether the TSPA was sufficiently describing the postclosure behavior of the repository. The TSPA-VA review contributed to the development of the TSPA-SR. The TSPA-SR was then subjected to a peer review conducted by an IRT in 2001. The IRT review, described in Section 7.9.2, was undertaken to evaluate the soundness of the Project's decision for site recommendation and, more especially, to seek recommendations from the international perspective for preparation of the next TSPA for LA, which is the TSPA-LA Model documented in this model report. In turn, the earlier drafts of the TSPA-LA Model, along with their supporting analyses and model reports, were subjected to a technical review conducted by an IVRT as mentioned in Section 7.1. The IVRT review was convened in order to gain insight into the state of the validation status of the model as reflected in its early drafts and seek comments and recommendations that were to be applied to the development of the TSPA-LA Model. The IVRT was completed in 2006. The IVRT review is presented in Section 7.9.3.

Before the individual reviews are presented, some discussion on the function of technical reviews in model validation and evolution of the TSPA-LA Model as a result of the Project's previous technical reviews is provided below in order to put the presentation into perspective.

Technical Reviews and Model Validation Requirements

During the last decade the YMP conducted three empanelled technical reviews on the previous versions of the TSPA that led to the current TSPA-LA Model. The reviews were conducted by teams of experts. Although the emphasis and criteria for the reviews varied somewhat from one review to the next as the TSPA Model development process progressively matured from the viability assessment to site recommendation to LA, the underlying single common purpose for all reviews remained the same. That purpose was to continue to improve the model development process as envisioned in the NRC guidance for preparation of model development (Eisenberg et al. 1999 [DIRS 155354]) in order to ultimately develop the TSPA-LA Model, via a successful TSPA-SR, that would comply with the requirements for an LA to the NRC for authorizing construction of the repository at the Yucca Mountain site.

SCI-PRO-006 requires performing two of the activities that are identified therein for the post-model development phase. Technical reviews may be included as one of the activities undertaken in order to produce a valid model. A brief summary of the requirements for developing a valid TSPA Model is included below in order to provide a perspective on the TSPA-LA Model validation strategy (Section 7.1) and the role of technical review in that strategy.

Development of a valid model is an iterative process as described by the NRC (Eisenberg et al. 1999 [DIRS 155354]) and alluded to in Section 7.1. The iterative process involves continuing to validate the model, often with change in compliance strategy, to enhance confidence that the model would meet and exceed the goal for its intended use. In the case of developing a model for a system with a high potential human health and environmental consequence, such as the postclosure performance of a geologic repository for disposal of high-level radioactive waste, the progressive model development process must be controlled by an established quality assurance procedure in order to ensure a high degree of traceability and transparency of the model development process. The development of the TSPA-LA Model evolved through such a controlled iterative process. The TSPA-LA Model development and validation process is guided by *Quality Assurance Requirements and Description* (QARD) (DOE 2007 [DIRS 182051], Supplement SIII-2) and implemented by the QA procedures developed for the purpose. As discussed in Section 7.1, SCI-PRO-006, which controls the development of the TSPA-LA Model, requires that the needed pre- and post-development model verification and validation activities are identified and described in the TSPA-LA technical work plan (SNL 2008 [DIRS 184920]). The technical work plan identified and described the activities required for developing and validating the TSPA-LA Model. The TSPA-LA Model validation approach is presented on Figure 7.1-2.

The governing procedure for the TSPA-LA Model development (SCI-PRO-006 by reference to SCI-PRO-002) identified six criteria to ensure that the model is valid for its intended purpose. At least two of the nine post-development activities identified are required to ensure that the model is valid for its intended purpose.

Two of the nine post-development validation activities identified by SCI-PRO-006 involve a technical review of two kinds. The first is the critical review for which the instructions are described in Attachment 4 of this procedure. The second kind of optional review is peer review, which is governed by SO-PRO-001, *Peer Review*. The earlier versions of the TSPA models received both types of technical reviews. The TSPA-VA and the TSPA-SR models each received a peer review, and the earlier drafts of the TSPA-LA Model received a critical review. SCI-PRO-006 (Section 6.4.10) requires an independent technical reviewer as a part of the model development activities regardless of whether or not a critical review or a peer review is used as one of the post-development model validation criteria. The independent technical review ensured that the TSPA-LA Model was developed as per the requirements stated in the technical work plan (SNL 2008 [DIRS 184920]), and confirms the adequacy of the validation portion of the model documentation.

The TSPA-LA technical work plan (SNL 2008 [DIRS 184920]) incorporated the required criteria for the development of the TSPA-LA Model. As mentioned earlier, the technical work plan did not select a technical review as one of the activities for post-development validation of the

TSPA-LA Model. The rationale for this decision is that another technical review on the TSPA-LA Model was deemed unnecessary given that during the past decade of its iterative development the predecessor TSPA models, as well as their input process models, underwent a number of technical reviews, including the recent IVRT review on the early drafts of the TSPA-LA Model as discussed below. Instead, as a post-development validation criteria, the technical work plan required documenting the Project responses to the comments and implementation of the recommendations from the reviews already conducted on the predecessor TSPAs; in particular, responding to the remaining IVRT issues and continuing to implement the IVRT recommendations.

The technical work plan (SNL 2008 [DIRS 184920]) selected a number of post-development model validation activities from among the nine identified by SCI-PRO-006 (Section 7.1, Figure 7.1-2) to build confidence in the TSPA-LA Model (Section 7.1, Figure 7.1-2). These technical work plan activities include: (1) corroborating the TSPA-LA direct input abstraction results with those of the respective underlying process models (Section 7.6); (2) auxiliary analyses (Section 7.7) that include (a) analyses of single realizations, (b) comparison of the TSPA-LA Model with a separately developed Simplified TSPA-LA Analysis, (c) comparison of the TSPA-LA Model with a TSPA Model for the repository independently developed by EPRI using their own code (IMARC), and (d) the PMA; and (3) evaluation of man-made and natural analogues that are relevant to the different components of the TSPA-LA Model (Section 7.8). In addition, post-development model validation criteria presented in the technical work plan (SNL 2008 [DIRS 184920]) required documenting the Project to the comments and implementation of the recommendations from the prior reviews of the past Project TSPAs to enhance confidence in the final product.

Past Technical Reviews and Evolution of Methodology for the TSPA-LA Model

The TSPA methodology is iterative, as mentioned above. The general TSPA process adopted by the DOE follows the methodology developed by the NRC (Codell et al. 1992 [DIRS 103714] and Westcott et al. 1995 [DIRS 100476]). Over time, the methodology has been enhanced and applied to numerous Projects by various international organizations involved in radioactive waste management. The TSPA-LA Model was developed to analyze the ability of the natural and engineered systems of the Yucca Mountain repository to isolate nuclear waste following repository closure. Performance assessments and related supplemental analyses of the Yucca Mountain repository have been conducted following the publication of the Nuclear Waste Policy Act as Amended in 1987, Public Law No. 100-203 [DIRS 100016]. The TSPAs of the Yucca Mountain repository have been iterative and periodically updated, each building on and extending the scope and results of the previous TSPA. The iterative assessments incorporate both an improved understanding of the processes affecting repository performance and, through additional field observations and laboratory analyses, better identification and quantification of the values of the parameters used in the TSPA.

Early iterations of probabilistic TSPAs for the Yucca Mountain repository include TSPA-91 (Barnard et al. 1992 [DIRS 100309]); TSPA-93 (Wilson et al. 1994 [DIRS 100191]); TSPA-95 (CRWMS M&O 1995 [DIRS 100198]); and *Total System Performance Assessment – Viability Assessment of a Repository at Yucca Mountain* (DOE 1998 [DIRS 100550], Volume 3). The more recent TSPA iterations include *Total System Performance Assessment for the Site*

Recommendation (CRWMS M&O 2000 [DIRS 153246]) and the application of the Total System Performance Assessment-Site Recommendation Model to the Final Environmental Impact Statement for the Yucca Mountain Repository (Williams 2001 [DIRS 157307]).

TSPA iterations are evaluated and independently reviewed by technical staff and various independent organizations. Reviewers generally make recommendations for improvements for consideration in future TSPA iterations. Examples of empanelled technical reviews that contributed to the development of the TSPA-LA Model include the peer review of the TSPA-VA completed in 1999 by a panel of experts and an evaluation of the TSPA-SR by an IRT of peers completed in 2002. More recently, an IVRT performed a critical review of the initial drafts of the TSPA-LA Model. The IVRT review was completed in 2006. The TSPA-VA, IRT, and IVRT reviews are discussed below in Sections 7.9.1, 7.9.2, and 7.9.3, respectively.

In addition to the three empanelled reviews, the Nuclear Waste Technical Review Board (NWTRB) performs routine reviews on key areas of the Project as mandated by Congress. The NWTRB focuses its review effort on three broad technical areas of the Project: Preclosure Operations, Postclosure Repository Performance, and System Integration. The NWTRB reviews on the TSPA effort are captured by its focus on postclosure repository performance. The NWTRB comments on the TSPA, and the Project responses to their comments along with the implementation of the recommendations, are captured in the NWTRB reports and correspondences presented in the NWTRB websites: http://www.nwtrb.gov/reports/reports.html and http://www.nwtrb.gov/corr/corr.html, respectively. These comments and recommendations made significant contributions to the development of the TSPA-LA Model on an on-going basis.

7.9.1 TSPA-VA Review

This section summarizes the TSPA-VA peer review with respect to the scope and methodology of the review, the comments and recommendations made by the review panel, and the Project's response to the comments and implementation of the recommendations. The details are documented in the panel report (Budnitz et al. 1999 [DIRS 102726]) and the Project's response document (CRWMS M&O 1999 [DIRS 153111]).

7.9.1.1 Scope and Methodology for the TSPA-VA Peer Review

The TSPA-VA peer review was conducted to provide a formal, independent evaluation and critique of the TSPA-VA. The peer review was planned and managed by the DOE Management and Operating Contractor at that time. The specific scope was for the review panel to conduct a phased review over a two-year period to observe the development and completion of the TSPA-VA. The comments, concerns, conclusions, and recommendations of the review panel were to be provided in a final report to the Management and Operating Contractor to support the eventual development and conduct of the TSPA-LA. The panel was expected to evaluate the TSPA-VA Model for its analytical approach, including the following within the context of their significance to the long-term performance of the repository:

- Physical events and processes considered in analyses
- Use of appropriate and relevant data
- Assumptions made

- Abstraction of process models into total system models
- Application of accepted analytical methods
- Treatment of uncertainties.

In addition to the review of the TSPA analytical approach, the panel was also to consider traceability and transparency of the TSPA-VA analyses.

The TSPA-VA peer review was conducted in accordance with the Management and Operating Contractor QAP-3-3, *Peer Review,* that was in effect at that time and consistent with the NRC guidance for conducting peer reviews (Altman et al. 1988 [DIRS 103597]). The peer review was conducted during the period 1997 through 1998, with the final panel report submitted in early 1999. As a part of the phased approach of the peer review, the panel submitted three interim reports that were based on observations on the draft documents supporting the TSPA-VA and formal and informal interactions with the Project technical staff, which collectively led to the final TSPA-VA report (DOE 1998 [DIRS 100550], Volume 3) on which the panel's final report was based.

The panel was comprised of six members distinguished in their individual area of expertise. Details of the purpose, methods, panel members, and findings of the peer review on the TSPA-VA model are provided in the panel's final report (Budnitz et al. 1999 [DIRS 102726]). The final report includes the major points from the three interim reports, updated as appropriate, as well as the new findings the panel developed during its review of the TSPA-VA (DOE 1998 [DIRS 100550], Volume 3).

7.9.1.2 TSPA-VA Panel Comments and Recommendations and the Project Responses

The objective of the TSPA-VA review panel in reviewing the completed TSPA-VA (DOE 1998 [DIRS 100550], Volume 3) was to provide comments, concerns, conclusions, and recommendations that could be used in the development of a TSPA Model that would ultimately support development of the LA. The panel drew no conclusion regarding acceptability of the proposed repository or readiness for preparation of the LA and stated that the comments and recommendations it made should be considered with that fact in mind.

The TSPA-VA review panel's key conclusions include:

- Overall, the approach demonstrated in the TSPA-VA for assessing the behavior of the repository during the postclosure period was sound (Budnitz et al. 1999 [DIRS 102726], Section C, p. 3).

- The panel stated that "it is unlikely that the TSPA-VA, taken as a whole, describes the long-term probable behavior of the proposed repository". In the panel's judgment, a number of components of the TSPA-VA analysis were not supported by adequate evidence that they represent systems, components, and processes they were designed to represent. In addition, several of the component models were likely to be conservative and others non-conservative. For these reasons, the panel stated that the decisions based on the TSPA-VA should be made cautiously (Budnitz et al. 1999 [DIRS 102726], Section B, p. 1).

- The TSPA-VA was a necessary and useful step in evolving the understanding of how a repository could be expected to perform at Yucca Mountain. It has produced valuable insights into performance of the various repository components and helped identify issues where additional data and analyses could improve understanding of the repository performance and where additional work is unlikely to make significant contributions (Budnitz et al. 1999 [DIRS 102726], Section B, p. 1). The panel noted the inherent difficulty in developing the TSPA Model that is required to predict the repository behavior such a long time into the future (Budnitz et al. 1999 [DIRS 102726], Section B, p. 1). (Note that 10,000 years after the repository closure was the regulatory compliance period at that time).

- The panel noted the many experiments that were planned to be performed, which would be valuable in confirming, calibrating, or invalidating models that were developed for analyses of conditions at the proposed repository (Budnitz et al. 1999 [DIRS 102726], Section B, p. 2).

The Project reviewed and identified the comments and recommendations that were presented in a discussion format in the panel's final report (Budnitz et al. 1999 [DIRS 102726]) and listed them in the comment-response report (CRWMS M&O 1999 [DIRS 153111]). As mentioned earlier, the panel viewed that the objective of the TSPA-LA Model was to demonstrate that the repository would comply with the applicable regulatory standards with reasonable assurance rather than to describe the probable behavior of the repository system, which was the objective of the TSPA-VA Model. The panel thought the TSPA-LA Model objective would be significantly different from the TSPA-VA Model (DOE 1998 [DIRS 100550], Volume 3) objective and recommended the following approaches for achieving the upcoming TSPA-LA objective (Budnitz et al. 1999 [DIRS 102726], Section D, p. 40):

- Updating the component models
- Expanding the quality and quantity of data for analyses
- Using bounding assumption
- Making design changes
- Incorporating the defense-in-depth concept.

The panel also stated: (1) efforts should be made where improvements are feasible in the component models or underlying data if such efforts would affect the overall assessment, (2) it may not be cost effective to make additional efforts where conservative bounding analyses do not result in unduly pessimistic estimates of total system performance, and (3) for complex issues where development of realistic models supported by data is not feasible, a combination of bounding analyses and design changes should be applied.

The YMP found the panel recommendations were consistent with the Project's strategy for development of the postclosure safety cases for the upcoming site recommendation and subsequent LA and the design selection and work-prioritization efforts that were underway for developing the safety case.

The YMP fully implemented the panel recommendations as demonstrated in the significant updates of the component models based on the highly expanded site-scale test data collection

efforts. This collection of test data came from the ESF; single-heater and drift-scale thermal tests; ECRB tests; various (radionuclide-surrogate) tracer tests in the UZ and SZ of the natural system such as the Busted Butte tests, Alluvium Tracer tests, and Natural Gradient tests; and also several supporting laboratory tests (e.g., the long-term corrosion tests). Some of these tests in the ESF and ECRB are ongoing long-term tests and will continue as a part of the Performance Confirmation program after the LA submittal. The Project also made significant design changes since the panel recommendations. The key changes include the use of a DS and, more recently, incorporating the TAD canister to enhance safety during waste transportation to the repository site, aging at the site, and finally the disposal in the underground repository. Parallel to and complementing these data collection and design-change efforts, the Project significantly improved its ability to treat uncertainty in the TSPA Model and its submodels; enhanced the ability of the TSPA-LA computational software; and improved implementation of quality assurance procedures and issue-identification, tracking, and the correcting process such as the Corrective Action Program. The Project vigorously incorporated the defense-in-depth concept in order to increase the safety margin. For the TSPA, the effort included (a) incorporating the design-changes mentioned above in the TSPA computations, (b) performing additional auxiliary analyses of the total system and its subsystems to better understand the TSPA results and reduce the associated uncertainty, (c) ensuring qualitative and quantitative comparison of the TSPA Model components with several man-made and natural analogues, and (d) performing empanelled technical reviews such as the peer review of the TSPA-SR by an IRT, and more recently, the critical review of the earlier drafts of this TSPA-LA Model by an IVRT. The purpose and outcome of the IRT and IVRT reviews are described below.

Utilizing input from the TSPA-VA review group and, where appropriate, modifying modeling and design elements, the Project has subsequently produced much improved TSPAs, which in turn made achieving significant Project goals possible, for example, the submittal of the TSPA-SR (CRWMS M&O 2000 [DIRS 153246]) and the Environmental Impact Statement (EIS) (DOE 2002 [DIRS 155970]) supporting the Site Recommendation. This resulted in the Presidential and Congressional approval of the repository site and authorizing the DOE to proceed with the LA for the NRC authorization to begin construction of the repository. The TSPA-LA Model is the latest product of the above mentioned testing, modeling, and documentation activities performed during the last decade.

7.9.2 International Review Team Peer Review

This section summarizes the IRT peer review with respect to the scope and methodology of the review, the comments and recommendations made by the IRT, and the Project's response to these comments and implementation of the recommendations. The details are referred to in the IRT final report (OECD and IAEA 2002 [DIRS 158098]); Appendix E (TSPA-LA, Volume III) provides the effort the Project made in implementing the IRT recommendations.

7.9.2.1 Scope and Methodology for the International Review Team Peer Review

The IRT peer review was requested by the Project and conducted by a team of experts organized by a Joint Secretariat formed by the NEA and IAEA. The overall objective of the IRT review was to provide, based on the available international standards and guidance as appropriate, an independent assessment of the methodology developed by the Yucca Mountain Site

Characterization Project, as reported in *Total System Performance Assessment for the Site Recommendation* (CRWMS M&O 2000 [DIRS 153246]). The IRT peer review entailed a review and critical analysis of the performance assessment methodology and rationale being used in support of the site-recommendation decision-process.

The IRT review was conducted while taking into account the international experience in preparing for and conducting system-level postclosure performance assessments. In addition, the IRT was to consider in its review the requirements proposed at that time by the EPA and NRC for disposal of high-level radioactive waste in a geologic repository. The IRT was to identify consistencies and inconsistencies between methods being used by the Project and those being considered or developed in international recommendations, standards, or practices. More importantly, the IRT review was to comment on the adequacy of the overall performance assessment approach for supporting the programmatic decision for site recommendation. In addition, recommendations were expected on specific technical improvements that would help the Project's performance assessment effort better support the next programmatic decision point (i.e., the preparation and submission of an LA, specifically the TSPA-LA Model documented in this report).

The IRT review was primarily based on the TSPA-SR (CRWMS M&O 2000 [DIRS 153246]) Model and some of its key scientific basis documents selected by the IRT panel. Consistent with the IRT review objective and scope in conducting the review, the IRT considered (OECD and IAEA 2002 [DIRS 158098], Appendix 1, Section 3):

- The technical basis for the performance assessment, including identification and justification of the conditions and characteristics modeled at the system level. This would include a review of the abstractions of the adopted design and the scientific basis for determining future environments in the system and its materials and natural systems behavior.

- The development of the key conceptual models, including the assumptions made with respect to the representations of relevant FEPs.

- The adequacy of the treatment of the undisturbed and disturbed system performance.

- The adequacy of the methods used and the cases considered in sensitivity and uncertainty evaluations.

- The overall clarity and completeness of the technical report describing this system-level performance evaluation.

The IRT review was conducted through interactions with the technical and management staff, as necessary, and a site visit and meetings open to the public where technical presentations were made by the Project staff and a few invited public participants. As reported in the IRT final report (OECD and IAEA 2002 [DIRS 158098]), the review was performed during June 2001 through December 2001, culminating in a final review report presented to the DOE in January 2002. Additional detail on the scope and methodology of the IRT review is presented in the IRT final review report (OECD and IAEA 2002 [DIRS 158098]).

International Review Team Comments and Recommendation and the Project Responses

The IRT made several recommendations (OECD and IAEA 2002 [DIRS 158098], Section 5.1) on the rationale the Project was pursuing in developing the SR, specifically the TSPA-SR Model; methodology to be used in developing the ensuing TSPA-LA; and the EPA and NRC proposed regulations for the repository. The IRT made these recommendations from the international perspective of the performance assessment methods being considered or recommendations, standards, or practices being developed. The IRT made the following statement (OECD and IAEA 2002 [DIRS 158098], Section 5.2) regarding the overall performance assessment approach used in the TSPA-SR:

> "While presenting room for improvement, the TSPA-SR methodology is soundly based and has been implemented in a competent manner. Moreover, the modeling incorporates many conservatisms, including the extent to which water is able to contact the WPs, performance of engineered barriers, and retardation provided by the geosphere.
>
> Overall, the international review team considers that the implemented performance assessment approach provides an adequate basis for supporting a statement on likely compliance within the regulatory period of 10,000 years and, accordingly, for the site recommendation decision.
>
> On the basis of a growing international consensus, the international review team stressed that understanding the repository system and its performance and how it provides for safety should be emphasized more in future iterations, both during and beyond the regulatory period. Also, further work would be required to increase confidence in the robustness of the TSPA."

The IRT made a set of 27 specific recommendations in its final report (OECD and IAEA 2002 [DIRS 158098], Section 5.3) for future improvements in the preparation and submission of the LA. The Project implemented these recommendations. Table E-1 in Appendix E (Volume III of the TSPA-LA Model report) tabulates the IRT recommendations and describes the work the Project completed implementing these recommendations and provides references to where the work is documented.

7.9.3 Independent Validation Review Team Review

This section summarizes the IVRT review with respect to the review scope as provided by the prevailing TSPA technical work plan, methodology of the review, comments and recommendations made by the review panel, and the Project's response to these comments and implementation of the recommendations. The details are presented in the draft TSPA-LA Model (Gibson 2007 [DIRS 181099]). The IVRT final report is included as Appendix C of the draft TSPA-LA Model, Rev 01E (Gibson 2007 [DIRS 181099]). In addition, a complete tabulation of the IVRT comments and the Project responses, as well as the Project positions on several difficult-to-resolve issues raised early during the review process, are presented in an interoffice memorandum from T.C. Booth (2006 [DIRS 176638]). Several IVRT issues were not fully addressed according to the IVRT panel when these documentations were completed. The Project

has since planned, performed, and documented the additional work to address these issues as discussed below and summarized in Table 7.9-1.

7.9.3.1 Scope and Methodology for the IVRT Review

The IVRT performed the review during 2004, 2005, and 2006 on the earlier draft of the TSPA-LA Model and its supporting draft documentations. The draft material was prepared for the 10,000-year postclosure compliance period rather than the 10,000 year and 1,000,000 year compliance periods covered by the TSPA-LA Model for the current proposed regulations. Therefore, the TSPA-LA Model is based on a changed compliance strategy from the one the IVRT review drafts were based. In developing the TSPA-LA Model, the Project fully utilized the perspective gained from the IVRT review. The Project considered and responded to all IVRT comments and implemented all of its recommendations as described under IVRT Panel Comments and Recommendation and the Project Responses below.

The IVRT conducted its review in two parts. The 2004 part consisted of reviewing the process models that supported the initial TSPA-LA Model that was being drafted at that time and some of their submodels. This 2004 part of the IVRT review was incorporated as a part of the Repository Integration Team (RIT) review that was ongoing independent of the IVRT at the time the IVRT was convened. The 2004 part of the IVRT review was governed by the review criteria in *Technical Work Plan for: TSPA-LA Model Development, Initial Use, and Documentation* (BSC 2004 [DIRS 168449]). The second part of the review conducted in 2005 and 2006 was governed by the review criteria in the technical work plan revised in March 2005 (BSC 2005 [DIRS 173309]). The entire IVRT review was performed in accordance with the then effective LP-SIII.10Q-BSC, *Models.*

The IVRT adopted the iterative model validation process described in *Regulatory Perspectives on Model Validation in High-Level Radioactive Waste Management Programs: a Joint NRC/SKI White Paper* (Eisenberg et al. 1999 [DIRS 155354]) as the strategy for conducting its review. In addition to the RIT part of the IVRT review conducted in 2004 during its review period, the IVRT reviewed several versions of the draft TSPA-LA Model that resulted from the IVRT comment resolutions starting with the 2004 initial draft. The IVRT comments and recommendations for these drafts were incorporated into the draft TSPA-LA (Gibson 2007 [DIRS 181099]), as mentioned earlier. The IVRT review documented in its draft final report of 2005, which incorporated the results of the 2004 review, was conducted within the context of whether or not the TSPA-LA drafts satisfy the intended purpose specifically included in the following two model validation goals (BSC 2005 [DIRS 173309], Section 2.10.1):

1. Describe the postclosure performance of the repository system for the nominal, igneous, and seismic scenario classes.

2. Produce an estimate of mean dose (and other performance measures, as appropriate) that is consistent with the degree of conservatism representative of the component abstraction models and parameters (and their uncertainty) that are input to the TSPA-LA Model.

In July 2004, the IVRT produced a draft report documenting the findings of its review based on the information it had examined up to that time and as per the scope of the 2004 technical work

plan (BSC 2004 [DIRS 168449]). The IVRT focused its review of 2005 drafts of the TSPA-LA Model on evaluating the compliance status of the 20 review criteria given in the 2005 technical work plan (BSC 2005 [DIRS 173309], Section 2.10.1). Ten of these criteria are in the TSPA draft under review, five are in the submodels area, and the remaining five were of general category. Specifically, the technical work plan (BSC 2005 [DIRS 173309]) identified the following as the objective for the technical review (BSC 2005 [DIRS 173309], Section 2.10.1, pp. 17 and 18):

1. The independent review team should determine and document:
   - Whether or not, in their judgment, the criteria are met
   - Whether or not, in their judgment, the TSPA-LA Model is valid for its intended purpose
   - How the judgment for each criterion was weighted in reaching the valid or not-valid decision for the overall TSPA-LA Model.
2. The independent review team was to categorize their judgments regarding whether or not each criterion has been met as follows:
   - Meeting the criterion is significant for the intended purpose of estimating conservative mean dose and the criterion is met.
   - Meeting the criterion is not significant for the intended purpose of estimating conservative mean dose.
   - Meeting the criterion is significant for the intended purpose of estimating conservative mean dose and the criterion is not met.

In August 2005, the IVRT provided interim information to the project that updated the 2004 review and concluded that an evaluation against the review criteria in the 2005 TWP (BSC 2005 [DIRS 173309]) indicated that the model, as then documented, was not valid for its intended purpose. The IVRT findings are documented in the draft final report. Based on a number of information exchanges between the Management and Operating Contractor technical staff and IVRT panel members on comment resolution and the adverse findings by the IVRT documented in the draft final report, the Management and Operating Contractor requested the IVRT to provide recommendations for future improvements for the TSPA-LA Model validation status. In response to this request, the IVRT revised the 2005 draft final report to reiterate their conclusion that the model had not satisfied all review criteria and to include a total of seven recommendations. This report was submitted to records as the IVRT's final report (Gibson 2007 [DIRS 181099], Appendix C).

The following section provides a summary of the IVRT comments and recommendations and the Project responses to these comments and implementation of the recommendations in developing this TSPA-LA Model.

7.9.3.2 IVRT Panel Comments and Recommendations and the Project Response

The detail of the IVRT comments on the TSPA material and its RIT review of the supporting process models and submodels are in the IVRT final report (Gibson 2007 [DIRS 181099], Appendix C). A summary of the IVRT conclusions and the Project status of addressing the IVRT comments and implementation of its recommendations is presented below.

As mentioned earlier, in July 2004 the IVRT produced a draft report documenting the findings of its review based on the information it had examined up to that time. That draft IVRT report was incorporated in the IVRT final report cited above, which was submitted by the IVRT in February 2006. In the course of its RIT and TSPA-LA initial draft reviews in 2004, the IVRT concluded in its final report that, as of December 2004, "the IVRT found that the technical issues that caused some review criteria to be not met were not significant to the determination of validity and that the TSPA Model as configured at that time was valid for its intended purpose, given that the IVRT believed that the model provided a highly conservative estimate of mean dose and that the intended purpose was to demonstrate compliance with the quantitative requirements at 10 CFR 63.311 [DIRS 178394], and 10 CFR 63.331 [DIRS 180319]. The IVRT therefore determined that, notwithstanding the many concerns it had with the TSPA Model, it nonetheless met the established validation goals due to a number of extreme conservatisms embedded in the model."

The IVRT stated in the final report (Gibson 2007 [DIRS 181099]) that in response to the RIT and the IVRT comments the Project modified the draft TSPA Model to remove some extreme conservatism and made numerous other changes, thereby revising the compliance strategy. The Project also performed a series of impact analyses to provide objective evidence of the effect of apparently significant conservatisms on mean dose as well as to provide responses to the IVRT's comments on the submodel reports, thereby generating additional information. The IVRT further noted that one of the most significant changes to the TSPA Model from 2004 to 2005 was the removal of several of the extreme conservatisms embedded in the model. The IVRT felt that the removal of these extreme conservatisms substantially relaxed the conservative basis that the IVRT had relied on for its 2004 conclusion regarding model validity. The Project incorporated these changes in the revised drafts of the TSPA-LA Model that were produced in 2005, which the IVRT reviewed as mentioned above, and developed its draft final report in late 2005.

In the draft final report, the IVRT concluded that, unlike its conclusion documented in the July 2004 draft report, the draft 2005 TSPA Model could no longer be considered valid for its intended purpose because the information available at the time did not adequately support a conclusion that the drafts of the 2005 TSPA Model they reviewed met the two validation goals mentioned earlier. The IVRT reached this conclusion because the 2005 TSPA Model drafts appeared to contain potentially significant optimisms as well as conservatisms and there were no estimates of the performance measures that the IVRT could use as a basis for comparison and for determining the degree of conservatism of the model. This gap of information led the panel to conclude that it could no longer consider the model valid for its intended purpose.

The Project documented, analyzed, responded to all, and resolved most of the IVRT comments, which numbered in excess of 500, before the panel was dissolved with the submittal of its final report. However, some issues remained not fully addressed according to the panel. As

mentioned earlier, based on the IVRT's adverse conclusion regarding the validation status of the 2005 draft TSPA-LA Model in the draft IVRT final report, the Management and Operating Contractor (Bechtel SAIC Company, LLC) requested the IVRT to provide recommendations for future work that could generate additional information to address the most salient issues that led the IVRT to the new conclusion documented in the 2005 draft IVRT final report. In response, the IVRT revised its draft final report to include seven recommendations for potential future work and submitted the final report in February 2006. The IVRT noted in the final report that the iterative approach that was followed in its review was consistent with the model validation process described in NUREG-1636 (Eisenberg et al. 1999 [DIRS 155354]). The IVRT observed in its final report that "Consistent with the model validation process documented in Addendum C.I, the Project will undertake a number of activities that may result in a revised compliance strategy. It is the IVRT's opinion that this is a prudent approach for achieving the goal of developing and implementing an acceptable TSPA Model for supporting a license application."

The Project agreed with the IVRT that successful completion of additional activities planned for FY06 to FY07 would help achieve the goal of a credible TSPA Model for supporting the LA. The Project has since planned and completed these activities as summarized below and shown in Table 7.9-1. The results of these completed additional activities, along with the continued implementation of the IVRT recommendation for improvements, significantly contributed to the TSPA-LA Model as documented in the three volumes of this report.

Subsequent to the IVRT review, the Project revised the draft version of the TSPA-LA Model the IVRT commented on into the draft TSPA-LA Model report (Gibson 2007 [DIRS 181099]). The draft TSPA-LA Model report contains the IVRT final report (summary in Section 7.7 and full report as Appendix C) and the Project's status of responses to the IVRT comments that were in the IVRT final report. Section 7.8 of the TSPA-LA Model report provides a detailed discussion on the Project responses to the IVRT comments and recommendations especially in the context of the validation status of the draft TSPA-LA Model at that time. Implementation of all seven recommendations was substantially completed by the Project at that time, as indicated and discussed in Section 7.7 and Section 7.8 of TSPA-LA Model report (Gibson 2007 [DIRS 181099]). In March 2006, the Project completed documenting (Booth 2006 [DIRS 176638]) all comments that were generated by the IVRT during its review. Booth (2006 [DIRS 176638]) also documented the Project responses to the IVRT comments, including the ones that were considered by the IVRT not fully addressed at the time when the IVRT submitted its final report in February 2006. In addition, Booth (2006 [DIRS 176638]) shows the Project position statements on the difficult-to-address RIT comments generated in 2004. As mentioned earlier, by the close of the IVRT review with its final report submitted in February 2006, a relatively small number of issues remained not fully addressed according to the IVRT panel members (Booth 2006 [DIRS 176638]). The Project continued to work on the remaining issues and implementation of the IVRT recommendations after the IVRT was dissolved and the current status is discussed below.

As mentioned above and in its final report (Gibson 2007 [DIRS 181099], Appendix C), the IVRT made a total of seven recommendations in response to the Project request to improve the validation status of the TSPA-LA Model. Details of these recommendations are discussed in the final IVRT report. In response to the Project request, the IVRT designed the recommendations

so that when implemented, they would remove the key factors that were responsible for the IVRT-designated overall not-met validation status of the 2005 drafts of the TSPA-LA Model. The IVRT recommendations and their implementation by the Project are summarized below.

Three of the IVRT recommendations (numbers 4, 5, and 6) were related to the potential impact on the model due to changes in GoldSim (V. 8.02.500, STN: 10344-8.02-05 [DIRS 174650]), timely identification and managing model file errors, and performing analysis of impact, if any, due to the errors. The remaining four recommendations (numbers 1, 2, 3, and 7) focused on resolving the technical issues that led the IVRT to conclude that the 2005 drafts of the TSPA Model could not be considered valid for the model's intended use based on the review criteria in the governing technical work plan (BSC 2005 [DIRS 173309]). The discussion on the four recommendations to resolve technical issues is presented first, followed by the discussion on the recommendations on GoldSim software and the related modeling file error management issues.

7.9.3.3 Implementation of the IVRT Recommendations

The IVRT recommendations to resolve technical issues and the status of implementation of these recommendations are as follows.

IVRT Recommendation #1: Conduct a sensitivity analysis for the Nominal and Early Failure Modeling Cases in a manner similar to that used in the analysis for the seismic ground motion and igneous intrusion modeling cases in Appendix M of the 2005 drafts of the TSPA-LA Model report. Include the results of the expanded sensitivity analysis in Appendix M of the next revision of the TSPA Model report. The IVRT suggested this expanded sensitivity analysis in response to concerns regarding not-met Review Criteria 1.5, 3.8, and 3.9 (BSC 2005 [DIRS 173309]).

Status: The Project provided supplemental information to the IVRT along with an expanded version of Appendix M as documented in the draft TSPA-LA Model (Gibson 2007 [DIRS 181099]). The IVRT examined the information and concluded that this activity yielded satisfactory results. The Project continued to perform relevant uncertainty and sensitivity analyses (Appendix K in Volume III of this TSPA-LA Model report) in order to enhance the TSPA-LA Model description and especially the confidence in its results. The TSPA-LA Model contains early failure analysis for DS as well as WP barriers. In addition, the appropriateness and reliability of the TSPA-LA Model was evaluated by a set of auxiliary analyses as discussed in Section 7.7.

IVRT Recommendation #2: Examine the potential for risk dilution for all important uncertain parameters identified in the expanded Appendix M sensitivity analyses described in Recommendation #1. The IVRT suggested this risk dilution analysis in response to the concerns regarding not-met technical work plan Review Criteria 1.1 and 3.3 (BSC 2005 [DIRS 173309]). Risk dilution is a potential nonconservatism that is a concern in a performance assessment model.

Status: In support of the IVRT concerns, the Project reported preliminary findings to the IVRT that indicated (1) the original process of including a normative expert may not have been fully utilized to ensure a consistent treatment of uncertainty, (2) the uncertainty describing some

parameters has a conservative bias, and (3) some parameters may need to be evaluated in TSPA sensitivity analyses as they may have inappropriate ranges with the potential for introducing risk dilution in TSPA calculations. Condition Report 7538 was filed to document these preliminary findings and track the completion of the work. The Project reported that as part of the condition report closure, additional work in this area might be required during the next TSPA Model revision cycle for any parameters found to be contributing to risk dilution. The condition report was closed with the completion of the planned work. The Project has since then initiated more rigorous additional analyses to ensure elimination of the potential for risk dilution concerns. For example, the TSPA-LA Model is supported by a number of auxiliary analyses as discussed in Section 7.7. Section 7.7.4 (with details in Appendix C of the TSPA-LA Model report, Volume III) includes a set of PMA that was specifically conducted to ensure that the TSPA-LA results are reasonable, reliable, and do not result from unmanaged optimistic and conservative modeling approaches. The PMA provides objective evidence for assessing performance margin and the degree of conservatism or non-conservatism in the TSPA-LA compliance model.

The Project established a parameter uncertainty team consisting of a group of the Project's subject matter experts in order to ensure uniform treatment of the uncertainty associated with the TSPA parameters. The parameter uncertainty team performed the uncertainty analyses (Section 6.1.3) and remediated the issues.

IVRT Recommendation #3: Revisit the screening arguments for EBS FEPs that were screened out on the basis of low consequence and provide substantiated arguments, preferably quantitative, that confirm they were of low consequence relative to mean dose. The IVRT suggested this analysis in response to concerns regarding not-met technical work plan Review Criterion 1.1 (BSC 2005 [DIRS 173309]). The objective of this recommendation was to ensure that there are no significant non-conservatisms indirectly included in the total system conceptual model because FEPs that could have potentially significant effects, if included, had been screened out on the basis of low consequence.

Status: The Project completed an initial re-evaluation of certain EBS FEPs that were excluded on the basis of low consequence and initiated condition report 7523 to track the completion of the work. The Project also re-evaluated several other FEPs in addition to those recommended by IVRT in order to further strengthen the Project's FEPs screening results. The condition report was closed as planned. Since the time this effort was completed, the Project has revised its entire FEPs database (SNL 2008 [DIRS 179476]) in order to implement a further enhanced screening process of the FEPs on the repository performance as well as the transparency and traceability of the individual FEPs' screening logic.

IVRT Recommendation #7: Perform an uncertainty and sensitivity analysis using the 2005 draft TSPA Model with model and input modifications proposed by the IVRT. The IVRT believed that the proposed uncertainty and sensitivity analysis addressed those fundamental issues responsible for the IVRT's not-valid decision on the 2005 drafts of the TSPA-LA Model. Achieving these goals requires performing uncertainty analyses for all modeling cases and the related Appendix M sensitivity analyses referred to in Recommendation #1 plus interpretation of all results. The IVRT has provided the TSPA department with a design for this uncertainty and sensitivity analysis, which was included in the IVRT final report (Gibson 2007 [DIRS 181099], Appendix C, Addendum C.III).

Status: The Project evaluated the IVRT recommended design for the uncertainty and sensitivity analysis analyses and responded to the IVRT by presenting a plan for performing the work needed to implement Recommendation 7 during FY06 to FY07. The proposed work plan consisted of two parts as summarized below:

- Revisions to process models and the TSPA Model placed a high priority on evaluating and mitigating potential non-conservatisms in the models. The work scope includes activities to: (1) address potential optimism in the representation of DS degradation, including improper emplacement as well as advective flow through cracks; (2) address potential optimism in the WP degradation representation, including advective flow through cracks; (3) obtain additional laboratory data to strengthen the basis for not including corrosion due to dust deliquescence in the TSPA Model, if possible; (4) include sorption on degraded corrosion products in the revised model, although changes to the EBS due to the incorporation of multipurpose TAD canisters are expected to result in modifications to the models for radionuclide mobilization and transport; (5) strengthen the basis for use of NpO_2 as the controlling phase for neptunium solubility in the in-package solubility model and address the unrealistic approach to solubility caps; and 6) revise the ash redistribution model to provide a more defensible representation for the effect of alluvial fan depositional and erosional processes on ash fall.

- Supplemental analysis to be performed using the TSPA Model. Expert judgment would be used to define alternative models and parameter ranges for input to the TSPA Model to address topics where the IVRT has expressed concerns relevant to recommendation #7 (e.g., incorporate additional realism). Results from this case could be used as a basis for comparison to results from the base case to provide improved understanding of sources of margin and to gain further insights into other impacts of conservatisms in the base case model.

As a result of the proposed implementation of some aspects of the modifications recommended by the IVRT, the model validation process evolved from the not-valid-for-intended purpose conclusion in the 2005 IVRT draft final report toward a new iteration of the validation process. This new iteration in turn would involve revising the compliance strategy, which would then result in revising the TSPA Model. The IVRT noted that although the revised TSPA Model resulting from the proposed work scope by the Project might not include all of the model modifications recommended by the IVRT, the progress made at that time in undertaking the activity suggested in Recommendation #7 was a positive step toward developing a TSPA Model adequate for supporting the LA.

The Project has since revised the technical work plans of the relevant supporting models in order to document the plans for completing the work mentioned in the first bullet and completed the planned work as documented in the respective revised supporting model reports referenced in Table 7.9-1. The Project also completed the initial supplemental analyses mentioned in the second bullet, which have been since superseded by additional auxiliary analyses (Section 7.7). The auxiliary analyses include a set of performance margin analyses (Section 7.7.4 and Appendix C). The performance margin analysis was designed to provide objective evidence for assessing performance margin and degree of conservatism or non-conservatism in the TSPA-LA

Model. As mentioned earlier, the Project also continued to perform other relevant uncertainty and sensitivity analyses (Appendix K in Volume III of the TSPA-LA Model report) in order enhance the TSPA-LA Model description, and especially the confidence in its results.

It was mentioned earlier that a relatively small number of IVRT issues remained not fully addressed according to the responsible IVRT panel members (Booth 2006 [DIRS 176638]). The Project continued to work on these remaining issues since the IVRT was closed with its final report in February 2006 (Gibson 2007 [DIRS 181099], Appendix C). As mentioned in the preceding paragraph, the Project revised the technical work plans (Table 7.9-1) for the relevant process models to include a plan for the work needed to address these remaining issues. The planned work has been completed and documented in the respective supporting model reports. Table 7.9-1 summarizes the nature of these remaining IVRT issues and identifies the technical work plan where the work was planned and the model reports where the completed work is documented. There were a few IVRT issues for which no additional work was deemed necessary by the Project and the reasons for this decision are also provided in Table 7.9-1.

Recommendations on GoldSim Software and the Related Modeling File Error Management Issues

It should be noted that the TSPA-LA Model is based on an updated version of GoldSim (V. 9.60, STN: 10344-9.60-00 [DIRS 181903]) with advanced features, as well as a number of supporting model softwares. However, the Project considered that the IVRT recommendations are also applicable to model execution using the updated versions of these softwares.

IVRT Recommendation #4: Provide objective evidence that the changes in the TSPA Model do not change the current TSPA Model results obtained using earlier GoldSim service packs used in the drafts of the TSPA-LA Model the IVRT reviewed.

Status: The Project provided the IVRT with plots comparing results from GoldSim V. 8.02.400 (STN: 10344-8.02-04 [DIRS 173352]) (using Service Pack 4) with GoldSim V. 8.02.500 (STN: 10344-8.02-05 [DIRS 174650]) (using Service Pack 5). Comparisons of calculated mean dose were provided for the nominal early failure, igneous intrusive, volcanic eruption, and seismic mechanical damage modeling cases. No differences were observed between the results for any of the cases. The IVRT concluded that the current TSPA Model results were not changed by the changes in the TSPA Model.

IVRT Recommendation #5: The IVRT should be kept informed on a timely basis (within one week) if additional GoldSim model file errors are identified.

Status: The Project response to the IVRT stated that during model development, any errors found in the model file are identified internally as the in-process model evolves. It further stated that the TSPA department has provided the IVRT with access to the model file error log during the IVRT review and provided monthly updates on an ongoing basis. The response further stated that as part of the Performance Document Management System process, formalized desktop instructions would document this developmental error-tracking process via Condition Report 7539. In addition, the response stated that after the model is finalized and the document is

approved, any further errors would also be identified in the Corrective Action Program. Condition Report 7539 was subsequently closed as planned.

IVRT Recommendation #6: Any new model file errors identified should be evaluated for impact on modeling cases reported in the TSPA-LA (Gibson 2007 [DIRS 181099], Appendix C]).

Status: The Project explained to the IVRT the procedure that is followed by the TSPA department to identify and log errors and conduct updates to the model and correct the errors as necessary. After the model is finalized and the document is approved, further identification of errors would require documentation in the Corrective Action Program. The response to the IVRT indicated that Performance Document Management System planned to formalize this process into a desktop instruction via Condition Report 7539. The IVRT considered filing a condition report regarding formalizing the developmental error tracking and impact assessment process as a positive step toward ensuring the constructive resolution of this issue. The Project since then formalized the process in the TSPA Configuration Management Desktop Guide, desktop Error Tracking and Evaluation for TSPA Modeling Activities, and Condition Report 7539 was closed.

Summarizing, the IVRT review comments and recommendations, which have been addressed and implemented by the Project, strengthened the TSPA-LA Model as intended. The iterative model development process that the Project pursued during the last decade, of which the IVRT review was an integral part, resulted in the TSPA-LA Model documented in this report. The TSPA-LA Model is based on a sound technical database, fully compliant with the quality assurance requirements, and verified and valid for its intended use by a number of criteria applied during and after the model development. The three empanelled reviews presented in this section played an important role in the development of the TSPA-LA Model.

Table 7.9-1. Summary of Responses to the Remaining IVRT Comments

Remaining IVRT Comment	Additional Work Conducted since the IVRT Review and Documentation where the Work is Located
Remaining IVRT Comments (1) Booth (2006 [DIRS 176638]) provides a full description of all IVRT comments, including those that remained not fully addressed as per the IVRT panel members. These remaining comments are listed here. See Booth (2006 [DIRS 176638]) for full descriptions of the individual remaining comments, which are only abstracted below for brevity. (2) For certain comments, the comment numbers in Booth (2006 [DIRS 176638]) have a zero in front of the number. For example, SZT-02 and UZF-01 in Booth (2006 [DIRS 176638]) are same as SZT-2, UZF-1, respectively, in Section 7.8 of the TSPA-LA (Gibson 2007 [DIRS 181099]).	**Additional Work Conducted since the IVRT Review and Documentation where the Work is Located.** (Note: The project responded to all of the IVRT comments and developed position statements on some of the comments that were difficult to resolve. The IVRT reviewed the Project responses and positions, and found that a relatively small set of comments were not fully addressed to their satisfaction when the IVRT was closed in February 2006. These comment-responses are documented in *Independent Validation Review Team (IVRT) Issues, Bechtel-SAIC Responses, and IVRT Assessment of Responses Related to Review of the TSPA Model and Supporting Analyses and Model Reports* (Booth 2006 [DIRS 176638]). Since the time the IVRT review was closed, the Project completed additional work to address the remaining comments and documented that work as shown below).
Natural Barrier System	
SZT-02: The IVRT was concerned that the 1-D model was not compared to either the 3-D model or the Site-Scale Transport Model under multiple climate changes or with intermittent WP failure and radionuclide release.	The project completed the work planned (BSC 2006 [DIRS 177375]) to address this comment. The comparison work for the base-case model is documented in the *Saturated Zone Flow and Transport Model Abstraction* (SNL 2008 [DIRS 183750], Section 7). The implementation of the 1-D model in dose calculations for the following modeling cases is presented in this TSPA-LA as follows: DS and WP early failure modeling cases in Sections 6.4.1 and 6.4.2, respectively; the disruptive events due to igneous and seismic events in Sections 6.5.1 and 6.5 and Sections 6.6.1 and 6.6.2, respectively; and human intrusion in Sections 6.7.1 and 6.7.2.
UZF-01: The IVRT was concerned that the UZ Flow Model and Submodels analysis and/or model reports do not demonstrate that the three calibrated flow fields developed to address uncertainty in the infiltration rates also capture the uncertainty in the flow fields.	Booth 2006 [DIRS 176638] concluded that the project position was appropriate and that no further work was needed. However, the project subsequently developed a new infiltration model (SNL 2007 [DIRS 182145]) and expanded the treatment of uncertainty in the UZ (SNL 2007 [DIRS 184614]) to use four, rather than three, calibrated flow fields.
UZF-02: The IVRT felt that the comparison between matrix properties measured at Busted Butte with properties calculated for the CHnv did not justify a lack of fracture flow in the CHnv because there was little evidence that hydrologic conditions in the CHnv at Busted Butte are similar to hydrologic conditions in the deeply buried CHnv beneath the repository location, and no correlation was presented between matrix and fracture properties at either location.	The project completed planned (BSC 2006 [DIRS 177465]) work to address this comment. A dual continuum model replaced the single fracture flow model approach that was used in the version of the UZ Flow analysis and/or model report that the IVRT reviewed. The work is documented in *UZ Flow Models and Submodels* (SNL 2007 [DIRS 184614], Sections 6 and 7).

Table 7.9-1. Summary of Responses to the Remaining IVRT Comments (Continued)

Remaining IVRT Comment	Additional Work Conducted since the IVRT Review and Documentation where the Work is Located
Natural Barrier System (Continued)	
CPMS-09(CPM-16): As in UZF-1, this comment deals with uncertainty in UZ flow fields. The remaining questions related to this comment are: (1) whether uncertainty in unsaturated zone flow fields is adequately captured through the use of three calibrated property sets for the low, mean, and high infiltration cases; and (2) the appropriateness of using relaxed constraints for measurements with large uncertainties to develop calibrated property sets for a given infiltration rate.	The project position presented in Booth (2006 [DIRS 176638]) adequately addressed the remaining two parts of this comment. The uncertainties in the flow fields and calibrated properties are not hydraulically significant relative to the uncertainty in the magnitude of the infiltration, which is being addressed in UZ flow with discrete flow fields spanning different climates. Consequently, no additional work is planned on the calibrated properties model.
CPMS-14(CPM-21): This comment deals with uncertainty in UZ flow calibrated parameters. The IVRT was concerned that while the individual parameter uncertainties were used to bound the calibration process, it was not clear that all of the types of parameter uncertainty mentioned in its comment were adequately captured in the CPM.	The project position presented in Booth (2006 [DIRS 176638]) addressed the remaining parts of the comment, especially by the comparison with the bore-hole data approach used. Additional work was considered not likely to make a significant contribution because the uncertainties in the flow fields and calibrated properties are not hydraulically significant relative to the uncertainty in the magnitude of the infiltration, which is being addressed in UZ flow with discrete flow fields spanning different climates.
Disruptive Events—Volcanic Eruption (VE) and Igneous Activity (IGI)	
CMT-062105-112723-09: The IVRT was concerned with the lack of treatment of the possible effects of dike swarms due to future igneous intrusion on the UZ and SZ flow and transport and how the treatment would impact the TSPA results.	The IVRT and TSPA were unable to reach a compromise resolution acceptable to both parties. This impasse was to be recorded in the TSPA-LA Model report as a part of Section 7 with a response from the Project as to its significance in the overall validation of the TSPA-LA Model (Booth 2006 [DIRS 176638]). The project response as to the significance of the comment in the overall validation of the TSPA-LA Model is as follows: The disruptive event FEP disposition argument for 1.2.10.02.0A, Hydrologic Response to Igneous Activity (BSC 2005 [DIRS 173981], Section 6.2.2.10), addressed the comment. The basis argument is that at the scale of the UZ site scale model or the SZ regional model, the effects of dikes on UZ and SZ flow, if they occur at all, are too localized to affect TSPA results. Analyses based on analog results show that mineralogical changes in the host rock adjacent to contacts with dikes typically extend for a few tens of cm to perhaps a couple of meters into the host. Again, at the scales of the SZ and UZ models, the extent of such effects is negligible. Much of the analog work is documented in (SNL 2007 [DIRS 174260], Appendix F).

Table 7.9-1. Summary of Responses to the Remaining IVRT Comments (Continued)

Remaining IVRT Comment	Additional Work Conducted since the IVRT Review and Documentation where the Work is Located
Disruptive Events—Volcanic Eruption (VE) and Igneous Activity (IGI) (Continued)	
IGI-01: The IVRT was concerned that the Project treated dike intrusion effect conservatively; the repository block is a strong monolith, but the path of dike ascent will be structurally controlled to follow primary faults such that few if any dikes will penetrate the Yucca Mountain structural block and can be demonstrated readily by numerical analysis.	The planned work that addresses this IVRT concern is in *Technical Work Plan for: Igneous Activity Assessment for Disruptive Events* (BSC 2006 [DIRS 182219]). The report, *Characterize Eruptive Processes at Yucca Mountain, Nevada* (SNL 2007 [DIRS 174260], Section 6.3.3), includes analog information about the relationship between dike propagation and geologic structures and the tendency of dikes to follow pre-existing structures. Revision 02 of *Dike/Drift Interactions* (SNL 2007 [DIRS 177430]) includes descriptions of analyses of 2 D dike propagation driven by compressible magma, a 2 D model of a rising dike encountering faults and/or stratigraphic discontinuities, and an extension of an analysis of secondary breakout consistent with higher magma pressures described in Revision 01 (BSC 2004 [DIRS 177430], Section 6.5). These discussions show that the repository block does not behave as a strong monolith and will support the abstraction that an ascending dike would propagate through the repository. The analysis in *Dike/Drift Interactions* (SNL 2007 [DIRS 177430], Section 6.3.4) shows that dikes will not be diverted into faults in the rocks of Yucca Mountain except for steeply dipping faults at depths of only a few hundred meters.
IGI-02: As in the case of IGI-01, the IVRT was concerned that an ascending dike will tend to follow pre-existing fractures that it encounters.	The planned work that addresses this IVRT concern, is in *Technical Work Plan for: Igneous Activity Assessment for Disruptive Events* (BSC 2006 [DIRS 182219]), which discusses the differences between the conceptual models and TSPA implementation of dike interactions with rock. *Characterize Eruptive Processes at Yucca Mountain, Nevada* (SNL 2007 [DIRS 174260], Section 6.3.3) includes results of analogue work that shows an ascending dike will tend to follow preexisting fractures. *Dike/Drift Interactions* (SNL 2007 [DIRS 177430], Section 6) provides descriptions of 3D representation of dike propagation driven by compressible magma, a 2 D model of a rising dike encountering faults and/or stratigraphic discontinuities, and topographic effects on dike propagation. The results of these investigations will address the nature of interactions between ascending dikes and intruded rocks. The analysis in *Dike/Drift Interactions* (SNL 2007 [DIRS 177430], Section 6.3.4), shows that dikes will not be diverted into faults in the rocks of Yucca Mountain except for steeply dipping faults at depths of only a few hundred meters.

Table 7.9-1. Summary of Responses to the Remaining IVRT Comments (Continued)

Remaining IVRT Comment	Additional Work Conducted since the IVRT Review and Documentation where the Work is Located
Disruptive Events—Volcanic Eruption (VE) and Igneous Activity (IGI) (Continued)	
IGI-05: The IVRT question asked for the basis for assuming the behavior of the WP to be radically different in the Igneous Intrusion Modeling Case compared with the Nominal Modeling Case. The IVRT believed that additional analyses were necessary to re-evaluate WP performance under magmatic conditions with more representative confining pressures generated by magma filling the drifts and would help address the comment.	The planned work that addresses this IVRT concern is in *Technical Work Plan for: Igneous Activity Assessment for Disruptive Events* (BSC 2006 [DIRS 182219]). Analyses of WP degradation after magma intrusion, described in *Dike/Drift Interactions* (SNL 2007 [DIRS 177430]), provides descriptions of an analysis that shows the TAD canister lid weld fails after exposure to magmatic temperatures and effusive and multiphase flow conditions. That analysis provides the basis for the assumption about WP damage after contact by magma. The 2 D model for magma cooling considers the effects of hot and cold WPs. *Dike/Drift Interactions* (SNL 2007 [DIRS 177430]) also includes an estimate of invert performance. An estimate of WP degradation after combined (igneous + seismic) events (SNL 2007 [DIRS 177432]), includes an assumption about the severity of WP damage following an intrusion. Magmatic pressures following an intrusion are discussed in *Dike/Drift Interactions* (SNL 2007 [DIRS 177430], Section 6.4.8.1). The effect of magmatic temperatures, pressures, and gas composition on the WPs and waste form is discussed in Section 6.4.8.3 of *Dike/Drift Interactions* (SNL 2007 [DIRS 177430]). An analysis of WP failure due to external pressurization is included in Appendix E in *Dike/Drift Interactions* (SNL 2007 [DIRS 177430]).
IGI-WP/WF-04: The IVRT felt that the disconnect on how the WP responds to the magma was still remaining in that magma does not contact the waste, but there is no impedance to the flow of water through the magma-filled drift and the WP. Additionally, in Appendix J of *Atmospheric Dispersal and Deposition of Tephra from a Potential Volcanic Eruption at Yucca Mountain, Nevada* (BSC 2005 [DIRS 174067], a historic document cited for background information), it is stated that the WP is breached and magma enters the WP before the dike turns into a volcanic event; again a disconnect between different parts of the TSPA.	The planned work that addresses this IVRT concern is in *Technical Work Plan for: Igneous Activity Assessment for Disruptive Events* (BSC 2006 [DIRS 182219]). *Dike/Drift Interactions* (SNL 2007 [DIRS 177430]) includes descriptions of the mechanism of TAD canister failures at end cap welds. This failure mechanism is the basis for an assumption that WPs contacted by magma provide no protection for waste, which is documented in *Number of Waste Packages Hit by Igneous Intrusion* (SNL 2007 [DIRS 177432], Section 5.1). In addition, the TSPA-LA Section 6.5 includes descriptions of assumptions about the form of radionuclides suspended in cooled basalt. The radionuclide inventory is available in the first TSPA timestep, but the magnitude of release is controlled by radionuclide solubilities. An analysis of WP failure due to external pressurization is included in Appendix E of *Dike/Drift Interactions* (SNL 2007 [DIRS 177430], Section 6.4.8.3.1).

Table 7.9-1. Summary of Responses to the Remaining IVRT Comments (Continued)

Remaining IVRT Comment	Additional Work Conducted since the IVRT Review and Documentation where the Work is Located
Disruptive Events—Volcanic Eruption (VE) and Igneous Activity (IGI) (Continued)	
IGI-WP/WF-05: The IVRT was concerned that no impact analysis was done to account for the heat sink effect of the WP.	The planned work that addresses this IVRT concern is in *Technical Work Plan for: Igneous Activity Assessment for Disruptive Events* (BSC 2006 [DIRS 182219]). *Dike/Drift Interactions* (SNL 2007 [DIRS 177430]) provides and documents an alternative model that is a tabulation of drift centerline temperatures based on a 2 D model for magma cooling, while considering effects of hot and cold WPs (SNL 2007 [DIRS 177430], Section 6.4.7.2). The analysis results support an assumption about the severity of WP damage following contact with magma (SNL 2007 [DIRS 177432], Section 5.1).
VE-01: This IVRT comment is similar to IGI-01. The geologic block containing the repository was chosen for its strong monolithic qualities, as discussed in the 'siting' criteria; however, in the Igneous Intrusion Modeling Case, the repository geologic block is assumed to be a weak monolith and, therefore, a dike would penetrate the block rather than follow planes of weakness within the surrounding formation. There seems to be an inconsistency in the assumption made for the Igneous Intrusion Modeling Case and the 'siting' criteria.	The relevant work plan is the *Technical Work Plan for: Igneous Activity Assessment for Disruptive Events* (BSC 2006 [DIRS 182219]). The report, *Characterize Eruptive Processes at Yucca Mountain, Nevada* (SNL 2007 [DIRS 174260]), includes analogue information about the relationship between dike propagation and geologic structures and the tendency of dikes to follow pre-existing structures. *Dike/Drift Interactions* (SNL 2007 [DIRS 177430]) includes descriptions of analyses of 2 D dike propagation driven by compressible magma (Section 6.3), a model of a rising dike encountering faults and/or stratigraphic discontinuities (Section 6.3), and an extension of analysis of secondary breakout consistent with higher magma pressures (SNL 2007 [DIRS 177430], Section 6.5). These discussions show that the repository block does not behave as a strong monolith and will support the abstraction that an ascending dike would propagate through the repository.
VE-02: The IVRT was concerned with the extreme mass balance error in the old tephra redistribution model.	The relevant work plan is the *Technical Work Plan for: Igneous Activity Assessment for Disruptive Events* (BSC 2006 [DIRS 182219]). The report, *Redistribution of Tephra and Waste by Geomorphic Processes Following a Potential Volcanic Eruption at Yucca Mountain, Nevada* (SNL 2007 [DIRS 179347], Section 6.5), documents a new ash redistribution model that provides estimates of the amount of waste in remobilized tephra for each cell in the model grid and includes geomorphic processes for landscape features characteristic of the Fortymile Wash watershed. Tephra-soil mixing rates (dilution) are explicitly addressed in the new ash redistribution model. The new model eliminates the mass balance error that was inherent in the previous model by using a mass conservative analytical method to calculate diffusion into the soil on distributary channels and interchannel divides at the RMEI location.

Table 7.9-1. Summary of Responses to the Remaining IVRT Comments (Continued)

Remaining IVRT Comment	Additional Work Conducted since the IVRT Review and Documentation where the Work is Located
Disruptive Events—Volcanic Eruption (VE) and Igneous Activity (IGI) (Continued)	
VE-03: The IVRT commented that the ash distribution model they reviewed for leaching radionuclides from ash deposits and redepositing them in the underlying soil does not seem to account for residence time, rainfall, and depletion of radionuclides in the overlying ash. The current model most likely overestimates the amount and duration of exposure to radionuclides from an ash deposit, perhaps significantly.	Work has been planned in *Technical Work Plan for: Igneous Activity Assessment for Disruptive Events* (BSC 2006 [DIRS 182219]) to address the ash leaching aspect. *Redistribution of Tephra and Waste by Geomorphic Processes Following a Potential Volcanic Eruption at Yucca Mountain, Nevada* (SNL 2007 [DIRS 179347], Section 6.5) documents a new ash redistribution model that addresses the temporal near-surface and at-depth concentrations of fuel (waste) in soil at the location of the RMEI. In the modeling method, a single value of diffusivity is applied to fuel (waste), representing all radionuclides. Support for this approximation comes from measurements that indicate that different radionuclide species are dispersed in the soil column at similar rates (Anspaugh et al. 2002 [DIRS 169793]). Diffusion is assumed to occur within a finite thickness corresponding to the distance from the surface to impermeable soil horizons at depth (with a different thickness for the divide and channel).
VE-04: The IVRT was concerned that active alluvial fans are distributary environments with long-term deposition rather than erosion, as apparently assumed in the TSPA model. It believes that floodwaters rework stream channel gravels and transport them downstream, replacing them with upstream gravel. When the deposited gravel sufficiently raises the channel bed, water will escape and create a new channel. The net effect is to build the fan higher while continually mixing gravel and moving it toward the toe. The process is much more dynamic than what is captured in the TSPA conceptual model.	The work planned in the *Technical Work Plan for: Igneous Activity Assessment for Disruptive Events* (BSC 2006 [DIRS 182219]) to address the comment of alluvial fan deposition was completed. *Redistribution of Tephra and Waste by Geomorphic Processes Following a Potential Volcanic Eruption at Yucca Mountain, Nevada* (SNL 2007 [DIRS 179347], Section 6.5), documents a new ash redistribution model that is based on detailed geomorphic descriptions of the upper part of the Fortymile Wash alluvial fan. The work includes a description of the stability of interchannel divides and erosion/deposition rates for distributary channels.

Table 7.9-1. Summary of Responses to the Remaining IVRT Comments (Continued)

Remaining IVRT Comment	Additional Work Conducted since the IVRT Review and Documentation where the Work is Located
Disruptive Events—Volcanic Eruption (VE) and Igneous Activity (IGI) (Continued)	
VE-05: The IVRT comment deals with the instantaneous incorporation of waste in ash. The IVRT was concerned that the Project treatment of instantaneous incorporation of waste (radionuclides) into erupted ash is not justified and inconsistent with the regulatory expectation that the DOE should use a full range of defensible and reasonable parameters in their performance model rather than relying on extreme physical situations and parameter values. Project treatment of instantaneous incorporation of waste is an example where the use of extreme assumptions leads to results that may be very difficult to defend.	The comment has been addressed by the analyses documented in *Atmospheric Dispersal and Deposition of Tephra from a Potential Volcanic Eruption at Yucca Mountain, Nevada* (SNL 2007 [DIRS 177431]), as described below. Significant progress has been made in defining the processes for the incorporation of exposed waste into the tephra transported in the ASHPLUME model and adding realism in how they are incorporated into the eruptive case model. An analysis of the effects of contact with a WP and the waste form in the intrusion scenario indicates that the integrity of the WP would be compromised (SNL 2007 [DIRS 177430], Section 6.4.8.3). For the Volcanic Eruption Modeling Case, once intrusion of the repository occurs, a volcanic conduit does not form immediately, but rather forms gradually as continued magma flow locally widens the dike. This process may take hours to days to reach the repository depth. If a developing conduit intersects an emplacement drift, the WPs located partially or entirely within the conduit would experience elevated temperatures (1,000˚C) for an extended period (100s of hours) as well as other degrading conditions. The WPs located within the boundaries of the developing conduit would also be subjected to magma pressure fluctuations, differential movement by unsteady magma flow, impact by failing wall-rock, and physical degradation by fragmenting melt particles (SNL 2007 [DIRS 174260], Appendix F); (SNL 2007 [DIRS 177430], Section 6.4.8.3.2)). Physical damage to the WP in this energetic conduit environment is assumed to result in failure of the WPs and entrainment of fragmented waste within the rising magma (SNL 2007 [DIRS 177431], Section 5.1.2). A review of international literature on waste form particle size indicates that the likely range resulting from magma/waste interaction in the conduit is 0.0001 cm to 0.2 cm, based on studies of spent fuel pellet size, mechanical shock, crushing and milling, dry and aqueous oxidation/corrosion, and the Chernobyl reactor accident analogue (SNL 2007 [DIRS 177431], Appendix F). Some portion of these waste particles is assumed to be suspended and well-mixed with the magma, carried to the surface through the conduit, and erupted at the vent. The waste particles within the magma are treated as refractory particles (analogous to xenoliths) that form a component of tephra particles upon fragmentation of the magma (SNL 2007 [DIRS 177431], Section 6.5.2.6). The value for the input parameter, waste incorporation ratio, has therefore been revised to reflect a neutral combination of the tephra and waste particle size distributions. The ASHPLUME model abstraction assumes that the various eruption phases are condensed into a single violent Strombolian phase (SNL 2007 [DIRS 177431], Section 5.1.1) with concurrent effusion of lava, sustained eruption column, and construction of a scoria cone. The waste incorporated into the magma is therefore distributed among the various eruptive products—scoria cone, lava flows, and tephra blanket—over the course of the eruption. Accounting is made, by means of a magma partitioning factor, for the proportion of waste-containing magma that is eventually deposited in geologically resistant eruptive products (scoria cone, lava flows) that do not contribute to dose (SNL 2007 [DIRS 177431], Section 6.5.2.22).

Table 7.9-1. Summary of Responses to the Remaining IVRT Comments (Continued)

Remaining IVRT Comment	Additional Work Conducted since the IVRT Review and Documentation where the Work is Located
Disruptive Events—Volcanic Eruption (VE) and Igneous Activity (IGI) (Continued)	
CMT-062105-124045-60; CMT-062005-125053-19; CMT-062105-112025-93; CMT-062105-112302-53; CMT-062105-124255-71; CMT-062105-124619-89: These similar IVRT comments deal with inconsistent treatment of basalt properties in the drift and above and below it. Response to IGI-06 addressed the subsurface aspects of these comments. See Booth (2006 [DIRS 176638]) and the material presented in the column at the right for the specific aspects associated with the unresolved parts of the individual comments and the corresponding work the Project completed to address these parts.	The following analysis and model reports were updated to address the remaining parts of the comments in this group: *Characterize Eruptive Processes at Yucca Mountain, Nevada* (SNL 2007 [DIRS 174260]); *Dike/Drift Interactions* (SNL 2007 [DIRS 177430]); *Magma Dynamics at Yucca Mountain, Nevada* (Dartevelle and Valentine 2007 [DIRS 182090]); *Number of Waste Packages Hit by Igneous Intrusion* (SNL 2007 [DIRS 177432]); *Atmospheric Dispersal and Deposition of Tephra from a Potential Volcanic Eruption at Yucca Mountain, Nevada* (SNL 2007 [DIRS 177431]); and the model report, *Redistribution of Tephra and Waste by Geomorphic Processes Following a Potential Volcanic Eruption at Yucca Mountain, Nevada* (SNL 2007 [DIRS 179347]). The work completed in response to the individual comments in this group is summarized below. **CMT-062105-124045-60:** Comment items related to inconsistent properties of intrusive and eruptive phases, magma characteristics, and eruption energies associated with various eruption phases are described in *Characterize Eruptive Processes at Yucca Mountain, Nevada* (SNL 2007 [DIRS 174260], Section 6.3.2). Partitioning of erupted material into lava, cone forming facies (scoria), and tephra (ash), consistent with the eruption phases described in *Characterize Eruptive Processes at Yucca Mountain, Nevada* (SNL 2007 [DIRS 174260], Section C.9), was used in *Atmospheric Dispersal and Deposition of Tephra from a Potential Volcanic Eruption at Yucca Mountain, Nevada* (SNL 2007 [DIRS 177431]) to divide the mass of entrained waste among the erupted products and provide consistency between the erupted products and eruption phases. **CMT-062005-125053-19:** For the Igneous Intrusion Modeling Case, this comment (i.e., inconsistent properties of intrusive and eruptive phases, magma characteristics, and eruption energies associated with various eruption phases) is addressed (SNL 2007 [DIRS 177430], Section 6) by clarifying that the magma in the drift offers no additional resistance to flow beyond that of the surrounding host rock. In the case of the Hawaiian dike complexes, water table elevations are found to be as much as 1,000 m higher inside the complexes as compared with locations outside the dike complexes (Booth 2006 [DIRS 176638], pp. 349 to 351). Water table elevation changes caused by dike complexes in more arid climates such as Yucca Mountain are expected to be much smaller and should be bound by the existing rise in the water table as modeled for future climates (SNL 2008 [DIRS 184748], Section 6.4.8). Intrusive dikes have been observed to reach the ground surface in Hawaii (Booth 2006 [DIRS 176638], pp. 349 to 351). Nevertheless, surface eruptions by dikes have not led to large surface impoundments of water in Hawaii despite high levels of rainfall that occur on some parts of the islands. Based on these observations, the effects of dikes on surface water flow at Yucca Mountain are not expected to result in significant changes in infiltration behavior or the generation of significant surface water impoundments. Therefore, the effects of dikes on unsaturated zone flow, radionuclide transport, and infiltration are expected to be beneficial to the performance of the natural barriers, but minimal. However, the overall effects on changes in drift seepage are less certain.

Table 7.9-1. Summary of Responses to the Remaining IVRT Comments (Continued)

Remaining IVRT Comment	Additional Work Conducted since the IVRT Review and Documentation where the Work is Located
	The comment is beyond the scope considered in the analyses of the Volcanic Eruption Modeling Case, which examines the direct deposition and redistribution of contaminated waste on the ground surface but does not include percolation through the subsurface components of an igneous event. *Dike/Drift Interactions* (SNL 2007 [DIRS 177430], Section 5.4.1) said, "The permeability of any contact metamorphic aureole surrounding the intruded drifts is assumed to be as great as that of the bulk host rock. The basalt will undoubtedly fracture during cooling, but will fracture to such an extent that the resulting secondary permeability will not provide an additional impediment to seepage." That was an assumption that was used in the seepage water section that has been converted into a literature review. The assumption was, therefore, no longer needed for Revision 02 of *Dike/Drift Interactions* (SNL 2007 [DIRS 177430]) and was not included. **CMT-062105-112025-93:** TSPA-LA Model for the Igneous Scenario Class—FEPs disposition. The surface effects are addressed in the Volcanic Eruption Modeling Case by inclusion of the partitioning of erupted products into lava, cone forming facies, and tephra (ash) in *Atmospheric Dispersal and Deposition of Tephra from a Potential Volcanic Eruption at Yucca Mountain, Nevada* (SNL 2007 [DIRS 177431]), and by redistribution of contaminated ash as described in the new FAR model report, *Redistribution of Tephra and Waste by Geomorphic Processes Following a Potential Volcanic Eruption at Yucca Mountain, Nevada* (SNL 2007 [DIRS 179347]). For the lava, data from field observations indicate that the surfaces of flows are geomorphically stable for long time periods. Hence, the bulk of radionuclides in lava flows would be isolated from redistributed materials moved into distributary channels. In addition, lava flows in the immediate vicinity of Yucca Mountain are of small volume and aerially restricted. If a future volcano penetrated the repository, such flows, if they occurred, would be localized and distant from the location of the RMEI. For the cone-forming facies, a user-defined parameter (radius) in the tephra redistribution model determines the amount of the cone-forming material that is prevented from being redistributed. Cone forming material beyond this user-defined radius is treated the same as tephra dispersed during the eruption. The steepness of the pre-eruption slopes is compared with a critical slope angle and material on slopes equal to or greater than the critical angle that is considered available for redistribution. Partitioning of erupted material into lava, cone forming facies (scoria), and tephra (ash), consistent with the eruption phases described in *Characterize Eruptive Processes at Yucca Mountain, Nevada* (SNL 2007 [DIRS 174260], Section C.9), was used in *Atmospheric Dispersal and Deposition of Tephra from a Potential Volcanic Eruption at Yucca Mountain, Nevada* (SNL 2007 [DIRS 177431]) to divide the mass of entrained waste among the erupted products and provide consistency between the erupted products and eruption phases. The parts of the comment that deal with development of potential fast pathways for groundwater flow in cooled basalt are beyond the scope considered in analyses of the eruption modeling case, which examines the direct deposition and redistribution of contaminated waste on the ground surface but does not include percolation through the subsurface components of an igneous event. Those effects are described for CMT-062005-125053-19. **CMT-062105-112302-53:** This comment addresses long-term (post-cooling) effects of igneous activity on

Table 7.9-1. Summary of Responses to the Remaining IVRT Comments (Continued)

Remaining IVRT Comment	Additional Work Conducted since the IVRT Review and Documentation where the Work is Located
	groundwater flow and transport during the postclosure period. The parts of the comment that are related to the flow of groundwater through cooled basalt and the potential for development of fast pathways are addressed by the response to IGI-06. Analog information included in *Dike/Drift Interactions* (SNL 2007 [DIRS 177430], Section 6.7) addresses changes to groundwater chemistry resulting from percolation through cooled basalt. However, *Dike/Drift Interactions* (SNL 2007 [DIRS 177430]) will no longer include basalt-water chemistry as an abstraction for TSPA, and the text specified above is not needed. The text was included in the TSPA model report (Section 6.5). The TSPA inputs for pH and ionic strength of water that has reacted with cooled basalt is provided by the *In-Package Chemistry Abstraction* (SNL 2007 [DIRS 180506], Section 6[a]). **CMT-062105-124255-71:** This comment is addressed by the response to comment IGI-06. **CMT-062105-124619-89:** This comment was addressed consistent with responses to CMT-062005-125053-19 and IGI-06 in Booth (2006 [DIRS 176638]). The Project noted that the TSPA and DDI reports treat the flux the same. The flux entering the drift is assumed to be the percolation flux from the base of the PTn. The flux remains the same through the magma filled drift (after wall rock and magma cool to below boiling). The confusion lies with the statement in *Dike/Drift Interactions* (SNL 2007 [DIRS 177430]), "the magma in the drift offers no resistance to flow." This statement is misleading and was modified to state (SNL 2007 [DIRS 177430], Section 6) that the magma in the drift offers no additional resistance to flow beyond that of the surrounding host rock. The text in the TSPA-LA (Section 6.5.1) states that the intruded basalt in the drift is assumed to provide no resistance to water flow; because the entire WP and DS are failed, the entire seepage flux enters the WP and is available for advective transport of radionuclides from the EBS (SNL 2007 [DIRS 181244], Section 6.7.1.1).

Table 7.9-1. Summary of Responses to the Remaining IVRT Comments (Continued)

Remaining IVRT Comment	Additional Work Conducted since the IVRT Review and Documentation where the Work is Located
Engineered Barrier System	
CMT-062105-121205-14 and **CMT-062105-113319-24:** The IVRT was concerned that even though the TSPA Seismic Scenario Class represented a commendable attempt to address a very complex problem and state of the art modeling was used intelligently to provide a reasonable assessment of damage due to severe ground motions, the key assumption that translates the predictions is the assumption of stress corrosion cracking that eliminates advective flow as a result of the damage to vibratory ground motion. The IVRT felt that this assumption needed to be more fully described and justified.	The Project has made a significant enhancement of the FEPs screening process and revised the FEPs database since the IVRT review was closed. The advective flow and transport of radionuclides through the WP as a result of the damage due to vibratory ground motionwas evaluated and screened out. A detailed discussion of the FEPs screening process, including the WP and DS degradation due to stress corrosion cracking, is presented in the FEPs database (DTN: MO0706SPAFEPLA.001 [DIRS 181613]).
EBS-21, CMT-062005-130513-66, CMT-062105-104839-19, CMT-062105-100225-22, and CMT-062105-100349-08: In these similar comments, the IVRT expressed the concern that the Project's treatment of radionuclides transport due to the processes of irreversible and reversible sorption to colloids was inconsistent across the EBS components.	The planned work to address this IVRT concern is in *Technical Work Plan for: Near-Field Environment: Engineered Barrier System: Radionuclide Transport Abstraction Model Report* (BSC 2006 [DIRS 177739]) and *Technical Work Plan for Waste Form Testing and Modeling* (BSC 2006 [DIRS 177389]). The planned work was completed. Colloids assisted radionuclide transport through the EBS components is treated consistently as due to equilibrium and kinetic sorption processes as appropriate (SNL 2007 [DIRS 177407], Section 6.3.4.4).
EBS-29, EBS-49, and CMT-062105-101939-31: The IVRT concern for these comments is similar—water balance within WP. The IVRT was concerned that the basis for the (1) rind product from the reacted spent nuclear fuel becoming fully saturated quickly with water in both seep and non-seep environments reported in the reviewed version of *EBS Radionuclide Transport Abstraction* (SNL 2007 [DIRS 177407]). Section 6.5.3 was not provided and felt that this assumption may result in very conservative-release concentrations for radionuclides not controlled by solubility limits (Tc, I, and C) and discard a more realistic conceptual model (Section 6.6.2 of the reviewed check copy draft of EBS Radionuclide Transport Abstraction), and (2) diffusive release of colloids of larger diameter than the assumed thin water film, was not provided.	The planned work to address this IVRT concern is in *Technical Work Plan for: Near-Field Environment: Engineered Barrier System: Radionuclide Transport Abstraction Model Report* (BSC 2006 [DIRS 177739]) and the *Technical Work Plan for Waste Form Testing and Modeling* (BSC 2006 [DIRS 177389]). The planned work was completed. A detailed discussion on the water saturation of the DSNF and CSNF degradation products (i.e., rind) in seep and non-seep conditions is provided in *EBS Radionuclide Transport Abstraction* (SNL 2007 [DIRS 177407], Section 6.3.4.6)

Table 7.9-1. Summary of Responses to the Remaining IVRT Comments (Continued)

Remaining IVRT Comment	Additional Work Conducted since the IVRT Review and Documentation where the Work is Located
Engineered Barrier System (Continued)	
CMT-062105-100851-03: The IVRT was concerned that there seemed to be a lack of a consistent treatment of water saturation degree in different parts of the EBS system. In CNSF, the saturation degree in corrosion products is calculated using a sorption isotherm of water onto hematite surfaces, while in the DSNF, it is just simply set to 1, though both domains consist of the same material. In addition, in the invert, the van Genuchten moisture retention relationship is used to calculate the intergranular water saturation. This comment is related to those of comments EBS-49 and CLAD-05b discussed above.	See pages 364 and 365 of Booth (2006 [DIRS 176638]) for the Project technical position on the comment where the Project justified the saturation states used in the different parts of EBS. Nonetheless, the Project planned the additional work to further enhance consistency of the degree of water saturation across the EBS. The work has been completed as planned and is reported in the *EBS Radionuclide Transport Abstraction* (SNL 2007 [DIRS 177407], Sections 6.2.4.6 and 6.5.2.2); and *In-Package Chemistry Abstraction* (SNL 2007 [DIRS 180506], Sections 6.6.1[a] and 6.10.9.1 [a]) model reports.
IDC-01: The comment IDC-01 is the same as the last part of comment IDC-02. They both deal with possible compositional differences between the fracture and matrix water. The IVRT was concerned that the compositional differences were not considered.	The comment was addressed in the revised version of *Engineered Barrier System: Physical and Chemical Environment* (SNL 2007 [DIRS 177412], Section 6.6).
IDC-02: In addition to the fracture-matrix water compositional differences comment mentioned above in IDC-01, the IVRT commented that since more data have become available, it would be helpful to show that with more data accumulated the original assumption of equal probability for five waters is still justified. Since no seepage is assumed for temperature greater than100^{o}C, the water compositions calculated from the THC model for temperatures greater than 100^{o}C should be excluded in the P&CE model analysis.	The planned work (SNL 2007 [DIRS 179287]) was completed to address both parts of the comment and is documented in *Engineered Barrier System: Physical and Chemical Environment* (SNL 2007 [DIRS 177412], Section 6.6). The cited section provides a detailed description of how the four end-member starting waters were selected for the Near-Field Chemistry Model based on the latest available pore-water database.

Table 7.9-1. Summary of Responses to the Remaining IVRT Comments (Continued)

Remaining IVRT Comment	Additional Work Conducted since the IVRT Review and Documentation where the Work is Located
Engineered Barrier System (Continued)	
IDC-04: The IVRT stated that the initial draft P&CE model they reviewed takes the water compositions calculated by the THC model as inputs to its evaporation calculations. These water compositions are calculated using a given set of values of reaction rate constants, which generally vary over several orders of magnitude. No sensitivity analysis has been done on how these reaction rate constants affect the calculated water chemistry. They mentioned that in the P&CE Model a small change in the initial water composition could result in quite a different chemical divide pathway.	The work planned in *Technical Work Plan for: Revision of Model Reports for Near-Field and In-Drift Water Chemistry* (SNL 2007 [DIRS 179287]) to address the comment was completed by performing sensitivity studies on THC seepage and is documented in *Drift-Scale THC Seepage Model* (SNL 2007 [DIRS 177404]). The PC&E Model uses the Near-Field Chemistry Model, which was developed independent of the THC model. The results of the THC model were used to corroborate the Near-Field Chemistry Model with agreeable results (SNL 2007 [DIRS 177412], Section 7.1.3 and Figure 7.1-10).
IDC-10: The IVRT stated that the water chemistry calculations in the P&CE Model (REV 02, DRAFT A) are valid only for drift-center temperatures; however, they are also applied at the drift ends. It is not clear how applicable water chemistries at elevated temperatures (i.e., the center of the drift) can be applicable at lower temperatures (i.e., at the end of the drift). This is believed to be conservative because this assumption should result in more corrosive water conditions; however, the adequacy of this assumption has not been demonstrated. Similarly, chemistry is passed as a function of time, yet in reality it is a function of the thermal history (which is spatially variable). The chemistry is for the center of the drift and it is not clear how it applies across the entire drift.	The work planned in *Technical Work Plan for: Revision of Model Reports for Near-Field and In-Drift Water Chemistry* (SNL 2007 [DIRS 179287]), as a part of the work needed to close Condition Report 7037, was completed. The completed work is documented in *Drift-Scale THC Seepage Model* (SNL 2007 [DIRS 177404]). The variations of the modeled water composition at the repository center and edge as the repository heats up and cools off as a function of time are discussed in Section 6.5.5.4 and shown on Figures 6.5-10 through 6.5-24 of the *Drift-Scale THC Seepage Model* (SNL 2007 [DIRS 177404], Section 6.5).

Table 7.9-1. Summary of Responses to the Remaining IVRT Comments (Continued)

Remaining IVRT Comment	Additional Work Conducted since the IVRT Review and Documentation where the Work is Located
Engineered Barrier System (Continued)	
IDC-11: The IVRT was concerned that different types of brines (e.g., NaCl, $CaCl_2$) would be quite different in total volumes, which reflect relative probabilistic distributions. This volume constraint on probabilistic distributions is not captured in the TSPA conceptual model. A similar comment can also be raised for the dust deliquescence model. It is expected that the amount of water potentially condensed on dust will be very small, perhaps not enough to form a continuous water film for metal corrosion.	The total volume of brine that may be residing on the WP due to seepage is not currently determinable. There are several dynamic processes that are occurring simultaneously (e.g., intermittent seepage flow events, seepage flowing off the package, evaporation, mineral precipitation), so the conceptual model falls back to an equilibrium brine composition that covers the entire seeped-on area and results in the most concentrated brine that has the highest potential to trigger localized corrosion. Thus, the brine volumes from different seepage compositions are reasonably assumed to be irrelevant in determining localized corrosion of the WP (SNL 2007 [DIRS 178519], Section 5.5). The IVRT comment no longer applies to dust deliquescence as there are no dust brines chemistry being modeled. Dust brines are all excluded from TSPA because they are of low-consequence, where low brine volume is a part of that justification (SNL 2007 [DIRS 181267], Sections 7.1).
IDC-12: The IVRT was of the opinion that there was a large inconsistency in water chemistries among the P&CE Model (REV 02, DRAFT A), the long-term corrosion testing to support the *WAPDEG Analysis of Waste Package and Drip Shield Degradation Model* (BSC 2003 [DIRS 161317] , a historic document cited for background information), the general corrosion and localized corrosion of WP outer barrier model which they reviewed, the *In-Package Chemistry Abstraction Model* (BSC 2003 [DIRS 161962] , a historic document cited for background information), and the *Dissolved Concentration Limits of Radioactive Elements* (BSC 2003 [DIRS 163152] , a historic document cited for background information). These inconsistencies must be addressed and the analysis and/or model reports for these affected models made consistent, and/or the justification for the inconsistencies being inconsequential.	The Project position (Booth 2006 [DIRS 176638]) is that the alleged inconsistencies no longer exist. Nonetheless, the Project made strides to further consistency between the WP localized corrosion model and seepage chemistry (SNL 2007 [DIRS 177412]) and utilized the same pH scales, which were the largest chemical disconnect.
IDC-19: The IVRT was concerned that the treatment of invert chemistry based on surface evaporation might have resulted in unrealistically high ionic strength, which may overly predict colloidal instability, which is not conservative.	The work needed to address the comment was planned in *Technical Work Plan for: Revision of Model Reports for Near-Field and In-Drift Water Chemistry* (SNL 2007 [DIRS 179287]) and completed. As part of this effort, pH and *p*CO2 covariance was evaluated to constrain, to the extent possible, the uncertainty of conditions that control radionuclide solubility and colloids stability in the invert. This new abstraction was based on fracture and matrix water compositions from the THC seepage model for the drip and no-drip cases, respectively. The work is documented in *Engineered Barrier System: Physical and Chemical Environment* (SNL 2007 [DIRS 177412], Section 6.15.2).

Table 7.9-1. Summary of Responses to the Remaining IVRT Comments (Continued)

Remaining IVRT Comment	Additional Work Conducted since the IVRT Review and Documentation where the Work is Located
Engineered Barrier System (Continued)	
Clad-05b: The IVRT was of the opinion that the Project calculations showed that assuming the rind was always saturated, regardless of temperature, had no effect on the peak mean dose to the RMEI. Therefore, it is not conservative to assume that the rind is saturated. Furthermore, the IVRT believed that it is not physically reasonable to assume that the rind is saturated given that the spent fuel rods are the hottest part of the repository.	No work is needed for this comment because no performance credit due to cladding will be claimed in the TSPA-LA Model (Section 6.3.8). However, additional work was performed by the Project to enhance water-balance treatment as mentioned in this table under the IVRT comments IPC-08, EBS-29, and EBS-49. In addition, Appendix C 5.6 of the TSPA-LA Model includes performance margin analysis on cladding degradation.
IPC-01: The IVRT was of the opinion that no model validation has been provided in the version of the In-Package Chemistry Abstraction model report the IVRT reviewed. The data used for validation in Sections 7-1 to 7-4 of the reviewed TSPA model are not specific, or not relevant, to the system to be validated.	The work planned in *Technical Work Plan for Waste Form Testing and Modeling* (BSC 2006 [DIRS 177389]) to address the comment was completed. The work included enhancing the model validation by incorporating quantitative comparisons of the in-package chemistry modeling results with laboratory data as discussed in Section 7.4[a] of *In-Package Chemistry Abstraction* (SNL 2007 [DIRS 180506]). In addition, the model results by EQ6 were corroborated with the model results from an independently developed code (PHREEQC) as discussed in *In-Package Chemistry Abstraction* (SNL 2007 [DIRS 180506], Section 7.10[a]).
IPC-08: The IVRT concern was the same as in CLAD-05b above and deals with the general water balance comment within the EBS. The related comments are EBS-29 and EBS-49.	Work was planned in *Technical Work Plan for Waste Form Testing and Modeling* (BSC 2006 [DIRS 177389]) to address the comment and was completed as reported above under the comments EBS-29 and EBS-49.
IPC-09: The IVRT was concerned that the version of the In-Package Chemistry Abstraction report that the IVRT reviewed assumed no evaporation inside a WP. This is not consistent with the EBS physical and chemical environment report the IVRT reviewed. No convincing justification has been provided. This comment is also similar to the IVRT comments CLAD-05b, EBS-29, EBS-49, and IPC-08—all related to a more general comment of water balance inside the drift.	Additional work was performed by the Project to enhance water-balance treatment as mentioned in this table under the IVRT comments CLAD-05b, IPC-08, EBS-29, and EBS-49. The objective of the PMA is to obtain a realistic estimate of the quantity of water available inside a breached WP for interaction with waste components and, consequently, radionuclide transport. This analysis involves the fully coupling of thermal evolution, waste degradation, and water transport. The amount of water is modeled as a function of RH in the engineered barrier system, dripping rate, distribution of failed openings on the WP outer layers, and extent of waste degradation.

Table 7.9-1. Summary of Responses to the Remaining IVRT Comments (Continued)

Remaining IVRT Comment	Additional Work Conducted since the IVRT Review and Documentation where the Work is Located
Engineered Barrier System (Continued)	
RNS-02: The IVRT was concerned that although uncertainty in fluoride concentration as a function of pH was explicitly accounted for in the models of Pu, Np, U, Th, and Am dissolved concentration limits, these uncertainties were not correlated. Because every modeled radio element will experience the same fluoride concentration and because the concentration of every modeled radioelement increases with increasing fluoride concentration, these uncertainties should be correlated.	Work has been planned in *Technical Work Plan for Waste Form Testing and Modeling* (BSC 2006 [DIRS 177389]) to address the comment. The planned work was completed and documented in *Dissolved Concentration Limits of Radioactive Elements* (SNL 2007 [DIRS 177418]). The work entailed evaluation of fluoride uncertainty with new values from *In-Package Chemistry Abstraction* (SNL 2007 [DIRS 180506]). The resolution approach was to add a statement to the model report and output DTN that fluoride uncertainties are to be correlated. The impact to TSPA from this change was that, when sampling fluoride, the same fluoride concentration was used for all radionuclides in a WP instead of allowing fluoride to differ for different radionuclides in any one package. The update to achieve consistency with in-package chemistry changed the fluoride uncertainty parameter values (Epsilon 2 parameters). No additional validation is required; this change only affects the implementation of the sampling of uncertainty distributions associated with the effects of fluoride on dissolved concentration limits.
RNS-04: The IVRT was concerned that the *Dissolved Concentration Limits of Radioactive Elements* (REV 03A) suggested using an unconstrained concentration for the chemical condition outside the valid ranges. This treatment will cause serious problems for the Igneous Intrusion Modeling Case, where pH can be around 10, which falls outside the model's valid pH range for some radionuclides. It is not physically credible for radionuclide solubilities under this condition to be unconstrained. Solubilities must have a finite value!	The work was planned in *Technical Work Plan for Waste Form Testing and Modeling* (BSC 2006 [DIRS 177389]) to address the comment. The planned work was completed and reported in Dissolved Concentration Limits of Radioactive Elements (SNL 2007 [DIRS 177418]). The scientific approach used was to set caps, (i.e., setting limits on dissolved concentrations (SNL 2007 [DIRS 177418], Section 6.22)) by exploring the maximum concentration of radionuclides that are possible based on using all the available water to solvate the solute ions. This approach would still give a conservative upper bound for the dissolved concentration while lowering the caps significantly. The resulting change in the numerical values used in TSPA from the metal densities to lower values based on maximum utilization of the available water for salvation of solute ions was implemented.
RNS-07: The IVRT was concerned that the proposed extension of B-dot model calculations to ionic strength up to 3 M was stretchy. The justification provided in Section 6.3.3.4 of the *Dissolved Concentration Limits of Radioactive Elements* (BSC 2004 [DIRS 169425, a historic document cited for background information]) was not fully convincing.	Work was planned in *Technical Work Plan for Waste Form Testing and Modeling* (BSC 2006 [DIRS 177389]) to address the comment. The objective of the planned work was to augment the technical basis for assessing the effects of higher ionic strength (greater than 1 Molal) on confidence in activity coefficients calculated using the B-dot equation. The planned work was completed and documented in *Dissolved Concentration Limits of Radioactive Elements* (SNL 2007 [DIRS 177418], Sections 6.3.3.4 and 6.4.4).

Table 7.9-1. Summary of Responses to the Remaining IVRT Comments (Continued)

Remaining IVRT Comment	Additional Work Conducted since the IVRT Review and Documentation where the Work is Located
Engineered Barrier System (Continued)	
CMT-062705-091834-96: The IVRT was concerned that the general corrosion rate of the order of 0.0001 mm/year was based on the extrapolation of data taken over a period of 1 to 5 years and at temperatures of 60°C and 90°C, to time periods of up to 35,000 years and high temperatures without sufficient justification.	No additional work on this comment is planned. Use of short-term data relative to the regulatory time frame will always be a consideration in performance assessment. The IVRT should reconsider this comment. In addition, this comment is of little consequence to the current TSPA Model because only 1/3 of the thickness of the DS will be corroded in 10,000 years. Because the rates used in TSPA are early time rates and rates decrease with time, the use of lower corrosion rates will only reduce the thickness corroded. The CDF is based on data collected between temperatures of 60°C and 90°C and is constant. However, the general corrosion rate is a function of temperature. The repository temperature drops (Section 6.3.2) to this range (60°C to 90°C) within 1,000 years making it reasonable to use data collected in this temperature range for the whole duration. Moreover, the chemistry becomes less corrosive with time and the corrosion rate should decrease with time.
CMT-062105-123501-09: The IVRT's concern was that it is not known how appropriate it is to apply the evaporation look-up tables directly to the invert since the invert is a porous medium and the capillary effect should play an important role in controlling water saturation degrees.	The comment is not applicable since the Project does not use evaporation look-up tables the IVRT referred to any longer. This is now accomplished by using a relationship between relative humidity and water saturation, as explained in a 9/7-8/2005 meeting between IVRT and TSPA staff as documented in *Independent Validation Review Team (IVRT) Issues, Bechtel-SAIC Responses, and IVRT Assessment of Responses Related to Review of the TSPA Model and Supporting Analyses and Model Reports* (Booth 2006 [DIRS 176638]). Consequently, no additional work was deemed necessary.
General Comment	
CMT-062005-120938-57: The IVRT was concerned that many of the pdfs for characterizing uncertainty in parameter values in analysis and/or model report submodels where very broad pdfs were developed that often (1) were not supported by the existing data or information and (2) does not provide evidence that risk dilution is not likely to occur when implementing the TSPA-LA Model. In addition, the submodel analysis and/or model reports did not seem to have followed and applied the guidelines for developing pdfs presented in *Guidelines for Developing and Documenting Alternative Conceptual Models, Model Abstractions, and Parameter Uncertainty in the Total System Performance Assessment for the License Application* (BSC 2002 [DIRS 158794]), and adequate justification was not provided for why these guidelines were not followed.	The Project conducted an initial scoping evaluation of pdfs for 60 key parameters among the 388 parameters used in the draft TSPA-LA report, which the IVRT reviewed. Sensitivity to dose was analyzed on six of these 60 parameters. The six parameters were selected for their high significance to dose. This initial scoping work was the subject of a Condition Report 7538, which was closed as planned after the initial work was completed. The Project since then undertook a focused effort by a team of SMEs to ensure that the uncertainty-treatment and the pdf development for the TSPA-LA input parameters are uniformly performed. The uncertainty treatment is discussed in Section 6.1.3 and an uncertainty characterization review is presented in Section 7.4 of this TSPA-LA Model report. The review in Section 7.4 was aimed at making an evaluation of the manner in which the uncertainty associated with the TSPA input parameters were treated in developing the TSPA Model, and ensuring that any inconsistencies or inappropriateness in the treatment of uncertainty was detected and corrected so that the TSPA-LA Model results are reliable and reasonable.

Table 7.9-1. Summary of Responses to the Remaining IVRT Comments (Continued)

Remaining IVRT Comment	Additional Work Conducted since the IVRT Review and Documentation where the Work is Located
General Comment (Continued)	
CMT-062005-143936-34: The IVRT commented that the five observed pore waters in the THC-seepage abstraction model were selected only to capture the variability of water samples and no probability was associated with the original selection. Therefore, the equal probability for these five waters is not justified. These five waters were selected from limited early field measurements. Since more data have become available, it would be helpful to show that with more data accumulated, the original assumption of equal probability for five waters is still justified.	This comment is similar to the part of the comment IDC-2 dealing with the probability assignment of the five water samples and the use of the more water data now available to justify the equal probability assignment made. The work planned in *Technical Work Plan for: Revision of Model Reports for Near-Field and In-Drift Water Chemistry* (SNL 2007 [DIRS 179287]) to address the comment was completed and documented in *Engineered Barrier System: Physical and Chemical Environment* (SNL 2007 [DIRS 177412], Section 6.6). The cited section provides a detailed description of how the four end-member starting waters were selected for the Near-Field Chemistry Model (CFM) based on the latest available pore-water database.
CMT-062705-093311-25: The IVRT thought that the basis for using NpO2, summarized in Section 6.6 and Appendix IV in the version of the *Dissolved Concentration Limits of Radioactive Elements* model report that the IVRT reviewed, was not convincing.	Additional work on the subject was planned in *Technical Work Plan for: Revision of Model Reports for Near-Field and In-Drift Water Chemistry* (BSC 2006 [DIRS 179287]) to address the comment. The technical objective of the neptunium testing work was to enhance the technical basis for using NpO2 (as opposed to Np2O5) as the pure neptunium phase limiting the dissolved concentration of neptunium inside the WPs. The technical objective also included determination of the effective activation energy for NpO2 precipitation in systems where active reductants may be scarce or absent. The scope involved examination of the behavior of neptunium in corroded spent fuel samples and assessing the homogenous and heterogeneous precipitation kinetics for precipitation of Np(IV) from Np(V) solutions. The goal was to obtain an improved scientific basis for the redox behavior and precipitation kinetics of neptunium in heterogeneous environments similar to those inside the breached WP and in the low-temperature environments outside the WP, where active reductants may be scarce or absent. The planned work was completed and documented in *Dissolved Concentration Limits of Radioactive Elements* (SNL 2007 [DIRS 177418], Section 6.6).
CMT-062705-093723-54: The IVRT comment was that using solubility equal to the density of the solid metal violated basic physical principles (Darcy's Law and Fick's law) in terms of radionuclide transport as a dilute species. Other related submodels that assume transport of dilute solutions are, therefore, incorrectly linked.	This is an expansion of RNS-04. Work was planned in *Technical Work Plan for: Revision of Model Reports for Near-Field and In-Drift Water Chemistry* (BSC 2006 [DIRS 179287], Section 1.2.1) to address the comment. The planned work was completed and reported in *Dissolved Concentration Limits of Radioactive Elements* (SNL 2007 [DIRS 177418]). The scientific approach used was to set caps that set limits on dissolved concentrations (SNL 2007 [DIRS 177418], Section 6.22) to the maximum concentration of radionuclides that are possible, based on using all the available water to solvate the solute ions. This approach would still give a conservative upper bound for the dissolved concentration while lowering the caps significantly. The resulting change in the numerical values used in TSPA from the metal densities to lower values based on maximum utilization of the available water for solvation of solute ions was implemented.

Table 7.9-1. Summary of Responses to the Remaining IVRT Comments (Continued)

Remaining IVRT Comment	Additional Work Conducted since the IVRT Review and Documentation where the Work is Located
General Comment (Continued)	
CMT-062105-100625-71: The IVRT was concerned that with respect to radionuclides transport in the EBS, the two-cell model used by the Project may not be appropriate because in reality, Cell 1 and Cell 2 in the EBS Transport Model are not completely physically separated in space. Even with a purely advective flow, the water will percolate through multiple fuel rods and corrosion product domains and significant flow mixing is expected.	In order to model this type of transport, two distinct domains are needed: one that acts as a source of dissolved mass and the other that acts as the porous medium. The Project believes the approach (i.e., relying on multiple batch-reactor cells for EBS transport modeling) used is reasonable and consistent with the conceptualization of the in-package environment. The Project's current approach, which is somewhat modified, is discussed in *Technical Work Plan for: Near-Field Environment: Engineered Barrier System: Radionuclide Transport Abstraction Model Report* (BSC 2006 [DIRS 177739]). The planned work was completed and presented in *EBS Radionuclide Transport Abstraction* (SNL 2007 [DIRS 177407], Section 6).

INTENTIONALLY LEFT BLANK

7.10 SUMMARY OF MODEL CONFIDENCE BUILDING

The intended purpose of the TSPA-LA Model, as defined in *Technical Work Plan for: Total System Performance Assessment FY 07-08 Activities* (SNL 2008 [DIRS 184920], Section 2.3.5), is to provide the TSPA-LA Model appropriate for use in the evaluations of compliance with the quantitative postclosure requirements of NRC Proposed Rule 10 CFR Part 63 ([DIRS 178394] and [DIRS 180319]). The TSPA-LA Model was validated by performing activities required by SCI-PRO-006, *Models*. The *Technical Work Plan for: Total System Performance Assessment FY 07-08 Activities* (SNL 2008 [DIRS 184920], Section 2.3.5) implements these procedural requirements and describes and plans the tests and analyses activities that are to be performed to build confidence in the TSPA-LA Model and ensure that the model is valid for its intended purpose. As described in Section 2, results of the activities presented in Sections 7.2 through 7.9 are summarized below, in order to assess the validation status of the TSPA-LA Model for its intended purpose. Once the during-development activities were performed and it was established that the requirements of the technical work were satisfied, the relative significance of the post-development activities in building confidence in the reasonableness of the TSPA-LA Model results were evaluated and determined to meet the required Level II validation status of the model as specified in SCI-PRO-006. While the results of all four groups of the post-development validation activities, summarized below added confidence in making the decision on whether the model achieved the required validation status, the auxiliary analyses and in particular the performance margin analyses (PMA) results, were of special significance in this regard. As required by the technical work plan, the PMA utilized revisions to selected component models in the TSPA-LA compliance model including conceptual or uncertainty alternatives, to assess the performance margin in the compliance model, and to evaluate whether the compliance model dose is underestimated. The cumulative results of the pre- and post-development activities led the responsible performance assessment manager to the conclusion that the TSPA-LA Model indeed satisfied the Level II validation requirements and met its intended purpose.

Section 7.10 summarizes the above validation activities. Section 7.10.1 provides a synopsis of the validation strategy. Sections 7.10.2 through 7.10.9 summarize the validation activities performed. Concluding remarks are presented in Section 7.10.10. Validation of the TSPA-LA Model consisted of a series of activities to provide confidence in the analysis of transport processes for radionuclides that occur between the waste form in the repository and the RMEI. The validation process begins with the verification of model input and verification that the valid supporting models and analyses and their abstractions are incorporated properly into the TSPA-LA Model (Section 7.2). Supporting models, analyses, and abstractions undergo appropriate verification and validation prior to their final implementation in the TSPA-LA Model. The TSPA-LA model is then evaluated for statistical, temporal, and spatial stability (i.e., number of realizations, timesteps, and spatial discretization) and accuracy of the calculated dose (Section 7.3). Treatment of uncertainty in the development of the TSPA-LA Model is documented in Section 6.1.3. Uncertainty characterization reviews on the TSPA-LA Model direct-input parameters were conducted in order to ensure that uncertainty with respect to the input parameters was treated uniformly and consistently throughout the TSPA-LA Model (Section 7.4). Additionally, uncertainty and sensitivity analyses were conducted to gain confidence that uncertainty in parameters, models, and scenarios were propagated correctly into the results provided by the TSPA-LA Model (Section 7.4 and Appendix K). The uncertainty

and sensitivity analyses examined subsystem radionuclide release and transport processes and system results to gain confidence in the TSPA-LA Model results. Surrogate waste form analyses representing the DOE spent fuel Categories 2 through 11 and the NSNF, Category 1, ensured that the TSPA-LA Model appropriately incorporates these waste types (Section 7.5).

Post-development activities are conducted to ensure that the TSPA-LA Model is valid for its intended purpose. The results of these validation activities are documented in Sections 7.6 through 7.9. Section 7.6 documents corroboration of the direct input abstraction parameters with their respective underlying validated process models and demonstrates that the results are consistent with these supporting models. Several auxiliary analyses were conducted to: (1) determine that the submodels are coupled as intended by evaluating selected key single-realization curves that contribute to the calculation of mean annual dose (Section 7.7.1); (2) compare the TSPA-LA Model mean annual dose results with the results from a simplified, independently developed TSPA analysis (Section 7.7.2); (3) compare model results with a TSPA developed independently by the EPRI (Section 7.7.3); and (4) provide objective evidence for assessing a performance margin analysis, and the degree of conservatism or non-conservatism in the TSPA compliance model (Section 7.7.4). In addition, analogues were examined to provide confidence in the results provided by the TSPA-LA Model (Section 7.8).

As an additional confidence-building activity, reviews by three independent teams of external experts were described (Section 7.9) showing that the comments and recommendations from these reviews were addressed in the development of the TSPA-LA Model. This summary includes a description of the implementation of the work planned to address the several remaining comments from the most recent IVRT review of earlier drafts of the TSPA-LA Model.

Validation of the TSPA-LA Model applies directly to the estimates of the performance measures for the Yucca Mountain repository as established by NRC Proposed Rule 10 CFR Part 63 ([DIRS 178394] and [DIRS 180319]). The TSPA-LA Model provides estimates of the groundwater protection performance measures in terms of groundwater concentration and dose. The last step in the annual dose calculation is the conversion of radionuclide concentrations in the groundwater to an annual dose to the RMEI using a BDCF. Thus, a model that is valid for the calculation of annual dose is also valid for calculation of groundwater protection performance measures in terms of concentration and dose (Section 8.1.2).

The activities described in Section 7 are conducted to gain confidence in the TSPA-LA Model through the model validation activities required by SCI-PRO-006. These activities examine the internal supporting models and components of the TSPA-LA Model separately and in combination to determine whether or not they are producing plausible and reasonable inputs to the TSPA-LA Model. The results of the activities demonstrate that the TSPA-LA Model inputs represent the underlying process models as expected; the inputs were accurately implemented in the TSPA-LA Model; the TSPA-LA Model is numerically, temporally, and spatially stable; and the resultant dose calculations are accurate. The subsequent post-development validation activities (Table7.1-1) demonstrate that the TSPA-LA Model produces reliable estimates of repository performance compliance measures such as estimates of the individual and groundwater protection standards.

7.10.1 Validation Strategy

This section summarizes the approach applied to validate the TSPA-LA Model as required by SCI-PRO-006 and as planned in the TSPA-LA technical work plan (SNL 2008 [DIRS 184920]) that implements the procedural requirements. The technical work plan identifies the general activities that need to be performed during and after the model development in order to ensure that the TSPA-LA Model is valid for its intended purpose. This section highlights the tests and analyses that are performed (Table 7.1-1) in support of these activities.

7.10.1.1 Introduction

The general TSPA process adopted by the DOE follows the methodology developed by Cranwell et al. (1990 [DIRS 101234], Sections 2 and 3). Over time, the methodology has been enhanced and applied to numerous projects by various international organizations involved in radioactive waste management. The TSPA-LA Model was developed to analyze the ability of the natural and engineered systems of the Yucca Mountain repository to safely isolate nuclear waste following repository closure. Performance assessments and related supplemental analyses of the Yucca Mountain repository were conducted following the publication of the Nuclear Waste Policy Amendments Act of 1987 (Public Law No. 100-203 [DIRS 100016]). The TSPAs of the Yucca Mountain repository have been iterative and periodically updated, each building on and extending the scope and results of the previous TSPAs. The iterative assessments incorporate both an improved understanding of the processes affecting repository performance and, through additional field observations and laboratory analyses, better identification and quantification of the values of the parameters used in the TSPA models.

The TSPA iterations have been evaluated and independently reviewed by technical staff and various external organizations, and these reviewers have made recommendations for improvements for consideration in future TSPAs. Examples include a TSPA peer review conducted of the TSPA-VA by Budnitz et al. (1999 [DIRS 102726]), an evaluation of the TSPA-SR by an IRT (OECD and IAEA 2002 [DIRS 158098]), and a technical review of the earlier drafts of the TSPA-LA Model by an IVRT (Gibson 2007 [DIRS 181099]). The criteria for these independent technical reviews were designed within the framework of procedural compliance as required by the prevailing model development procedure (precursors of SCI-PRO-006, and per the requirements of the QARD applicable at the time) and the respective technical work plans that were in effect during the review periods. The review criteria especially focused on evaluating two critical aspects of the TSPA under review: (1) the adequacy of the TSPA methodology being developed, and (2) whether the TSPA satisfied its intended purposes. Section 7.9 describes the criteria used for the TSPA-VA, IRT, and IVRT reviews. The TSPA-VA, TSPA-SR, and the early drafts of the TSPA-LA models were developed to assess the repository performance for a 10,000-year postclosure compliance period reflecting the regulations in effect at that time. The TSPA-LA Model assesses repository performance with respect to the NRC Proposed Rule 10 Part CFR 63 ([DIRS 178394] and [DIRS 180319]) for a postclosure compliance period of 10,000 years and the period of geologic stability, defined as 1,000,000 years at NRC Proposed Rule 10 CFR 63.302 [DIRS 178394]. Nonetheless, the comments and recommendations made by these reviews that were implemented in development of the TSPA-LA Model contributed to the development of the TSPA-LA Model as valid for its intended purpose.

Validation of the TSPA-LA Model consists of a sequence of activities that are designed to build confidence in the results of the model. The TSPA-LA Model analyzes the FEPs expected to affect the repository system; that is, the FEPs leading to the development of the Nominal Scenario Class. TSPA-LA Model analyses include the Nominal Scenario Class Modeling Case, the low probability Drip Shield EF and Waste Package EF Modeling Cases, as well as the low probability modeling cases due to postclosure disruptive events that could occur at the Yucca Mountain repository site, such as those represented by the Igneous Intrusion Modeling Case, Volcanic Eruption Modeling Case, Seismic GM Modeling Case, and Seismic FD Modeling Case. The TSPA-LA Model analyses also include evaluation of a Human Intrusion Scenario per NRC Proposed Rule 10 CFR 63.322 [DIRS 180319].

Validation of a computer model for a physical system involves a series of steps designed to generate and enhance confidence in the model's results during and after model development. The modeling process starts with the developer's understanding of the physical system. A model is then conceptualized based on available information using appropriate assumptions, simplifications, and idealizations. The conceptual model is formulated into a mathematical model and then into a numerical model. An appropriate computer code/software suite is selected or developed to implement the numerical model. The input to the computer code is prepared, and the code is executed to obtain the model results.

A well-designed, correctly implemented numerical model should produce results that are explainable and are appropriate for the model's intended use. Validation of the TSPA-LA Model is a process of establishing that the results provided by the model, which requires performance prediction for many thousands of years into the future, are plausible and reasonable. Consequently, in contrast to modeling activities where validation may be achieved by comparing model results with direct measurements, such measurements are impossible to obtain at the temporal and spatial scales of interest for postclosure repository performance assessment. Instead, confidence in the results of the TSPA-LA Model is based on the successful completion of required activities described in the technical work plan (SNL 2008 [DIRS 184920], that are based on SCI-PRO-006. These activities are designed to ensure that the TSPA-LA Model is developed consistent with its intended use for the LA; that it captures the relevant features, events and processes (FEPs) through the implementation of its validated submodel components in which the FEPs are addressed; and that the confidence in the TSPA-LA Model results is demonstrated by independent lines of corroborative information after the model development. There are two main categories of procedural activities to validate the TSPA-LA Model (Figure 7.1-2): (1) those conducted during development of the model, and (2) those conducted after development of the model.

7.10.1.2 During-Development Model Validation Activities

The during-development activities listed in the technical work plan (SNL 2008 [DIRS 184920], Section 2.3.5.1), which are performed to demonstrate the TSPA-LA Model validation in relationship to the model's intended use and required level of confidence, are as follows:

1. Selection of input parameters and/or input data and a discussion of how the selection process builds confidence in the model (SCI-PRO-002, *Planning for Science Activities*, Attachment 3, Level 1, Validation 1).

2. Description of calibration activities, and/or initial boundary condition runs, and/or run convergences, and a discussion of how the activity or activities build confidence in the model. Includes a discussion of impacts of any run non-convergences (SCI-PRO-002, Attachment 3, Level 1,Validation 5).

3. Discussion of the impacts of uncertainties on model results (SCI-PRO-002, Attachment 3, Level 1, Validations 4 and 6).

Two additional factors are incorporated as appropriate during development of the TSPA-LA Model:

1. Formulation of defensible assumptions and simplifications (SCI-PRO-002, Attachment 3, Level 1, Validation 2).

2. Consistency with physical principles, such as conservation of mass, energy, and momentum (SCI-PRO-002, Attachment 3, Level 1, Validation 3).

Selection of input parameters and/or input data provides parameters and initial and boundary conditions for submodels and components that calculate input parameters and boundary conditions for successive submodels and model components. Based on analyses that show that these submodels and components are working as intended (Section 7.10.2), the model is then tested for stability (i.e., appropriate number of realizations, timesteps, and spatial discretization) (Section 7.10.3). The uncertainty characterization review ensures that uncertainty associated with the direct-input TSPA-LA parameters is being characterized adequately and uniformly, and the uncertainty and sensitivity analyses examine impacts of uncertainty on subsystem radionuclide release and transport processes, and the system results to gain confidence in the TSPA-LA Model. (Section 7.4 and Appendix K). These during-development activities test the integration of the submodels and components into the overall system model.

Completion of these during-development activities demonstrates that: (1) the input parameters for the model are correctly implemented into the model from source documents, including those parameters that are internally calculated; (2) the model is stable in terms of the number of realizations, length of timesteps, spatial discretization, that calculated doses are accurate; and the radionuclide transport model using the particle tracking method with FEHM code is stable; and (3) uncertainty in model inputs is treated properly and uniformly and is propagated through the model and correctly accounted for in the model results.

7.10.1.3 Post-Development Model Validation Activities

Post-development model validation activities (SNL 2008 [DIRS 184920], Sections 2.3.5.2 and 2.3.5.3) include activities that may be used to validate the TSPA-LA Model. For the TSPA-LA Model, the required level of confidence and validation falls into the Level II validation category (SCI-PRO-002, Attachment 3) that requires use of at least two of the activities from Section 6.3.2 of SCI-PRO-006. In order to provide confidence beyond the procedural requirements, the TSPA-LA Model utilized several post-development model validation activities:

- Corroboration of the direct-input abstraction results with the validated mathematical model or process model from which the abstraction was derived (Section 7.6)

- Auxiliary analyses for corroborating the results with the TSPA-LA Model or model abstractions and/or submodels used in the TSPA-LA (Section 7.7)

- Comparison of the relevant portions of the TSPA-LA Model with appropriate analogue information (Section 7.8)

- As an additional confidence-building exercise, the comments and recommendations by the past technical reviews, including those by the more recent IVRT on earlier drafts of this TSPA-LA Model were addressed and implemented as appropriate (Section 7.9).

The results of these post-development activities demonstrate that the overall system model is functioning as intended and the results are explainable and reasonable. Addressing the independent technical review comments and recommendations covers both during- and post-development activities and, along with auxiliary analyses, the natural analogues and the during-development activities mentioned earlier that provide confidence that the TSPA-LA Model is valid for its intended use.

In addition to the validation activities mentioned above, potential impact on the TSPA-LA Model results due to issues identified after the model runs were completed was evaluated as stated in *Technical Work Plan for: Total System Performance Assessment FY 07-08 Activities* (SNL 2008 [DIRS 184920], Section 2.3.5.3). Appendix P contains the results of this evaluation. No significant impact on the TSPA-LA results was noted. As a part of the continuing improvement effort by the Project, the impact on the results of this version of the TSPA-LA Model will be included in an addendum.

The goal of the model validation activities is to support the demonstration that the results of the procedurally validated TSPA-LA Model satisfy the applicable individual dose and groundwater protections requirements set by the NRC. The activities are also to address the applicable TSPA-LA Model acceptance criteria identified by the NRC in its Yucca Mountain Review Plan. Table H-1 in Appendix H provides a roadmap of the NRC requirements and the Yucca Mountain Review Plan acceptance criteria applicable to the TSPA-LA Model.

7.10.2 Code and Input Verification

The code and input verification was conducted to provide confidence in the software and the input used in the TSPA-LA Model and to comply with the requirements of SCI-PRO-006, Section 6.3.2. This includes: (1) verification of the integrated system software (GoldSim) that is the software platform for the TSPA-LA Model, (2) verification of DLLs from source documents and DLLs that are generated within the TSPA-LA Model, and (3) verification of model inputs from the TSPA Input Database. Submodels that originate from a source analysis and/or model report were verified by comparing submodel results from the TSPA-LA Model with results provided in the analysis and/or model report. Coupling between submodels was examined by verifying that the information generated by one submodel is input correctly to successive submodels and that this information does not exceed the applicable range of the successive

submodel. In other words, these activities were conducted to verify that the computer codes and model inputs that originated from an outside source (analysis and/or model reports), or are generated internally within the TSPA-LA Model, are implemented correctly. The results of these activities are as follows:

- GoldSim was selected as the TSPA integration code based on its capabilities and use in similar applications. GoldSim V9.60.100 (STN: 10344-9.60-01 [DIRS 181903]) was qualified per IM-PRO-004, *Qualification of Software.*

- Output of DLLs from other sources (analysis and/or model reports and DTNs) was found to be exact.

- Output of DLLs that calculate results within the TSPA-LA Model was found to be within the acceptance criteria (e.g., within five percent).

- Individual submodels were validated and documented in their respective analysis and/or model reports.

- Results from submodels within the TSPA-LA Model were compared to results contained in model reports (stand-alone or simple models) and were found to agree within the acceptance criteria.

- Outputs from one submodel to another were found to be correct and either does not exceed the valid range of the successive submodel or the value used is fixed within the range or at the upper bound of the range of the successive submodel.

- Input in the TSPA Input Database was verified to correspond with source data.

An important aspect of the during-development model validation identified in the technical work plan (SNL 2008 [DIRS 184920], Section 2.3.5.1) is the appropriate selection of input parameters and how the selection process builds confidence in the model. In the case of the TSPA-LA Model, this is a function of the selection process of each of the model abstractions and the appropriateness (i.e., validity) of those abstractions. This process included the formal review by TSPA technical staff of all supporting models and analyses used as input to the TSPA-LA Model. In addition, a formal review of the appropriate subsections of the TSPA-LA Model description, Sections 6.3, 6.4, 6.5, 6.6, and 6.7, was conducted by a SME responsible for these inputs to ensure the information was appropriately implemented in the TSPA-LA Model. This review is summarized and discussed in Section 4.

The activities above demonstrated that the system software for the TSPA-LA Model is appropriate and valid, that input is correct and verified, that the internal transfer of information within the model is correct and within the valid range of successive submodels, and that submodels are valid per their respective source analysis and/or model reports. In other words, incorporation of information and submodels from other sources into the TSPA-LA Model has not altered the validity of the information or the submodels or both.

7.10.3 Model Stability Testing

Demonstration of stability of the TSPA-LA Model is essential to validation and confidence building of the model results. As discussed in Section 7.3, the TSPA-LA Model computes mean annual dose in four steps: (1) selection of values for epistemic parameters and aleatory uncertainties; (2) numerically solving a complex, coupled system of differential equations describing radionuclide decay, flow, transport, and other physical processes; (3) integration over aleatory uncertainty, carried out either by quadrature or Monte Carlo techniques; and (4) integration over epistemic uncertainty, conducted by a Monte Carlo technique. Section 7.3 discusses the details of how the stability of the TSPA-LA Model is verified through implementation of the four steps during the TSPA-LA Model computations. TSPA-LA Model stability verification involved five different analyses: (1) statistical stability of mean annual dose, (2) numerical accuracy of expected annual dose, (3) temporal stability, (4) spatial stability, and (5) stability of the FEHM particle tracking model. A summary of each of these stability tests and their results obtained from them are provided below

Statistical Stability

A replicated sampling procedure was used to determine the statistical stability of the TSPA-LA Model results. With this procedure, the LHS is repeatedly generated with different random seeds. Mean annual dose is computed for each modeling case with each LHS. Confidence intervals for the mean annual dose are then estimated with the *t*-distribution.

Replicate sampling runs were performed in the GoldSim code for each of the TSPA-LA modeling cases: Nominal Modeling Case, Waste Package EF Modeling Case, Drip Shield EF Modeling Case, Igneous Intrusion Modeling Case, Volcanic Eruption Modeling Case, Seismic GM Modeling Case, Seismic FD Modeling Case, and Human Intrusion Modeling Case. The details of the stability analyses for these modeling cases are presented in Section 7.3.1. Results are presented for each modeling case and for total mean annual dose (summed over all modeling cases) in Section 7.3.1. The analysis concludes that the sample size used in the Monte Carlo technique is adequate to estimate mean annual dose in each modeling case as well as to estimate the total mean annual dose. Therefore, the results of the TSPA-LA Model are statistically stable.

Numerical Accuracy of Expected Annual Dose

Detailed discussions on the numerical accuracy analyses for each of the TSPA-LA modeling cases are provided in Section 7.3.2. The results are summarized below.

Because the expected annual dose for the Nominal Modeling Case is computed directly with the GoldSim code, the numerical accuracy of the mean annual dose for the Nominal Modeling Case was evaluated by increasing the size of the LHS size from 300 (used for the base case) to 1,000. The results show that the mean annual dose based on 300 realizations is adequate and numerically stable. The expected annual dose for the Waste Package EF Modeling Case and Drip Shield EF Modeling Case is calculated by summation rather than numeric integration, making the calculated expected annual dose exact, thus requiring no estimate of numerical accuracy.

For the Igneous Intrusion Modeling Case, the accuracy of the calculation of expected annual dose by numeric integration was verified by increasing the number of igneous intrusion times from 10 (base case) to 50. The similarity of the shape of the dose history curves for different times of intrusions within a climate period indicates that the interpolation techniques used within the EXDOC software are justified, and the 10 intrusion times are sufficient to obtain a numerically accurate expected dose. For the Volcanic Eruption Modeling Case, sufficiency of the LHS size for aleatory parameters is demonstrated by increasing the LHS size from 40 to 80. The results show that the LHS sample size of 40 used in the base case is adequate to estimate expected dose. Because the dose from volcanic eruption constitutes most of the total dose during the first 1,000 years, the accuracy of the first 1,000-year dose was verified by increasing the number of eruption events with no significant change in dose. The results imply that the expected dose for 1,000,000 years is also numerically stable.

Accuracy of both the 10,000-year and 1,000,000-year expected annual dose results was verified for the Seismic GM Modeling Case. Detailed discussions on execution of the steps performed for the verification and the results are provided in Section 7.3.2.6. For the 10,000-year Seismic GM Modeling Case, several steps were performed to verify accuracy of the expected annual dose for the 10,000-year modeling case. Summarizing here,

1. Demonstrated that increasing the number of times of seismic events (from 6 to 12) and damage fractions (from 5 to 8) does not change the expected dose calculation for any realization, verifying that the discretization used to calculate expected dose is adequate.

2. Justified the use of the assumption that the dose from a sequence of seismic events is reasonably approximated by the sum of the doses from each event where each event is modeled separately.

3. Justified the simplifications to the *Seismic Consequences Abstraction* (SNL 2007 [DIRS 176828]) by evaluating the effects of corrosion processes; the effects of DS plate or framework failure; magnitude of the volume of rockfall; the consequences of rupture and puncture of WPs; and seismic damage to TAD WPs.

For the 1,000,000-year Seismic GM Modeling Case, numerical stability of the expected annual dose calculated by the Monte Carlo technique was investigated by increasing the aleatory sample size from 30 to 90 for a suitable epistemic realization. Although the expected annual dose for each realization did not converge to a stable value, the results demonstrate that the sample size used in the base case calculation produces a statistically stable mean annual dose for the 1,000,000-year Seismic GM Modeling Case (Section 7.3.2.6.2).

In the case of the Seismic FD Modeling Case, it was shown that increasing the event size would result in an improved dose accuracy. However, given the relatively low significance of this modeling case, the event size used for the base case produces an adequate result. The numerical stability of the expected annual dose for the Human Intrusion Modeling Case was computed by the Monte Carlo technique. The results show no significant difference by increasing the size of the aleatory sample from 30 to 90**.**

Temporal Stability

Evaluation of temporal stability of the TSPA-LA Model was performed conducting simulations of the Waste Package EF Modeling Case, Igneous Intrusion Modeling Case, Seismic GM Modeling Case, and Human Intrusion Modeling Case. These modeling cases have the most influence on the system performance and are likely to be influenced by the changes in the timestep size used. The simulations were conducted by reducing the TSPA-LA Model timestep size to examine the timestep size sensitivity. The annual dose from the TSPA-LA Model runs with different timestep sizes were compared graphically with the base case results to determine the effect of refining the timesteps. The details of the approach and results are provided in Section 7.3.3. The results for the four modeling cases are summarized below.

In the case of the Waste Package EF Modeling Cases of the CDSP and CSNF WPs, comparison of the annual dose curves resulting from the refined two-timestep scheme runs shows that the temporal discretization used in the Waste Package EF Modeling Case for the TSPA-LA Model is suitable. In the Igneous Intrusion Modeling Case, temporal stability was tested for 1,000,000 years (with the intrusion fixed at 400,000 years) and 20,000 years (with the intrusion fixed at 1,000 years) and then applying separate sets of alternate timestep schemes in both cases. An increase of annual dose was observed for the alternate timesteps immediately after the intrusion events, and the increase was found to be insignificant to either the expected dose or the mean dose. Similarly for the 20,000-year three timestep runs, the overall shape of the dose history is very similar for all three timestep schemes. The results show that the timestep scheme used in the Igneous Intrusion Modeling Case is adequate. In the Seismic GM Modeling Case for 20,000 years, the annual dose is computed by employing three separate timesteps with the seismic event time fixed at 1,000 years and the damage fraction at 10^{-6}. The results demonstrate that the timestep scheme used in the 20,000-year dose calculation is adequate. The test results for the Human Intrusion Modeling Case also confirms that the timestep scheme used for dose calculation in this modeling case is adequate.

Spatial Stability

Section 7.3.4 describes the spatial discretization schemes of the process model abstractions (Mountain-Scale UZ Flow Submodel, the EBS TH Environment Submodel, the UZ Transport Submodel, and the SZ Flow and Transport Submodel) that feed the TSPA-LA Model. No impact on the TSPA-LA Model results due to these inherited (and verified as documented in their respective source documents) spatial discretizations are expected because they were used unchanged in the TSPA-LA Model simulations.

In addition, the TSPA-LA Model implements its own spatial discretization scheme to accommodate the use of the comprehensive EBS TH data set (provided by the MSTHM Process Model) by abstracting a representative TH data set that would capture the variability of the EBS TH environment across the repository footprint, while at the same time minimizing the computational burden associated with each additional subregion. This was accomplished and validated by two activities: (1) spatial discretization of the repository into a minimum but adequate number of subregions with percolation flux as a basis for discretization and binning percolation subregions by quantiles 0.0 to 0.05, 0.05 to 0.3, 0.3 to 0.7, 0.7 to 0.95, and 0.95 to 1.0; and (2) comparing TH-parameter curves (for single CSNF WP and a single CDSP WP for

each of the five percolation subregions) based on the representative TH data set with the corresponding curves based on the comprehensive EBS TH data set. The results demonstrate that the representative TH dataset can be used as a surrogate for the comprehensive EBS TH data set. The difference in EBS release times due to using the comprehensive EBS TH data set and the representative TH data set used in the TSPA-LA Model is insignificant.

Stability of FEHM Particle Tracking Model

Radionuclide transport processes in the TSPA-LA Model were modeled using the FEHM particle-tracking methodology. The model accuracy of this methodology increases with the number of particles released from the source until a plateau is reached, indicating stability. The maximum number of particles used in TSPA-LA Model for any species modeled is computationally limited to 900,000 particles. The UZ Radionuclide Transport Model was rerun in GoldSim with a lower number of released particles (500,000 and 750,000), and the results were compared with the 900,000-particle base case TSPA-LA Model runs to test stability of the FEHM Particle Tracking Model results of the TSPA-LA Model. The runs were made for the Drip Shield EF Modeling Case, Igneous Intrusion Modeling Case, and Seismic GM Modeling Case, and with the radionuclides ^{99}Tc, ^{233}U, ^{234}U, ^{237}Np, and Total ^{239}Pu (combined reversible and slow and fast irreversible colloids). The tests and test results are discussed in Section 7.3.5. A summary of the results is provided below.

The particle-tracking stability test indicates that the use of 900,000 particles in the TSPA-LA Model analyses provides stable results with respect to the number of particles used in all three of the modeling cases (Drip Shield EF Modeling Case, Igneous Intrusion Modeling Case, and Seismic GM Modeling Case). A reduction of the maximum number of particles to 750,000 or 500,000 is shown to have little effect on the annual dose results. Likewise, peak dose results showed that the reductions in the maximum number of particles used to represent the EBS releases had little influence on the TSPA-LA Model results. Therefore, the FEHM particle tracking model is stable. A detailed comparison of annual dose for representative radionuclide species and UZ mass flux releases shows that slight differences in particle tracking results associated with the reductions to the number of particles representing source releases (and in-growth contributions) represent differences in the refinement of source terms to the SZ. This difference in the source terms is dampened by the time mass has been transported 18 km.

7.10.4 Uncertainty Characterization Reviews and Sensitivity Analyses

Uncertainty Characterization Reviews

A substantive effort to systematically review the uncertainty/variability characterizations of the direct-input parameters for consistency, defensibility, and traceability was made for the TSPA-LA Model. These reviews resulted in ensuring that the inputs to the TSPA-LA Model are technically sound and appropriately reflect any significant uncertainty associated with the input parameters. Parameter uncertainty and sensitivity analyses were performed during and after the TSPA-LA Model development to ensure the uncertainty was propagated properly and its sensitivity on the dose calculations were represented accurately. A detailed discussion of the uncertainty characterization reviews, and the sensitivity analyses is presented in Section 7.4. A summary is provided below.

A multi-disciplinary team of scientists and engineers was formed to conduct the parameter uncertainty reviews. The skill composition of the review team was chosen to ensure relevant large breadth of expertise, experience, and knowledge needed to perform the review. While the uncertainty characterization reviews primarily focused on scrutinizing the technical basis, they also included consistency aspects of the NRC Review Method for data uncertainty described in the *Yucca Mountain Review Plan, Final Report* (NRC 2003 [DIRS 163274]) for the 14 abstraction topics. Parameter uncertainty and variability characterizations were judged appropriate based on the criteria consistent with the NRC Acceptance Criterion for data uncertainty. More specifically, the criteria consisted of: (1) must be technically defensible and reasonably account for major sources of uncertainties and variabilities, and (2) will not introduce inappropriate risk dilution when propagated through the TSPA-LA Model. The major scenario classes and their associated modeling cases were ranked according to their potential contribution to the overall dose-risk. Three disruptive scenario modeling cases were chosen as the focus of the formal uncertainty characterization reviews: (1) Seismic GM Modeling Case, (2) Igneous Intrusion Modeling Case, and (3) Volcanic Eruption Modeling Case. The Nominal Scenario Class was added to the list because many of its component models are used in the seismic and igneous modeling cases.

The uncertainty characterization review ensured that the uncertainty associated with the TSPA-LA input parameters was properly and consistently characterized and propagated, and the observed significant issues were addressed. For example, for the seismic hazard curve it was observed that while use of a bounded curve in the TSPA-LA Model may be conservative (with respect to the total dose CDF), this particular treatment of uncertainty is inconsistent with approaches used in other scenario classes. As a result of this finding, additional seismic analyses were performed and a quantitative representation of uncertainty in the mean hazard curve developed. Because this new result provides a better treatment of uncertainty, it was included in the TSPA calculations for the PMA (Appendix C, Volume III). The PMA calculation gives a perspective on the level of conservatism introduced by the bounded hazard curve approach. As a result of the review, the Igneous Intrusion Modeling Case and Drip Shield EF Modeling Case account for both aleatory and epistemic uncertainties, the effects of which are explicitly propagated to the dose CDF. In the case of the Nominal Scenario Class modeling cases, the review findings helped develop improved CDFs for stainless and carbon steel corrosion rates for EBS Transport Model, the groundwater specific discharge (GWSPD) parameter, and the flowing interval spacing (FISVO) parameter for the SZ Flow model.

Sensitivity Analyses

The detail of the final results of sensitivity analyses are documented in Appendix K. The during-development analyses followed the analysis scheme presented in Appendix K. The during-development sensitivity analyses generally confirmed that the uncertainty reviews had covered all key uncertain inputs. In addition, the during-development analyses provided a measure of confirmation that important uncertain inputs are propagated appropriately through the process models, and that the effects of these uncertainties are consistent with physical principles underlying the models. The during-development sensitivity analyses also uncovered a number of implementation errors in developmental versions of the model, which were subsequently corrected before the TSPA-LA Model became final. After model development, a final sensitivity analysis was conducted, and is documented in Appendix K. This analysis identifies the

dominant sources of uncertainty in total expected dose to the RMEI. The final sensitivity analysis confirms that uncertain inputs are propagated through the TSPA-LA Model and that the effects of uncertainty in these inputs are consistent with physical principles. The confirmation is demonstrated through causal explanations of the relationships between input and output variables. The final sensitivity analysis also identified a relatively small number of implementation errors present in version 5.000 of the TSPA-LA Model. The errors were found not to significantly affect the performance measures (i.e., mean dose, dominant modeling cases, etc) from the TSPA-LA Model (Appendix P).

7.10.5 Surrogate Waste Form Validation

The three waste forms included in the TSPA-LA Model are CSNF (stainless steel and Zircaloy clad), DSNF surrogates, and HLW. Of the DSNF fuel categories, the naval spent fuel (Category 1) is represented in the TSPA-LA Model by a CSNF surrogate. The remaining DSNF (Categories 2 through 11) packages are represented by a surrogate with a radionuclide inventory that is the average of the radionuclide inventories of Categories 2 through 11. The dissolution rate of the surrogates is instantaneous based on the rapid dissolution of Category 7 DSNF (i.e., uranium metal).

The analyses presented in Section 7.5 show that the use of surrogates to represent naval spent fuel and Categories 2 through 11 of DSNF is appropriate. The analyses of NSNF show that mean annual dose from NSNF is bounded by that from the Zircaloy-clad CSNF surrogate. In the analyses of Categories 2 through 11, the DSNF show that the surrogate spent fuel used in the TSPA-LA Model is a reasonable representation of the weighted sum of these categories of DSNF.

7.10.6 Corroboration of Abstraction Results with Validated Process Models

Abstraction is a quantitative simplification process utilized for numerical implementation of many of the process models in the TSPA-LA Model. Therefore, it is essential to ensure that the abstraction results corroborate with the underlying process models. That is, the abstractions represent their respective process models before and after their implementation in the TSPA-LA Model and, when applied together as the integral components of the TSPA-LA Model, they function coherently so that the TSPA-LA Model results are stable and properly represent the contributing abstractions. This consistency is achieved by ensuring that the individual abstractions are validated for their intended use in the TSPA-LA Model, performing input-verification activities during their implementation in the TSPA-LA Model and performing TSPA-LA Model stability-testing during its development process. After the integrity of the underlying process models is ensured through the abstraction validation and the TSPA-LA Model implementation processes, and the individual abstractions can be shown to be functioning correctly when they are applied together as TSPA-LA Model components and result in the needed stability of the TSPA-LA Model, certain post-development validation and confidence building activities that are unrelated to the TSPA-LA Model development activities need to be performed in order to determine that the TSPA-LA Model is appropriate for its intended use. Ensuring the integrity of the direct-input process models through abstractions and their successful application in the TSPA-LA Model is the first step towards defining and executing these follow-up post-development validation and confidence-building activities. As a follow up,

the technical work plan (SNL 2008 [DIRS 184920], Section 2.3.5.2) identified corroboration of abstractions with validated process models as a post-development TSPA-LA Model validation criterion in order to demonstrate that the actual abstraction results of the process models do, in fact, corroborate with the respective underlying process models that were abstracted. To accomplish this confirmation, the abstraction results were qualitatively and quantitatively compared with the respective process models. Details of the corroboration method applied and results are presented in Section 7.6 and summarized in Table 7.6-1.

The corroboration effort was performed for the process models and analyses that served as direct inputs (Table 4-1) to the TSPA-LA Model. The results demonstrate that the process model abstractions are validated and corroborated with their underlying process models. The results also show that the relevant analyses that support the TSPA-LA Model are also verified. Details of these validation and verification activities are documented in their respective source documents (Table 7.6-1). In summary, the results of the corroboration study documented in Section 7.6 confirm that the abstractions implemented in the TSPA-LA Model do, in fact, corroborate qualitatively and quantitatively with their underlying validated process models and analyses.

7.10.7 Corroboration of Results with Auxiliary Analyses

The auxiliary analyses are an important aspect of determining whether the TSPA-LA Model is yielding reasonable results (e.g., that the model is producing the results that would be expected). Four different sets of auxiliary analyses were performed: (1) single realization analysis (Section 7.7.1), (2) comparison of the results of the TSPA-LA Model with a Simplified TSPA Analysis (Section 7.7.2), (3) comparison of the results of the TSPA-LA Model with the TSPA independently developed by EPRI (Section 7.7.3), and (4) PMA (Section 7.7.4) of the TSPA-LA modeling cases. The sections cited above describe in detail the analytical approach applied and observations made regarding the reasonableness of the TSPA-LA Model construction and the results it produced. A summary of the auxiliary analyses is provided below.

Single Realization Analysis

A comprehensive explanation detailing how the transport of key radionuclides is affected by coupling various submodel components of the EBS, UZ, and SZ domains in the TSPA Model, following the WP failure under varying physical-chemical-thermal-mechanical conditions, provides confidence that these model components are working as expected and the aggregate TSPA-LA Model results (in terms of dose) are reflective of the model components. Single realization analyses provide insight into the inner workings of the model and allow one to describe the transport of key radionuclide in a transparent manner. Through examination and explanation of key aspects affecting the release of radionuclides, it is demonstrated that the TSPA-LA Model is functioning as intended and that the submodels are coupled correctly to yield the system level results. This demonstration provides confidence that the TSPA-LA Model is functioning as designed and helps validate the model.

Single realization analyses have been performed on four modeling cases that were chosen to cover the range of WP failure mechanisms considered in TSPA-LA and to highlight the various processes affecting and controlling the radionuclide releases under varying

thermal-physical-chemical conditions. The four modeling cases are: (1) Waste Package EF Modeling Case (Section 7.7.1.1), (2) Drip Shield EF Modeling Case (Section 7.7.1.2), (3) Igneous Intrusion Modeling Case (Section 7.7.1.3), and (4) Seismic GM Modeling Case (Section 7.7.1.4). Details of the analyses and ensuing results are discussed in the sections cited above. The Waste Package EF Modeling Case and Drip Shield EF Modeling Case typically highlight the processes and controls on transport at early times when the repository is at an elevated temperature, along with the effects of climate changes while the DS is still intact. In contrast, the Igneous Intrusion Modeling Case and Seismic GM Modeling Case show the effects of various processes occurring late in time and when the DSs are breached but with variable damage on the WP.

A realization for analysis is selected that has behavior similar to the mean expected dose and represents a unique combination of epistemic and aleatory uncertainty. The description of aleatory uncertainty is different for each modeling case. It represents (1) a spatial location in the Waste Package and Drip Shield EF Modeling Cases, (2) timing of the disruptive event in the Igneous Intrusion Modeling Case, and (3) a sequence of randomly generated seismic events of varying magnitudes in the Seismic GM Modeling Case. After selecting a particular realization, the analysis provides a comprehensive explanation on the WP and DS failure mechanism, determination of failure opening area, and how the various waste forms degrade under varying thermal-physical-chemical conditions. The mass release of key radionuclides and their transport characteristics in the EBS, UZ, and SZ as modified by sorption, radioactive decay, decay-chain ingrowth, dispersion, and dilution, are described in detail under conditions that are unique to the modeling cases. The effects of solubility and sorption in controlling the release of certain radionuclides from the EBS are especially highlighted along with transport through various subdomains in the EBS Transport Model. The partitioning of mass going into the UZ fractures versus UZ matrix at the EBS-UZ boundary is described, and then the mass released is tracked in the UZ and SZ to underscore their barrier capability with respect to various radionuclides for selected parameter values. The concentrations at the RMEI location in the SZ are calculated from which the dose to RMEI is determined.

The qualitative and quantitative aspect of mass transport of various selected radionuclides is described in each of the three barriers. Describing the coupling of various submodels, such as in-package chemistry with solubility and sorption calculations under given thermal-physical-chemical conditions, provides the transparency and traceability that the models are coupled together and are working together as expected. The retardation effects in the UZ and SZ, along with the effect of fracture-matrix interaction, are also described. In all modeling cases the early release following the WP breach is dominated by non-sorbing and non-solubility limited radionuclides such as ^{99}Tc and ^{129}I, while the late time release is dominated by longer-lasting solubility-limited radionuclides that undergo sorption such as ^{242}Pu, ^{237}Np, and ^{239}Pu.

Comparison with Simplified TSPA Analysis

Comparison of the TSPA-LA Model results to a stand-alone Simplified TSPA Analysis (Section 7.7.2 and Appendix L) was conducted to further confidence in the TSPA-LA Model. The Simplified TSPA Analysis, based on a stand-alone computer program written in FORTRAN 90 and compiled/linked using Compaq Visual Fortran, was developed to corroborate the TSPA-LA Model. In developing the TSPA-LA Model, a complex numerical model is

required to appropriately solve the couple differential equations while taking into account the spatial variability in properties and processes. The Simplified TSPA Analysis is a higher level abstraction than the TSPA-LA Model. The difference between the two models is described in Section 7.7.2 with additional detail provided in Appendix L. Briefly, the simplification primarily involves removing a considerable amount of detail included in the TSPA-LA Model to capture spatial and temporal variability and treating the repository system with a more average representation. In addition, process level modeling results are further abstracted for inclusion in the Simplified TSPA Analysis. Although its technical bases are identical to those of the TSPA-LA Model, the Simplified TSPA Analysis is different than the TSPA-LA Model both in its structure and computational method.

The Simplified TSPA Analysis simulated four TSPA-LA modeling cases: (1) Nominal Modeling Case, which considered degradation of the WPs and DSs from corrosion processes only. Early WP failure, mechanical damage of the DS and WP, and seismic induced rockfall and its subsequent effects on seepage were not considered. (2) Waste Package EF Modeling Case, which evaluated repository performance considering only those WPs that experience early failure, and no failure of the WPs is considered to occur due to general corrosion, SCC, or seismic mechanical damage. (3) Seismic GM Modeling Case, which considered (a) degradation of the WP and DSs from corrosion processes; (b) effects of seismic ground motion, including mechanical damage to the WPs and DSs, and seismic induced rockfall; (c) random sampling of both aleatory and epistemic uncertainty in each realization; and (d) assuming seismic events of varying magnitude to occur randomly following a Poisson. The subsequent effects on rockfall, DS damage, and WP damage were then calculated. (4) Igneous Intrusion Modeling Case, which (a) considered the degradation of the engineered barriers as a result of an intruding magma dike; (b) did not consider degradation of the WP and DSs due to corrosion processes, seismic mechanical damage, and early WP failure; and (c) randomly sampled both aleatory and epistemic uncertainty in each realization. A single igneous intrusion was assumed to occur randomly over the simulation period resulting in the failure of all DSs and WPs.

The results of the Simplified TSPA Analysis show that for all four modeling cases the total mean annual dose and the individual radionuclide mean annual dose are similar in magnitude to those obtained for the corresponding TSPA-LA modeling cases. In addition, the most significant radionuclides are also similar in the respective modeling cases of both the Simplified TSPA Analysis and TSPA-LA Model. Section 7.7.2 provides detailed discussion on the comparative results for the individual modeling cases for the Simplified TSPA Analysis and the TSPA-LA Model, as well as the minor differences in the prominence of certain radionuclides and mean annual doses calculated by the two approaches. The differences are found to be consistent with the simplifications made in the Simplified TSPA Analysis**.** Three examples of this follow: (1) reflective of the differences in the approaches in the two TSPAs, the Waste Package EF Modeling Case of the Simplified TSPA Analysis yields higher mean annual total and individual radionuclide doses than those of the TSPA-LA Model. (2) The Simplified TSPA Analysis for the Seismic GM Modeling Case indicates that the trend in the mean annual dose for the key radionuclides is similar with the TSPA-LA Model although the magnitude of their mean annual doses may be slightly different. For example, the TSPA-LA results do not show ^{229}Th to be a dominant radionuclide towards the end of the simulation period and that ^{239}Pu is a second-order contributor to the total mean annual dose, always less than ^{129}I and ^{99}Tc. The minor differences in the prominence of certain radionuclides and mean annual doses by the Simplified TSPA

Analysis are consistent with the simplifications made in the models as discussed in detail in Section 7.7.2. (3) For the Igneous Intrusion Modeling Case**,** the results indicate that the total probability-weighted mean annual dose is similar in magnitude to that obtained for the nominal scenario simulated over a 1,000,000-year period with the TSPA-LA Model. The most significant radionuclides for the Simplified TSPA Analysis show the same trends as for the TSPA-LA Model, but the latter has ^{229}Th being of lesser importance after 200,000 years following repository closure. The increased importan**ce** of ^{229}Th is attributed to how its transport in the natural system is being modeled in the Simplified TSPA Analysis.

Comparison with EPRI TSPA Analysis

The EPRI TSPA Analysis was developed independently by EPRI based on its own modeling approach and total systems performance code, Integrated Multiple Assumptions and Release Code (IMARC). The EPRI TSPA Analysis results available in the public domain were compared with those of the TSPA-LA for building further confidence in the TSPA-LA Model results. Like TSPA-LA Model, EPRI identifies scenario class modeling cases. The key features of the EPRI TSPA nominal modeling case were compared with the corresponding TSPA-LA modeling case (Section 7.7.3.2) in order to develop an understanding of the basis for the doses in the EPRI TSPA Analysis and TSPA-LA Model. The EPRI TSPA Analysis is based on the YMP data available in the earlier analysis and/or model reports that were primarily used for preparation of TSPA for the Site Recommendation (TSPA-SR), not the information used in the TSPA-LA. In general, the EPRI Analysis represents a more simplified implementation of the various process models and associated uncertainty compared to the TSPA-LA Model. It does not explicitly consider aleatory uncertainty, whereas the TSPA-LA Model considers both epistemic and aleatory uncertainty. Detail of the similarities and differences between the EPRI TSPA Analysis and the TSPA-LA Model is discussed in Section 7.7.3, with additional detail provided in Appendix M. For dose comparison, no model was rerun using the EPRI TSPA data. Rather, a preliminary comparison was made with the tables and figures in the EPRI report available on the EPRI website with the appropriate parts of the TSPA-LA Model results. The TSPA-LA Model mean annual doses of the Nominal Modeling Class and Waste Package EF Modeling Case were compared with those from the EPRI report.

The results show general similarities of dose curves and radionuclides trend as well as and some differences between the results from the two models. However, the differences in model results can broadly be accounted for by the differences between the two models in seepage rates through the repository; early-failure representation and EBS failure; inventory, both in terms of waste type and individual radionuclides; and solubility limits and sorption characteristics in the UZ and SZ as discussed in Section 7.7.3. For example, the results of the comparison indicate a similar pattern for the nominal scenario characterized by a significant increase in dose after 100,000 years. The early-failure dose is represented by the dose increase after about 1,000 years in the TSPA-LA Model, which is somewhat delayed in the EPRI TSPA Analysis. Overall, the total dose in the EPRI TSPA Analysis is about 0.02 mrem/yr compared to about 0.4 mrem/yr at one million years by the TSPA-LA Model. The main contributor to total dose at late time is ^{129}I in both cases.

Performance Margin Analysis

The PMA was developed to quantitatively evaluate the differences in repository performance due to significant explicit and implicit conservatisms, and simplifications embedded in the TSPA-LA Model subcomponents. The PMA (1) evaluated conservatism with respect to the mean annual dose of the TSPA-LA Model; (2) quantified the extent to which conservatisms and simplifications individually and collectively might overestimate the projected annual dose; and (3) assessed that the evaluated conservatisms and simplifications did not introduce any inappropriate risk dilution in the TSPA-LA results presented in support of the LA. The PMA was conducted by first modifying selected submodels and parameters of the TSPA-LA Model, including the additional submodels and parameters for the PMA and then repeating the sequence of calculation for a select set of modeling cases that were run for the TSPA-LA. PMA was conducted for both 10,000-year and 1,000,000-year time periods and on the same set of modeling cases as the TSPA-LA Model. The details of approach and results of the PMA are presented in Section 7.7.4 with additional supporting material in Appendix C. Summarizing here, the results show that the conservatisms and simplifications evaluated in the PMA are indeed conservative with respect to the total system performance measures (e.g., mean annual dose), as the largest doses calculated in the PMA for the 10,000 year and 1,000,000 year are significantly lower than the doses used in compliance demonstration. The largest calculated PMA mean annual doses are lower by over an order of magnitude and a factor of two over the largest mean annual dose relative to the TSPA-LA Model (Section 8.0) for the time periods of 10,000 years and 1,000,000 years, respectively. Further, the PMA analysis demonstrated that the conservatisms evaluated did not introduce risk dilution in the TSPA-LA results presented (Section 8.1.1 in Volume III) in support of compliance with the regulatory dose requirement, as demonstrated by the absence of higher peak doses in the PMA results for both the probabilistic projections of the expected annual dose and the comparison of the projected total mean annual dose for the PMA relative to the TSPA-LA. The PMA results also have different significant modeling cases than the TSPA-LA Model due primarily to the items selected for modification in PMA.

7.10.8 Corroboration of Results with Natural Analogues

Corroboration of the results of the TSPA-LA Model can be gained, in part, through comparison with characteristics of relevant analogues. Analogue information serves as indirect input to several of the process models and analyses that support the TSPA-LA Model and is used in validation and confidence building of these process models and analyses. The detail of description of the analogues and their application is provided in the source model and analysis reports cited in Table 6-1 and *Natural Analogue Synthesis Report* (BSC 2004 [DIRS 169218]).

Summarizing the results of the corroboration effort with the relevant analogues, the information from natural analogues has contributed to confidence in the submodels for drift stability, waste form and EBS degradation, seepage, UZ flow and transport, coupled processes, SZ transport, the biosphere, and disruptive events due to volcanism and seismicity. The use of this information during the development of these TSPA-LA submodels ensures that the submodels are grounded in reality and provides confidence that the TSPA-LA Model produces reasonable results. In addition to applying the relevant analogues on a qualitative basis for building confidence in the

TSPA-LA supporting process models and analyses, detailed comparisons were conducted with the Cerro Negro volcanic eruption and the Nopal I uranium mine at Peña Blanca (Section 7.8).

The ASHPLUME Model was used to simulate ash-fall thickness from the 1995 eruption of the Cerro Negro volcano. The results show that the ASHPLUME Model can reasonably predict the ash-fall distribution and ash-fall thickness from the eruption of a basaltic cinder cone volcano similar to Cerro Negro. The Cerro Negro ash-fall calculation method is used to simulate eruptive releases of ash either near the Yucca Mountain repository or through the repository involving WP destruction and aerial distribution of radionuclides. The uraninite degradation process at the analogue Peña Blanca Nopal I ore body appears to be similar to that described by the metal-fuel dissolution submodel used in the TSPA-LA Model. The measured values of uranium concentration in the groundwater beneath the Nopal I ore body and in boreholes downgradient on the groundwater flow path from the ore body appear to show, consistent with similar observations in other natural analogues, that uranium and its decay products are sequestered by natural geologic processes and do not migrate significant distances away from the source, even for geologically long times. The Peña Blanca analogue analysis provides confidence in the ability of the TSPA-LA Model to reasonably simulate the processes involved, and the outcome of the transport of radionuclides from the Yucca Mountain repository through a UZ and an SZ to a receptor location.

7.10.9 Technical Reviews Summary

Section 7.9 summarizes the empanelled technical reviews that were performed by the Project during the last decade on its TSPA methodology-development approach for ultimately producing a valid TSPA-LA Model. These reviews, conducted by teams of external experts, were undertaken in order to ensure that the TSPA-LA Model produced by the Project applying the methodology was credible, defensible to the regulatory authorities, and respected by the technical community.

The empanelled TSPA technical reviews that support development of the TSPA-LA Model include the TSPA-VA review completed in 1999, the TSPA-SR review by an IRT completed in 2002, and the critical review performed on initial drafts of the TSPA-LA Model by an IVRT completed in 2006. The TSPA-VA, IRT, and IVRT reviews are discussed in Sections 7.9.1, 7.9.2, and 7.9.3, respectively. In addition to the three empanelled reviews, the NWTRB performs routine reviews on key areas of the Project as mandated by Congress. These NWTRB comments and recommendations make significant contributions to the development of the TSPA-LA Model on an on-going basis. It is to be noted here that the TSPA-VA, TSPA-SR, and the initial drafts of the TSPA-LA were prepared for the 10,000 years after the repository closure period, which was the regulatory compliance period at that time. A summary of the TSPA-VA, IRT, and IVRT reviews are provided below.

TSPA-VA Peer Review

The TSPA-VA peer review was conducted to provide a formal, independent evaluation and critique of the TSPA-VA. The specific scope was for the review panel to conduct a phased review over a two-year period to observe the development and completion of the TSPA-VA. The TSPA-VA review panel's key conclusions include: (1) overall, the approach demonstrated

in the TSPA-VA for assessing the behavior of the repository during the postclosure period was sound; (2) the panel stated that, "it is unlikely that the TSPA-VA, taken as a whole, describes the long-term probable behavior of the proposed repository". In the panel's judgment, a number of components of the TSPA-VA analysis were not supported by adequate evidence that they represent systems, components, and processes they were designed to represent. In addition, several of the component models were likely to be conservative and others non-conservative. For these reasons, the panel stated that the decisions based on the TSPA-VA should be made cautiously (Budnitz et al. 1999 [DIRS 102726], Section B, p. 1); (3) the TSPA-VA was a necessary and useful step in the evolving understanding of how a repository could be expected to perform at Yucca Mountain. It has produced valuable insights into performance of the various repository components and helped identify issues where additional data and analyses could improve understanding of the repository performance and where additional work is unlikely to make significant contributions (Budnitz et al. 1999 [DIRS 102726], Section B, p. 1); (4) the panel noted the inherent difficulty in developing the TSPA model that is required to predict the repository behavior such a long time into the future (Budnitz et al. 1999 [DIRS 102726], Section B, p. 1); and (5) the panel noted the many experiments that were planned to be performed, which would be valuable in confirming, calibrating, or invalidating models that were developed for analyses of conditions at the proposed repository (Budnitz et al. 1999 [DIRS 102726], Section B, p. 2).

The Project responded to the comments (CRWMS M&O 1999 [DIRS 153111]) and found the panel recommendations consistent within the strategy for development of the postclosure safety cases for the upcoming site recommendation and subsequent LA and the design selection, and work-prioritization efforts that were underway for developing the safety cases. The Project fully implemented the panel recommendations as demonstrated in the significant updates of the component models based on the highly expanded site-scale test data collection efforts (Section 7.9.1.2). These bold and positive steps by the Project produced a much improved TSPA, which in turn made achieving significant Project goals possible. The most remarkable achievement is the submittal of the SR (Abraham, S 2002 [DIRS 159915]) and the associated Environmental Impact Statement (EIS) (DOE 2002 [DIRS 155970]). This resulted in the Presidential and Congressional approval of the repository site and authorization to the DOE to proceed with the LA for the NRC authorization of construction of the repository in accordance with the stipulations of NRC Proposed Rule 10 CFR Part 63 [DIRS 178394] and [DIRS 180319].

International Review Team Peer Review

The overall objective of the IRT review was to provide, based on the available international standards and guidance, as appropriate, an independent assessment of the methodology developed by the Yucca Mountain Site Characterization Project, as reported in *Total System Performance Assessment for the Site Recommendation* (CRWMS M&O 2000 [DIRS 153246]). Based on its review, the IRT made several recommendations (OECD and IAEA 2002 [DIRS 158098], Section 5.1) on the rationale the Project was pursuing in developing the SR, specifically the TSPA-SR Model, methodology to be used in developing the ensuing TSPA-LA, and the prevailing EPA and NRC proposed regulations at that time for the repository. The details of these observations are presented in Section 7.9.2. The key ITR included the following: (1) while presenting room for improvement, the TSPA-SR methodology is soundly based and has been implemented in a competent manner; (2) the performance assessment approach

provides an adequate basis for supporting a statement on likely compliance within the regulatory period of 10,000 years and, accordingly, for the site recommendation decision; and, (3) the IRT stressed that understanding the repository system and its performance and how it provides for safety should be emphasized more in future iterations, both during and beyond the regulatory period, and further work would be required to increase confidence in the robustness of the TSPA. The IRT made a set of 27 specific recommendations for future improvements in preparation and submission of the LA. The Project addressed these recommendations (Section 7.9.2.1 and Appendix E).

IVRT Technical Review

The IVRT review scope was defined by the then available TSPA technical work plans for the draft TSPA-LA Model under preparation and was conducted within the context of whether or not the TSPA-LA drafts satisfy the intended purpose specifically included in the following two model validation goals (BSC 2005 [DIRS 173309], Section 2.10.1): (1) describe the postclosure performance of the repository system for the Nominal, Igneous, and Seismic Scenario Classes; and, (2) produce an estimate of mean dose (and other performance measures, as appropriate) that is consistent with the degree of conservatism representative of the component abstraction models and parameters (and their uncertainty) that are input to the TSPA-LA Model. The details of the review are presented in Section 7.9.3. A summary is provided below.

The IVRT developed many comments and submitted seven recommendations (Section 7.9.3.2 and 7.9.3.3). The Project responded to these comments and implemented the recommendations as discussed in Section 7.9.3.2 and 7.9.3.3. The IVRT believed that the model provided highly conservative estimates of mean dose. In 2005, the IVRT issued a draft final report. The Project responded to the IVRT comments and additional changes were made to the process models and the TSPA Model. In their draft final report, the IVRT concluded that unlike its conclusion documented in the July 2004 they determined that the 2005 TSPA Model draft appeared to contain potentially significant optimisms as well as conservatisms and that there was no basis for determining the degree of conservatism of the model. The IVRT included seven recommendations as mentioned above, in its final report of February 2006. The Project recognized that successful completion of additional activities planned for FY06 to FY07 would help achieve the goal of a credible TSPA-LA Model for supporting a LA. The Project has since planned and completed these activities and fully implemented the seven IVRT recommendations (Section 7.9).

7.10.10 Conclusions

The TSPA-LA Model is a product of more than a decade of iterative TSPA development effort by the YMP. The during-development and post-development model validation activities presented in Section 7 of the TSPA-LA Model report are identified in the technical work plan to ensure that the TSPA-LA Model is developed and validated for its intended purpose and as required by procedure. The intended purpose is to provide the TSPA-LA Model for use in evaluations of compliance with the quantitative postclosure requirements of U.S. Nuclear Regulatory Commission (NRC) Proposed Rule 10 CFR Part 63 (DIRS [178394] and DIRS [180319]). The activities are also to address the applicable TSPA-LA Model acceptance criteria identified by the NRC in the Yucca Mountain Review Plan.

The activities presented in Section 7 examine the internal supporting models and components of the TSPA-LA Model separately and in combination to determine whether or not they are producing reasonable and plausible inputs to the TSPA-LA Model. These during-development TSPA-LA Model activities included (a) verification of the GoldSim code and the inputs used in computation of the TSPA-LA Model results using the code; (b) statistical, temporal and spatial stability and numerical accuracy of the computed results, and the radionuclide transport computation applying the particle-tracking method by the FEHM code produces reliable results; (c) performing uncertainty characterization reviews and implementing the review findings to ensure that the uncertainty associated with the TSPA-LA input parameters are properly and uniformly characterized; and, (d) verifying and validating the use of the CSNF and DSNF surrogates to represent the Navy and the DSNF wastes categories respectively, to be disposed of in the repository. The results of these during-development activities demonstrate that the GoldSim code functions as intended, inputs were accurately implemented in the TSPA-LA Model; the TSPA-LA Model is numerically, temporally, and spatially stable; and the resultant dose calculations are accurate for meeting the regulatory standards for disposing the high-level radioactive wastes.

The subsequent post-development validation activities included (a) documenting the demonstration that the abstracted direct inputs to the TSPA-LA Model do represent the respective supporting process models; (b) a number auxiliary analyses to examine that the TSPA-LA Model produces reasonable and plausible results and included several analyses of single realizations, comparison of the TSPA-LA Model results with a Simplified TSPA Analysis using a FORTRAN code and the EPRI TSPA Analysis, and a set of performance margin analyses to ensure that the TSPA-LA Model results are free of inadvertent risk dilution; (c) qualitative and quantitative evaluation of the component-models of TSPA-LA Model with the relevant natural analogues to provide additional confidence in the reasonableness of the TSPA-LA Model; and (d) implementing the recommendations and responding to the review comments by the independent national and international panels of experts on the methodology and validity of the Project's past TSPA models. The results of these post-development corroborative activities demonstrate and provide confidence that the TSPA-LA Model is valid for its intended purpose. A roadmap of the TSPA-LA sections to the applicable NRC requirements and the Yucca Mountain Review Plan acceptance criteria is provided in Table H-1 of Appendix H.